Mechanisms of Methylglyoxal-elicited Leukocyte Recruitment

A Thesis

Submitted to the College of

Graduate Studies and Research

In Partial Fulfillment of the Requirements

For the Degree of Doctor of Philosophy

In the Department of Pharmacology

University of Saskatchewan

Canada

By

Yang Su

PERMISSION TO USE

In presenting this thesis in partial fulfillment of the requirements for a Postgraduate degree from the University of Saskatchewan, I agree that the libraries of this University may make it freely available for inspection. I further agree that permission for copying of this thesis in any manner, in whole or in part, for scholarly purposes may be granted by the professor or professors who supervised my thesis work or, in their absence, by the Head of the Department or the Dean of the College in which my thesis work was done. It is understood that any copying or publication or use of this thesis or parts thereof for financial gain shall not be allowed without my written permission. It is also understood that due recognition shall be given to me and to the University of Saskatchewan in any scholarly use which may be made of any material in my thesis.

Requests for permission to copy or to make other use of material in this thesis in whole or part should be addressed to:

Head of the Department of Pharmacology

University of Saskatchewan

Saskatoon, Saskatchewan S7N 5E5

Canada

ABSTRACT

Methylglyoxal (MG) is a reactive dicarbonyl metabolite formed during glucose, protein and fatty acid metabolism. In hyperglycemic conditions, an increased MG level has been linked to the development of diabetes and the accompanying vascular inflammation encountered at both macro- and microvascular levels. The present study explores the mechanisms of MG-induced leukocyte recruitment in mouse cremasteric microvasculature. Biochemical and intravital microscopy studies performed suggest that administration of MG (25 and 50 mg/kg) to mouse cremaster muscle tissue induces dose-dependent leukocyte recruitment in cremasteric vasculature with 84-92% recruited cells being neutrophils. MG treatment up-regulated the expression of endothelial cell (EC) adhesion molecules P-selectin, E-selectin and intercellular adhesion molecule-1 (ICAM-1) via the activation of nuclear factor-κB (NF-κB) signalling pathway and contributed to the increased leukocyte rolling flux, reduced leukocyte rolling velocity, and increased leukocyte adhesion, respectively. The inhibition of NF-κB blunted MG-induced endothelial adhesion molecule expression and thus attenuated leukocyte recruitment.

Further study of signalling pathways revealed that MG induced Akt-regulated transient glycogen synthase kinase 3 (GSK3) activation in ECs, which was responsible for NF-κB activation at early time-points (< 1 h). After MG activation for 1 h, the endothelial GSK3 activity was decreased due to the up-regulation of serum- and glucocorticoid-regulated kinase 1 (SGK1), which was responsible for maintaining NF-κB activity at later time-points. Silencing GSK3 or SGK1 attenuated P-selectin, E-selectin and ICAM-1 expression in ECs, and abated MG-induced leukocyte recruitment. SGK1 also promoted cyclic adenosine monophosphate (cAMP) response element-binding protein (CREB) activity which was partially involved in ICAM-1 expression. Silencing CREB blunted ICAM-1 expression while P-selectin and E-selectin levels remained unaffected. MG also induced GSK3 activation in isolated neutrophils after 30 min treatment, an effect that was not responsible for MG-elicited Mac-1 expression. These data suggest the sequential activation of GSK3 and SGK1 in ECs as the pivotal signalling mechanism in MG-elicited leukocyte recruitment.

Additionally, MG-treatment led to uncoupling of endothelial nitric oxide synthase (eNOS) following MG-induced superoxide generation in ECs. MG triggered eNOS uncoupling and

hypophosphorylation associated with superoxide generation and biopterin depletion in EA.hy926 ECs. In cremaster muscle, as well as in cultured murine and human primary ECs, MG increased eNOS monomerization and decreased 5,6,7,8-tetrahydroboipterin (BH4)/total biopterin ratio, effects that were significantly mitigated by supplementation of BH4 or its precursor sepiapterin but not by N^G-nitro-L-arginine methyl ester (L-NAME) or 5,6,7,8-tetrahydroneopterin (NH4). These observations confirm that MG administration triggers eNOS uncoupling. In murine cremaster muscle, MG triggered the reduction of leukocyte rolling velocity and the increases in rolling flux, adhesion, emigration and microvascular permeability. MG-induced leukocyte recruitment was significantly attenuated by supplementation of BH4 or sepiapterin or suppression of superoxide by L-NAME confirming the role of eNOS uncoupling in MG-elicited leukocyte recruitment. MG treatment further decreased the expression of guanosine triphosphate cyclohydrolase I in murine primary ECs, suggesting the impaired BH4 biosynthesis caused by MG.

Taken together, these data suggest that vascular inflammation and endothelial dysfunction occurring in diabetes may be linked to GSK3/SGK1 regulated adhesion molecule expression, as well as the uncoupling of eNOS evoked by elevated levels of MG. These findings not only provide a better understanding of the role of MG in the development of diabetic vascular inflammation, but also suggest the potential therapeutic targets for MG-sensitive endothelial dysfunction in diabetes.

ACKNOWLEDGEMENTS

First of all, I would like to express my deepest appreciation to my supervisor Dr. Lixin Liu who gave me the precious opportunity to become his PhD student and supported me in my entire PhD study. I appreciate all his contributions of time, ideas, and financial support to make my PhD experience productive. His diligence and professionalism gives me an excellent example of a great scientist and supervisor. Specially, I want to thank him for always trusting me and giving me so much freedom to pursue the research areas that I am interested in. Without his guidance, I can never achieve what I have right now.

I would like to express my profound gratitude to my co-supervisor Dr. Lingyun Wu who generously offered her wisdom to improve my PhD work. Without the help from her and her lab, I could not get my project on track quickly at the beginning. From her, I saw a great scientist, and I know she will always be there when I need her. I want to thank her for her effort throughout my PhD study and in the preparation of each of our manuscript.

A special thank must go to Dr. Steven Richardson for his generous help in so many ways. He taught me how to make a good presentation, how to improve my English writing, and always remind us the characteristic we need to have to be a good researcher. He is a great man and a great mentor. I will always be grateful for his guidance.

I wish to express my heartiest thanks to my thesis committee members: Dr. Venkat Gopalakrishnan, Dr. Linda Hiebert, Dr. Lynn Weber and Dr. Kaushik Desai for their encouragement, insightful comments, and critical questions which always inspired me to improve my research. I must say that I could not make this far without your help.

I would also like to express my gratitude to Dr. Francisco Cayabyab for helping me with the confocal images and helping us with our manuscript.

I wish to express my sincerely thanks to my colleagues Md. Mokarram Hossain, Entesar Omran, Syed M. Qadri, and my friends Jianghai Liu, Arti Dhar, Indu Dhar, Simi Sandhawalia, Hanbin Lin and his wife Jiamin Li for their delightful companionship and friendship. I would like to thank our

technician Bo Jiang and Najia Xu, and also technicians from collaborated labs Arlene Drimmie and Karen Yuen for providing a helping hand whenever I needed.

I would also like to thank Cindy Wruck, Donna Dodge and Bob Wilcox for making the Pharmacology department a sweet home for all the students and helping us in every possible way.

I am sincerely thankful to the staff in lab animal services unit and health sciences supply centre of University of Saskatchewan for helping me by providing animals and reagents at appropriate time.

I would like to thank the College of Graduate Studies and Research and College of Medicine of University of Saskatchewan, and China Scholarship Council for kindly provide me the PhD scholarship.

Last but not least, no words can express my feelings for my loving parents and my Fianc éZhengxin Ying. Words have no power to express my gratitude for having them in my life. Their love, dedication, understanding and encouragement are the power of getting me closer to my dream step by step.

DEDICATION

To my parents

Jianqing Su and Jiqin Yao

To my Fianc é

Zhengxin Ying

For their constant encouragement, never ending love, care and support

TABLE OF CONTENTS

LIST OF TABLES

LIST OF FIGURES

LIST OF ABBREVIATIONS

3NT	3-nitrotyrosine
ADP	Adenosine diphosphate
AGE	Advanced glycation end-products
AMP	Adenosine monophosphate
ANOVA	Analysis of variance
Apo	Apocynin
ATP	Adenosine triphosphate
BH2	7,8-dihydrobiopterin
BH4	5,6,7,8-tetrahydroboipterin
Ca^{2+}	Calcium ion
CalDAG-GEF1	Ca^{2+} and diacylglycerol-regulated guanine nucleotide exchange factor 1
CEC	Carboxyethyl cysteine
CEL	N^{ε} –(carboxyethyl) lysine
CML	N^{ε} –(carboxymethyl) lysine
COX2	Cyclooxygenase-2
CREB	Cyclic AMP response element-binding protein
CRP	C-reactive protein
DAG	Diacylglycerol
DCF	Fluorescent 2',7'-dichlorofluorescein
DHAP	Dihydroxacetone phosphate
DHE	Dihydroethidium
DHFR	Dihydrofolate reductase
DM	Diabetes mellitus
DPI	Diphenylene iodonium
EC(s)	Endothelial cell(s)
ECM	Extracellular matrix
EE2 ECs	SVEC4-10EE2 endothelial cell line cells
ELISA	Enzyme-linked immunosorbent assay

eNOS	Endothelial nitric oxide synthase
ER	Endoplasmic reticulum
ERK	Extracellular signal-regulated kinase
ESL-1	E-selectin ligand-1
FFAs	Free fatty acids
fMLP	N-formyl-methionyl-leucyl-phenylalanine
GA3P	Glyceraldehyde 3-phosphate
GLUT4	Glucose transporter type 4
GPCR	G protein-coupled receptor
GS	Glycogen synthase
GSH	Reduced glutathione
GSH-Px	Glutathione peroxidase
GSH-red	Glutathione reductase
GSK3	Glycogen synthase kinase 3
GSSG	Glutathione disulfide
GTPCH1	Guanosine triphosphate cyclohydrolase 1
H & E	Haematoxylin and eosin
H2DCF-DA	2',7'-dichlorodihydrofluorescein diacetate
H_2O_2	Hydrogen peroxide
HPLC	High-performance liquid chromatography
HUVECs	Human umbilical vein endothelial cells
ICAM-1	Intercellular adhesion molecule-1
IFN-γ	Interferon-γ
IGT	Impaired glucose tolerance
IKK	Iκb kinase
IL-1	Interleukin-1
IL-6	Interleukin-6
IL-8	Interleukin-8
IMP	Inosine monophosphate
iNOS	Inducible nitric oxide synthase
IP3	Inositol triphosphate

IR	Insulin receptor
IRS-1	Insulin receptor substrate-1
ITAM	Immunoreceptor tyrosine-based activation motif
IκB	Inhibitory protein-κb
JNK	c-Jun N-terminal kinase
LFA-1	Lymphocyte function-associated antigen-1
L-NAME	N^{ω}-Nitro-L-arginine methyl ester
LOX-1	Lectin-like oxidized low-density lipoprotein receptor 1
LPAM	Lymphocyte Peyer's patch adhesion molecule
LTB4	Leukotriene B4
mAbp1	Mammalian actin binding protein 1
Mac-1	Macrophage-1 antigen (CD11b/CD18)
MAP kinase	Mitogen-activated protein kinase
MCP-1	Monocyte chemotactic protein-1
MG	Methylglyoxal
MG-H1	5-hydro-5-methylimidazolone
MLCK	Myosin light chain kinase
MnTBAP	Manganese (iii) tetrakis (4-benzoic acid) porphyrin
MOLD	Methylglyoxal-derived lysine dimer
NAC	N-acetyl cysteine
NADPH oxidase	Nicotinamide adenine dinucleotide phosphate oxidase
NDRG1	N-myc down-regulated gene 1
NF-κB	Nuclear factor-κB
NH4	5,6,7,8-tetrahydroneopterin
NK cells	Natural killer cells
NO	Nitric oxide
$O_2^{\bullet-}$	Superoxide
$ONOO^-$	Peroxynitrite
o-PD	*o*-Phenylenediamine
p38 MAPK	p38 mitogen-activated protein kinase
PDK1	Phosphoinositide-dependent kinase-1

PI3K	Phosphoinositide 3-kinase
PI3Kδ	Phosphoinositide 3-kinase δ
PIP2	Phosphatidylinositol 4,5-bisphosphate
PIP3	Phosphatidylinositol (3,4,5)-trisphosphate
PLCβ	Phospholipase Cβ
PPAR	Peroxisome proliferator-activated receptor
PSGL-1	P-selectin glycoprotein ligand-1
RAGE	Receptor for advanced glycosylated end-products
Rap-1	Ras-related protein 1
RIAM	Rap1-GTP-interacting adapter molecule
ROS	Reactive oxygen species
SGK1	Serum- and glucocorticoid-inducible kinase 1
SGLT1	Na^+-coupled glucose transporter 1
siRNA	Small interfering RNA
SOD	Superoxide dismutase
SSAO	Semicarbazide-sensitive amine oxidase
T1DM	Type 1 diabetes mellitus
TEMPOL	2,2,6,6-tetramethylpiperidinyl-N-oxy
TLR	Toll-like receptors
TNF-α	Tumor necrosis factor-α
VCAM-1	Vascular cell adhesion molecule-1
VE-cadherin	Vascular endothelial cadherin
VEGF	Vascular endothelial growth factor
VLA-4	Very late antigen-4
VSMCs	Vascular smooth muscle cells

CHAPTER 1

INTRODUCTION AND LITERATURE REVIEW

1.1 Diabetes

Diabetes mellitus (DM), or simply diabetes, is "a group of common metabolic disorders that share the phenotype of hyperglycemia" [1]. It is a group of chronic conditions that take place when the body is not able to sufficiently produce insulin or properly respond to insulin. As a hormone secreted by β cells in the pancreas, insulin enables the cells in the body to uptake sugar from bloodstream and use it to produce energy. Thus, diabetes is usually characterized by hyperglycemia. With the progression of the condition, hyperglycemia damages blood vessels and organs, for example the kidneys, eyes, heart, and nerves. These pathological changes can lead to serious complications and ultimately death [2, 3]. Hyperglycemia, hypertension and hyperlipidemia, which are associatively seen in diabetes patients, accelerate blood vessel damage, thus they need to be carefully controlled [4]. According to the most recent statistics on the burden of diabetes in Canada, in 2008/09, nearly 2.4 million Canadians (about 6.8%) were living with diabetes. Further estimates suggest that this number will reach 3.7 million by 2018/19 if the incidence and mortality rates remain the same [2, 5, 6]. Diabetes brings economic, physical and psychological burdens to the patient and their family. However, it is expected that this burden will only increase in the future.

1.1.1 Type 1 diabetes mellitus

Type 1 diabetes mellitus (T1DM) is considered an autoimmune disease. In T1DM, the body's immune system specifically destroys the insulin-secreting β cells in the pancreas [7]. Therefore the patients have to rely on an exogenous source of insulin for life. Type 1 diabetes usually occurs at a young age. It is partially genetically inherited, but the details are not fully known. Among all the diabetes patients, the prevalence of T1DM is about 10% [5].

1.1.2 Type 2 diabetes mellitus

Type 2 diabetes mellitus (T2DM) is a metabolic disorder caused by either insufficient production of insulin in the pancreas or an inappropriate response to insulin in the body (insulin resistance) [8]. In the early stage of T2DM, insulin resistance causes a compensatory increase in pancreatic insulin production which results in elevated plasma insulin levels. Because of the compensatory

effect, there may be no symptoms at this stage. However, with the development of the disease, the release of insulin is finally reduced due to apoptosis of β cells, causing decreased plasma insulin levels and hyperglycemia [9, 10]. It is shown that T2DM has a strong genetic predisposition. However, other risk factors such as poor eating habits, overweight, and physical inactivity also make people more vulnerable to T2DM. The onset of type 2 diabetes usually occurs in adults at the age of 40 or above. Among all the diabetes patients, the prevalence of T2DM is about 90% [2, 5].

1.1.3 Gestational diabetes

Gestational diabetes refers to the condition in which the females without previously diagnosed diabetes show hyperglycemia during pregnancy [11]. Although the elevated glycemic levels usually disappear after delivery, females who experienced gestational diabetes have a higher risk of developing T2DM in the following five to ten years [12].

1.2 Diabetic vascular complications

Vascular dysfunction is the main feature of diabetic complications and involves both micro- and macro-angiopathy [13]. The development of diabetic vascular complications leads to cardiovascular diseases (including coronary artery disease, peripheral arterial disease, and stroke), retinal damage, chronic renal failure, poor wound healing and neuropathy [2, 14]. The most recent diabetes statistics in Canada showed that diabetes patients increase their chances to develop heart disease by 3.8 times. They also increase the chance to have end-stage renal disease and non-traumatic lower limb amputations by 12 times and 20 times, respectively [2, 5, 6]. Despite the serious burden and threats that diabetic vascular complications bring to our life, the mechanism underlying hyperglycemia-induced micro- and macro-angiopathy is not fully understood.

1.2.1 Diabetic microvascular complications

Diabetic microvascular complications includes diabetic retinopathy, diabetic nephropathy and diabetic neuropathy [15]. With the extended duration and poor control of hyperglycemia, the patients will have higher risk of developing diabetic microvascular complications [2]. Diabetic

retinopathy, the leading cause of blindness in diabetes patients, harms small blood vessels in the retina of the eye and might show no symptoms at all until it causes bleeding or retinal detachment-induced acute vision loss [16]. Diabetic nephropathy which damages the blood vessels in the kidneys is the primary cause of renal failure in diabetes patients. The early stage of diabetic nephropathy shows leakage of blood proteins into the urine. As damage progresses, with compromised kidney function, eventually the patient will depend on dialysis or kidney transplant for survival [17]. Diabetic neuropathy is a result of damaged small blood vessels which provide oxygen to and remove toxins from nerves. It compromises both the structure and function of the nerves. Typically, patients experience numbness, tingling, burning, or pain. Patients with diabetic neuropathy are at high risk to develop foot ulceration [18].

Several proposed mechanisms explain how hyperglycemia leads to the development of microvascular complications. The overflow of the polyol pathway under hyperglycemia is considered to be important in this process. Aldose reductase, which converts glucose into sorbitol, is the initial enzyme in the polyol pathway. Under the physiological conditions, glucose is metabolized via the glycolytic pathway since aldose reductase has less affinity for glucose than hexokinase. However, hyperglycemia forces the metabolism of glucose via polyol pathway and causes the accumulation of sorbitol, which results in osmotic stress in cells [19-21]. There is evidence showing that sorbitol accumulation is related to thickening of the vascular basement membrane, microaneurysm formation, and loss of pericytes [22, 23]. More importantly, sorbitol can be oxidized into fructose by sorbitol dehydrogenase, and the latter can be converted into dihydroxyacetone phosphate (DHAP) which is known to be a primary source of endogenous methylglyoxal (MG) generation [24, 25]. The formation of MG and other by-products under hyperglycemia further promotes nonenzymatic formation of advanced glycation end products (AGE), which is identified as another important mechanism underlying the development of microvascular complications [26]. AGE are formed when MG, 3-deoxy glucosone or glyoxal reacts with certain proteins, resulting in the alteration of protein structures and functions [27]. AGE formation in collagens causes cross-linking of extracellular matrix (ECM) molecules, which impairs matrix-matrix interactions and promotes vascular stiffness [28, 29]. Another mechanism involved in this process is oxidative stress. High glucose levels foster reactive oxygen species (ROS) and free radical formation [30]. Despite their nonspecific attack on the cell membrane and

proteins, increased ROS also promotes the reaction of nitric oxide (NO) with superoxide anion to produce peroxynitrite [31]. This reaction further reduces the bioavailability of NO and leads to endothelial dysfunction [31, 32]. Beside the mechanisms mentioned above, some growth factors, including transforming growth factor-β, growth hormone, and vascular endothelial growth factor (VEGF), are also involved in the progression of diabetic microvascular complications, especially in diabetic retinopathy [33-35]. The growth factors foster angiogenesis in retinal capillaries, which causes functional and anatomical damage to the capillary network [36]. Consistently, suppressing VEGF formation results in lower progression of retinopathy in animal models [35].

1.2.2 Diabetic macrovascular complications

Diabetic macrovascular complications increase the risk of cardiovascular diseases such as stroke, peripheral arterial disease, and coronary artery disease [2]. Diabetes fosters the progression of atherosclerosis, leading to the narrowing of arterial blood vessels in the body. The damage in the coronary blood vessels causes unstable angina and acute myocardial infarction, whereas the narrowing of the vessels in brain can result in stroke [37, 38]. In general, people with diabetes have a two to four times greater risk to have cardiovascular disease than those without diabetes [3].

The most identified pathological mechanism of diabetic macrovascular disease is the progression of atherosclerosis. Atherosclerosis is induced by chronic inflammation and arterial endothelium injury in the coronary or peripheral vascular system. It is initiated with endothelial cell (EC) injury and increased plasma LDL levels, which foster the accumulation of LDL and oxidized LDL particles in the arterial wall. In the next step, monocytes migrate into the arterial wall where they further differentiate into macrophages. Macrophages ingest oxidized LDL and become foam cells, which then stimulate macrophage proliferation and attract more monocytes/macrophages to the injury site. During this process, the presence of angiotensin II further promotes the uptake of oxidized LDL by macrophages, thus accelerating the progression of the disease [39]. The injury in the local arterial walls also induces smooth muscle proliferation and promotes collagen accumulation. Finally, the result of this process is to form a lipid-rich atherosclerotic lesion covered with a fibrous cap, and the rupture of the atherosclerotic lesion is the leading cause of acute infarction [40-42]. In addition to atheroma formation, reduced NO production, elevated ROS

formation, and impaired calcium regulation in platelets were also found in diabetic patients. These changes promote platelet hyperaggregation, which increases the possibility of vascular occlusions [43, 44]. Besides, evidence showed that diabetes patients may have impaired fibrinolysis because of increased plasminogen activator inhibitor type 1 levels [45, 46]. The combination of impaired fibrinolysis and increased coagulability is an important mechanism involved in diabetic macrovascular complications as well.

1.3 Inflammation and diabetes

In the last decade, the perspective of diabetes has gradually evolved. It is now widely accepted that chronic inflammation and the activated immune system are essentially involved in the development of diabetes [47]. Inflammation can be induced by stress, aging, overnutrition, obesity and infection [48]. It is a protective response to remove the harmful stimuli and to start the healing process. However, long-term innate immune system activation, which results in chronic inflammation, causes disease instead of repair. Chronic inflammation is shown to be involved closely in the pathogenesis of diabetes. In addition, the findings that anti-inflammatory agents may decrease the risk of type 2 diabetes are of great interest [49].

1.3.1 Inflammation and type 1 diabetes

Type 1 diabetes is due to the over-reactive immune response. As a result, the insulin-producing β cells in pancreas are selectively destroyed by the immune system [7]. This disease is characterized by the infiltration of $CD8^+$ and $CD4^+$ T-cells and macrophages to islets in the pancreas. A series of mechanisms have been suggested to participate in β-cell killing. For instance, $CD8^+$ T-cells which produce lytic granules may kill β-cells by direct cytotoxicity. T effector cells, which express Fas ligand (FASL), bind with the Fas domain expressed on β-cells and induce apoptosis through FAS-FASL death domain signalling. Macrophages that release cytokines and ROS directly trigger apoptosis of β-cells [7]. Excessive cytokine signalling in β-cells also lead to endoplasmic reticulum (ER) stress. In addition, cytokines also indirectly activate and recruit immune cells to attack β-cells [7].

1.3.2 Inflammation and type 2 diabetes

In the last a few years, the link between cytokine production, insulin resistance and type 2 diabetes has been intensively established. Studies using non-diabetic subjects, people with impaired glucose tolerance (IGT) and lately diagnosed type 2 diabetes patients, showed that the levels of proinflammatory mediators and cytokines, such as C-reactive protein (CRP), tumor necrosis factor-α (TNF-α), and interleukin-6 (IL-6), are positively correlated with insulin resistance and the development of type 2 diabetes [47, 50].

TNF-α is produced by macrophages, T cells, natural killer cells, *etc.* [51]. It promotes endothelial activation as well as vascular hyperpermeability [52]. Recent experimental studies have shown that chronic elevation of TNF- α and IL-6 levels directly impairs insulin-induced glucose uptake [53, 54]. Over production of TNF-α and IL-6 activates intracellular signalling pathways, such as Jun N-terminal kinase (JNK) and protein kinase C (PKC), which produce serine phosphorylation of insulin receptor (IR) and insulin receptor substrate 1 (IRS-1) [55, 56]. This phosphorylation impairs insulin-induced tyrosine phosphorylation on IRS via the activation of phosphoinositide 3-kinase (PI3K) and Akt, and thus blocks the signalling transduction in insulin pathway [57]. Besides, *in vitro* studies have shown that TNF-α depresses glucose transporter type 4 (GLUT4) gene transcription and decreases GLUT4 mRNA stability [58]. Additionally, IL-6 and TNF-α also stimulate CRP production from the liver. The expression of CRP then promotes the expression of monocyte chemotactic protein-1 (MCP-1) and intercellular adhesion molecule-1 (ICAM-1) by ECs, which accelerates the progression of diabetic vascular complications [59, 60].

On the other hand, the elevation of cellular free fatty acids (FFAs), commonly observed in pre-diabetic and diabetes patients, also contributes to insulin resistance via the activation of toll-like receptors (TLRs) [61, 62]. The binding of FFA to TLRs stimulates proinflammatory cytokines expression in macrophages [61]. In addition, FFAs also directly activate JNK pathway, which leads to the phosporylation of IRS-1 on serine residues and results in insulin resistance [63, 64]. Under pathological conditions, the increases of FFAs combined with excessive glucose lead to oxidative stress. Such an oxidative stress in turn activates redox-sensitive transcription factors such as NF-κB, which further promotes the transcription of TNF-α and IL-6 [65].

1.3.3 Inflammation and diabetic vascular complications

Besides its critical role in diabetes pathogenesis, inflammation also plays a critical role in the development of diabetic vascular complications [66, 67]. The mechanism of diabetes-induced vascular inflammation involves pathological changes in vascular ECs, smooth muscle cells, and the migration and transformation of macrophages. Hyperglycemia, hyperlipidemia, increased serum and cellular FFAs and AGE all contribute to vascular inflammation, and finally result in micro- and macrovascular damage [68, 69].

1.3.3.1 The impact on endothelial cells

Pro-inflammatory signals are involved in the mechanism of hyperglycemia-induced endothelial dysfunction. It has been shown that high glucose or glucose metabolites, such as MG, reduce nitric oxide (NO) production in ECs [70]. As an important anti-inflammatory molecule in ECs, NO reduction causes pro-inflammatory gene expression via the activation of pro-inflammatory signalling pathways [71]. On the other hand, the reactive glucose metabolite production under hyperglycemic conditions also promotes the formation of AGE, which exert multiple effects on cells via binding and activating RAGE (receptor for AGE). The activation of AGE-RAGE pathway results in excessive production of ROS through nicotinamide adenine dinucleotide phosphate (NADPH) oxidase and the activation of pro-inflammatory signalling events [72, 73]. A key target among these activated signals is NF-κB, which is responsible for the expression of EC adhesion molecules and cytokines [74]. Increased EC adhesion molecules, such as ICAM-1 and VCAM-1, together with the decreased NO and increased cytokines foster leukocyte adhesion and transmigration from the blood stream into the local tissue [75]. The movement of macrophages into the lipid-rich lesions on the vessel wall is the key step in the progression of atherosclerosis [76, 77]. Such a process in arterioles, especially renal arterioles, leads to hypertension and diabetic nephropathy over time [78]. Thus, it is clear that vascular inflammation, which is initiated by endothelial dysfunction, is deeply involved in the development of diabetic vascular complications.

1.3.3.2 The impact on vascular smooth muscle cells

Endothelial dysfunction directly affects the microenvironment of vascular smooth muscle cells (VSMCs) and causes pathological changes. The expression of pro-inflammatory molecules is

highly involved in this process. It was shown that high glucose induces adhesion molecule and cytokine expression in VSMCs [79, 80]. The expression of cytokines such as IL-1, MCP-1, IFN, IL-6 results in VSMCs proliferation, migration and over-expression of ECM proteins [79]. In the progression of diabetic macrovascular complications, for example atherosclerosis, the proliferation and migration of VSMCs towards the lipid-rich atherosclerotic lesion contributes to the formation of the fibrous cap which strengthens the atheromatous plaque [81]. In the progression of diabetic microvascular complications, such as arteriolosclerosis, VSMC-mediated excessive ECM production results in the thickening of arteriole walls and the deposition of homogeneous pink hyaline material, which is known as hyaline arteriolosclerosis [82, 83]. These changes narrow the lumen of the arteries in both macro- and microvasculature. In large vessels, the rupture of atheromatous plaque is the leading cause of coronary artery disease in diabetes patients [84]. In small vessels, reduced lumen size in renal arterioles decreases renal blood flow, and therefore reduces glomerular filtration rate. This could in turn cause increased renin secretion, which further increases the blood pressure, and finally the decreased kidney function [85]. All these changes can not be achieved without the presence of pro-inflammatory signals.

1.3.3.3 The impact on monocytes/macrophages

The role of monocytes/macrophages in diabetic vascular inflammation is widely studied in macrovasculature [65, 86]. As we know, the most identified pathological mechanism of diabetic macrovascular disease is the progression of atherosclerosis. In this process, increased FFA and lipoproteins firstly activate monocytes/macrophages via TLR signalling [61, 87, 88]. The activated cells are then attracted to the lesion site in the arterial wall by cytokines that are expressed locally by activated ECs or VSMCs. The pro-inflammatory cytokines IL-8 and MCP-1 are involved in this process [89-91]. In addition, the activated monocytes/macrophages also secret cytokines, which are important for recruiting more monocytes to the lesion site [81]. It is clear that the migration of monocytes/macrophages plays a major role in the pathogenesis of diabetic macrovascular diseases. However, the behavior of leukocytes in diabetic microvascular diseases is still poorly studied. In those small vessels, it remains unclear as to how leukocyte recruitment is involved in diabetic vascular complications.

1.4 Leukocyte recruitment

Our immune system is a complex network of organs, tissues, and cells that work together to defend the body against infections and foreign materials. Being the key components in the immune system, leukocytes are tightly associated with the immune functions in our body. In most cases, leukocytes are produced and derived from hematopoietic stem cells in the bone marrow. As the hematopoietic stem cells mature, they differentiate into diverse subtypes of leukocytes, including neutrophils, eosinophils, basophils, lymphocytes and monocytes. Each of them have unique functions in immune defence [92].

Neutrophils are usually the first responders to infections or tissue damage. They are commonly seen in the early stages of acute inflammation. These cells are not able to renew their lysosomes which are used to digest microbes, thus will die after phagocytosing a few pathogens [93]. Lymphocytes are much more common in the lymphatic system than in the blood. They include 3 types of cells: T cells, which function in cell-mediated cytotoxicity in adaptive immunity; B cells, which function in antibody-mediated humoral immunity in adaptive immunity; and natural killer cells (NK cells), which function in cell-mediated cytotoxicity in innate immunity [93]. Monocytes can move to the infection sites and differentiate into macrophages or dendritic cells. Monocytes also have phagocyte function as do neutrophils, but are capable of replacing their lysosomal contents and thus have a much longer active life. They also act as antigen presenting cells which present pieces of processed pathogens to T cells so that the pathogens can be recognized and killed by the adaptive immune system. Eosinophils are primarily involved in parasitic infections and allergic reactions, whereas basophils are mainly responsible for allergic and antigen responses by releasing histamine [94].

1.4.1 Mechanisms of leukocyte recruitment

Leukocyte recruitment refers to the movement of leukocytes from the blood stream to the extravascular space. However, it is known that leukocyte recruitment, although essential to survival, can also be harmful to the host [95-97]. Figure 1-1 illustrates the leukocyte recruitment paradigm that is commonly seen in immunology textbooks. This process occurs at postcapillary venules and requires the presence of selectins to support rolling, and integrins to support adhesion.

The activation of integrins requires the presents of chemokines and other proinflammatory molecules on the surface of endothelium. Rolling and adhesion are essential for the migration of leukocytes. In most cases, the blockade of rolling by anti-selectin antibodies prevents firm adhesion of leukocytes, and thus inhibits leukocyte diapedesis [98-100].

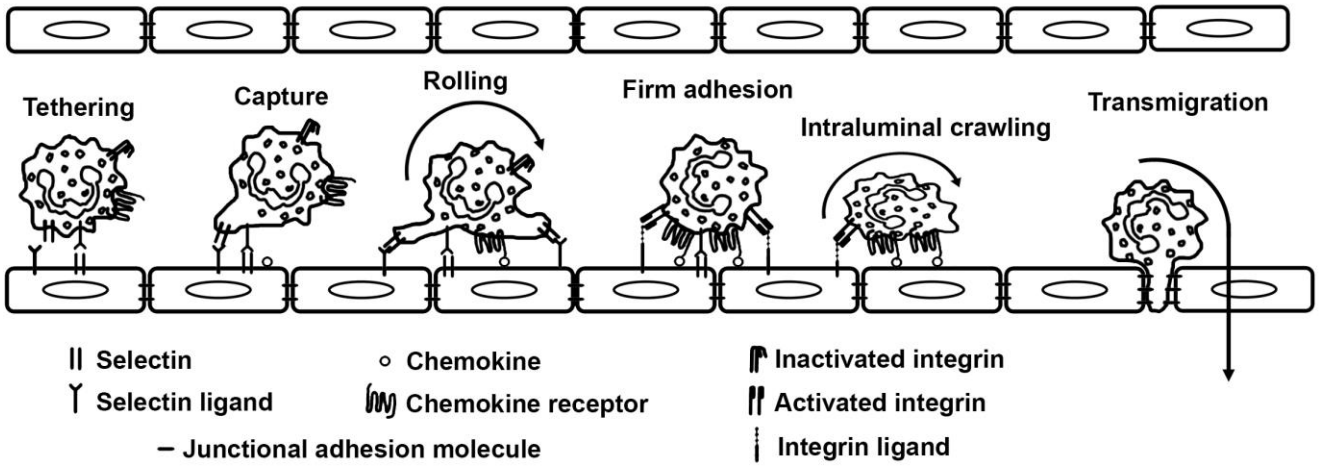

Figure 1-1. Sequential phases of leukocyte recruitment from the blood stream to the inflamed tissue. Tethering and rolling are mostly selectin-dependent, while adhesion and intraluminal crawling are integrin-mediated. Endothelium-expressed chemokines activate the surface-expressed integrins on the rolling leukocytes, resulting in conformational changes of the integrins. The transmigration of leukocytes requires the interaction of junctional adhesion molecules that are expressed on both leukocytes and ECs [100].

1.4.1.1 Tethering and rolling

The initial contact between leukocytes and endothelium is termed tethering. Under physiological conditions, leukocytes move along with red blood cells at a high speed in the blood stream. Therefore, to initiate tethering, a greatly reduced velocity must take place. During inflammation, vascular hyperpermeability and vasodilation change the velocity and shear force of the blood. It was shown that during low shear, smaller cells, such as red blood cells, tend to move near the center of the bloodstream, while the larger cells, such as leukocytes, are pushed outward to the vessel wall. This physical property provides the chances for leukocyte-endothelium interaction, however it is not sufficient to slow down the high speed leukocytes [96, 97, 101]. The following

rotational movement of leukocytes along the vessel wall, which is named rolling, is dependent on the expression of selectins. It is well accepted that selectins are critical for initiating leukocytes tethering and rolling on endothelium [97, 102].

The selectins are calcium-dependent type I transmembrane glycoproteins. E-selectin and P-selectin are expressed on activated endothelium, while L-selectin is found on leukocytes. P-selectin (CD62P) is not constitutively expressed. In platelets it is stored in alpha-granules, while in ECs it is stored in Weibel-Palade bodies. In ECs, upon the stimulation of inflammatory mediators (such as cysteinyl leukotrienes, histamine, thrombin, and oxidants, *etc.*), the Weibel-Palade bodies fuse with the plasma membrane within minutes and increase the level of P-selectin on the surface of ECs. Thus, it is anticipated that P-selectin participates in the early stage of leukocyte recruitment [101]. Upon activation by cytokines, the transcriptional upregulation of P-selectin is also observed in endothelium. TNF-α, IL-1, and LPS are shown to increase P-selectin expression in murine, while IL-4 and IL-13 are functioning in human ECs [97, 100]. The blockade of P-selectin prevents leukocytes rolling and the subsequent adhesion in postcapillary venules. E-selectin (CD62E) is *de novo* synthesized in ECs upon the stimulation of proinflammatory cytokines such as TNF-α or IL-1β. On the endothelium of non-inflamed tissue, minimal or no E-selectin is expressed. The expression of E-selectin takes place within 4 h and generally decreases within 24 h. Thus, it mediates leukocyte rolling at a delayed time point. E-selectin expression leads to a dramatic decline of rolling velocity (slow rolling), which facilitates the subsequent adhesion. The blockade of E-selectin results in higher rolling velocity and lower chance to adhere [95, 102]. On leukocytes, the binding to endothelial P-selectin and E-selectin is mediated by P-selectin glycoprotein ligand-1 (PSGL-1), while other ligands such as E-selectin ligand 1 (ESL1), CD43, CD44 and L-selectin (in human neutrophils) are also responsible for E-selectin binding. L-selectin (CD62L) is constitutively expressed on most leukocytes. It is a homing molecule that is involved in lymphocyte recirculation. The binding between L-selectin and endothelial PSGL-1 is reported in postcapillary venules. L-selectin is involved in leukocyte rolling, however, its role may be limited. In the absence of L-selectin, leukocytes still rolled and adhered but failed to emigrate out of the vasculature, suggesting it is involved not just in the rolling process [97, 99]. Despite the differences, the three selectins functionally overlap with each other, and play a significant role in leukocyte recruitment during inflammation.

1.4.1.2 Activation of leukocytes

The tethering and the rolling of leukocytes along the inflamed endothelium allow the leukocytes to contact chemokines on the surface of endothelium. Chemokines are critical for integrin activation. The binding between chemokine and its G protein-coupled receptor (GPCR) triggers the conformational change of the integrins which provides higher affinity to adhesion molecules. Both chemokines and activated integrins are required for the subsequent firm adhesion of the leukocyte.

The activation of leukocyte integrins requires an "inside-out signalling": the activation of intracellular signalling finally results in the conformational change of surface-expressed integrins, thus affects intercellular action. The binding of the chemokine to its receptor activates GPCR signalling, thus the Gβγ subunit is released from the receptor complex then activates phospholipase Cβ (PLCβ) which cleaves phosphatidylinositol 4,5-bisphosphate (PIP2) into diacylglycerol (DAG) and inositol triphosphate (IP3). Increased IP3 causes Ca^{2+} release from the endoplasmic reticulum, which leads to the activation of Ca^{2+} and DAG sensitive protein Ca^{2+} and diacylglycerol-regulated guanine nucleotide exchange factor 1 (CalDAG-GEF-1). This activation results in the binding of several proteins including Ras-related protein 1 (Rap-1), Rap1-GTP-interacting adapter molecule (RIAM), talin-1 and kindling-3 to form a complex. Finally, the contact between talin-1, kindling-3 and the tail of β chain causes the conformational change of bended ligand-binding headpiece into an upright position, which allows the integrins to have higher affinity [103, 104]. It must be noted that the integrin activation occurs within seconds or subsecond time frames. Thus the "activation" is usually not considered as a specific stage in leukocyte recruitment paradigm.

1.4.1.3 Firm adhesion

With the presence of chemokines, lipid mediators or other proinflammatory molecules on the surface of the endothelium, the selectin-dependent rolling is followed by integrin-dependent firm adhesion. Integrins are heterodimers containing two distinct chains, named α and β subunits. In mammals, 18 α subunits couples with 8 β subunits to yield 24 different integrin molecules. It was shown that the expression of β2-integrins (CD18), such as LFA-1 (lymphocyte function-associated

antigen 1, αLβ2), Mac-1 (also known as macrophage-1 antigen, integrin αMβ2), p150, 95 (αXβ2) and αDβ2 on neutrophils, are important for their adhesion. Administration of anti-CD18 antibody blocks ischemia/reperfusion-induced leukocyte recruitment. Similar effects are observed in mesentery and other tissues. However, lack of β2-integrin gene could result in impaired wound healing and severe infectious complications. Besides β2-integrin, α4-integrin is another dominant integrin that required for adhesion. It can associate with either β1-integrin to form α4β1integrin (also known as very late antigen-4, VLA-4), which is observed in most mononuclear cells, or β7-integrin to become α4β7 integrin (also known as lymphocyte Peyer's patch adhesion molecule, LPAM) which is found primarily in lymphocytes. The α4-integrins primarily mediate the adhesion, and rolling in some cases, of monocytes, lymphocytes, and eosinophils. On ECs, the identified ligands for these integrins are ICAM-1 and VCAM-1. Both ICAM-1 and VCAM-1 can be *de novo* synthesised upon the stimulation. The ICAM-1/β2-integrin binding is shown to be important for neutrophil recruitment, while VCAM-1/α4-integrin binding recruits monocytes, lymphocytes and eosinophils. It should be noticed that the function of those molecules are usually not restricted in one certain stage. In some cases, integrins are capable of mediating leukocyte rolling, while selectins can also be important for initiating adhesion [95, 97, 99, 101, 102].

1.4.1.4 Intraluminal crawling

After firm adhesion, leukocytes crawl on the luminal surface of the endothelium to reach to their optimal extravasation sites. To initiate this stage, the binding between integrins and ICAM is required since blocking of ICAM-1 prevents adherent leukocyte from crawling and subsequent emigration. Additionally, the binding between ICAM-1 and β2 integrin activates the “outside-in signalling”: the interaction between ICAM-1 and integrin on the cell surface triggers the intracellular signalling cascade that increases the functionality of the integrins and that is required for the crawling of leukocytes. Although the mechanism is not fully understood, the “outside-in signalling” is shown to be critical for leukocyte intraluminal crawling.

The activation of “outside-in signalling” leads to proper localization of proteins that are crucial for intraluminal crawling at the edge of lamellipodium. For example, the translocation of phosphoinositide 3-kinase δ (PI3Kδ) results in the accumulation of PI3K products at the lamellipodium, which is essential for the stabilization of cell polarity and chemotactic migration.

The subsequent interaction between mAbp1 and actin at the leading edge of polarized cells controls the shape change of lamellipodium, and therefore facilitates the intraluminal crawling. It was shown that leukocyte intraluminal crawling does not require a chemotactic gradient. However, the established gradient of chemokines in the vasculature is able to guide the leukocytes crawling towards their transmigration sites, with the mechanism not yet demonstrated [97, 101, 103, 104].

1.4.1.5 Transendothelial migration

Leukocytes migrate into inflammatory sites by passing through the layer of ECs. However, ECs are tightly connected to each other through junctional structures. Therefore, these junctions must apparently be opened for transmigrating leukocytes, while the vascular integrity remains intact. On ECs, there are several well-identified junctional expressed molecules that are involved in leukocytes transmigration, including JAM-A, JAM-B, JAM-C, PECAM and CD99. Vascular endothelial cadherin (VE-cadherin) is another junctional-expressed molecule which is critical for maintaining vascular integrity and regulating vascular permeability. These junctional expressed molecules are capable of homophilic interactions, which means a molecule on one cell can bind to the same molecule on the apposing cell. On leukocytes, PECAM, JAM-A, JAM-C and CD99 are also expressed. Besides, integrins such as VLA-4, Mac-1 and LFA-1 also bind to JAMs on ECs. Upon the stimulation by inflammatory cytokines, the rearrangement of junctional expressed molecules is observed in ECs. This step is required for leukocyte transmigration to proceed since the rearrangement increases the contacts of leukocytes with ECs and guides leukocytes into the junction between ECs. To complete the transmigration, a transient rise of intracellular free calcium is also required in ECs. Leukocytes can only adhere to the endothelium but cannot complete the transmigration if this transient calcium rise is cushioned. The increase of intracellular calcium also activates myosin light chain kinase (MLCK), which leads to unfolding of myosin II, and subsequent cell retraction which facilitates leukocyte passage [97, 101, 103-106].

1.4.1.6 Fate of extravasated leukocytes

Leukocyte transendothelial migration must follow the chemokine gradient which is produced by the endothelium. After transendothelial migration, the leukocyte must then migrate against this gradient towards the infection or damaged tissue. This suggests there is a new chemotactic signal

in the tissue which overrides the first gradient that exists on endothelium. A number of studies have shown the hierarchy of chemotactic signals in an inflamed tissue. For example, the chemoattractant molecules which are presented by infecting bacteria [such as bacteria-derived N-formyl-methionyl-leucyl-phenylalanine (fMLP)] or the endogenous expressed complement component C5a override the endothelium-generated chemotactic signals [such as, interleukin 8 (IL-8) and leukotriene B4 (LTB4)]. Therefore, according to their leukocyte attracting ability, chemoattractants can be divided into "end-target" and "intermediate" chemoattractants. Chemotaxis was controlled by the activation of several pathways, among them the phosphatidylinositol 3-kinase (PI3K) signalling is most well-studied. The accumulation of PIP3 at the leading edge of chemotaxing neutrophils is required for their directional migration. Besides, p38 mitogen-activated protein kinase (p38 MAPK) signalling and extracellular signal-regulated kinase (ERK) signalling are also involved in the chemotaxis triggered by end-target chemoattractants [107, 108].

1.4.2 Leukocyte recruitment and microvasculature damage

Besides the mechanism of monocyte/macrophage recruitment in the development of atherosclerosis (reviewed in 1.2.2), little is known about the mechanisms and the impact of leukocytes recruitment on microvasculature. There are two major limitations to perform an *in vivo* study on this: the limited methods to perform *in vivo* leukocyte tracking during inflammation, as well as the limited techniques to evaluation the long-term impact of leukocyte recruitment on the development of microangiopathy. Although the detailed mechanisms are not completely understood, evidence shows that leukocyte recruitment is highly involved in microvascular injury, especially in diabetic nephropathy.

Endothelial dysfunction is associated with nearly all forms of diabetic microvascular complications. There is an increasing body of evidence showing that leukocyte transmigration increases vascular bed inflammation and changes the functions of ECs. For example, activated monocytes/macrophages release excessive ROS, NO, TNF-α, IL-1, metalloproteinases, and complement factors, all of which promote EC activation [79, 109]. Thus, the interactions between activated macrophages and ECs could result in endothelial dysfunction. Besides, macrophage-

derived factors such as IL-1 and platelet-derived growth factor (PDGF) also induce the proliferation of mesangial cells in kidney, resulting in diabetic nephropathy [109]. On the other hand, activated T lymphocytes, which are widely observed in diabetes patients, also secrete inflammatory factors such as IFN-γ, TNF-α, which activate ECs and macrophages [110]. Neutrophils can induce endothelial dysfunction by producing reactive oxygen species (ROS) and releasing cytotoxic proteinases [111]. There is clear evidence that neutrophils from diabetes patients exert an activated phenotype, which is revealed by increased TNF-α-induced superoxide generation and enhanced spontaneous adhesion [109, 112]. It has also benn shown that neutrophils from diabetes patients have increased level of ROS, which may impair ECs and promote the development of diabetic nephropathy [109, 112]. Thus, the contact between neutrophils and ECs is potentially harmful. The increased recruitment and impaired functions of leukocytes were both observed in diabetes mouse models. Hanses *et al.* observed defects in neutrophil apoptosis and in their ability to clear staphylococcal infections in diabetic mice [113]. In the physiological condition, neutrophil apoptosis promotes their elimination by macrophages at the site of infection, which subsequently terminates the inflammatory process. Thus, these defects prolong production of proinflammatory TNF-α by neutrophils and may contribute to the chronic inflammation and impaired wound healing. Judging from the evidence above, leukocyte recruitment brings more damage than healing in the microvasculature. Although the mechanisms are poorly understood, it is clear that leukocyte recruitment is involved in the progression of diabetic microvascular complications.

1.4.3 Intravital microscopy

Intravital microscopy is a cutting-edge technique for studying the molecular mechanisms of leukocyte recruitment by visualizing leukocyte-EC interactions *in vivo*. Many studies using this technique are performed with translucent tissues, such as mesentery and cremaster muscle, using brightfield intravital microscopy (Figure 1-2). In fact, the identification of the neutrophil recruitment paradigm was largely dependent on the use of this technique. Recently, with the application of spinning-disc confocal and two-photon microscopes which are suitable for thicker tissue penetration, more organs and tissues, for example skin, lymph nodes, brain, lung and liver, can also be visualized and studied. These advanced techniques allowed people to visualise the

different cell populations or anatomical structures that are labelled by fluorescent antibodies, thus allowing a better understanding of the mechanism of leukocyte recruitment [96, 114].

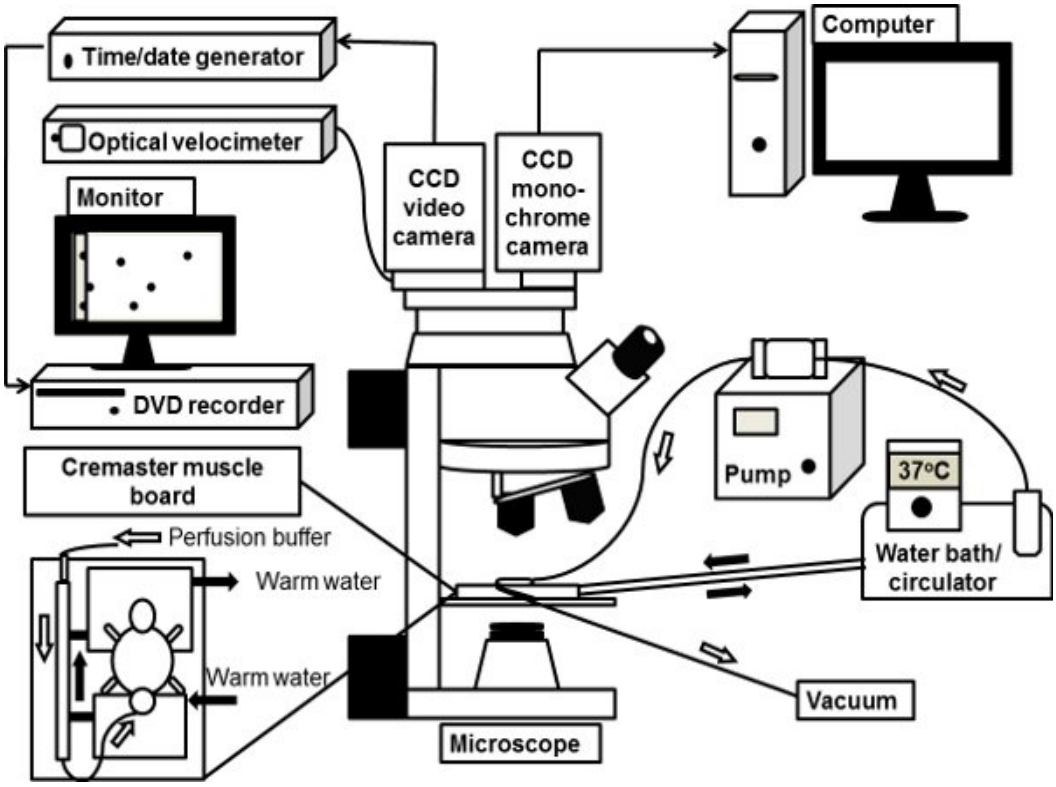

Figure 1-2. The schematic diagram of an intravital microscope system [114]. The mouse cremaster muscle is surgically exposed on an optically clear viewing pedestal, secured along the edges with 5-0 suture, and superfused with 37 ℃ bicarbonate buffered saline. A CCD color video camera is connected to the upright microscope for brightfield intravital microscopy. The leukocyte recruitment in cremaster muscle is recorded by a color video camera and stored by a DVD recorder. A monochrome deep-cooled CCD digital camera is also connected to the microscope for fluorescence intravital microscopy used in the vascular permeability assay. (Figure is adapted from Xu *et al.* J Vis Exp. 2011; (55): 3296.)

1.5 Methylglyoxal (MG)

1.5.1 The generation and metabolism of MG *in vivo*

1.5.1.1 Formation

MG is endogenously formed during glucose or fructose metabolism, protein catabolism and fatty acid oxidation. The primary source of MG is from the triosephosphate intermediates of glucose and fructose metabolism. In the first step of glycolysis, glucose is phosphorylated into glucose 6-phosphate by hexokinase, the latter is then enzymatically converted into fructose-6-phosphate which is further metabolized into fructose 1,6-bisphosphate. Fructose 1,6-bisphosphate can be cleaved by aldolase A to generate two triosephosphate intermediates glyceraldehyde 3-phosphate (GA3P) and dihydroxyacetone phosphate (DHAP), and from here they can either be part of glycolysis and generate pyruvate or be the precursor of MG [115, 116]. DHAP and GA3P can be readily inter-converted by triosephosphate isomerase. In pathological conditions, both of them can spontaneously and non-enzymatically be degraded into MG [115]. However, it was shown that in microorganisms, DHAP can be metabolized into MG by MG synthase. MG synthase was first purified from *E(scherichia) coli* in 1971 [117, 118]. Since then it has been found in other prokaryotic and in mammalian systems [115, 119]. However, the role of MG synthase in hyperglycemia and hyperglycemia-induced vascular injury has not yet been studied (Figure 1-3).

Under hyperglycemic condition, the overabundance of glucose influx saturates hexokinase and thus activates the polyol pathway (also known as aldose reductase pathway). In this pathway, glucose is converted into sorbitol by aldose reductase and then oxidised by sorbitol dehydrogenase to form fructose. Fructose can be quickly phosphorylated by fructokinase to fructose 1-phosphate and subsequently split by aldolase B into glyceraldehyde and DHAP. Considering the non-enzymatic formation of MG from DHAP, any pathways that increase DHAP formation are possibly linked to MG formation, such as the glycolysis pathway under physiological conditions, the polyol pathway under hyperglycemic conditions as well as excessive fructose intake from the diet [115, 120].

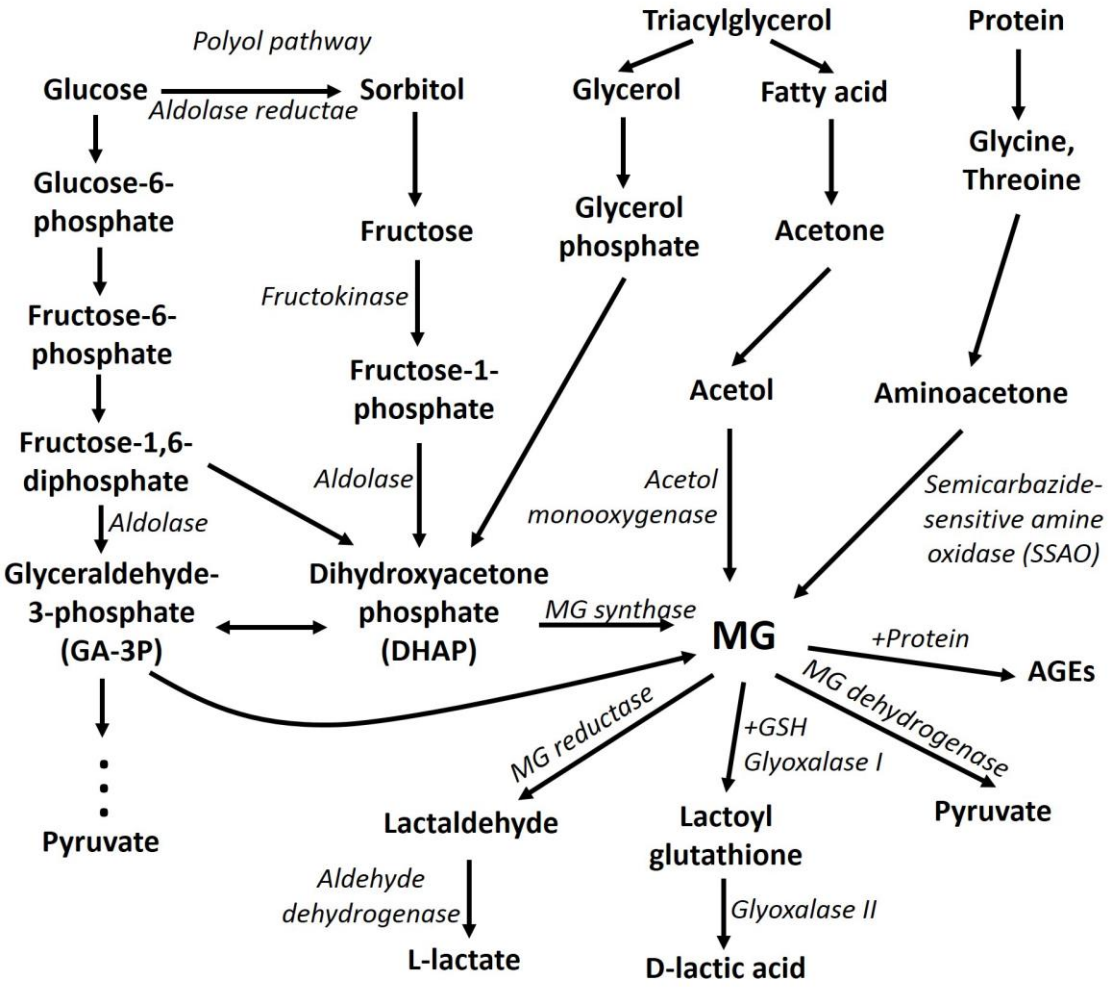

Figure 1-3. The formation and degradation of MG. Glyceraldehyde 3-phosphate (GA-3P) and dihydroxyacetone phosphate (DHAP) that produced through glycolysis or the polyol pathway are the main sources of MG formation. In addition, acetone from fatty acid oxidation and aminoacetone from protein catabolism also contribute to MG formation. The key enzymes are labelled in italics.

Besides the pathways mentioned above, proteins and fatty acids can also be the sources for MG formation. Acetone from fatty acid oxidation and aminoacetone from protein catabolism are important precursors of MG. The conversion of acetone into MG involves two consecutive catalytic steps which require the activity of enzymes belonging to cytochrome P450 2E1 gene

subfamily [121]. First, acetone is oxidized by acetone monooxygenase to generate acetol as an intermediate. Then acetol is converted into MG by acetol monooxygenase [115]. On the other hand, MG can also be produced from the catabolism of the amino acids threonine and glycine. Aminoacetone is an intermediate of threonine and glycine metabolism and is known as the substrate of amine oxidases. Semicarbazide-sensitive amine oxidase (SSAO), the enzyme catalyzes the deamination of aminoacetone into MG, exists in two forms: the tissue bound form in the plasmalemmal membrane and the soluble form in plasma, and both are capable of converting aminoacetone into MG. It was shown that SSAO is located in the outer membrane surface and in the cytoplasm of adipose tissue, vascular smooth muscle cells, and ECs, indicating its potential role in hyperglycemia-induced vascular damage [115, 122, 123].

1.5.1.2 Degradation

The degradation of MG involves MG reductase, glyoxalase and MG dehydrogenase, each leading to a distinct pathway of MG degradation (Figure 1-3) [115]. Among them, the glyoxalase system in the cytosol of all mammalian cells is the most common pathway for MG break-down. In the presence of glyoxalase I and its cofactor reduced glutathione (GSH), MG is firstly converted irreversibly to D-lactoylglutathione, and then to D-lactate by glyoxalase II. Thus, the degradation of MG is largely dependent on the presence of cellular GSH and the activities of GSH-related enzymes, such as glutathione peroxidase (GSH-Px) and glutathione reductase (GSH-red). It should be pointed out that excessive MG formation inhibits the activity of glutathione reductase and reduces the level of GSH, which further prevents MG degradation [124-126].

Besides the major degradation pathway, there are other pathways engaged in MG degradation. Since MG contains two functional groups that can be either reduced or oxidized, it is not surprising that the enzymes involved in oxidoreductions are able to convert MG. For example, MG reductase (also known as aldehyde reductase) located in cytosol is able to metabolise MG to lactaldehyde, which is then further converted to L-lactate with the help of aldehyde dehydrogenase. On the other hand, with NAD^+ as cofactor, MG can be converted into pyruvate by MG dehydrogenase (also known as α-ketoaldehyde dehydrogenase or 2-oxoaldehyde dehydrogenase) [116]. Although well studied in microorganisms, the functions of these two degradation pathways in mammals are still poorly understood.

The third way to eliminate MG brings more harm than good to our body. MG promotes the formation of advanced glycation end-products (AGE) which are highly associated in the progression of diabetes and diabetic complications [115, 116]. MG firstly reacts with proteins at lysine, arginine, or cysteine residues, and the subsequent irreversible reaction yields AGE. Irreversible formation of AGE on proteins changes their structures and disturbs their physicochemical and biochemical properties as well as their stability. Moreover, AGE bind to and activate the receptor for AGE (RAGE) on the cell surface, leading to either excessive generation of ROS through NADPH oxidase or the activation of multiple signalling pathways, such as p38 mitogen-activated protein kinases (MAPK) and c-jun N-terminal kinases (JNK) [127, 128]. By this way, MG causes damage to proteins, cells and the cardiovascular system.

1.5.2 The debate of MG dose

Despite the endogenous formation, there are multiple exogenous sources that bring MG into the body. The presence of MG was reported in rice, wheat and tobacco, so as a broad range of commercial foods and beverages, such as bread, coffee, honey, wine, and beer [129, 130]. Therefore, the important question is how much MG will put our body in danger. Unfortunately, the answer of this question is still largely debated. It is now commonly accepted that plasma MG levels in healthy humans is about 1 μmol/L or less, but is about 2—3 fold increased in type 2 diabetes patients and 5—6 fold increased in type 1 diabetes patients. This conclusion is mainly based on the observation by McLellan *et al.* in 1994 [131], which showed the plasma MG level was 79.8 pmol/g range 25.3 to 892.9 in healthy people (21 subjects), 470.7 pmol/g range 85.6 to 1044.3 in insulin-dependent patients (42 subjects) and 286.8 pmol/g range 54.7 to 2370 in non-insulin-dependent patients (105 subjects). The following study by Lapolla *et al.* showed that in healthy individuals the plasma MG level was about 8.5 ± 0.5 μg/mL, whereas in diabetes patients it was increased to 29.3 ± 5.5 μg/mL [132]. Another study conducted by Wang *et al.* reported that the plasma MG levels in type 2 diabetes patients was 77% higher than those in non-diabetic subjects (5.9 ± 0.7 μM versus 3.3 ± 0.4 μM) [112]. Despite the differences in the unit of measurements in the above studies, the fold increase of MG in diabetes patients versus control subjects seems consistent. However, Beisswenger and colleagues reported that plasma MG levels

in control subjects were 123.0 ± 37.0 nM, and in diabetic subjects 189.3 ± 38.7 nM [133], which is about 30 times lower than Wang's observation. The inconsistent MG values measured by different research groups complicates the research. Actually, the MG levels claimed by different research groups using *in vitro* or *in vivo* diabetic models have even greater differences.

Regardless of the debate over MG measurement, it is widely accepted that the plasma MG level is significantly increased in diabetes patients [131]. Based on this, exogenous MG was added to cultured cell or given to animals to study the role of MG in the development of diabetes. However, the dose of MG used in these studies are also largely debated. Dhar *et al.* reported that in Sprague-Dawley rats, 60 mg/kg/day and 28 days of chronic methylglyoxal infusion by minipump was required to increase the plasma MG level by about 2 fold, and with this dose the rat showed impaired glucose tolerance, apoptosis in pancreatic islets and reduced pancreatic insulin content [134]. This finding suggests that it requires large dose of exogenous MG to establish a diabetic animal model and reach the similar plasma MG level as in diabetic patient. In patients, the progression of diabetes takes several years, and during this process MG is not the only factor that causes damage to the cells and tissues. Therefore, it is reasonable and acceptable to use a high MG dose (sometimes even higher than pathological conditions) to establish the *in vitro* or *in vivo* model, especially in a short-term study. On the other side, the data regarding MG levels in the tissue in diabetes patients are still missing. Judging from high fructose diet-induced diabetic animal model, it is likely that MG tends to accumulate in certain tissues [135]. Randell *et al.* showed that in normal Sprague-Dawley rats, the MG level was highest in aorta followed by heart, liver, kidney and blood [136]. This result indicates that MG concentration in local tissue might be much higher than it is in the plasma. Taken together, in the studies using exogenous MG to induce diabetes-related syndromes, especially in the short-term studies, the given dose of MG should not be judged only by the plasma MG level in diabetes patients.

1.5.3 MG and insulin resistance

Insulin resistance is commonly observed in conditions like diabetes and obesity [86]. Chronic hyperglycemia-induced insulin resistance is the primary etiological causes of diabetes and diabetic complications [137]. In the physiological condition, binding of insulin to its receptor induces the

autophosphorylation of tyrosine residues present in the intracellular portion of insulin receptor. Insulin receptor activation then results in the phosphorylation of tyrosine residues on the insulin receptor substrate (IRS), which will be further recognised by p85 regulatory subunit of PI3K. The activation of PI3K leads to the formation of PIP3. Being a key downstream effector of PIP3, Akt is attracted to the plasma membrane, where it is phosphorylated hence activated by phosphoinositide-dependent kinase-1 (PDK1). Once activated, Akt enters the cytoplasm to phosphorylate and inactivate glycogen synthase kinase 3 (GSK3). Glycogen synthase (GS) which catalyses the final step of glycogen synthesis is the downstream target of GSK3. GSK3 negatively regulates GS activity by phosphorylating GS on the serine residue. Therefore, the inactivation of GSK3 by Akt activates GS and promotes glucose storage as glycogen [138].

However, under pathological conditions, the insulin pathway is blocked due to hyperglycemia. Both *in vivo* and *in vitro* evidence showed that the formation of MG may be responsible for this change [139, 140]. It was shown that MG inhibits insulin stimulated phosphorylation of Akt in cultured L6 muscle cells [140]. In cultured 3T3 adipocytes, MG significantly reduced PI3K activity and tyrosine phosphorylation of IRS-1, the effects that were reversed by N-acetyl cysteine (NAC), an MG scavenger [141]. It was also demonstrated that the incubation of MG with human insulin *in vitro* produced MG-insulin adducts which led to impaired autocrine control of insulin release from pancreatic β-cells, reduced insulin-mediated glucose uptake by the target cells, and decreased hepatic clearance of insulin in liver [142]. In the *in vivo* study, Dhar *et al.* showed that chronic MG infusion by minipump caused elevated fasting plasma glucose and reduced insulin in the rat. The impaired glucose tolerance, together with decreased insulin-stimulated glucose uptake in adipose tissue, as well as reduced GLUT4 level and PI3K activity were also observed. This study provides the direct evidence that MG itself is able to induce pancreatic β-cell dysfunction and type 2 diabetes [134]. All of the above evidence supports the critical role of MG in the impaired insulin-stimulated glucose uptake.

1.5.4 MG and oxidative stress

1.5.4.1 Association of MG formation and ROS generation

Oxidative stress is one of the important factors in causing diabetes and diabetes-related diseases [115]. Hyperactivities of xanthine oxidase, NADPH oxidase and mitochondrial dysfunction, which all cause excessive ROS production, are observed in pathological conditions such as aging, hypertension and diabetes [115, 143]. Under the hyperglycemic conditions, with the activation of enzymes in the polyol pathway, glucose is first converted into sorbitol, and then into fructose (reviewed in 1.5.1). The conversion of sorbitol into fructose consumes NADPH which is an important reducing agent for maintaining redox balance in the cells [144]. Thus, paralleled with MG generation, the over activation of the polyol pathway also increases oxidative stress. Likewise, fructose metabolism promotes oxidative stress as well. Unlike glycolysis, fructolysis doesn't have a negative feedback mechanism, which means all the ingested fructose will be metabolized without any storage. The first step of fructolysis, which converts fructose into fructose-1-phosphate, consumes adenosine triphosphate (ATP) and generates adenosine diphosphate (ADP). Therefore, the overload of fructose will lead to ADP accumulation. With the catalyzing of multi-enzymes, ADP will be metabolised into adenosine monophosphate (AMP), inosine monophosphate (IMP), hypoxanthine, xanthine and finally uric acid. The last step of this reaction requires the activity of xanthine oxidase and produces superoxide as the by-product [145-147]. Therefore, fructose overload can eventually lead to increased oxidative stress. It is evident that excessive fructose intake for 2 weeks leads to insulin resistance and hypertension in rats, the process of which is highly related to increased oxidative stress [148].

1.5.4.2 MG induces ROS formation

MG-induced ROS formation has been shown in many types of cells. In vascular smooth muscle cells (VSMCs), both cell line cells and primary cultured cells from rat mesenteric artery showed that incubation with MG increased total ROS in a time- and concentration-dependent manner [31, 149]. The induction of oxidative stress by MG has been also reported in Jurkat T leukemia cells and cultured rat hepatocytes [150, 151]. Moreover, the *in vivo* study using spontaneously hypertensive rats showed that, the level of MG in VSMCs from hypertensive rats were more than 2-fold higher than in VSMCs from normotensive Wistar-Kyoto rats [126]. Accordingly,

exogenous MG induced a greater increase in oxidative stress in VSMCs from hypertensive rats compared with normotensive rats [126]. These findings support the link between increased MG levels and elevated ROS formation in either *in vitro* cell models or *in vivo* animal models. Our own observation in the hybrid human umbilical vein EC line cells also showed that MG induced a dose- and time-dependent increase of superoxide and total ROS [152]. The *in vivo* permeability assay showed that MG induces hyperpermeability in postcapillary venules, an effect that can be blocked by ROS scavengers [153]. These results suggest that MG induces ROS formation which may be related to the progression of vascular disease.

1.5.4.3 The mechanism of MG-induced oxidative stress

1.5.4.3.1 MG-induced mitochondrial superoxide generation

The mitochondrial respiratory chain uses glucose to generate ATP via oxidative phosphorylation. During mitochondrial respiration, electrons from donors pass through the complexes I–IV of the respiration chain. The dysfunction or disruption of the mitochondrial respiratory chain contributes to ROS formation due to the leakage of electrons to oxygen [154]. There are two main sites of electron leakage, complex I (NADH-ubiquinone oxidoreductase) and complex III (ubiquinol-cytochrome c reductase) of the electron transport chain [154]. In diabetes, with the excessive glucose supplementation, it has been speculated that excess production of ROS could change the mitochondrial membrane potential, thus decreases ATP synthesis, leading to energy depletion [155, 156]. The role of MG in inducing mitochondrial superoxide generation has been widely reported. It has been shown that MG is able to inhibit mitochondrial complex activities and to increase mitochondrial superoxide generation [157]. In isolated rat renal mitochondria, MG incubation dose-dependently reduced the mitochondrial respiration rate [158]. In VSMCs, MG specifically inhibited complex III activity and increased mitochondrial superoxide generation, the effect possibly due to MG-induced AGE formation [157]. In osteoblastic MC3T3-E1 cells, MG decreased osteoblast differentiation and caused osteoblast cytotoxicity by inducing oxidative stress and mitochondrial dysfunction [159]. A similar phenomenon was also observed in neuroblastoma cell line cells [160].

1.5.4.3.2 MG-induced NADPH oxidase activation

MG-induced NADPH oxidase activation was first studied in rat kidney mesangial cells. It was shown that the superoxide production in mesangial cells was rapidly elevated after 2-h incubation with MG, and stayed at a high level for 24 h [161]. This effect was significantly reduced by an NADPH-oxidase inhibitor pretreatment, suggesting NADPH oxidase is responsible for the formation of superoxide and may be subsequently responsible for renal fibrosis under diabetic conditions [161]. The study in VSMCs similarly showed that MG-induced superoxide production was suppressed by NADPH-oxidase inhibitor diphenylene iodonium (DPI) [31]. In parallel with the decreased NADPH-oxidase activity, MG-induced VSMCs proliferation was also inhibited [115]. In both human umbilical vein ECs and rat aortic ECs, MG-induced superoxide production was blocked by another NADPH oxidase inhibitor, apocynin (Apo) [70]. Accordingly, MG-induced endothelial dysfunction was also partially restored [70]. Despite enormous evidence shown in *in vitro* and *in vivo* studies, the mechanism of MG-induced NADPH oxidase activation is not fully understood. It was shown that MG-induced AGE formation and the binding of AGE to its receptor RAGE may activate NADPH oxidases and promote the generation of ROS [162]. It is clear that MG-induced NADPH-oxidase activation plays an important role in the development of diabetic vascular complications.

1.5.4.3.3 MG-induced peroxynitrite formation

Peroxynitrite is a strong endogenous oxidation and nitration agent which damages a wide number of molecules, including DNA and proteins [163]. In patients, nitrosylated proteins is considered as a biomarker of peroxynitrite-related stress in diabetic patients with macroangiopathy [164]. In *in vitro* studies, peroxynitrite-mediated oxidative stress were observed from high glucose-treated retinal ECs [165]. Furthermore, peroxynitrite has been shown to induce vascular permeability increases in the retinal microvasculature [165]. The formation of peroxynitrite was also related to retinal ischemia/reperfusion injury [166]. Observations in human aortic ECs confirmed that high glucose induces tyrosine nitration via peroxynitrite formation, which leads to functional changes of enzymes as well as apoptosis [167]. In streptozotocin-induced diabetic mice and leptin deficient ob/ob mice, peroxynitrite decomposition improves neuronal functions and counteracts peripheral neuropathy [168-170].

Formation of peroxynitrite *in vivo* is mainly through the spontaneous reaction of nitric oxide (NO) and superoxide. In MG-treated cells, MG-induced NADPH oxidase activation provides large amount of superoxide, and NO can be produced either by endothelial nitric oxide synthase (eNOS) or inducible nitric oxide synthase (iNOS) depending on the different cell types [31, 115]. In ECs, eNOS is the dominant form of NOS, whereas iNOS is primarily expressed in VSMCs or macrophages upon stimulation [171]. Both *in vitro* and *in vivo* studies showed that in VSMCs, iNOS expression and NO were increased and associated with increased MG level, suggesting the role of MG in stimulating NO production [124, 172]. In ECs, eNOS is constitutively expressed, thus peroxynitrite is produced upon the activation of eNOS and the generation of superoxide [171]. However, unlike VSMCs, research data also showed that the expression of eNOS and bioavailability of NO were actually decreased with the elevated MG concentration [70]. In our own study, we found that the expression of 3-nitrotyrosine, which indicates the level of protein nitration thus reflecting the level of peroxynitrite, was increased in MG-treated ECs, indicating increased peroxynitrite formation even with decreased NO levels [70, 152]. Despite the differential role of MG in regulating NOS activity in ECs and VSMCs, the bioavailability of NO was decreased in both types of cells [31, 70]. In VSMCs, the formation of peroxynitrite was shown to be one of the reasons of MG-induced NO depletion, while in ECs both peroxynitrite formation and eNOS inhibition were involved [31, 70, 152].

1.5.4.3.4 MG-induced depression of antioxidant systems

MG increases intracellular oxidative stress levels by supressing antioxidative defense systems and reducing cellular antioxidant levels. Superoxide dismutase (SOD), glutathione peroxidase (GSH-Px), glutathione reductase (GSH-red), catalase, and glutathione (GSH) are usually the targets of MG [173, 174]. Under physiological condition, the superoxide produced in cells is dismutated by SOD into hydrogen peroxide (H_2O_2) [175]. H_2O_2 is decomposed by catalase or glutathione peroxidase into water [176]. In the glutathione peroxidase pathway, the decomposition of H_2O_2 requires the abundance of GSH [115]. With the catalyzing of GSH-Px, H_2O_2 and GSH are converted into water and glutathione disulfide (GSSG). The GSH-red then converts GSSG back into GSH, thus recycles GSSG to GSH [177]. It was reported that the activities of the purified SOD, GSH-Px and GSH-red were inhibited after incubation with MG in test tubes [173, 174]. In

VSMCs and ECs, the activities of SOD, GSH-Px, GSH-red and the levels of GSH were both significantly decreased upon incubation with MG [134, 157]. The *in vivo* studies showed that MG administration decreased SOD and catalase activities in the mouse liver [178]. In rats, chronic MG infusion by minipump also significantly reduced GSH levels in the plasma, skeletal muscle, and pancreas [134]. It was found that AGE formation is involved in MG-induced depression of the cellular antioxidant systems. Evidence showed that AGE formation directly impairs the functions of SOD and GSH-Px, while alagebrium, an AGE breaker, partially reduced MG-increased superoxide generation in VSMCs [157, 174]. Although the mechanism is not fully understood, it is clear that MG suppresses the activity of cellular antioxidant systems and thus further increases the oxidative stress.

1.5.5 MG and AGE formation

Spontaneous formation of AGE at lysine, arginine, or cysteine residues of proteins changes protein structures, and disturbs their physicochemical and biochemical properties as well as their stability [28, 29, 179]. Increased AGE formation in the blood and tissues occurs with aging. However, it is excessively increased during hyperglycemia and in diabetes [115, 124]. In Type 1 diabetes patients, levels of AGE in kidney and the retina were correlated with the development of nephropathy and retinopathy [180]. Studies in patients with type 2 diabetes showed that the increased AGE level in blood was correlated with decreased endothelium-dependent vasodilation, the thickness of intima-media of blood vessels, vascular stiffness, and increased systolic blood pressure [181, 182]. In diabetic rats, increased renal AGE level causes glomerular basement membrane thickening, the morphological change associated with diabetic nephropathy [183]. The increased retina AGE level is related to abnormal EC proliferation, the pathological change that is also associated with diabetic retinopathy [184]. Based on the enormous evidence found in patients and in animal models, increased AGE level is considered as the leading cause of vascular complications in diabetes.

MG has an essential role in AGE formation. It produces various types of AGE by reacting with lysine, arginine, or cysteine residues in proteins [185]. For example, its reaction with arginine residue produces 5-hydro-5-methylimidazolone (MG-H1) and argpyrimidine, the reaction with lysine residue generates N(ε)-carboxyethyl-lysine (CEL), methylglyoxal-derived lysine dimer

(MOLD), and the reaction with cysteine residue forms carboxyethyl cysteine (CEC) [28, 29, 179]. The *in vitro* studies showed that incubating purified human insulin with MG at 37 ℃ for 24-72 h modifies insulin at the arginine residue of the β chain, while its incubation with purified Akt1 leads to the modification of Akt1 at the cysteine residue [142, 186]. On the other hand, the experiments using MG inhibitor also showed decreased AGE level associated with suppressed MG level. Alagebrium, an AGE breaker, was shown to have the ability to scavenge MG [187]. In VSMCs, the application of alagebrium completely prevented MG-induced AGE formation [134, 187]. Another MG inhibitor, aminoguanidine (also known as pimagedine), also inhibited AGE formation by directly reacting with MG and significantly reduceding cellular MG levels in high glucose- or MG-treated ECs [70]. Metformin, an oral hypoglycemic drug which also reacts with MG to generate stable triazepinone derivatives, reduced AGE formation in the lens, kidney and nerves in diabetic rats [188]. It is believed that the application of MG inhibitors which react with MG to form stable adducts reduces the chances of MG to react with proteins, thus reduces MG-induced AGE formation and cytotoxicity. These findings further support the role of MG in AGE formation.

1.5.6 MG-activated and MG-related signalling pathways

1.5.6.1 MAPKs pathway

The mitogen activated protein kinases (MAPKs), which are responsible for various cellular activities downstream of cell membrane receptors, comprise mainly three members: extracellular signal regulated kinases (ERKs), p38 MAPKs and c-Jun N-terminal kinases (JNKs) [189]. Among them, p38 MAPKs and JNK are shown to be associated with the progression of diabetes [190-192]. Recent evidence suggests that due to its influences on vascular smooth muscle cells, vascular ECs, and monocytes/macrophages, p38 MAPKs may be the key linking endothelial dysfunction, insulin resistance, and the pathogenesis of type 2 diseases [191]. Consistently, inhibition of JNK using a cell-permeable peptide restores insulin sensitivity in mice, while genetic disruption of the JNK gene inhibits the progression of insulin resistance in diabetic and obese mice [192].

The role of MG in activating MAPK pathway has been shown in many cell types. In mouse fibroblast cell line and human embryonic kidney cell line, MG treatment was demonstrated to induce the activation of ERKs [193, 194], an important signalling of cell proliferation [195]. In

Jurkat leukemia T cells, MG induces apoptosis by activating JNK [196]. In human ECs, MG mediates JNK- and p38-dependent inflammatory responses such as the over expression of cyclooxygenase-2 (COX2) [197]. In immune cells such as neutrophils and monocytes, the activation of MAPK pathway results in cell adhesion, chemotaxis, oxidative burst and degranulation [198-201]. The activation of immune cells is suggested to be important in producing chronic low-degree inflammation in the macro- and micro-vasculature. However, under hyperglycemic conditions, whether MG induces immune cells activation via MAPK pathway is still unclear.

1.5.6.2 PKC pathway

Protein kinase C (PKC) is a family of protein kinase enzymes that are involved in regulating the functions of other proteins by phosphorylating the downstream proteins on their serine and threonine residues. The PKC family consists of fifteen isozymes in humans. It can be activated by calcium ion (Ca^{2+}), diacylglycerol (DAG), or phospholipid such as phosphatidylserine [202, 203]. Under hyperglycemic conditions, the synthesis of DAG is increased due to the over production of dihydroxyacetone phosphate (DHAP), an intermediate product of glycolysis [204]. Thus, it is not surprising that the activation of PKC was observed in high glucose-treated VSMCs and ECs [205, 206]. The downstream events of PKC activation include NADPH oxidase activation, NF-κB activation, TGF-β1, fibronectin and collagen expression, and eNOS inhibition [206-209]. The consequence of PKC activation includes basement membrane thickening, vasoconstriction and chronic inflammation in the vasculature [210].

It is known that MG induces PKC activation via AGE formation. Inhibition of AGE decreased PKC activation in cultured VSMCs and in the kidney of STZ-diabetic rats [211]. In addition, Hadas *et al.* reported that MG-induced accelerated thrombus formation and decreased thrombus stability is PKC dependent [212]. At the molecular level, MG activates the PKC pathway by increasing intracellular Ca^{2+} levels [213]. However, how MG increases intracellular Ca^{2+} level is still a mystery.

1.5.6.3 AGE-RAGE pathway

The receptor-dependent effects of AGE are mediated via the binding with RAGE. The AGE-RAGE interactions trigger the activation of a series of downstream pathways such as PKC, MAPK and NF-κB [214, 215]. The promoter region of RAGE contains the binding sequence of NF-κB, thus one of the consequences of NF-κB activation is RAGE up-regulation [216, 217]. Soluble RAGE (also known as sRAGE) is an isoform of the RAGE protein without the transmembrane and the signalling domain. It binds to AGE, but does not activate downstream signalling pathways as a full-length receptor [218]. It was shown that administration of sRAGE inhibited vascular hyperpermeability in the intestine, skin, and kidney of diabetic rats, and also suppressed hyperglycemia-induced atherosclerosis in the diabetic mouse model [219]. Besides, the interaction between RAGE and its ligands is involved in pro-inflammatory gene activation. In ECs, AGE-induced VCAM-1 expression and Molt-4 cells (a human T lymphoblast cell line) adhesion were inhibited by sRAGE administration, indicating the role of AGE-RAGE pathway in vascular inflammation [220].

It is well established that MG treatment induces the formation of AGE and up-regulates the expression of RAGE, but the mechanism of RAGE up-regulation is still unknown. Since the activation of NF-κB also up-regulates RAGE expression [221], it is reasonable to infer that the expression of RAGE and activation of NF-κB may establish a vicious circle and amplify the inflammation signal in the cells.

1.5.6.4 GSK3 pathway

It was reported that many chronic inflammation-related diseases such as Alzheimer's disease, diabetes, and cancer are associated with GSK3 activity [222]. In diabetes, GSK3 regulates glucose homeostasis via insulin-activated PI3K/Akt/GSK3 pathway (reviewed in 1.5.3). In addition, GSK3 also plays a proinflammatory role through the activation of NF-kB [223], and thus, lies at the mechanistic interface of both diabetes and inflammation. It was shown that type 2 diabetes patient have approximately 2 times higher GSK3 activity than those without diabetes in their biopsy skeletal muscle samples [224]. Accordingly, the inhibition of GSK3 showed promising therapeutic effects. GSK3 inhibitors dose-dependently lowered the plasma glucose levels in diabetic animal

models [225-229]. For example, a GSK3 peptide inhibitor is shown to be effective in improving glucose tolerance in insulin-resistant obese C57BL/6 mice [230], suggesting the suppression of GSK3 improves glucose regulation. Consistently, GSK3 overexpression is shown to be related to glucose intolerance [231]. Based on the findings above, the inhibition of GSK3 has become a promising therapeutic target in diabetes.

Despite the potential role of GSK3 in the development of diabetes, the effects of MG on GSK3 activity are barely understood. MG-induced activation of GSK3 was previously reported in pancreatic β cells [232]. Similarly, MG was shown to foster Tau protein hyperphosphorylation by activating GSK3 in neuroblastoma 2a cells [233]. However, in VSMC, MG was shown to activate Akt, the upstream negative regulator of GSK3, thus inhibiting the activity of GSK3 by increasing the inhibitory phosphorylation on serine residue [186]. In ECs, MG was shown to have no effect on Akt, while the downstream GSK3 activity was not known [70]. These results suggest that the effect of MG on GSK3 could be cell-specific. Given the proinflammatory effect of GSK3, it is worthy to study the role of GSK3 in both ECs and leukocytes in the context of MG-induced diabetic vascular inflammation.

1.5.6.5 SGK1 pathway

Being another signalling molecule involved in both diabetes and inflammation, SGK1 was reported to have dual effect in the pathophysiology of diabetes. It assists the development of obesity, which increases the risk for the development of type 2 diabetes. On the other hand, the expression of SGK1 itself is also upregulated by hyperglycemia, and shown to be involved in the progression of hypertension, fibrosis and excessive coagulation in diabetes patients [234]. SGK1 promotes the progression of obesity at least partly by accelerating the intestinal uptake of glucose through Na^+-coupled glucose transporter 1 (SGLT1) upregulation [235]. Given the upregulation of SGK1 by hyperglycemia, the increased plasma glucose levels may, at least in theory, cause intestinal SGK1 overexpression, which further enhances SGK1-dependent SGLT1 expression, thus establishes a vicious cycle that maintains obesity [234]. Additionally, SGK1 was shown to affect helper T-cell function [236], macrophage polarization [237] and regulation of neutrophil apoptosis [238] alluding to its role in immunity. Beyond the regulation of EC survival, migration and vascular remodelling [239, 240], the functions of endothelial-expressed SGK1 are not

completely understood. Noticeably, SGK1 was shown to foster the activation of NF-κB [241] and cyclic AMP response element-binding protein (CREB) [242], two transcription factors that are important in inflammatory responses. However, the role of MG on SGK1 activity has never been shown before. Similar to GSK3, the proinflammatory and pro-diabetic effects of SGK1 suggest that it can be involved in MG-induced diabetic vascular inflammation, although more evidence is needed.

1.5.6.6 NF-κB pathway

NF-κB, a heterodimeric complex consisting of p50 and p65, exists in the cytoplasm in an inactive form when binding with the inhibitory protein κB (IκB). The activation of NF-κB starts with the activation of IκB kinase (IKK). Activated IKK phosphorylates IκB, leading to the ubiquitination and degradation of IκB. The exposed p65 and p50 heterodimeric complex is translocated into the nucleus where it binds to specific sequences of DNA and initiates the downstream gene transcription. The activation of NF-κB has been found to be important in many pathological processes such as the development of inflammation, cancer, neurodegeneration disease and diabetes. A large number of genes that are involved in the immune response, inflammation, apoptosis, cell proliferation and differentiation are proven to be regulated by NF-κB pathway [243-245].

In diabetic animal model, the activation of NF-κB was observed in different vascular tissues associated with increased MG levels. In VSMCs and ECs, high glucose-induced NF-κB activation results in VSMCs proliferation and EC dysfunction via the expression of growth factors (such as VEGF) and proinflammatory cytokines (such as TNF-α and IL-1β) [246, 247]. Studies using exogenous MG showed that MG directly activates NF-κB in cultured VSMCs and retinal capillary pericytes [126, 248]. These findings indicate that MG formation may be the reason for high glucose-induced NF-κB activation. It is believed that MG induces NF-κB activation mainly through ROS or AGE formation [126, 221]. Blockade of ROS or AGE partially inhibits MG-induced NF-κB activation and its downstream gene expression [75, 249].

It is well known that NF-κB plays a central role in the development of inflammation by upregulating the expression of pro-inflammatory cytokines, adhesion molecules such as P-selectin,

E-selectin, ICAM-1 and VCAM-1, as well as other pro-inflammatory molecules such as COX2 and iNOS [250]. These changes are considered to be involved in the progression of vascular inflammation in diabetes. Wang *et al*. reported that the neutrophils from T2DM patients presented a greater tendency for apoptosis, and MG-induced cytokine release may be responsible for this phenomenon [112]. Our own study revealed that MG induces endothelial adhesion molecule expression via the activation of NF-κB, and this effect promotes leukocyte recruitment in microvasculature [75]. Therefore, MG-induced NF-κB activation may play an important role in the progression of vascular inflammation in diabetes.

1.5.7 MG and leukocyte recruitment

Elevated MG levels and increased leukocyte recruitment are both involved in the progression of diabetic vascular complications [28, 109]. Accumulating data from clinical and experimental studies suggest that increased formation of MG is linked to the development of diabetic vascular complications as well as the dysfunctions of various cells including ECs, vascular smooth muscle cells and neutrophils [31, 251, 252]. However, the role of MG in inducing leukocyte recruitment is a whole new research area. Increased recruitment but impaired functions of leukocytes during inflammation were observed in mouse models of type 1 and type 2 diabetes [253], but whether it is related to MG formation is not clear. Our own observation showed that exogenous MG is able to induce leukocyte recruitment in mouse cremasteric microvasculature, indicating that MG-induced leukocyte recruitment may be one of the mechanisms underlying hyperglycemia-induced vascular inflammation in diabetes [75]. Using intravital microscopy, immunohistochemistry and biochemical analysis, we are able to determine the types of leukocytes that are recruited by exogenous MG, the molecules that are upregulated in leukocytes and ECs, and the signalling pathways that are activated in leukocytes and ECs. Revealing the mechanisms of MG-induced inflammation may unveil the mystery of vascular complications and immune dysfunctions in diabetes and may provide a new clue for possible therapeutic strategies for diabetes.

CHAPTER 2

HYPOTHESIS AND OBJECTIVES

2.1 Rationale and hypothesis

In the past decades, increased production of MG has been observed in both diabetes patients and diabetic animal models [112, 131]. In blood vessels, the abnormal elevation of MG increases oxidative stress, promotes AGE formation and activates cellular signalling pathways [31, 124, 254] leading to endothelial dysfunction and vascular inflammation [255]. Being the first responders of inflammation, leukocytes are recruited at the site of inflammation. However, under pathological conditions, hyperglycemia-induced interactions between leukocytes and ECs are believed to bring more damage than cure to the microvasculature [109, 112, 113]. Despite the critical role of leukocyte recruitment in the development of diabetic vascular inflammation, the mechanism of hyperglycemia-induced leukocyte recruitment is poorly understood. It is not clear whether and how MG is involved in this process. However, given the reported role of MG in inducing endothelial dysfunction [70], we speculate that the increase of MG levels is likely to play a critical role in inducing leukocyte recruitment in the microvasculature. The study of MG-induced leukocyte recruitment will not only help us to understand the pathogenesis of diabetic vascular inflammation, but may also reveal the potential therapeutic target for the treatment of disease.

Hypotheses: MG-regulated GSK3/SGK1 signalling and eNOS uncoupling are responsible for the upregulation of endothelial adhesion molecules which promote leukocyte-EC interaction and leukocyte recruitment in the microvasculature.

2.2 Objectives and experimental approaches

To investigate whether exogenous MG administration induces leukocyte recruitment in cremasteric microvasculature

Although both elevated MG levels and increased leukocyte recruitment are shown to be involved in the development of diabetic vascular inflammation, whether MG induces leukocyte recruitment has never been studied. Our aim is to determine the effect of MG in inducing leukocyte recruitment, and establish an acute MG treatment model for further mechanistic studies. Using intravital microscopy, the leukocyte rolling velocity, rolling flux, adhesion, and emigration after MG treatment will be determined. Based on these results, an optimal MG dose will be established. Additionally, immunohistochemistry will be used to identify the subtypes of recruited leukocytes

in the cremasteric microvasculature, the result of which will demonstrate the nature of MG-induced vascular inflammation.

To investigate the role of endothelial adhesion molecules in MG-induced leukocyte recruitment

Leukocyte recruitment is a well-defined cascade of cellular events, and many of the steps require the presence and functions of endothelial adhesion molecules. Additionally, the overexpression of adhesion molecules is important in the early stage of diabetic vascular complications [256]. The aim here is to demonstrate the role of endothelial adhesion molecules in MG-induced leukocyte recruitment. Using intravital microscopy combined with functional blocking antibodies, we are able to functionally block P-selectin, E-selectin and ICAM-1, respectively, and observe the changes in recruitment parameters. This study will demonstrate the importance of endothelial adhesion molecules in MG-induced leukocyte recruitment, and reveal the role of P-selectin, E-selectin and ICAM-1 in this process.

To investigate the signalling pathways involved in MG-induced upregulation of endothelial adhesion molecules

The expression of adhesion molecules is regulated by the activity of transcriptional factors [250]. However, the signalling mechanisms involved in MG-induced endothelial adhesion molecule upregulation is not clear. Using enzyme-linked immunosorbent assay (ELISA), Western blotting combined with pharmacological inhibition and gene silencing, we will determine the role of transcriptional factors NF-κB and CREB in MG-induced adhesion molecule upregulation in *in vitro* and *in vivo* models. Additionally, GSK3 and SGK1, the upstream signalling molecules of NF-κB, are reportedly positioning at the mechanistic interface of both diabetes and inflammation [223, 234, 241]. Using cultured EC line cells, we will investigate whether GSK3 and SGK1 are activated upon MG administration. The specific inhibitors of these signalling pathways will be used to reveal the role of GSK3 and SGK1 signalling in MG-induced leukocyte recruitment. The *in vitro* kinetics study of MG-induced GSK3 and SGK1 activation in ECs and the *in vivo* study of MG-induced leukocyte recruitment upon the administration of GSK3 or SGK1 inhibitors will reveal the network of these signalling pathways and their importance in MG-induced leukocyte recruitment.

To investigate the role of eNOS uncoupling in MG-induced leukocyte recruitment

A growing body of evidence suggests that MG decreases NO availability in ECs, and this effect plays an important role in endothelial dysfunction and diabetic vascular inflammation [70, 115]. The mechanistic studies showed that the reduced NO availability is possibly due to MG-induced inhibition of eNOS and the formation of peroxynitrite [31, 70]. Recently, the observation of eNOS uncoupling, which shifts the functions of eNOS from producing NO to superoxide in diabetic and aging animal models, provides a novel insight into the mechanism of reduced NO availability in ECs [257-259]. Therefore, the aim of this part of my study is to determine whether MG is able to induce eNOS uncoupling in ECs and to reveal the role of eNOS uncoupling in MG-induced leukocyte recruitment. Using non-reducing SDS-PAGE and Western blotting, I will determine whether MG induces eNOS uncoupling in cultured EC line cells. The levels of tetrahydrobiopterin (BH4), 3-nitrotyrosine (3NT) and guanosine triphosphate cyclohydrolase I (GTPCH1) will also be determined to reveal the mechanisms of MG-induced eNOS uncoupling. Intravital microscopy together with specific inhibitors will be used to study the role of eNOS uncoupling in MG-induced leukocyte recruitment.

CHAPTER 3

THE ROLE OF ENDOTHELIAL CELL ADHESION MOLECULES P-SELECTIN, E-SELECTIN AND ICAM-1 IN LEUKOCYTE RECRUITMENT INDUCED BY EXOGENOUS METHYLGLYOXAL

As the first approach of this project, we demonstrated that exogenous MG-elicited leukocyte recruitment in mouse cremasteric microvasculature is largely dependent on the expression of adhesion molecules on endothelium. The study shown in this chapter aimed at the role of MG-induced adhesion molecules expression as the research interest, and our results also provides the foundation for pursuing the mechanism underlying MG-induced adhesion molecules in the following chapter.

This chapter has been published as a research paper by Yang Su, Xi Lei, Lingyun Wu, Lixin Liu in *Immunology* 2012 Sep; 137(1):65-79. Contents of this chapter have been adapted/reproduced from the published article with permission from the journal *Immunology*. In this paper Y.S. conducted all the experiments, acquired and analyzed all the data, and also participated in the design of the study and manuscript writing.

3.1 Abstract

Methylglyoxal (MG) is a reactive dicarbonyl metabolite formed during glucose, protein and fatty acid metabolism. In hyperglycemic conditionss, increased MG level has been linked to the development of diabetes and its vascular complications at the macro- and micro-vascular levels where inflammation plays a role. To study the mechanism of MG-induced inflammation *in vivo*, we applied MG locally to healthy mice and used intravital microscopy to investigate the role of EC adhesion molecules in MG-induced leukocyte recruitment in cremasteric microvasculature. Administration of MG (25 and 50 mg/kg) to the tissue dose-dependently induced leukocyte recruitment at 4.0—5.5 h, with 84—92% recruited cells being neutrophils. Such MG treatment upregulated the expression of EC adhesion molecules P-selectin, E-selectin, ICAM-1, but not VCAM-1. The activation of NF-κB signalling pathway contributed to MG-induced upregulation of these adhesion molecules and leukocyte recruitment. The role of the upregulated EC adhesion molecules in MG-induced leukocyte recruitment was determined by applying specific functional blocking antibodies to MG-treated animals and observing changes in leukocyte recruitment parameters. Our data demonstrate that the upregulation of P-selectin, E-selectin and ICAM-1 contributes to the increased leukocyte rolling flux, reduced leukocyte rolling velocity, and increased leukocyte adhesion, respectively. Our results reveal the role of EC adhesion molecules in MG-induced leukocyte recruitment in microvasculature, an inflammatory condition related to diabetic vascular complications.

3.2 Introduction

Vascular dysfunction is a main feature of diabetic complications and involves both micro- and macro-angiopathy [13]. The progression of diabetic vascular complications results in cardiovascular disease, chronic renal failure, retinal damage, neuropathy and poor wound healing. The pathological changes in the macro- and micro-vasculature in diabetes are linked to inflammation [67, 260-262]. In blood vessels and tissues, an abnormal elevation of the highly reactive glycolytic byproduct methylglyoxal (MG) increases oxidative stress and the generation of advanced glycation end-products (AGE) [31, 124, 254], which lead to vascular inflammation [255]. However, the mechanism of vascular inflammation induced by MG itself in diabetes and diabetic vascular complications is unclear.

MG is a reactive carbonyl metabolite formed during glucose, protein and fatty acid metabolism [124]. In physiological conditions, MG is endogenously produced by various metabolic pathways [125, 263]. It is one of the most powerful glycation agents of proteins and other important cellular components such as DNA and key enzymes. Increased MG levels have been reported in diabetes patients and animals [112, 264]. Besides its strong glycation capability, increased MG level is involved in the inflammatory response in diabetes by upregulating the expression of inflammatory mediators [251, 265-267]. It is reported that increased plasma MG level is related to the expression of cytokines in diabetic nephropathy patients and type 2 diabetes mellitus patients [112, 251]. Yamawaki *et al.* showed that MG is a very strong inducer of inflammation in human ECs [197]. It has also been shown that MG activates various signalling pathways such as nuclear factor-κ B (NF-κB), c-Jun N-terminal kinase (JNK) and p38 mitogen-activated protein kinase (MAP kinase) pathways in ECs and leukocytes [197, 268, 269]. The activation of these pathways further triggers downstream inflammatory cascade events [197, 270, 271] such as the production of cytokines and chemokines and upregulation of cell adhesion molecules which mediate leukocyte recruitment. Thus elevated MG may play a role in inducing inflammation in diabetes patients.

Leukocyte recruitment from the blood stream into the extravascular space is essential for developing an appropriate inflammatory response to injury or infection. In many tissues, this process follows a well-defined cascade of events, beginning with the capture of free-flowing blood leukocytes to the vessel wall, and followed by rolling and adhesion of leukocytes to the inflamed endothelium and, then by leukocyte transendothelial migration. Studies have shown that various cytokines, chemokines and adhesion molecules are essential for this process [95, 272]. In the initial phase of the adhesion cascade, leukocyte rolling is mediated by members of the selectin family (L-selectin on leukocytes, and P-selectin and E-selectin on activated ECs), and adhesion by intercellular adhesion molecule-1 (ICAM-1), which binds to β2 integrins such as LFA-1 and Mac-1 on the leukocyte membrane. This latter interaction results in the arrest and firm adhesion of the leukocytes to the endothelium, and is required for the subsequent leukocyte transendothelial migration. Although the process of leukocyte-EC interaction has been extensively investigated, the mechanism of MG-induced inflammatory response in macro- and micro-vasculature in diabetic vascular complications is not clear. The questions of whether and which adhesion molecules are

upregulated and which particular step in the recruitment process is affected by their upregulation still remain unanswered.

Previous studies demonstrated that the expression of ICAM-1, E-selectin and VCAM-1 in the blood vessels is increased in spontaneously hypertensive rats [273, 274]. The serum concentrations of VCAM-1 and ICAM-1 are increased in patients with systemic vascular inflammation, type 2 diabetes and cardiovascular diseases [275-278]. Since these diseases are related to hyperglycemia, inflammation and increased MG formation, it is reasonable to infer that there is a potential relationship between MG production, EC adhesion molecule expression, and inflammation. In this study, we used intravital microscopy to investigate the effects of MG on leukocyte recruitment and the role of EC adhesion molecules P-selectin, E-selectin and ICAM-1 in MG-induced leukocyte recruitment. We evaluated the changes in recruitment parameters (leukocyte rolling, adhesion and emigration) in the microvasculature of the cremaster muscle after intrascrotal injection of different doses of MG at different time points. We also explored the involvement of NF-κB signalling pathway in this process. Based on the time-course data, we established an MG-induced inflammation model and investigated the mechanism of MG-induced leukocyte recruitment. The expression of P-selectin, E-selectin, ICAM-1 and VCAM-1 after MG treatment was determined by immunohistochemistry. The role of each upregulated adhesion molecule was determined by using functional blocking antibodies. The role of NF-κB involved in MG-induced leukocyte recruitment was investigated by using specific inhibitor.

3.3 Materials and methods

Animals

Male C57BL/6 mice between 8 and 12 weeks old were obtained from Charles River Canada (Saint-Constant, QC, Canada). All animal protocols were approved by the University of Saskatchewan Committee on Animal Care and Supply, and met the standards of the Canadian Council on Animal Care.

Cell culture

EA.hy926 cell, a hybrid human umbilical vein EC line, was obtained from American Type Culture Collection (Rockville, MD, USA). Cells were cultured in Dulbecco's modified Eagle's medium (Cellgro, VA, USA) with 10% fetal bovine serum (Hyclone, UT, USA) and 100 U/mL penicillin-streptomycin (Amresco, OH, USA) with 5% CO_2 and maximal humidity at 37 ℃. Cells between passage 3 and 6 were used for the experiments.

MG administration

MG (Sigma-Aldrich, Oakville, ON, Canada) was dissolved in saline. To give MG doses of 0, 1, 5, 25, 50 mg/kg, 200 μL of the MG solution were injected into the right side of the scrotum using a 30G needle beneath the scrotum skin without puncturing any underlying tissue (intrascrotal injection). At various time points after MG injection, the mice were prepared for intravital microscopy (described below). Intrascrotal injection of 500 ng recombinant murine TNF-α (R & D systems, MN, USA) in 200 μL saline was used as positive control for immunohistochemistry studies.

MG assay

MG levels in plasma and cremaster muscle tissue were measured by a specific and sensitive HPLC method as described previously [252, 279]. Briefly, MG was derivatized with *o*-phenylenediamine (*o*-PD) to specifically form 2-methylquinoxaline. Samples were incubated in the dark for 24 h with PCA solution (1 M $HClO_4$, 4 mM $Na_2S_2O_5$, 0.1 mM EDTA) and 100 mM *o*-PD at room temperature. 2-Methylquinoxaline and quinoxaline internal standard (5-methylquinoxaline) were quantified on a Hitachi D-7000 HPLC system (Hitachi, Ltd., Mississauga, ON, Canada) via Nova-Pak® C18 column (3.9×150 mm, and 4 μm particle diameter, Waters, MA, USA). The protein concentrations in the samples were determined by BCA assay kit (Sigma-Aldrich).

Intravital microscopy

Mice were anesthetized by intraperitoneal injection of a mixture of 10 mg/kg xylazine (Bayer Inc., Toronto, ON, Canada) and 200 mg/kg ketamine hydrochloride (Bioniche Inc., Belleville, ON, Canada). The right jugular vein was cannulated for the administration of additional anesthetics and the antibodies. An incision was made in the scrotal skin to expose the left cremaster muscle, which was then carefully separated from the associated fascia. A lengthwise incision was made on the

ventral surface of the cremaster muscle. The testicle and epididymis were separated from the underlying muscle and reintroduced into the abdominal cavity. The muscle was then spread out over an optically clear viewing pedestal, secured along the edges with 5—0 suture, and superfused with 37 ℃ bicarbonate buffered saline (pH 7.4). The cremaster microcirculation was observed on a TV monitor through an intravital microscope (BX61WI, Olympus, Tokyo, Japan) using 10× eyepieces and a 20× objective lens. Single unbranched venules (25—35 μm in diameter) were selected for study and images of the microcirculation were recorded using a video camera (model DXC-990, SONY, Tokyo, Japan) and video recorder (model LRH-890, LG, Seoul, South Korea). To minimize variability, the same section of cremasteric venule was observed throughout the experiment. The number of rolling, adherent, and emigrated leukocytes was determined offline during video playback analysis. Rolling leukocytes were defined as cells moving at a velocity less than that of erythrocytes within a given vessel. The flux of rolling cells was measured as the number of rolling cells passing a given point in the venule per minute. The rolling velocity was determined as 100-μm length of distance on the venule divided by the average time that the first 20 rolling cells covered this distance at the recording time point. A leukocyte was considered to be adherent if it remained stationary for ≥30 s, and total leukocyte adhesion was quantified as the number of adherent cells within a 100-μm length of venule in 5 min. Leukocyte emigration was defined as the number of cells in the extravascular space within 443 × 286 μm^2 area (2 fields of view on TV monitor) on both sides of the venule. Only cells adjacent to and clearly outside the vessel under study were counted as emigrated [280].

Histological examination

Haematoxylin and eosin (H & E) staining

H & E staining of paraffin sections was used to determine the subtypes of emigrated leukocytes. After intravital microscopy, the cremaster muscle was collected and fixed for 16 h in 4% paraformaldehyde (Sigma-Aldrich) in PBS solution (pH 7.4). After fixation, the tissue was processed by an automatic vacuum tissue processor (model RVG/1, Belair, NJ, USA) for dehydration, clearing and infiltration with embedding medium. The tissue was then embedded into paraffin blocks and sliced at 5 μm by a microtome. H & E staining was carried out as previously described [281]. After H & E staining, cremasteric venules (25–35 μm diameter) were selected under a microscope, the emigrated cells in the same area (443 × 286 μm^2) as intravital microscopy

experiment were observed and counted. The subtypes of leukocytes recruited in the extravascular space were determined by their morphology under the microscope.

Immunohistochemistry

Immunohistochemistry of frozen sections of cremaster muscle was used to determine the expression of adhesion molecules. After intravital microscopy, the cremaster muscle was collected and fixed for 16 h by 4% buffered paraformaldehyde solution. After fixation, the tissue was dehydrated by hypertonic sucrose solution (10% 4 h, 15% 4 h, and 30% 16 h). Then the tissue was embedded in OCT compound and sectioned by a cryostat microtone (model HM 500, Microm, Walldorf, Germany) at 7 μm. The blocks were kept at -70 ℃ until use.

Tissue slices were mounted on microscope slides and washed in TBST (50 mM Tris-HCl, 150 mM NaCl, 0.1% Triton X-100, pH 7.4) twice (10 min each) for permeabilization, and then in TBS (50 mM Tris-HCl, 150 mM NaCl, pH 7.4) 3 times. The sections were immersed in 0.3% (v/v) H_2O_2 in TBS for 15 min to remove the endogenous peroxidase activity. After washing twice with TBS, blocking solution [10% goat serum (Abcam, MA, USA) plus 5%BSA in TBS] was added for 2 h. After blocking, sections were incubated for 16 h in a humidity chamber at 4 ℃ with diluted primary antibodies: anti-E-selectin (UZ6, Abcam) at 1:100, anti-P-selectin (polyclonal, LifeSpan BioSciences, WA, USA) at 1:50, anti-ICAM-1 (YN1/1.7.4, Abcam) at 1:100 or anti-VCAM-1 (MVCAM.A (429), Abcam) at 1:100. After washing with TBS 3 times (10 min each), the diluted secondary antibodies HRP-conjugated goat anti-rabbit (Abcam) at 1:200 and HRP-conjugated goat anti-rat (Abcam) at 1:200 were applied for 1 h in a humidity chamber at room temperature. Slides were washed with TBS 3 times (10 min each), developed with diaminobenzidine chromogen for 3 min, and rinsed in distilled water for 5 min. Coverslips were mounted with permanent mounting medium.

Western blotting

After treating with PBS (control), MG or TNF-α, EA.hy926 cells were harvested and lysed on ice for 30 min by RIPA buffer (50 mM Tris-HCl pH 8.0, 150 mM NaCl, 1% NP-40, 0.5% sodium deoxycholate, 0.1% SDS and protease inhibitors cocktail). The lysate was centrifuged at 10,000× *g* for 10 min, and the supernatant was collected, mixed with 4× sample loading buffer (200 mM Tris-HCl pH 6.8, 50% glycerol, 2% SDS, 20% β-mercaptoethanol, 0.04% bromophenol bule),

boiled for 5 min and centrifuged at 10,000× *g* for 5 min before loading. The same amount of proteins in cell lysates were separated on 7.5% SDS-PAGE, electrotransferred to a nitrocellulose membrane (Bio-Rad, CA, USA), blocked with 5% nonfat milk in TBS-Tween buffer for 1.5 h at room temperature, and incubated overnight at 4℃ with the primary antibodies against P-selectin (1:1000, Lifespan BioSciences), E-selectin (1:1000, Abcam), ICAM-1 (1:1000, Abcam), and β-actin (1:2000, Santa Cruz, CA, USA), and then incubated with horseradish peroxidase-conjugated secondary antibody (Abcam) for 1 h at room temperature. After extensive washing, the bands were visualized with enhanced chemiluminescence reagents (GE Healthcare Life Sciences, NJ, USA) and exposed to X-ray film (Kodak scientific imaging film, ON, Canada).

Functional blocking study

Mice were injected with MG and prepared for intravital microscopy as above. The functional blocking antibody was injected i.v. 5 min after the start of intravital microscopy. The antibodies were: anti-E-selectin antibody (9A9, 100 μg/mouse; a gift from Dr. Paul Kubes, University of Calgary, AB, Canada), anti-P-selectin antibody (RB40.34, 25 μg/mouse; BD Pharmingen, CA, USA), anti-ICAM-1 antibody (YN1/1.7.4, 100 μg/mouse; eBioscience, CA, USA), rat anti-mouse negative control IgG1 (for E-selectin and P-selectin; BD Pharmingen) and rat anti-mouse negative control IgG2b (for ICAM-1; eBioscience).

Administration of NF-κB inhibitor

BAY 11-7082 (Sigma-Aldrich), a specific NF-κB inhibitor, was first dissolved in DMSO as a 30 mg/mL stock solution, the appropriate amount of which was dissolved by 0.4 mL saline and injected to the animal at 20 mg/kg i.p. 30 min before MG administration. The same concentration of DMSO was used in the vehicle control group.

Statistical analysis

Data are expressed as mean ± SEM from at least three independent experiments. Statistical differences between mean values in two groups were analyzed by Student's *t* test, and the differences among more than two groups were analyzed by one-way ANOVA and Tukey's post-hoc test. $P < 0.05$ was considered as statistically significant.

3.4 Results

MG levels in plasma and cremaster muscle after exogenous MG administration

We measured MG levels in plasma and cremaster muscle after 4-h MG intrascrotal injection. Table 3-1 shows that as MG dose increased (0－50 mg/kg), the mean MG levels in plasma dose-dependently increased from 0.934 μM to 1.660 μM, and the mean MG levels in the local tissue increased from 0.999 nmol/mg protein to 3.878 nmol/mg protein. MG local injection significantly increased MG levels in plasma and local tissue in a dose-dependent manner. The MG levels in plasma and tissue in our model are consistent with those in previously established acute MG-treated animal models [134, 187].

Dose-response effects of MG on leukocyte recruitment

To determine the effect of a local MG increase on leukocyte recruitment in microvasculature, we examined leukocyte recruitment after intrascrotal injection of various doses of MG (1, 5, 25, and 50 mg/kg). Figure 3-1 shows leukocyte recruitment in cremaster muscle at 4.0—5.5 h after local administration of MG. In response to increasing doses of MG, leukocyte rolling flux did not increase until the dose of MG reached 25 mg/kg, and leukocyte rolling velocity was dose-dependently decreased when MG was 5 mg/kg or higher. The adhesion and emigration of leukocytes were increased in an MG dose-dependent manner. As the MG dose increased, the leukocyte adhesion and emigration increased from 2 cells to > 10 cells, and from 0 to > 8 cells, respectively. Low dose MG treatment at 1 mg/kg or 5 mg/kg showed no significant statistical change compared to saline control group. For 25 mg/kg and 50 mg/kg MG treatment groups, significant differences were always observed on rolling flux, rolling velocity, adhesion, and emigration. These results indicate that MG induces a dose-dependent increase of leukocyte recruitment.

Table 3-1. The levels of MG in plasma and local tissue

MG doses	Amount of MG detected by HPLC	
	Plasma (μM)	Cremaster muscle (nmol/mg protein)
0 mg/kg	0.934 ± 0.055	0.999 ± 0.040
1 mg/kg	1.051 ± 0.061	1.476 ± 0.135*
5 mg/kg	1.170 ± 0.061*	2.494 ± 0.007*
25 mg/kg	1.486 ± 0.109*	3.149 ± 0.172*
50 mg/kg	1.660 ± 0.096*	3.878 ± 0.166*

Table 3-1. The MG levels in plasma and cremaster muscle were analyzed by HPLC after 4-h MG local treatment. The values are mean ± SEM (n = 3). *, $P < 0.05$ compared with saline-treated control group (0 mg/kg).

The time course of leukocyte recruitment after MG treatment

To investigate the kinetics of leukocyte recruitment after MG treatment, we examined leukocyte recruitment 4, 8, 16 or 24 h after 25 or 50 mg/kg MG. The results showed that the effects of MG treatment on leukocyte recruitment peaked at 8 h (Figure 3-2). For both 25 and 50 mg/kg treatment groups, the lowest rolling velocity, and highest adhesion and emigration were all observed in 8 h. After 8 h, the rolling velocity increased, and the adhesion and emigration decreased, towards the untreated level. These data indicate that MG treatment induces rapid leukocyte recruitment in local tissue, and the peak response happens at 8 h.

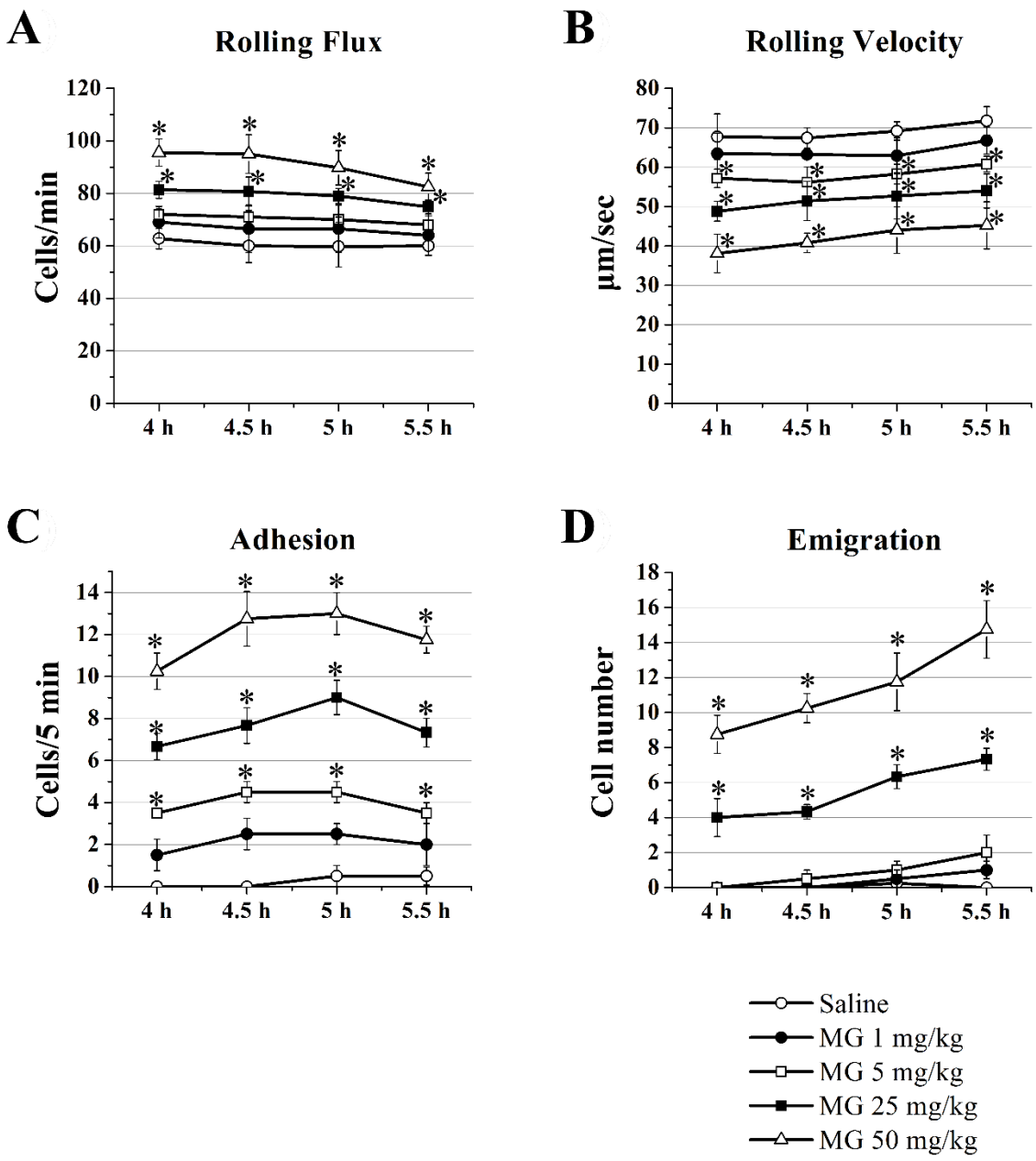

Figure 3-1. Dose-response effect of MG on leukocyte recruitment in cremasteric postcapillary venules. MG at different doses (dissolved in 200 μL saline) was injected intrascrotally, and the mouse cremaster muscle was prepared for intravital microscopy at 4 h. Leukocyte rolling flux (A), rolling velocity (B), number of adherent leukocytes (C) and the number of emigrated leukocytes (D) were determined at 4.0—5.5 h after MG treatment. Values are means ± SEM (n=4). *, $P < 0.05$ compared with saline-treated control group.

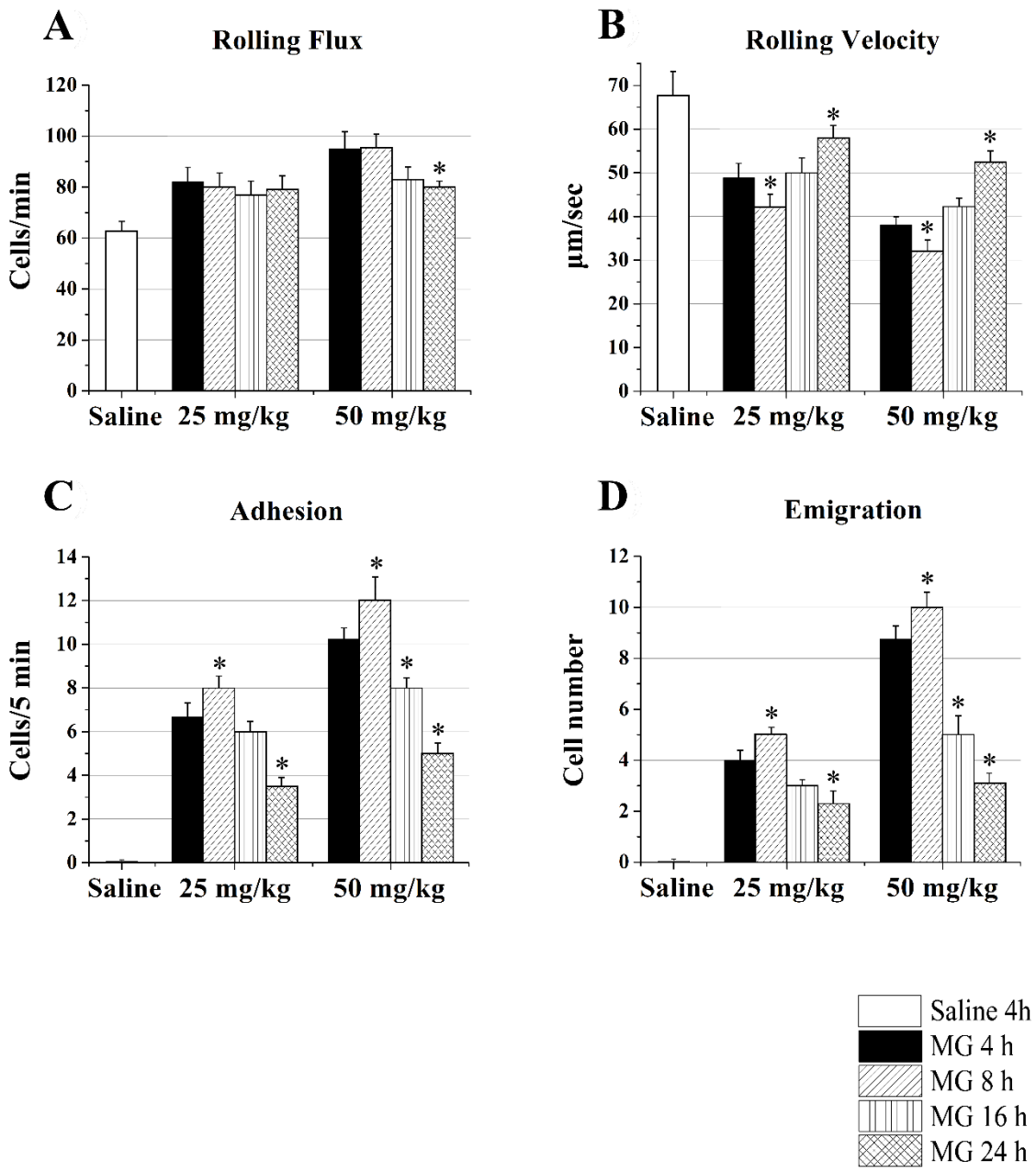

Figure 3-2. Time-course effect of MG on leukocyte recruitment in cremasteric postcapillary venules. MG, 25 mg/kg or 50 mg/kg (dissolved in 200 μL saline), was injected intrascrotally, and the mouse cremaster muscle was prepared for intravital microscopy at 4 h, 8 h, 16 h and 24 h, respectively. Leukocyte rolling flux (A), rolling velocity (B), number of adherent leukocytes (C) and the number of emigrated leukocytes (D) were determined. The 4 h saline group is shown as the control. Values are means ± SEM (n=3). *, $P < 0.05$ compared with the 4 h MG treatment group.

Neutrophils predominantly recruited by acute MG treatment

To determine whether MG induces a typical acute inflammation response in cremaster muscle, we measured the percentage of neutrophils and other subtypes of leukocytes in emigrated cells 5.5 h after the intrascrotal injection of 25 or 50 mg/kg of MG. The majority (~ 84—92%) of the emigrated leukocytes were neutrophils, ~ 7—14% were lymphocytes and monocytes, while eosinophils and basophils accounted for < 2% (Figure 3-3 and Table 3-2). Our results reveal that MG local treatment causes a typical, neutrophil-dominent, acute inflammation response in cremaster muscle.

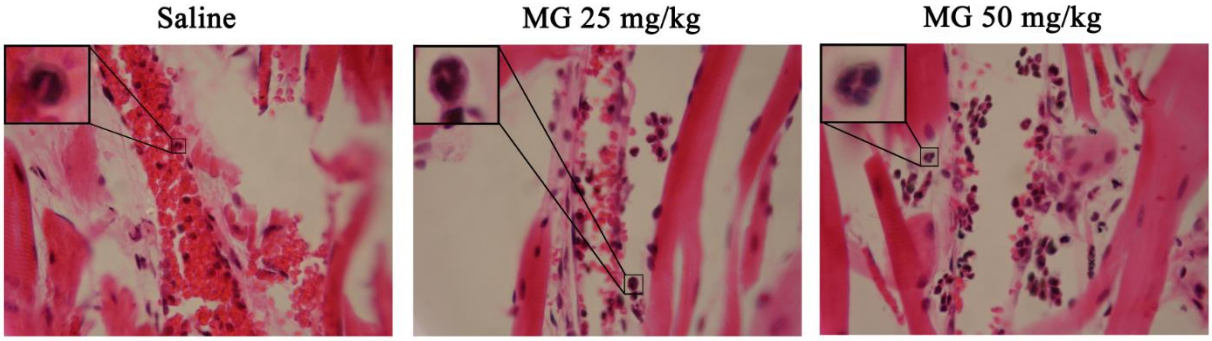

Figure 3-3. H & E staining of cremaster muscle sections. After 5.5 h MG or saline treatment, the cremaster muscles were collected and processed as described in *Materials and Methods*. After H & E staining, cremasteric venules (25–35 μm diameter) and adjacent tissues were examined under the microscope, and the emigrated leukocytes in the same area as intravital microscopy were counted (Table 3-2). The subtypes of leukocytes in the extravascular space were determined by their morphology (Magnification: 400×).

Table 3-2. The subtypes and percentage of recruited leukocytes after MG treatment

Dose and time of MG treatment	The percentage of each subtype of recruited leukocytes			
	Eosinophils	Basophils	Neutrophils	Lymphocytes/ Monocytes
25mg/kg, 5.5 h	0.38%	0.49%	91.78%	7.34%
50mg/kg, 5.5 h	0.91%	0.85%	84.24%	14.00%

Table 3-2. After H & E staining, the emigrated leukocytes in the same area as intravital microscopy experiment were examined and counted. The subtypes of cells in the extravenular space were determined by their morphology under microscope. For each treatment group, > 500 leukocytes in extravascular space were counted.

The acute inflammation model induced by MG

We found that MG treatment for 8 h or longer increased tissue damages such as scrotum swelling and interstitial tissue stickiness which were more apparent at 16 and 24 h, and that 25 mg/kg MG local treatment for 4.0—5.5 h induces a typical acute inflammation response with a high percentage of recruitment cells being neutrophils (Figure 3-1 and Table 3-2). In the following experiments, we chose 25 mg/kg MG local treatment for 4 h to study the role of EC adhesion molecules in MG-induced leukocyte recruitment.

Upregulation of endothelial adhesion molecule expression by MG treatment

By using immunohistochemistry, we determined the expression of EC adhesion molecules P-selectin, E-selectin, ICAM-1 and VCAM-1 on cremasteric postcapillary venules. After 25 mg/kg MG treatment for 4.0—5.5 h, the expression of P-selectin (Figure 3-4), E-selectin (Figure 3-5) and ICAM-1 (Figure 3-6) were increased, whereas VCAM-1 expression did not change (Figure 3-7).

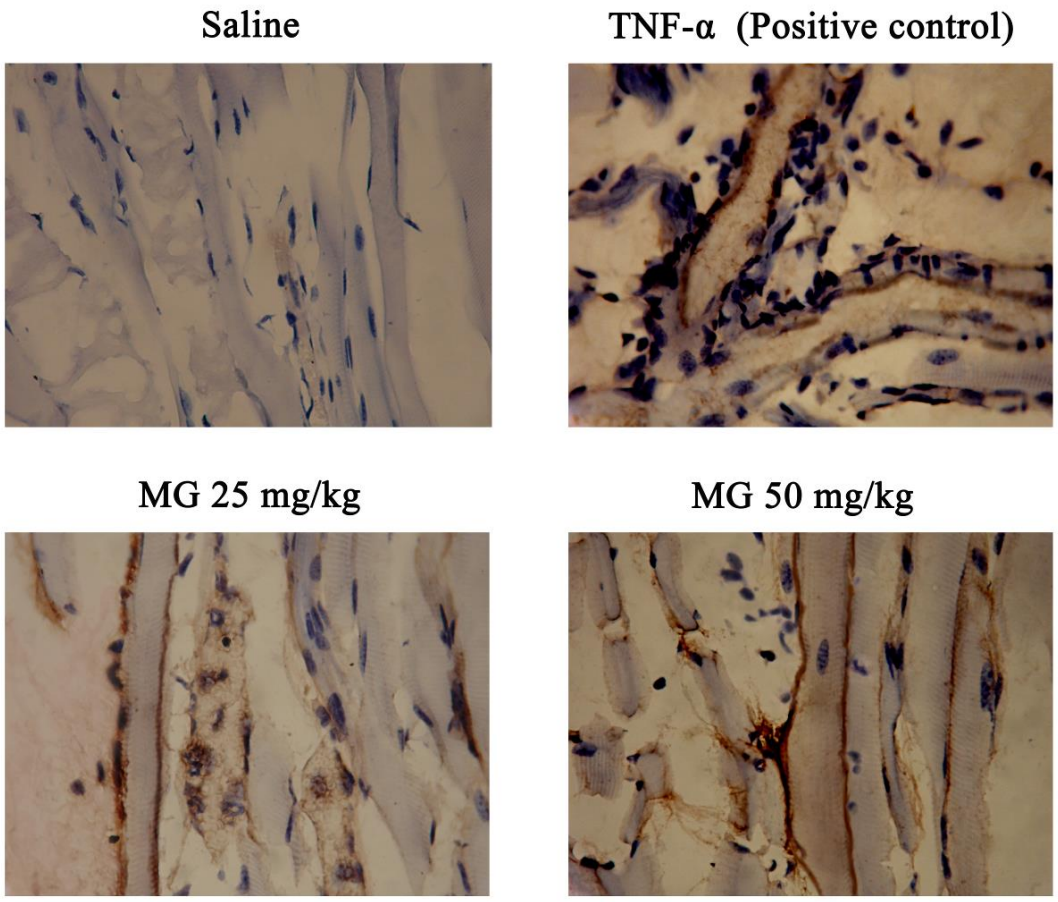

Figure 3-4. Immunohistochemistry staining of P-selectin in cremasteric endothelium after MG treatment. MG at 25 or 50 mg/kg (dissolved in 200 μL saline) was injected intrascrotally for 5.5 h, and the mouse cremaster muscles were collected and processed as described in *Materials and Methods*. The brown staining on the ECs of cremasteric postcapillary venules reveals the expression of P-selectin. Saline and 500 ng TNF-α were used as negative and positive control, respectively (Magnification: 400×).

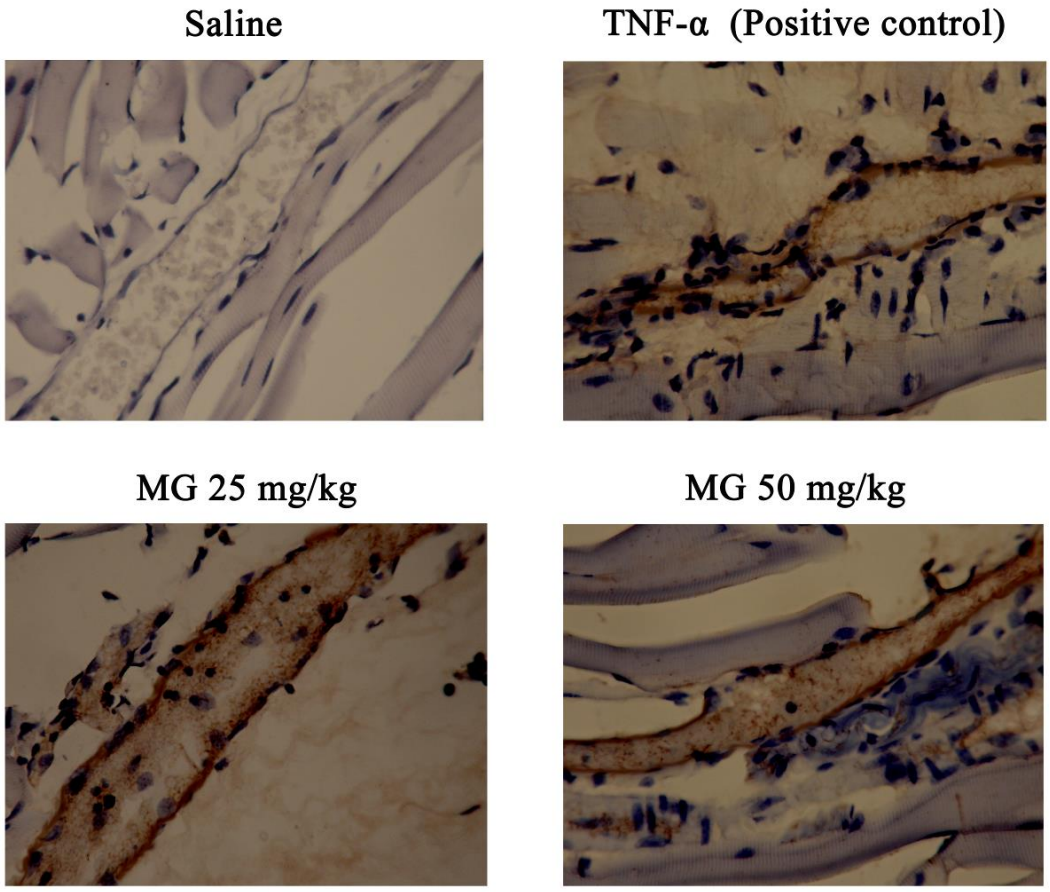

Figure 3-5. Immunohistochemistry staining of E-selectin on cremasteric endothlium after MG treatment. MG at 25 or 50 mg/kg (dissolved in 200 μL saline) was injected intrascrotally for 5.5 h, and the mouse cremaster muscles were collected and processed as described in *Materials and Methods*. The brown staining on the ECs of cremasteric postcapillary venules reveals the expression of E-selectin. Saline and 500 ng TNF-α were used as negative and positive control, respectively (Magnification: 400×).

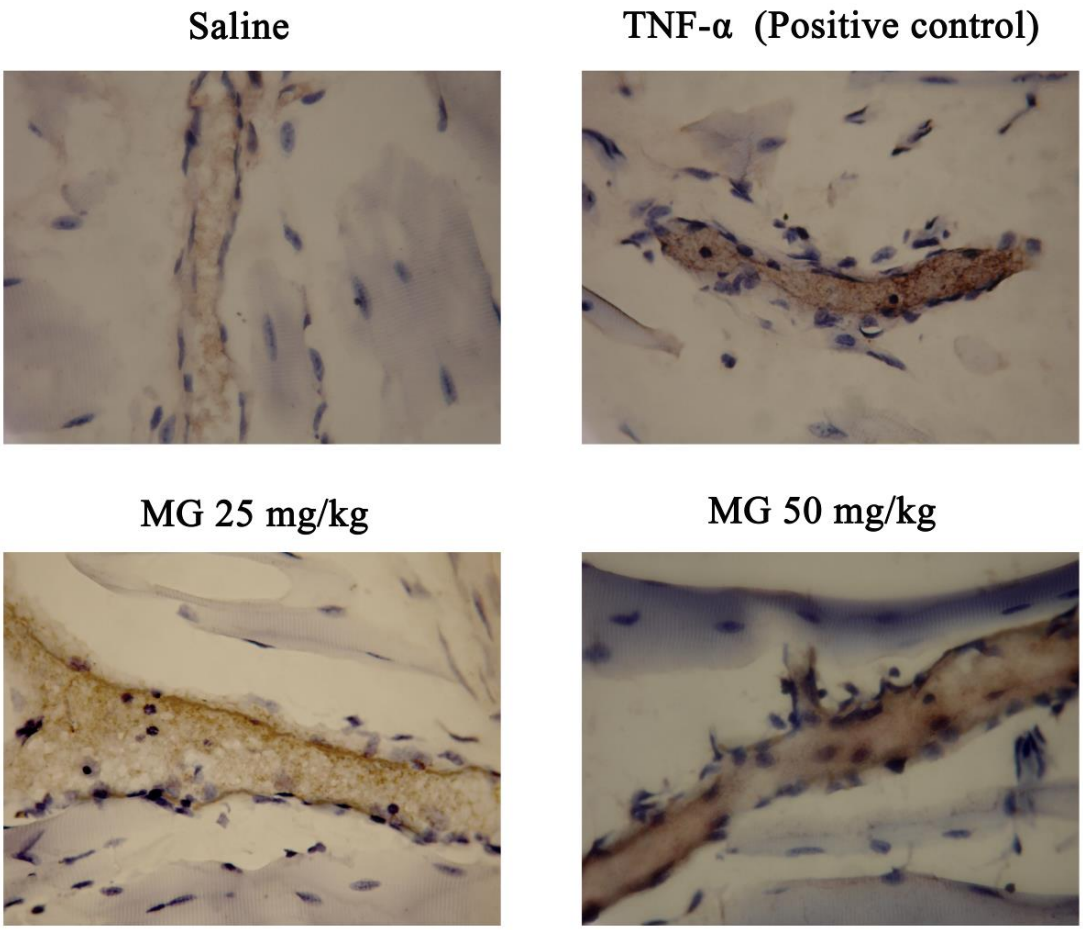

Figure 3-6. Immunohistochemistry staining of ICAM-1 on cremasteric endothelium after MG treatment. MG at 25 or 50 mg/kg (dissolved in 200 μL saline) was injected intrascrotally for 5.5 h, and the mouse cremaster muscles were collected and processed as described in *Materials and Methods*. The brown staining on the ECs of cremasteric postcapillary venules reveals the expression of ICAM-1. Saline and 500 ng TNF-α were used as negative and positive control, respectively (Magnification: 400×).

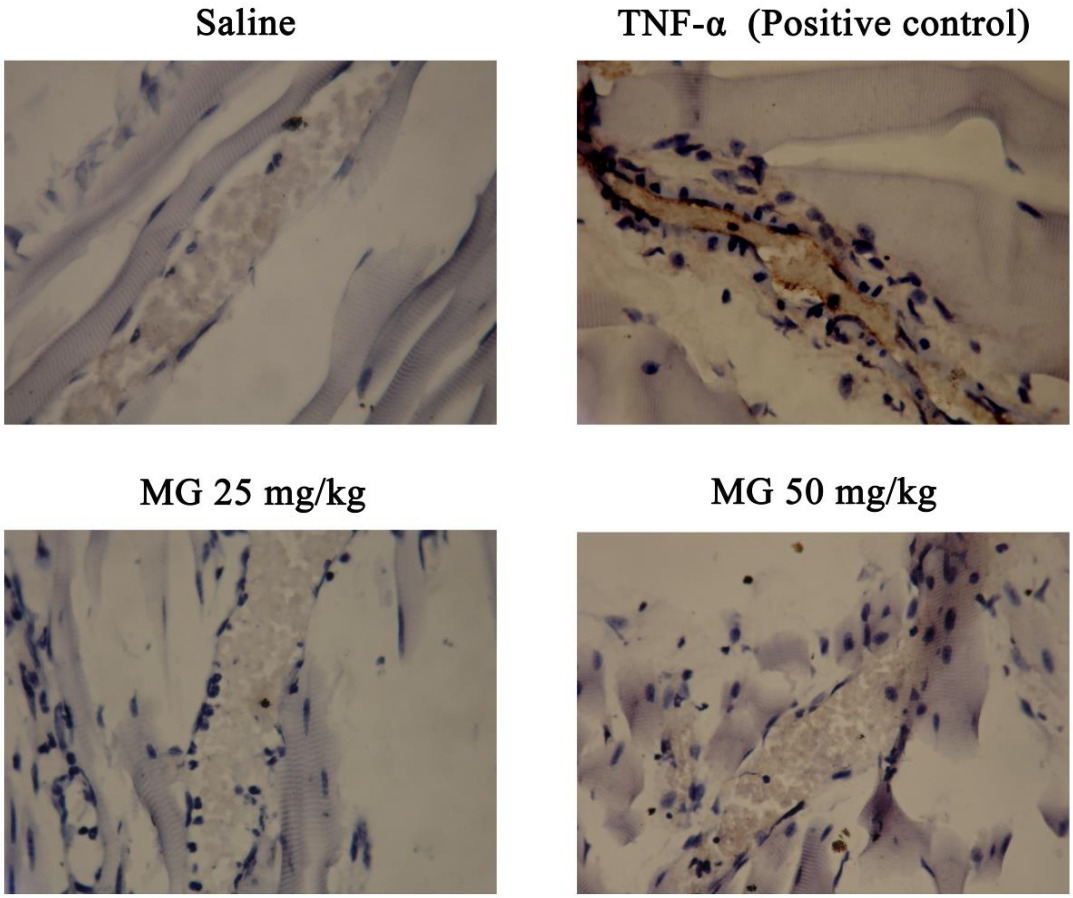

Figure 3-7. Immunohistochemistry staining of VCAM-1 on cremasteric endothelium after MG treatment. MG at 25 or 50 mg/kg (dissolved in 200μL saline) was injected intrascrotally for 5.5 h, and the mouse cremaster muscles were collected and processed as described in *Materials and Methods*. Saline and 500 ng TNF-α were used as negative and positive control respectively. The brown staining on the ECs of cremasteric postcapillary venules reveals the expression of VCAM-1 in TNF-α treated group. Both MG treatment groups show no apparent change of VCAM-1 expression after 5.5 h MG treatment compared to saline control group (Magnification: 400×).

The direct activation effect of MG on ECs

To investigate whether MG is directly activating ECs, we tested the effect of MG on the expression of endothelial adhesion molecules using *in vitro* system. Cultured EA.hy926 ECs were treated with 100 μM MG, PBS or 20 ng/mL TNF-α for 4 h, and the expression of P-selectin, E-selectin and ICAM-1 was determined by Western blot. Figure 3-8 shows that MG treatment increased the expression of these adhesion molecules in cultured EA.hy926 ECs demonstrating that the effect of MG was directly on the ECs.

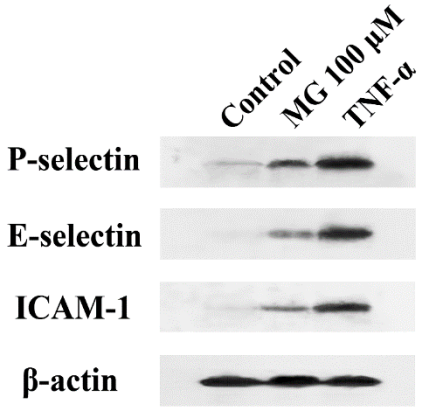

Figure 3-8. MG-induced expression of P-selectin, E-selectin and ICAM-1 in cultured ECs. EA.hy926 ECs were cultured to 90% confluence and treated with PBS (negative control), 100 μM MG or 20 ng/mL TNF-α (positive control) for 4 h. The expression of P-selectin, E-selectin and ICAM-1 in cell lysates were determined by Western blot.

The role of P-selectin, E-selectin and ICAM-1 in MG-induced leukocyte recruitment

To investigate the role of P-selectin, E-selectin and ICAM-1 during MG-induced leukocyte recruitment, we administered the functional blocking antibodies against these adhesion molecules 4 h after MG treatment, and determined leukocyte rolling velocity, rolling flux, adhesion and emigration by intravital microscopy over the next 1.5 h.

Suppression of MG-induced increase of leukocyte rolling flux by P-selectin blockade

Figure 3-9 illustrates that after anti-P-selectin antibody injection, the leukocyte rolling flux dropped to 0, indicating that the rolling of leukocytes on the venular wall depends on the functions of P-selectin. Since there were no leukocytes rolling on the venular wall after P-selectin blockade,

the rolling velocity was unable to be determined, and the further increases of leukocyte adhesion and emigration after MG were subsequently prevented (Figures 3-9C and 3-9D). These data indicate that MG-induced P-selectin upregulation results in more leukocytes rolling on the endothelium which increases the interactions between leukocytes and ECs.

Restoration of MG-induced reduction of leukocyte rolling velocity by E-selectin blockade

The intravital microscopy data demonstrate that anti-E-selectin antibody treatment significantly blocked the MG-induced decrease in rolling velocity, whereas the rolling flux had no significant change compared to the animals treated with the same dose of MG only (Figure 3-10). After blocking the functions of E-selecin, the rolling velocity increased back to the normal level and the adhesion and emigration were significantly decreased. Increasing the leukocyte rolling velocity reduces the time for leukocyte-EC interactions and decreases the subsequent increase of adhesion and emigration of leukocytes after MG treatment (Figures 3-10C and 3-10D). This result indicates that after MG treatment, the expression of E-selectin is important for the decrease in leukocyte rolling velocity.

Decreased MG-induced leukocyte adhesion by ICAM-1 blockade

After anti-ICAM-1 antibody administration, the adhesion cell number induced by MG dropped from ~7 to < 3, while the rolling velocity and rolling flux were not significantly changed (Figure 3-11). As adhesion was significantly decreased by anti-ICAM-1 treatment, the increased leukocyte emigration induced by MG was suppressed, and the emigration cell number remained ~4. These data indicate that ICAM-1 plays an important role in MG-induced adhesion of leukocytes to ECs, and may be crucial for MG-induced leukocyte emigration.

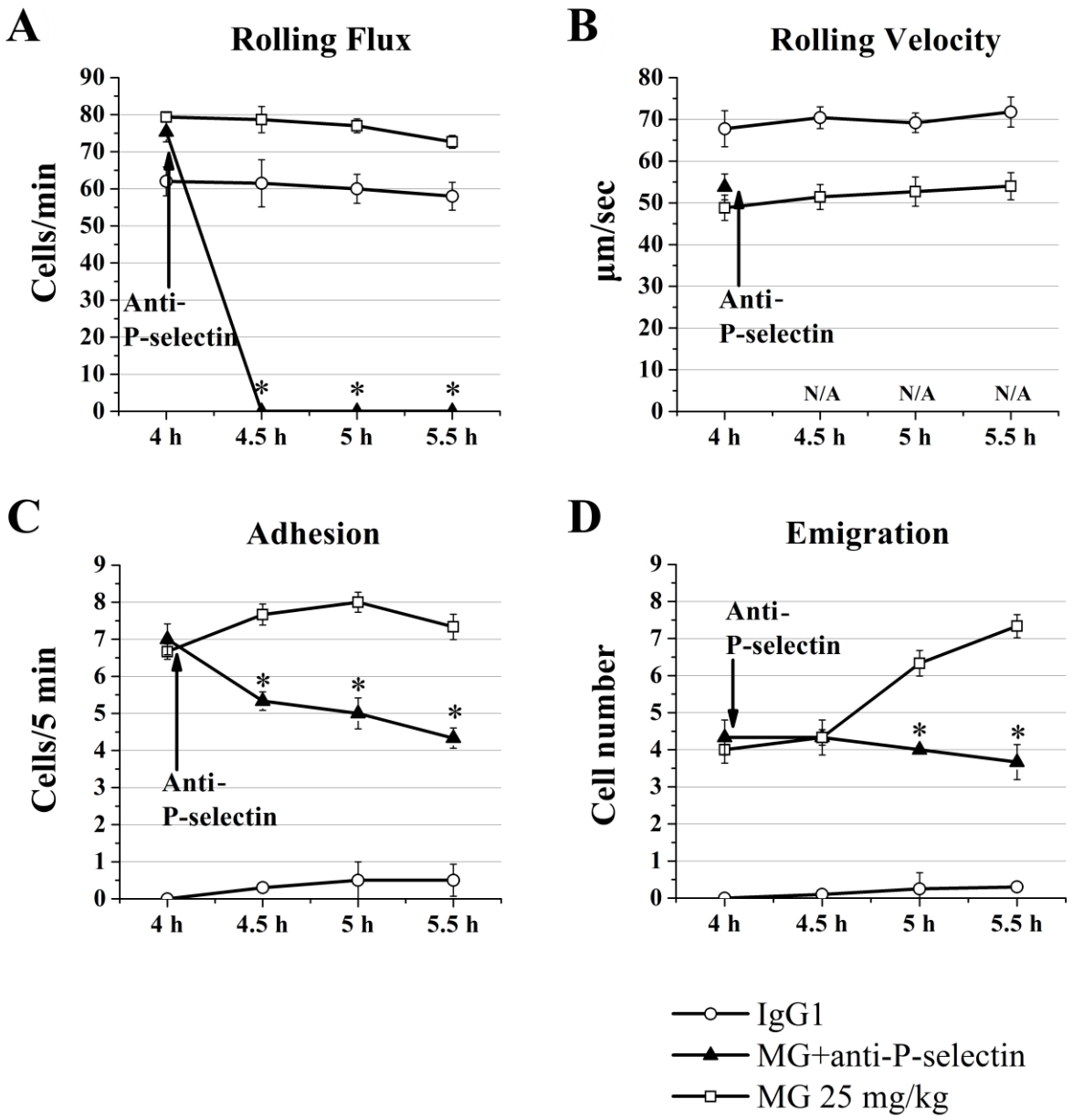

Figure 3-9. **Effect of P-selectin blocking antibody on leukocyte recruitment in cremasteric postcapillary venules after MG treatment.** Mice were treated with MG (25 mg/kg) as described in the legend of Figure 3-1, and leukocyte recruitment in cremaster muscle was measured at 4.0—5.5 h using intravital microscopy. After baseline measurement at 4 h, 25 µg anti-P-selectin antibody was infused *i.v.* (arrow). The leukocyte rolling flux (A), rolling velocity (B), number of adherent leukocytes (C) and the number of emigrated leukocytes (D) after antibody treatment were determined. Values are means ± SEM (n=3). *, $P < 0.05$ compared with 25 mg/kg MG-treated group without antibody.

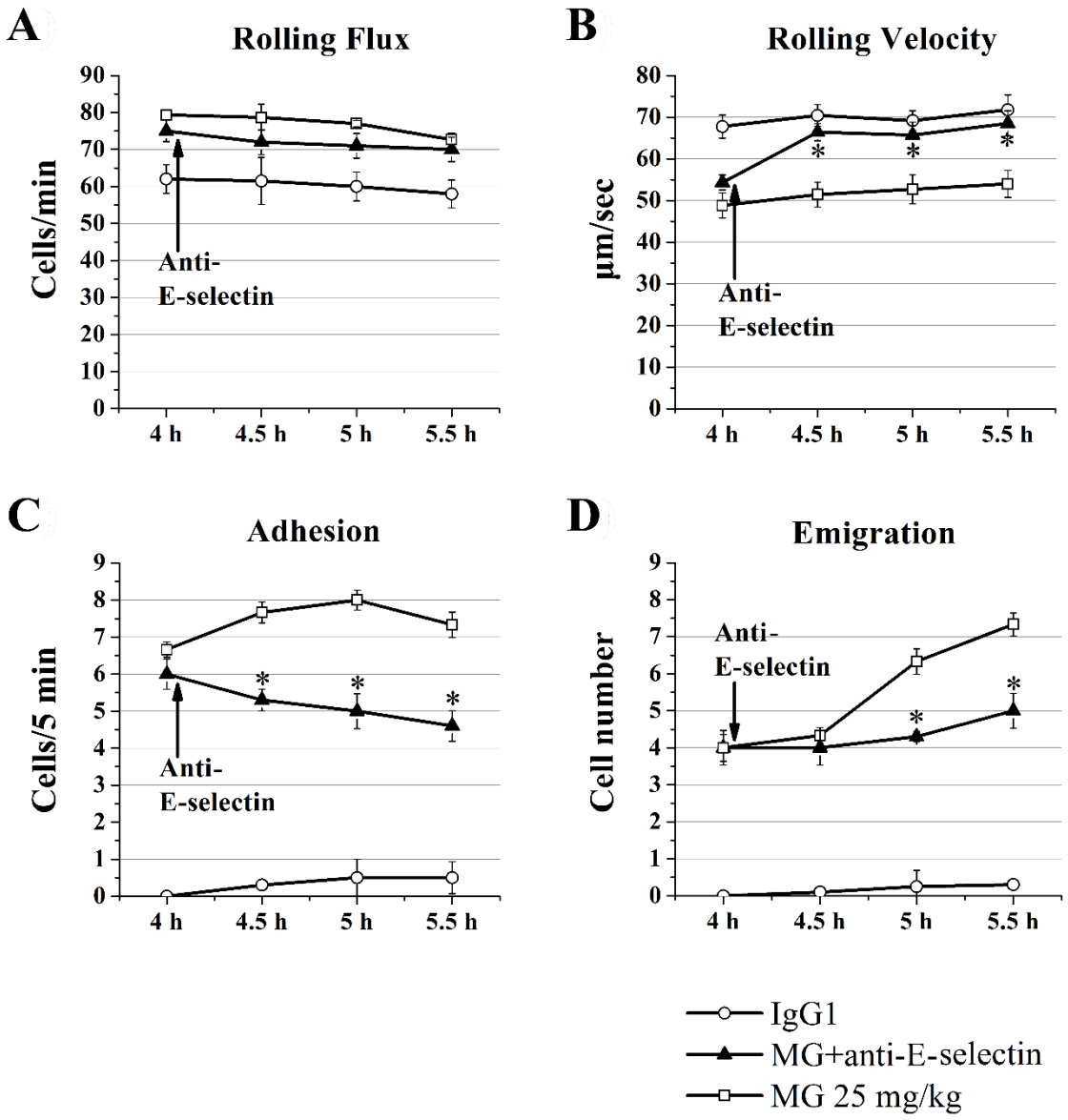

Figure 3-10. Effect of E-selectin blocking antibody on leukocyte recruitment in cremasteric postcapillary venules after MG treatment. Mice were treated with MG (25 mg/kg) as described in the legend of Figure 3-1, and leukocyte recruitment in cremaster muscle was measured at 4.0—5.5 h using intravital microscopy. After baseline measurement at 4 h, 100 µg anti-E-selectin antibody was infused *i.v.* (arrow). The leukocyte rolling flux (A), rolling velocity (B), number of adherent leukocytes (C) and the number of emigrated leukocytes (D) after antibody treatment were determined. Values are means ± SEM (n=3). *, $P < 0.05$ compared with 25 mg/kg MG-treated group without antibody.

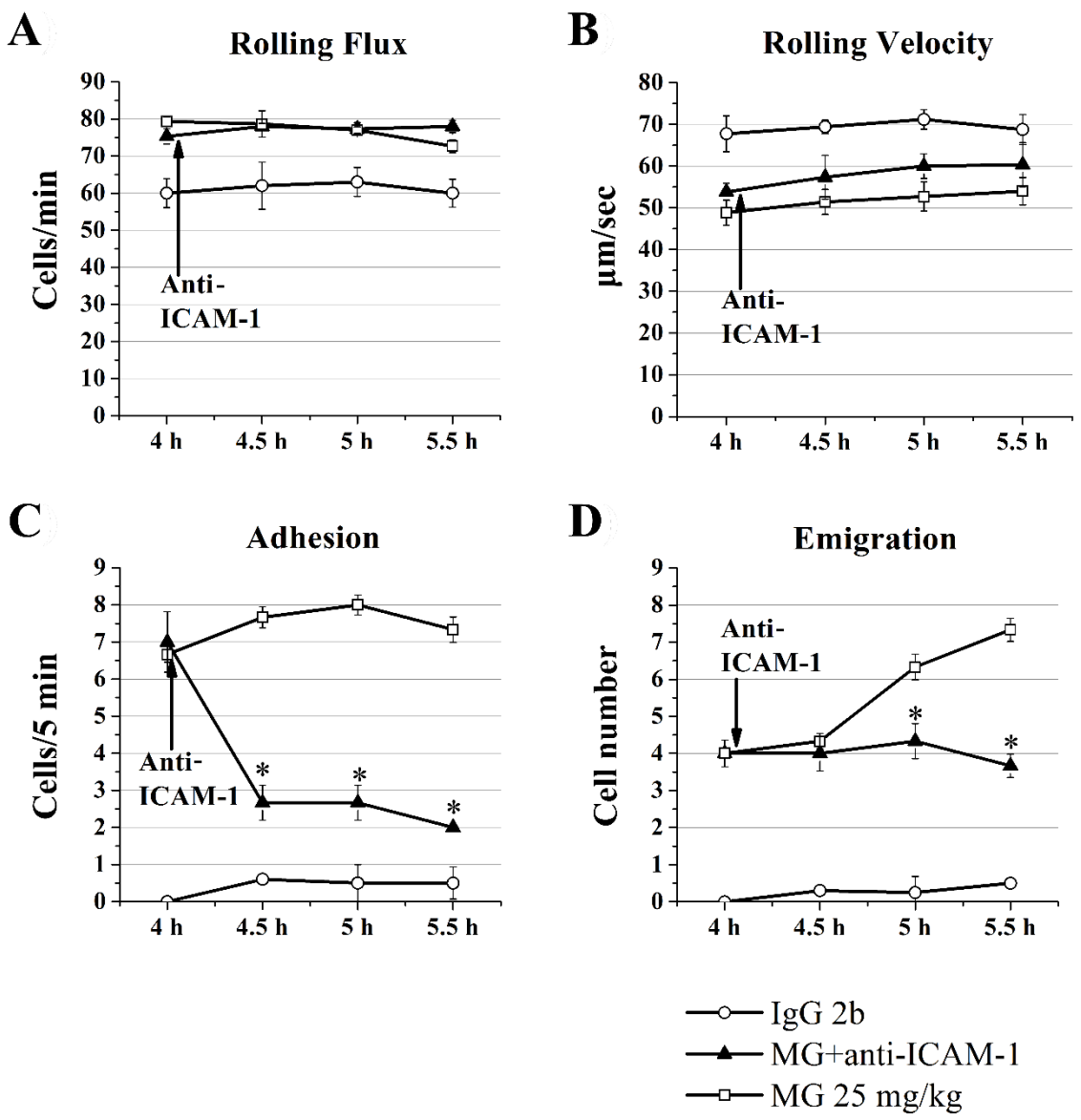

Figure 3-11. Effect of ICAM-1 blocking antibody on leukocyte recruitment in cremasteric postcapillary venules after MG treatment. Mice were treated with MG (25 mg/kg) as described in the legend of Figure 3-1, and leukocyte recruitment in cremaster muscle was measured at 4.0—5.5 h using intravital microscopy. After baseline measurement at 4 h, 100 µg anti-ICAM-1 antibody was infused *i.v.* (arrow). The leukocyte rolling flux (A), rolling velocity (B), number of adherent leukocytes (C) and the number of emigrated leukocytes (D) after antibody treatment were determined. Values are means ± SEM (n=3). *, $P < 0.05$ compared with 25 mg/kg MG-treated group without antibody.

The contribution of NF-κB signalling pathway to MG-induced adhesion molecule upregulation and leukocyte recruitment

To determine whether NF-κB pathway is involved in MG-induced adhesion molecule upregulation, we applied a specific NF-κB inhibitor, BAY 11-7082, 30 min before MG administration to observe the changes on adhesion molecule expression and leukocyte recruitment. Figure 3-12 shows that BAY 11-7082 pretreatment significantly suppressed the expression of MG-induced endothelial adhesion molecules P-selectin, E-selectin and ICAM-1, and attenuated MG-induced leukocyte recruitment. The immunostaining of P-selectin, E-selectin and ICAM-1 were much lighter in 25 mg/kg MG + NF-κB inhibitor-treated group than 25 mg/kg MG-treated group (Figure 3-12A). MG-induced leukocyte adhesion and emigration were also significantly reduced by BAY 11-7082 treatment (Figures 3-12D and 3-12E). Our data indicate that the activation of NF-κB pathway is involved in MG-induced endothelial adhesion molecule upregulation and leukocyte recruitment.

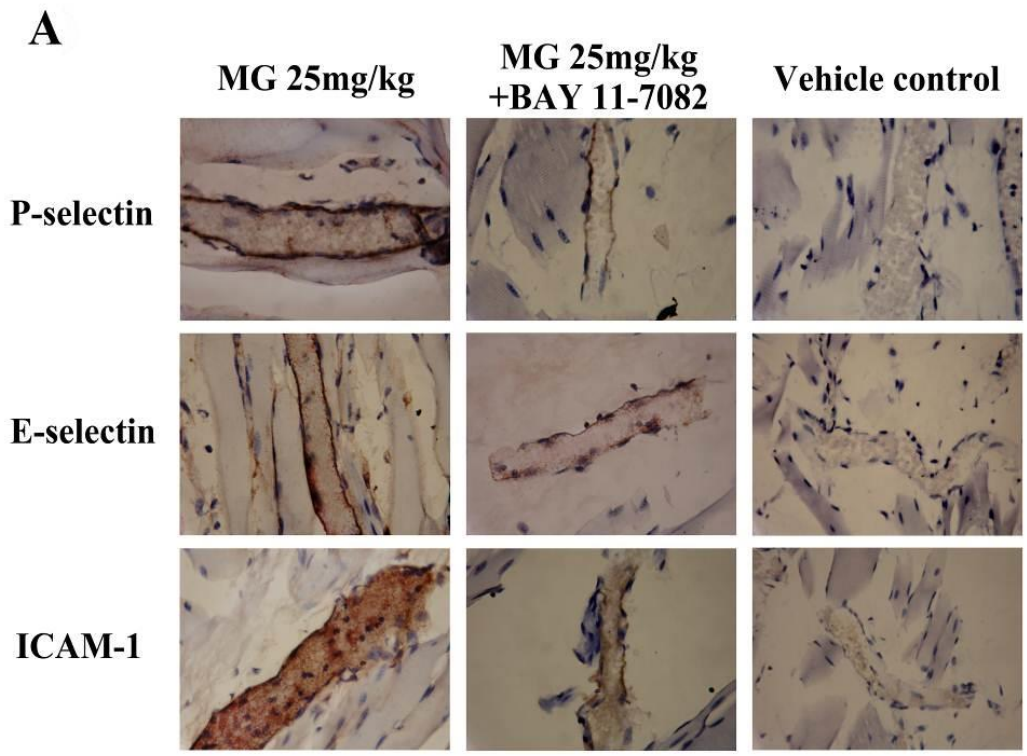

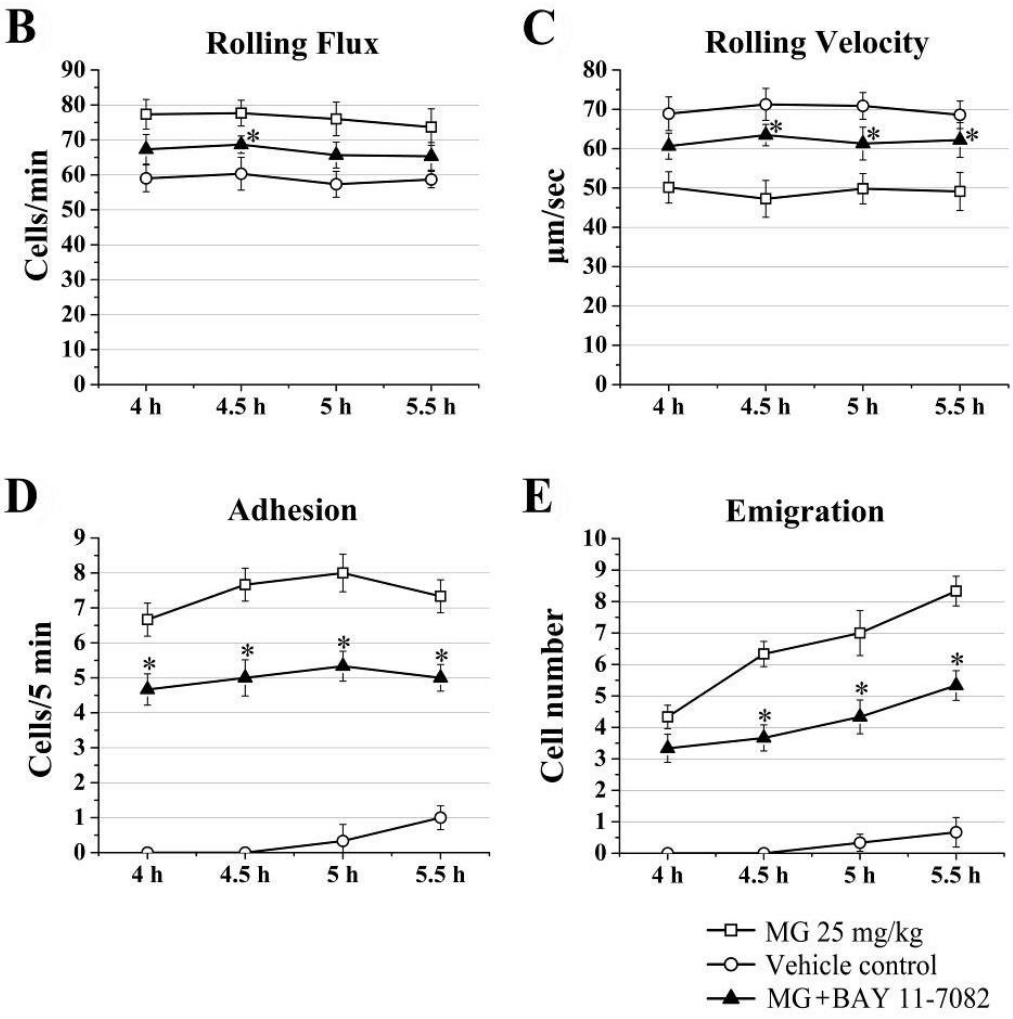

Figure 3-12. Effect of NF-κB inhibition on MG-induced endothelial adhesion molecule expression and leukocyte recruitment. BAY 11-7082 at 20 mg/kg was i.p. injected to the mice 30 min before 25 mg/kg MG administration. The vehicle control group was injected with the same concentration of the solvent for BAY 11-7082. After 4-h MG injection, the mouse cremaster muscle was prepared for intravital microscopy. The muscle samples were then collected and processed for immunostaining after 1.5 h intravital microscopy. The brown staining on the ECs of cremasteric postcapillary venules reveals the expression levels of P-selectin, E-selectin and ICAM-1 (Magnification: 400×) in the upper, middle and lower panels respectively (A). The inhibitory effects of BAY 11-7082 on MG-induced leukocyte rolling flux (B), rolling velocity (C), the number of adherent leukocytes (D) and the number of emigrated leukocytes (E) were determined. Values in B—E are means ± SEM (n=3). *, $P < 0.05$ compared with 25 mg/kg MG treatment group without BAY 11-7082.

3.5 Discussion

In the present study, using intravital microscopy, immunohistochemistry and functional blocking antibodies *in vivo*, we investigated the role of EC adhesion molecules P-selectin, E-selectin, ICAM-1 in leukocyte recruitment induced by exogenous MG. We applied MG locally to healthy mice to induce leukocyte recruitment in cremasteric microvasculature. MG-induced leukocyte recruitment is neutrophil-dominant, MG dose- and time-dependent; the decrease of leukocyte rolling velocity, and the increases of leukocyte rolling flux, adhesion and emigration are MG dose-dependent. MG treatment upregulates the expression of EC adhesion molecules P-selectin, E-selectin and ICAM-1, but not VCAM-1. Functional blocking studies confirmed that the expression of P-selectin and E-selectin is responsible for the decreased leukocyte rolling velocity and increased leukocyte rolling flux, respectively, and ICAM-1 upregulation is important for leukocyte adhesion. We show that the activation of NF-κB is involved and contributes to MG-induced endothelial adhesion molecule expression and leukocyte recruitment and that the effect of MG is, at least in part, directly through its action on ECs.

Accumulating data from clinical and experimental studies suggest that increased formation of MG is linked to the development of diabetic vascular complications and the dysfunction of various cells including ECs, neutrophils and vascular smooth muscle cells that are associated with vascular damage [31, 70, 251]. Plasma MG levels in healthy humans are 1 μmol/L or less but are 2—6 fold higher in diabetes patients [112, 131]. However, plasma MG concentrations as high as 400 μmol/L have been reported in poorly controlled human diabetes patients [282]. It has been suggested that local MG concentration in tissues could be much higher than its plasma levels [136, 197] although the exact local concentration of MG in diabetes patients is unclear. It was reported that cultured cells may produce larger amounts of MG (as much as 310 μM in cell extracts) [283]. In this study, we used MG local treatment to study the acute effect of MG on leucocyte recuitment, and determined the optimal dose and treatment time for MG based on intravital microscopy. We observed that systemic (i.p.) MG treatment for 4 h induced leukocyte recruitment similarly to the recruitment response elicited by local MG treatment but the systemic MG had to be at higher dose to have the same magnitude of recruitment response as local MG treatment (data not shown). Therefore, we used 25 mg/kg MG local injection for 4 h as the acute inflammation model to study the role of EC adhesion molecules in MG-induced leukocyte recruitment. We found that in 25

mg/kg MG-treated mice, plasma MG level was lower than 1.60 μM at all time points (5 min to 4 h) we tested (our unpublished observations) and even in the 50 mg/kg group, the plasma MG level (Table 3-1) was still lower than it was reported in diabetes patients [112, 124]. We also found that low dose of paraformaldehyde, a biological active chemical with active aldehyde group (similarly to MG) in solutions, induced leukocyte recruitment similar to MG but less potent than MG at 4 h, whereas the 4-h treatment with biological inactive D-glucose did not elicit leukocyte recruitment (data not shown), suggesting that the effect of MG in inducing leukocyte recruitment is possibly due to the presence of the biological active aldehyde group in its molecule. This suggests that the effect of MG may be indeed very local, that leukocyte recruitment induced by local MG treatment may not be the same as the systemic MG effect, and that there is a clear relationship between local MG dose and the degree of leukocyte recruitment in the tissue.

In this study, we focused on the role of EC adhesion molecules in MG-induced leukocyte recruitment. The upregulated EC adhesion molecules are the biomarkers of endothelial activation and dysfunction [284, 285] and the indication of the progression of diabetic complications in type 1 and type 2 diabetes [286-288]. It has been revealed that the role of adhesion molecules is important in the early stage of diabetic vascular complications [256, 289]. Evidence from patients also indicates that the increased expression of adhesion molecules in kidneys is directly associated with endothelial dysfunctions, renal tubular damage, and the progression of diabetic nephropathy [290, 291]. We found the upregulated expression of P-selectin, E-selectin and ICAM-1 but not VCAM-1 after acute MG local treatment. Because neutrophils are the first cells emigrated to the inflammation site, it is not surprising that they are the dominant leukocytes being recruited in tissue after acute MG treatment. We noted that after acute MG treatment, the level of VCAM-1 did not change. VCAM-1 is important for the recruitment of leukocytes other than neutrophils, such as lymphocytes, monocytes, eosinophils and basophils. In our results, these cells consisted of only a small percentage of the recruited leukocytes (Table 3-2). It has been shown that the level of VCAM-1 is increased with the progression of diabetic complications in type 1 and type 2 diabetes patients [292]. The unchanged VCAM-1 level in our experiment may be due to the short treatment time and/or relatively low MG dose. In this line, our experiments indeed found evidence of increased percentage of recruited lymphocyte, monocytes, eosinophils, and basophils with the

increasing MG dose (Table 3-2). Whether VCAM-1 expression and functions are increased as increasing time and dose of MG treatment warrants further investigation.

In this study, the role of each MG-upregulated EC adhesion molecule was determined by functional blocking studies. Our data suggest that acute MG treatment increases leukocyte rolling flux by upregulating P-selectin expression, reduces leukocyte rolling velocity by upregulating E-selectin expression, and increases cell adhesion by upregulating ICAM-1 expression. All these lead to the increased leukocyte-EC interactions that result in leukocyte emigration. How MG increases the expression or functions of these EC adhesion molecules is still unclear, but our data reveal that NF-κB signalling pathway appears to be involved. The activation of various intracellular signalling pathways including NF-κB is known to upregulate the expression inflammatory cytokines and chemokines and endothelial adhesion molecules [246]. Some studies have shown clear evidence that MG activates other signalling pathways such as JNK and p38 MAP kinases in ECs [197, 293]. Other studies have demonstrated that, in various cell types, MG induces the expression and production of cytokines such as TNF-α and IL-8 that are pro-inflammatory and able to induce leukocyte recruitment [266, 267, 294, 295]. In addition, research data from clinical studies show that MG levels are elevated in type 2 diabetes mellitus patients and diabetic nephropathy patients and are related to the increased expression of inflammatory cytokines such as TNF-α, IL-8 and IL-6 [112, 251]. Therefore, it is likely that, in our model system, MG upregulates the expression of EC adhesion molecules and induces leukocyte recruitment in the tissue at least in part through the activation of NF-κB signalling pathway in ECs.

In conclusion, our present study describes the role of EC adhesion molecules P-selectin, E-selectin and ICAM-1 in exogenous MG-induced leukocyte recruitment in local tissue. We demonstrate that increased MG in local tissue dose-dependently reduces leukocyte rolling velocity, increases leukocyte rolling flux and promotes cell adhesion by upregulating the expression of P-selectin, E-selectin and ICAM-1, respectively, and NF-κB is involved in these functional responses induced by MG. MG-induced upregulation of EC adhesion molecules may be important in leukocyte infiltration in the early stage of diabetic vascular complications and that revealing the mechanisms of MG-induced inflammation may unveil the mystery of vascular complications and immune dysfunctions in diabetes and may provide a new clue for possible therapeutic strategies.

CHAPTER 4

REGULATION OF METHYLGLYOXAL-ELICITED LEUKOCYTE RECRUITMENT BY ENDOTHELIAL SGK1/GSK3 SIGNALLING

For the molecular mechanistic study of the phenomena shown in the last chapter, in this chapter, we reveal that endothelial SGK1/GSK3 signalling plays an important regulatory role in MG-elicited adhesion molecule expression on endothelium. Here, we demonstrate SGK1/GSK3 signalling-regulated adhesion molecules expression in ECs as one of the mechanisms underlying MG-elicited leukocyte recruitment.

This chapter has been accepted as a research paper by Yang Su, Syed M. Qadri, Francisco S. Cayabyab, Lingyun Wu and Lixin Liu in *Biochimica et Biophysica Acta (BBA)-Molecular Cell Research*. Contents of this chapter have been adapted/reproduced from the accepted article with permission from the journal *BBA-Molecular Cell Research*. In this study, Y.S. conducted all the experiments, acquired and analyzed all the data, and also participated in the design of the study and manuscript writing.

4.1 Abstract

Excessive levels of the glycolysis metabolite methylglyoxal (MG) elicit enhanced expression of adhesion molecules which foster leukocyte-endothelial cell interactions. Signaling mechanisms of MG-induced leukocyte recruitment, however, remain elusive. To address this, we investigated signal transduction of leukocyte- and endothelial-expressed phosphoinositide 3-kinase (PI3K) effector kinases glycogen synthase kinase 3 (GSK3) and serum- and glucocorticoid-inducible kinase 1 (SGK1) in the regulation of MG-elicited leukocyte recruitment. Using intravital microscopy of mouse cremasteric microvasculature, we demonstrate that GSK3 inhibitors lithium and SB216763 mitigate MG-elicited leukocyte recruitment and microvascular hyperpermeability. In SVEC4-10EE2 endothelial cells, but not in neutrophils, MG transiently activates GSK3 as it reduces inhibitory phospho-GSK3α/β (Ser21/9) which parallels decrease of phospho-Akt at early time points (< 30 min). At later time points (≥ 1 h), MG induces GSK3 deactivation which is dissipated by siRNA silencing of SGK. MG treatment potentiates endothelial SGK1 mRNA, total SGK1, phospho-SGK1 and phospho-NDRG1. The SGK1 inhibitor GSK650394 attenuates MG-elicited leukocyte recruitment. Pharmacological inhibition or silencing endothelial GSK3 or SGK attenuates MG-triggered nuclear factor (NF)-κB activity. Inhibition of SGK1 or GSK3 mitigates the expression of endothelial adhesion molecules P- and E-selectins and ICAM-1. Silencing SGK blunts MG-triggered redox-sensitive phosphorylation of endothelial transcription factor CREB. Moreover, SGK1-dependent CREB activation participates in MG-elicited ICAM-1 upregulation. We conclude that temporal activation of endothelial SGK1 and GSK3 is decisive in MG-elicited upregulation of transcription factors, adhesion molecule expression, and leukocyte-vascular endothelium interactions. This novel regulatory pathway may link excessive MG levels *in vivo* to inflammation, thus, unravelling potential therapeutic targets.

4.2 Introduction

In conditions such as diabetes, which is associated with excessive levels of the glycolysis metabolite methylglyoxal (MG), pathological vascular changes and impaired leukocyte-endothelial cell interactions contribute to the pathophysiology of inflammatory sequelae [253, 296]. Contrary to the widely documented cytotoxic effects of MG, various studies have reported the relative safety of its treatment *in vivo* [297, 298] in addition to its anti-cancer [297, 299-301], anti-

microbial [302] and anxiolytic effects [303]. Ramifications of excessive levels of MG include increased expression of adhesion molecules on leukocytes and endothelial cells which fosters redox-sensitive leukocyte recruitment [75, 153, 255, 304]. MG modulates immune functions by stimulating macrophages [294], suppressing T-cell functions [265], triggering neutrophil apoptosis [255] and inducing cytokine production [267]. Putative signalling mechanisms that regulate leukocyte-endothelial interactions associated with excessive MG levels, however, remain elusive.

Phosphoinositide 3-kinases (PI3K) are crucial signal transducers in leukocyte recruitment and microvascular leakage during inflammation [305, 306]. The glycogen synthase kinase GSK3 is a pleiotropic serine/threonine kinase and critical downstream effector, in addition to Akt, of PI3K signalling [307]. Both Akt and serum- and glucocorticoid-inducible kinase 1 (SGK1) phosphorylate and inactivate GSK3 [308, 309]. GSK3 regulates glucose homeostasis and is inhibited by the stimulation of insulin receptors [307], thus playing a crucial role in energy metabolism. Remarkably, GSK3 is critical in inflammatory processes by playing either a positive or negative regulatory role [310]. GSK3 was previously shown to participate in leukocyte motility [311] and survival [312]. Interestingly, endothelial GSK3 was reported to regulate E-selectin expression [313] and vascular permeability [314], thus highlighting the significance of GSK3 signalling in non-hematopoietic endothelial cells. The GSK3 inhibitors lithium and SB216763 increase the inhibitory phosphorylation of GSK3 (Ser-21/9) and have been widely used to study putative functions of GSK3 [315].

Similar to Akt, the ubiquitously expressed SGK1 is activated by PI3K and phosphoinositide-dependent kinase-1 (PDK1) and is genomically regulated by a wide array of stimuli [316] including hyperglycemia [317]. In addition to its regulatory role in insulin secretion [318], SGK1 was previously shown to affect helper T-cell function [236], macrophage polarization [237] and regulation of neutrophil apoptosis [238] alluding to its role in immunity. Beyond the regulation of endothelial cell survival, migration and vascular remodelling [239, 240], the functions of endothelial-expressed SGK1 are not well understood. Noticeably, SGK1 was shown to activate nuclear factor-κB (NF-κB) [241] and cyclic AMP response element-binding protein (CREB) [242], two transcription factors that are important in mediating inflammatory responses. The small-

molecular inhibitor GSK650394 formulated for *in vivo* use is known to potently suppress the enzymatic activity of SGK1 [319].

SGK1- and GSK3-dependent signalling, therefore, lies at the mechanistic interface of both hyperglycemic pathophysiology and inflammation. In this study, using targeted gene silencing and pharmacological inhibition, we elucidate the regulatory role of SGK1 and GSK3 signalling on endothelial transcription factors and adhesion molecule expression, and use intravital microscopy to unravel their role in MG-triggered leukocyte-endothelial cell interactions *in vivo*.

4.3 Material and methods

Mice and intravital microscopy

Male C57BL/6 mice (Charles River, Saint-Constant, QC, Canada) aged between 8 and 12 wk-old were used in this study with the approval of animal protocols from UCACS (# 20070028) at the University of Saskatchewan. Mice were anesthetised using an i.p. injection of 10 mg/kg xylazine (Bayer, Toronto, ON, Canada) and 200 mg/kg ketamine hydrochloride (Rogar, Montreal, QC, Canada). The mouse cremaster muscle preparation was used to study dynamic leukocyte-endothelial interactions in microvasculature as described previously [75, 153, 306]. Velocity of rolling leukocytes (μm/sec), and the number of adherent (cells/100-μm venule), and emigrated leukocytes (cells/443×286 μm^2 field) were determined in the cremasteric postcapillary venule (25−40 μm diameter) using video playback analysis [75, 153, 306]. MG-triggered microvascular leakage was determined in postcapillary venules of the cremaster muscle by intravital microscopy measuring fluorescence intensity of FITC-labelled BSA (25 mg/kg b.w. i.v.; Sigma) inside and outside the vessel as described previously [153]. Where indicated, MG (50 mg/kg b.w. or 100 μM; Sigma, Oakville, ON, Canada), SB216763 (10 mg/kg b.w. or 20 μM; Sigma), lithium (LiCl, 20 mg/kg b.w.; Sigma), BAY11-7082 (20 mg/kg; Sigma) or GSK650394 (50 mg/kg b.w.; Sigma) were administered by an intrascrotal injection or superfusion.

Cell culture and gene silencing

Murine microvascular SVEC4-10EE2 endothelial cell line cells (EE2 ECs; ATCC, Manassas, VA) were cultured as described earlier [320]. Where indicated, Tempol (300 μM; Sigma) and other

pharmacological modulators were added at specified concentrations. Gene knock-down was accomplished by a 48-h transfection of EE2 ECs with siRNA specifically targeting GSK3 (Cell Signalling), CREB (Cell Signalling) and SGK (Santa Cruz) and by using siRNA transfection medium and reagent (Santa Cruz) as described previously [321]. The control cells were transfected with negative control scrambled siRNA (Santa Cruz) having no homology to any known RNA sequence.

Neutrophil isolation

Neutrophils from murine femurs and tibia were isolated using 3-step Percoll (GE Healthcare, Uppsala, Sweden) gradient (72%, 64% and 52%) centrifugation at 1060 g for 30 min as described [320].

FACS analysis

Neutrophil Mac-1 expression was determined using fluorescent anti-Mac-1 antibody (Anti-mouse CD11b FITC; clone M1/70; eBioscience) or its respective isotype control (Rat IgG2bκ FITC; eBioscience) using a previously reported protocol [322].

Immunoblotting

ECs or cremaster tissue homogenates were lysed using Phosphate Extraction Reagent (Novagen) or Nuclear Extraction Kit (Cayman). Proteins were solubilized in Laemmli buffer and resolved by 8−10% SDS-PAGE, and thereafter transferred to a nitrocellulose membrane and immunoblotted as described previously [320]. Primary antibodies (1:1000) were used against the following proteins of interest: CREB, GSK3 and phospho-GSK3-Ser-21/9 (Cell Signalling); phospho-CREB and phospho-GSK3-Tyr-279/216 (Millipore), Akt and phospho-Akt-Ser-473 (BD Pharmingen); P-selectin (LifeSpan Biosciences); E-selectin, ICAM-1, and SGK1 (Abcam); NDRG1 and phospho-NDRG1-Thr346 (Cell signalling) and phospo-SGK1-Thr-256 (Santa Cruz). Intensity values for the proteins were normalized to β-actin using anti-β-actin antibody (Santa Cruz).

Real-time PCR

RT-PCR was performed to determine SGK1 mRNA expression as described previously [264]. Briefly, RNA was isolated from the cells using RNA isolation kit (Qiagen) and reverse-transcribed

using reverse transcription kit (Qiagen). RT-PCR was carried out by SYBR green PCR kit (Qiagen) in an iCycler iQ apparatus (Bio-Rad, Hercules, CA) with primers targeting SGK1 (QT02379685; Qiagen), ICAM-1 (QT00155078; Qiagen) and β-actin (QT00095242; Qiagen). All PCRs were performed in triplicate and ran for 45 cycles at 95 ℃ for 30 sec, 55 ℃ for 30 sec, and 72 ℃ for 40 sec. The PCR product that increased within 30 cycles are considered as positive results.

Immunohistochemistry

Determination of adhesion molecule (E- and P-selectins and ICAM-1) expression in whole cremaster muscle was performed using the same primary antibodies in immunoblotting and a previously described method [75].

Analysis of NF-κB activity

After the indicated treatments, whole cremasteric tissue and EE2 ECs were subjected to nuclear extraction with Nuclear Extraction Kit (Cayman). Equal amounts of nuclear extracts were loaded on a 96-well plate of the NF-κB p65 Transcription Factor Activation Assay Kit (Abcam) and the manufacturer's instructions were followed.

Confocal imaging

EE2 ECs treated under different conditions (as indicated in the Results) were fixed using 4% paraformaldehyde for 30 min, washed twice with PBS, blocked for 1 h with 5% goat serum (Abcam) and then incubated overnight at 4 ℃ with antibodies against P-selectin (1:100; RB40.34; BD Pharmingen), E-selectin (1:100, 9A9, a gift from Dr. Paul Kubes, University of Calgary, AB, Canada) or ICAM-1 (eBioscience). After washing, the slides were incubated for 1 h with fluorescence goat anti-rat antibody (Alexa Fluor 488; Invitrogen) and cells were washed, permeabilized with 0.1% Triton-X-100 and stained with Hoechst 33342 (Invitrogen). The slides were mounted in ProLong® Gold Antifade Reagent (Invitrogen) and observed under a laser scanning confocal microscope (Zeiss, ConfoCor2/LSM510).

Statistical analysis

Data are shown as arithmetic mean ± SEM. Statistical analysis was made using Student *t* test or ANOVA with Tukey's post-hoc comparison test. *n* denotes the number of different mice, different

batches of cremasteric tissues or ECs studied in each group. Values of $p < 0.05$ were considered statistically significant.

4.4 Results

Inhibition of GSK3 ameliorates MG-induced upregulation of endothelial adhesion molecules, leukocyte recruitment and microvascular leakage

Firstly, we explored the effect of pharmacological GSK3 inhibitors SB216763 and lithium on MG-elicited leukocyte recruitment. The representative intravital images of cremasteric microvasculature are depicted in Fig. 4-1A. Both inhibitors themselves had no effect on leukocyte recruitment (data not shown). Fig. 4-1B shows increased numbers of adherent and emigrated leukocytes after MG treatment compared to saline treatment. Pretreatment with SB216763 or lithium significantly attenuated MG-induced increases in adherent and emigrated cells. Treatment with SB216763 or lithium significantly restored MG-triggered reduction of leukocyte rolling velocity (Fig. 4-1B). To determine whether pharmacological inhibition of GSK3 modulates microvascular permeability during leukocyte recruitment, we measured fluorescence changes of FITC-conjugated albumin inside and outside cremasteric postcapillary venule. Permeability index analysis revealed that superfusion of MG on the cremaster muscle increased microvascular permeability, an effect that was significantly inhibited by co-superfusion with SB216763 (Fig. 4-1C). We further examined whether GSK3 inhibition modulated the expression of endothelial adhesion molecules P- and E-selectins and ICAM-1. Histological evaluation of whole cremasteric tissue revealed enhanced expression of P- and E-selectins and ICAM-1 following treatment with MG, an effect that was blunted by treatment with SB216763 (Fig. 4-1D). These findings were further corroborated in murine EE2 ECs by silencing GSK3 with siRNA or treatment with SB216763. To this end, treatment of EE2 ECs with MG enhanced the expression of P- and E-selectins and ICAM-1, an effect that was significantly reduced by SB216763 or GSK3 silencing but not by the negative control siRNA (Fig. 4-1E).

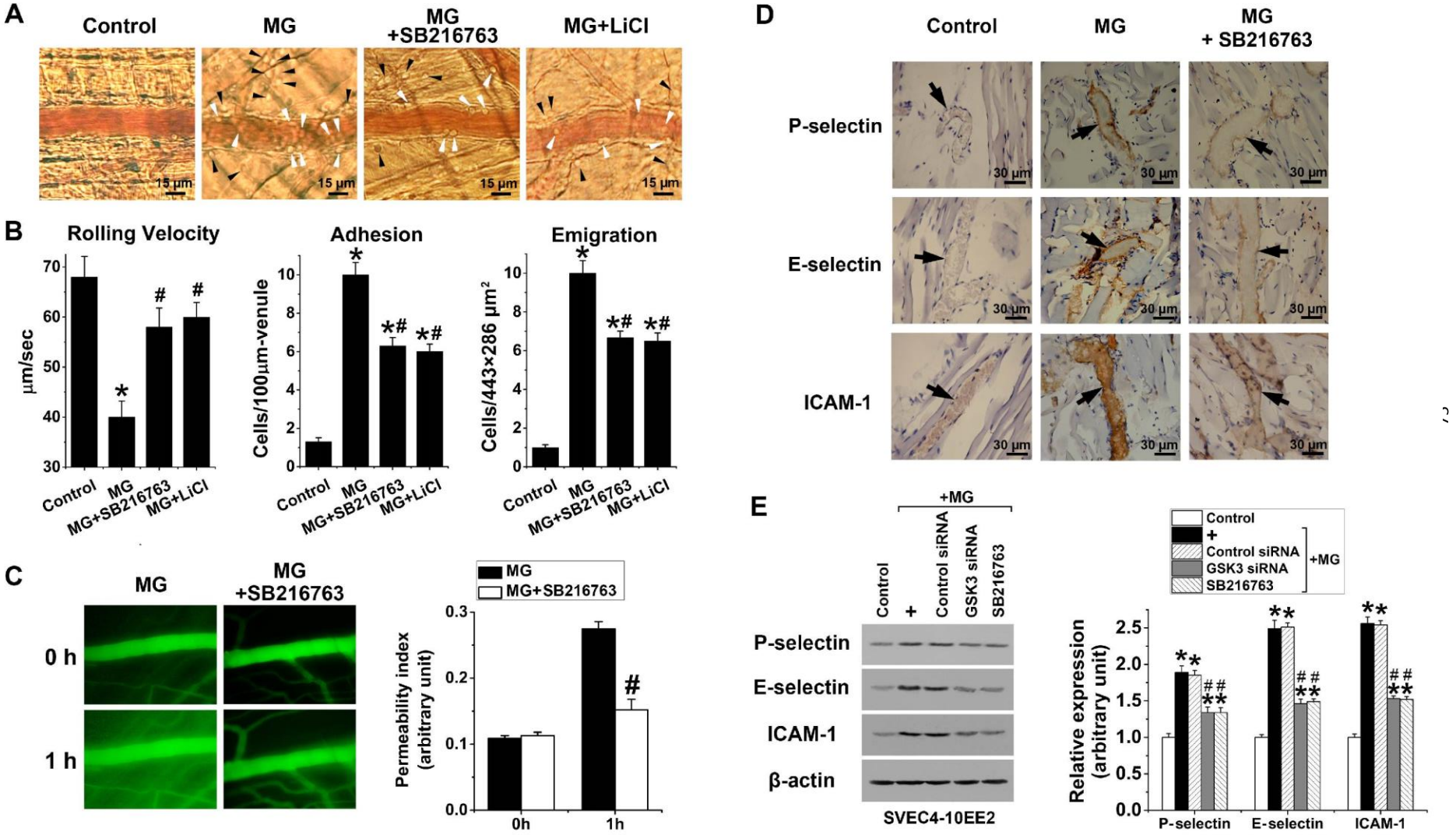
A
Control
MG
MG +SB216763
MG+LiCl
15 μm
B
Rolling Velocity
μm/sec
Adhesion
Cells/100μm-venule
Emigration
Cells/443×286 μm²
Control
MG
MG+SB216763
MG+LiCl
C
MG
MG +SB216763
0 h
1 h
MG
MG+SB216763
Permeability index (arbitrary unit)
0h
1h
D
Control
MG
MG + SB216763
P-selectin
E-selectin
ICAM-1
30 μm
E
+MG
Control
+
Control siRNA
GSK3 siRNA
SB216763
P-selectin
E-selectin
ICAM-1
β-actin
SVEC4-10EE2
Relative expression (arbitrary unit)

Figure 4-1. GSK3 inhibition ameliorates methylglyoxal-induced leukocyte recruitment, microvascular leakage and adhesion molecule upregulation. (A) Representative intravital images with adherent (white arrowheads) and emigrated (black arrowheads) leukocytes and (B) means ± SEM (n=6) of leukocyte rolling velocity (μm/sec), adherent (cells/100-μm venule) and emigrated (cells/443×286 μm2 field) leukocytes in mouse cremasteric postcapillary venules determined 4 h after an intrascrotal injection of saline (Control), MG (50 mg/kg) or co-treatment of MG with SB216763 (10 mg/kg) or lithium (20 mg/kg), both inhibitors administered 30 min prior to MG. (C) Representative fluorescence intravital images and means ± SEM (n=6) of permeability index analysis of mouse cremasteric postcapillary venules showing the leakage of FITC-conjugated BSA before (0 min) and 1 h after superfusion with MG (100 μM) alone or superfusion with SB216763 (20 μM) 30 min prior to and during 1-h MG superfusion. (D) Representative immunohistochemistry showing the staining of P-selectin, E-selectin and ICAM-1 determined in mouse cremasteric endothelium 4 h after an intrascrotal injection of saline (Control) or MG (50 mg/kg) or co-treatment of MG with SB216763 (10 mg/kg, intrascrotal, 30 min prior to MG). Arrow indicates cremasteric venule. (E) Original Western blot and means ± SEM (n=4) showing the expression of P-selectin, E-selectin and ICAM-1 (relative to β-actin) in EE2 ECs in the absence (Control) or in the presence of MG without (+) or treated with negative control siRNA, GSK3-targeted siRNA or SB216763 (20 μM, 30 min prior to the addition of MG). * ($p<0.05$) from Control. # ($p < 0.05$) from MG alone.

MG elicits acute and transient endothelial GSK3 activation

In view of the modulatory effects of GSK3 inhibitors on MG-elicited leukocyte recruitment, we studied the effect of MG on endothelial GSK3 downstream of PI3K signaling. To elucidate the activation of GSK3 by MG in EE2 ECs, we analyzed time-dependent changes in inhibitory (Ser-21/9) and activational (Tyr-279/216) GSK3α/β phosphorylation. As a result, MG treatment of EE2 ECs elicited a significant and transient reduction in Ser-21/9 and increase in Tyr-279/216 GSK3α/β phosphorylation at 15 min, with both phosphorylation returning to the basal level at 30 min. After 1−4 h of MG treatment, Ser-21/9 phosphorylation was significantly increased and Tyr-279/216 phosphorylation was significantly reduced (Fig. 4-2A). Fig. 4-2B shows that exposure of MG-treated EE2 ECs to SB216763, completely abrogated MG-induced GSK3 activation (reduced Ser-21/9 and increased Tyr-279/216 phosphorylation) at 15 min without affecting the GSK3

deactivation at later time points (1—4 h), indicative of the specificity of SB216763 in blocking GSK3 activation. To further define the role of Akt, the upstream negative regulator of GSK3, in MG-triggered modulation of GSK3 activity, we determined Akt phosphorylation in MG-treated EE2 ECs. Exposure of EE2 ECs to MG caused a transient and significant reduction of phosphorylated Akt (Ser-473) at 15 and 30 min, but not after 1−4 h MG exposure suggesting the inhibitory effect of MG on Akt in PI3K signalling only at early time points (Fig. 4-2C).

Neutrophil-expressed GSK3 does not participate in MG-induced leukocyte recruitment

We then sought to elucidate the role of neutrophil-expressed GSK3 in leukocyte recruitment by examining the effect of MG on neutrophil GSK3 activity. Treatment of neutrophils with MG for different time points significantly enhanced Tyr-279/216 and significantly reduced Ser-21/9 GSK3 phosphorylation, an effect reaching statistical significance at 30 min following MG exposure (Fig. 4-3A). To elucidate the relevance of GSK3 activation in neutrophils, we tested whether pharmacological GSK3 inhibition modulates the hitherto known effect of MG on the expression of neutrophil β2 integrin Mac-1 [255], the decisive molecule in leukocyte adhesion to endothelial cells [323]. Exposure of neutrophils to MG significantly enhanced Mac-1 expression, an effect that was not modified by SB216763 but was significantly reduced by Tempol, the scavenger of reactive oxygen species (ROS), suggesting that GSK3 in endothelial cells but not in neutrophils is critical in MG-elicited leukocyte recruitment (Fig. 4-3B).

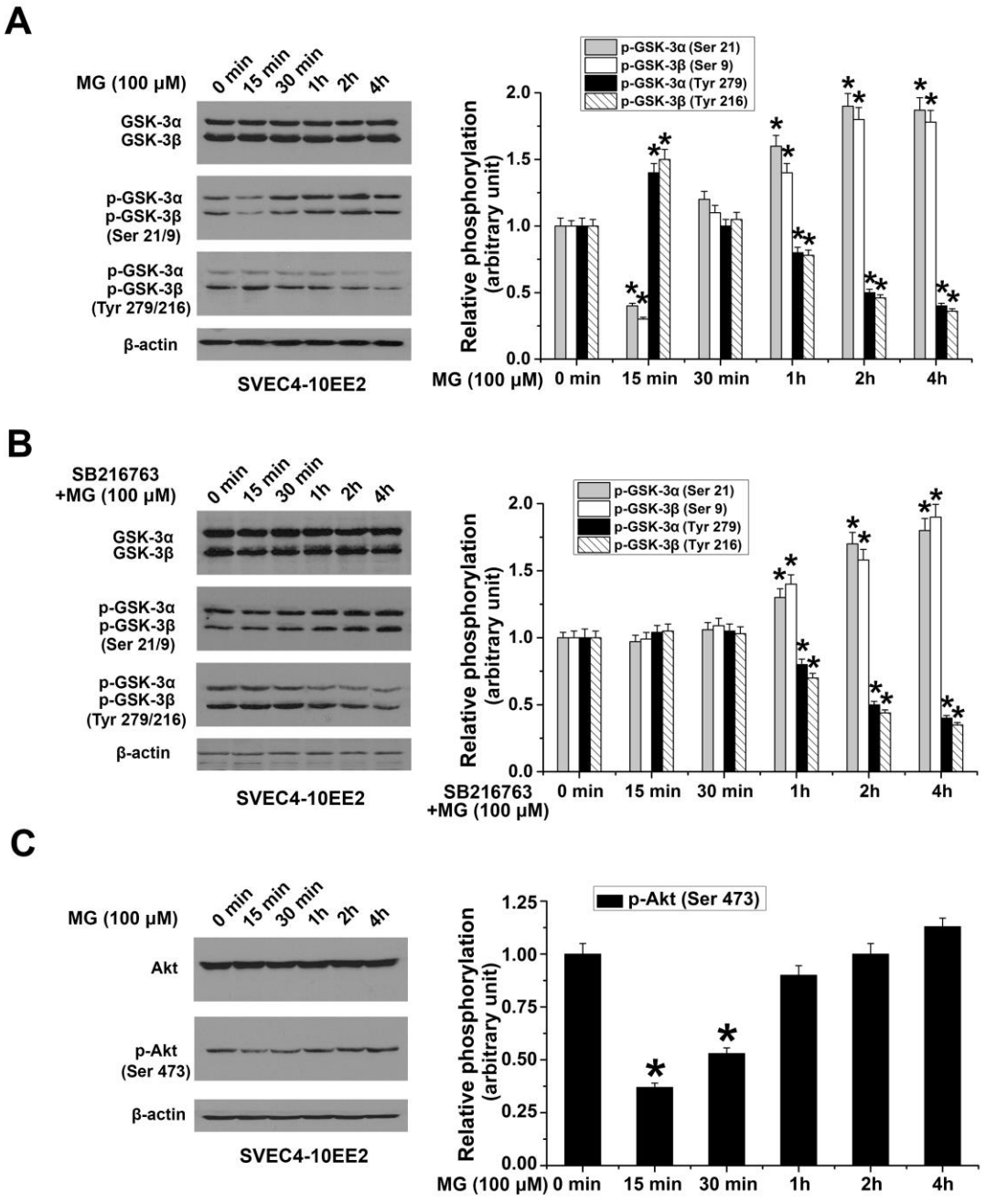

Figure 4-2. Methylglyoxal-sensitive modulation of endothelial Akt and GSK3 phosphorylation. Original Western blot and means ± SEM (n=4) showing total GSK3α/β and phosphorylated GSK3α/β (Ser-21/9 and Tyr-279/216) in the absence (A) or in the presence (B) of 20 μM SB216763 (added 30 min prior to MG treatment) determined in MG-treated (100 μM for 0−4 h) EE2 ECs (relative to β-actin). (C) Original Western blot and means ± SEM (n=4) showing total Akt and phosphorylated Akt (Ser-473) determined in MG-treated (100 μM for 0−4 h) EE2 ECs (relative to β-actin). * ($p<0.05$) from 0 min. * ($p<0.05$) from 0 min.

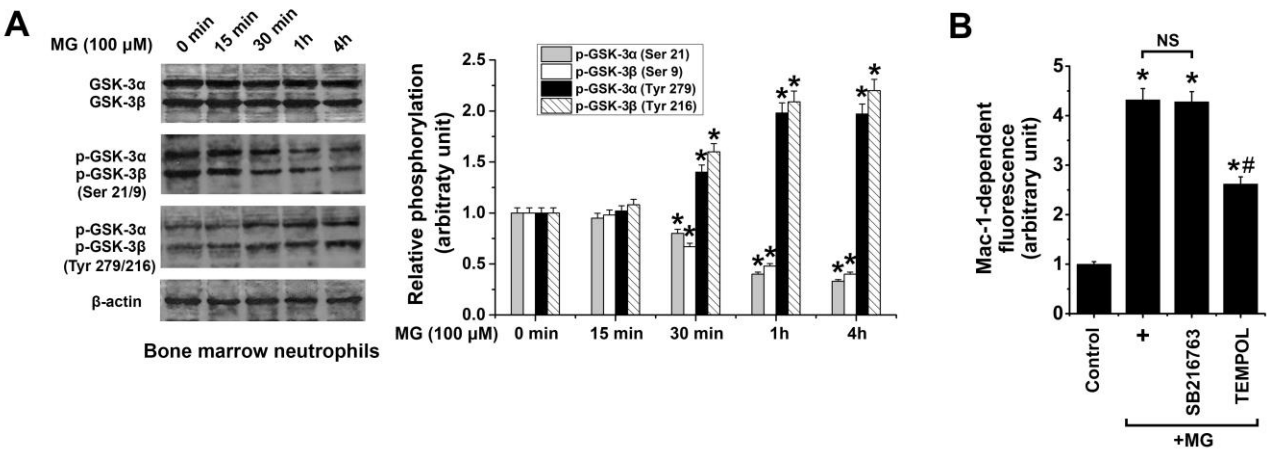

Figure 4-3. Effect of methylglyoxal on neutrophil-expressed GSK3. (A) Original Western blot and means ± SEM (n=4) showing total GSK3α/β and phosphorylated GSK3α/β (Ser-21/9 and Tyr-279/216) determined in MG-treated (100 μM for 0−4 h) bone marrow neutrophils (relative to β-actin). * ($p<0.05$) from 0 min. (B) Means ± SEM (n=4) of Mac-1-dependent fluorescence in neutrophils incubated without (Control) or with MG (100 μM for 1 h) in the absence (+) or in the presence of SB216763 (20 μM) or Tempol (300 μM) added 30 min prior to the addition of MG. * ($p < 0.05$) from Control. # ($p<0.05$) from MG alone.

MG triggers endothelial SGK1 upregulation and temporally late SGK1-dependent GSK3 inactivation

In addition to Akt, GSK3 is phosphorylated and inactivated by SGK1, a PI3K effector kinase [308]. We, therefore, explored the role of SGK1 in MG-induced leukocyte recruitment. First, we elucidated the transcriptional upregulation of endothelial SGK1 triggered by MG. Fig. 4-4A shows that endothelial SGK1 mRNA levels were significantly increased following MG treatment reaching statistical significance after 1 h MG exposure. The levels of phosphorylated (Thr-256) and total endothelial SGK1 were significantly enhanced at 1 h and 2 h, respectively, following MG-treatment of EE2 ECs (Fig. 4-4B). Furthermore, siRNA-targeted silencing of endothelial SGK1 (Fig. 4-4C) did not significantly modify the acute and transient GSK3 activation (15 min) that is depicted in Fig. 4-2A, but abrogated GSK3 deactivation after 1−4 h of MG treatment (Fig. 4-2A and Fig. 4-4D) indicating that SGK1 is not involved in early GSK3 activation but is a crucial upstream molecule in endothelial GSK3 deactivation at 1−4 h of MG treatment.

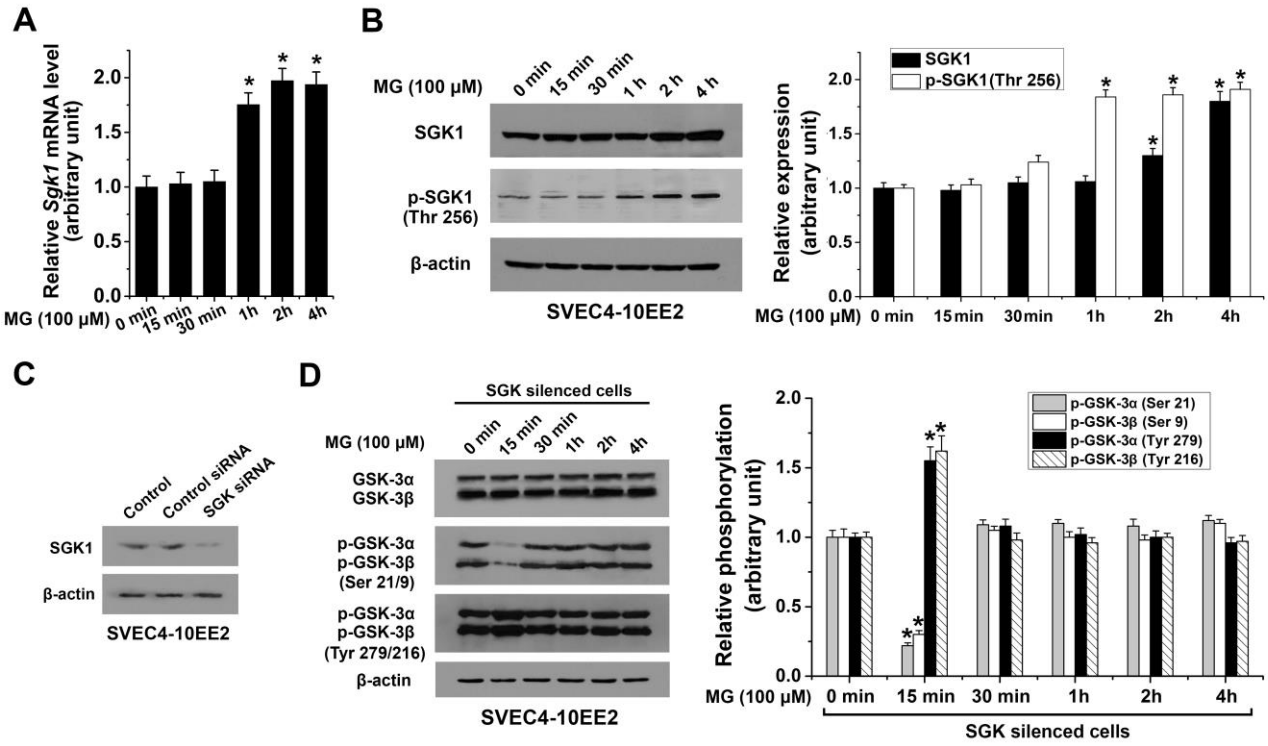

Figure 4-4. Effect of methylglyoxal on endothelial SGK1 expression. (A) Mean ± SEM of mRNA levels (n = 6) encoding SGK1 and (B) original Western blot and means ± SEM (n=4) showing total SGK1 and phosphorylated SGK1 (Thr-256) determined in MG-treated (100 μM for 0−4 h) EE2 ECs (relative to β-actin). (C) SGK-targeted siRNA silencing showing decreased SGK1 protein expression in EE2 ECs. (D) Original Western blot and arithmetic means ± SEM (n=4) showing total GSK3α/β and phosphorylated GSK3α/β (Ser-21/9 and Tyr-279/216) after SGK silencing determined in MG-treated (100 μM for 0−4 h) EE2 ECs (relative to β-actin). * ($p<0.05$) from 0 min.

Endothelial but not neutrophil SGK1 contributes to MG-induced leukocyte recruitment

Further experiments addressed the effect of SGK1 inhibition on MG-elicited leukocyte recruitment *in vivo*. Intravital microscopy analysis of mouse cremasteric microvasculature in Fig. 4-5A revealed that SGK1 inhibitor GSK650394 significantly reduced the number of adherent and emigrated leukocytes triggered by MG treatment. Leukocyte rolling velocity tended to be higher

in mice treated with both MG and GSK650394 compared to mice treated with MG alone, an effect not reaching statistical significance (Fig. 4-5A). MG treatment presented a dramatic upregulation of total and phosphorylated SGK1 in whole cremasteric tissue (Fig. 4-5B), thus, corroborating enhanced abundance of total and phosphorylated SGK1 observed *in vitro* (Fig. 4-4B). Furthermore, the specificity and efficacy of GSK650394 was determined by the phosphorylation of N-myc downstream-regulated gene 1 (NDRG1), a specific target of SGK1 [324, 325]. MG treatment enhanced NDRG1 phosphorylation in whole cremasteric tissue, an effect that was significantly blunted by GSK650394 (Fig. 4-5C) suggesting that GSK650394 specifically targets SGK1 in our model system. We further observed that in neutrophils, MG exposure for different durations had no appreciable changes in total or phosphorylated SGK1 (Fig. 4-5D), suggesting that SGK1 expressed in endothelial cells, but not in neutrophils, is critical in MG-induced leukocyte recruitment. To disclose the underlying mechanisms of SGK1-sensitive leukocyte recruitment, expression of endothelial adhesion molecules was determined in whole cremaster muscle using immunoblotting and visualized in EE2 ECs using confocal imaging. As depicted in Fig. 4-5E and 4-5F, exposure to MG enhanced the expression of P- and E-selectins and ICAM-1 in whole cremaster muscle and in EE2 ECs respectively, an effect abrogated after SGK knockdown or GSK650394 treatment.

MG induces GSK3- and SGK1-dependent activation of NF-κB

Expression of endothelial adhesion molecules is effectively accomplished by activation of transcription factors. Using GSK3- or SGK-targeted siRNA silencing, we examined dynamic changes of NF-κB activation in MG-treated EE2 ECs and whole cremasteric tissue. Silencing GSK3 or SGK significantly reduced NF-κB activity in silenced versus non-silenced MG-treated EE2 ECs, an effect reaching statistical significance at 15 min (for GSK3 silencing) and 1 h (for SGK silencing) respectively (Fig. 4-6A). To substantiate these data *in vivo*, we analysed NF-κB activity in whole cremasteric tissue. Treatment with MG significantly increased NF-κB activity as compared to saline treated cremaster muscle. Pretreatment with SB216763, GSK650394 or the NF-κB inhibitor BAY11-7082 significantly attenuated MG-induced NF-κB activation (Fig. 4-6B). These observations indicate that both GSK3 and SGK are sensitive to MG and decisive in the regulation of MG-triggered NF-κB activity in endothelial cells, albeit at different time points.

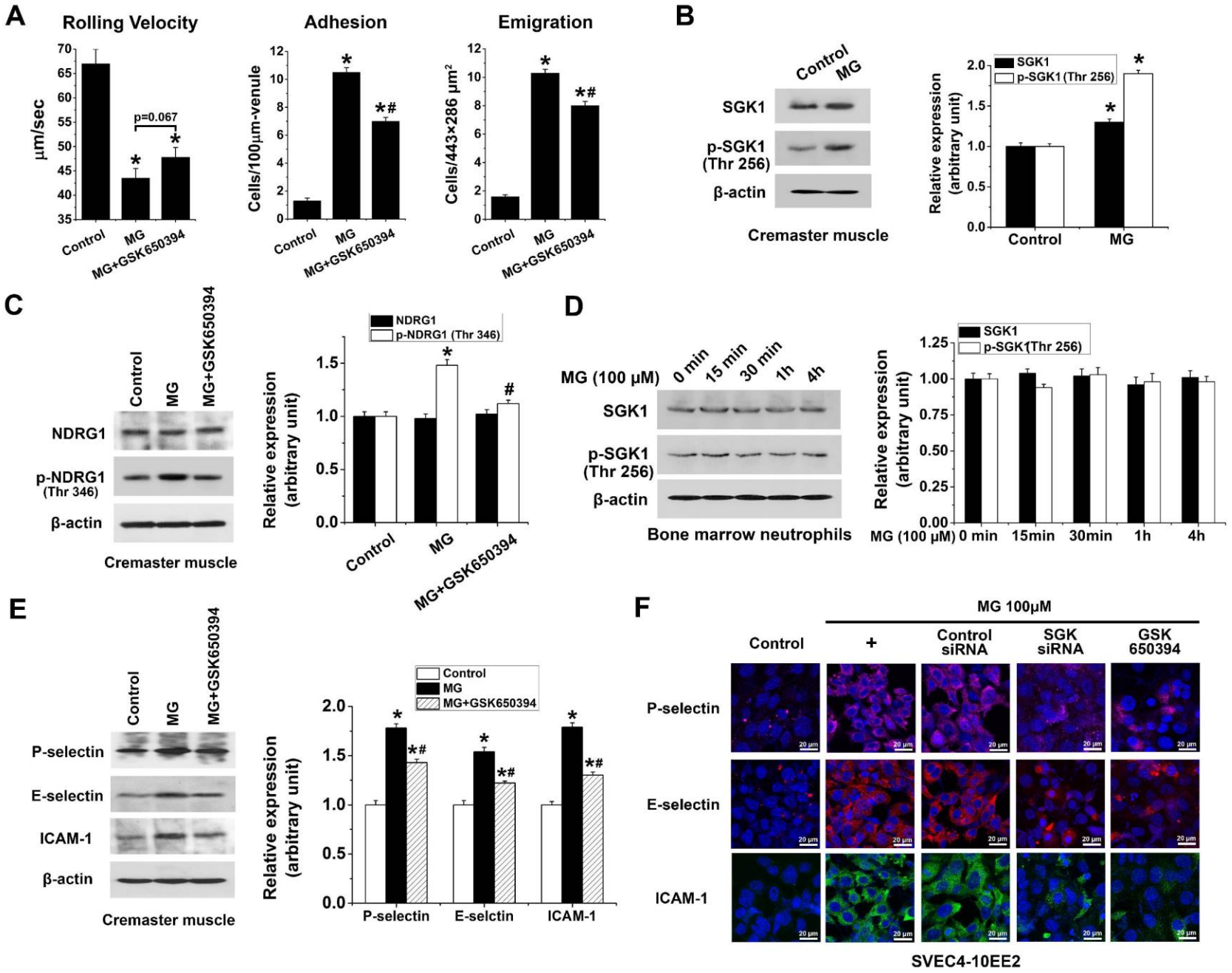
A
Rolling Velocity
μm/sec
p=0.067
Control
MG
MG+GSK650394
Adhesion
Cells/100μm-venule
Emigration
Cells/443×286 μm²
B
Control
MG
SGK1
p-SGK1 (Thr 256)
β-actin
Cremaster muscle
Relative expression (arbitrary unit)
C
NDRG1
p-NDRG1 (Thr 346)
D
MG (100 μM)
0 min
15 min
30 min
1h
4h
Bone marrow neutrophils
E
P-selectin
E-selectin
ICAM-1
F
MG 100μM
Control siRNA
SGK siRNA
GSK 650394
SVEC4-10EE2

Figure 4-5. Participation of SGK1 in methylglyoxal-induced leukocyte recruitment. (A) Means ± SEM (n=6) of leukocyte rolling velocity (μm/sec), adhesion (cells/100-μm venule) and emigration (cells/443×286 μm2 field) determined 4 h after an intrascrotal injection of saline (Control) or MG (50 mg/kg) with or without treatment with GSK650394 (50 mg/kg, 30 min prior to MG). (B) Original Western blot and means ± SEM (n=4) showing total SGK1and phosphorylated SGK1 (Thr-256) determined in whole cremaster tissue (relative to β-actin) 4 h after an intrascrotal injection of saline (Control) or MG (50 mg/kg). (C) Original Western blot and means ± SEM (n=4) showing total NDRG1 and phosphorylated NDRG1 (Thr-346) determined in whole cremaster tissue (relative to β-actin) at 4 h after an intrascrotal injection of saline (Control), or MG (50 mg/kg) with or without treatment with GSK650394 (50 mg/kg, 30 min prior to MG). * ($p<0.05$) from Control. # ($p< 0.05$) from MG alone. (D) Original Western blot and means ± SEM (n=4) showing total SGK1 and phosphorylated SGK1 (Thr-256) determined in MG-treated (100 μM for 0−4 h) neutrophils (relative to β-actin). (E) Original Western blot and means ± SEM (n=4) showing the expression of P-selectin, E-selectin and ICAM-1 determined in whole cremaster tissue (relative to β-actin) in the absence (Control) or MG (50 mg/kg) with or without treatment with GSK650394 (50 mg/kg, 30 min prior to MG). * ($p<0.05$) from Control. # ($p<0.05$) from MG alone. (F) Representative confocal micrographs of P-selectin, E-selectin and ICAM-1 immunostaining in EE2 ECs in the absence (Control) or in the presence of MG (100 μM, 4 h) alone (+) or co-treatment with negative control siRNA, SGK-targeted siRNA or SGK1 inhibitor GSK650394 (20 μM, 30 min prior to MG).

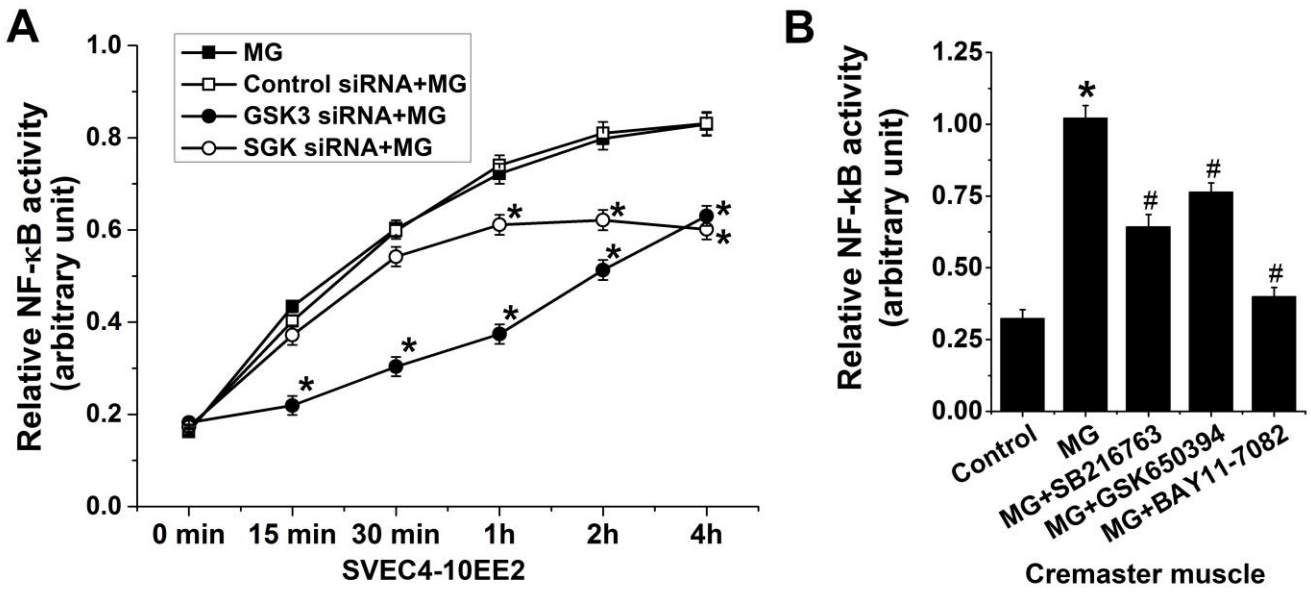

Figure 4-6. SGK1 and GSK3 orchestrate methylglyoxal-induced endothelial NF-κB activation. (A) Means ± SEM (n=4) of relative NF-κB activity determined in MG-treated EE2 ECs (100 μM for 0−4 h) in the absence (MG) or in the presence of prior treatment with negative control siRNA, GSK3-targeted siRNA or SGK1-targeted siRNA. * ($p<0.05$) from negative Control siRNA. (B) Means ± SEM (n=3) of relative NF-κB activity determined in determined 4 h after an intrascrotal injection of saline (Control), MG (50 mg/kg) or co-treatment of MG with GSK650394 (50 mg/kg), SB216763 (10 mg/kg) or BAY11-7082 (20 mg/kg), the inhibitors being administered 30 min prior to MG. * ($p<0.05$) from Control. # ($p<0.05$) from MG alone.

MG-elicited redox-sensitive activation of endothelial CREB transcription factor is regulated by SGK1

We further characterized the transcriptional regulation of endothelial adhesion molecule expression fostered by SGK1 by evaluating endothelial CREB expression and phosphorylation in nucleus after exposure of EE2 ECs to MG. As shown in Fig. 4-7A, the CREB phosphorylation and total CREB expression were significantly increased on exposure to MG, an effect reaching statistical significance at 1 h (phospho-CREB) and 2 h (total CREB) respectively. Silencing SGK in EE2 ECs completely abolished the increased total- and phospho-CREB expression induced by MG (Fig. 4-7A). Silencing CREB (Fig. 4-7B) significantly attenuated MG-triggered ICAM-1

expression, but not the expression of P- and E-selectins (Fig. 4-7C), suggesting that transcriptional regulation by SGK1-dependent CREB is endothelial adhesion molecule-specific. We also tested whether ROS was involved in MG-triggered CREB activation. As shown in Fig. 4-7D, upregulation of total- and phospho-CREB in EE2 ECs triggered by MG was significantly blunted by the treatment with the antioxidant Tempol indicating that CREB activation elicited by MG is ROS-dependent. To corroborate our in vitro findings, we further examined the expression of total and phosphorylated CREB in whole cremasteric tissue. As shown in Fig. 4-7E, MG-elicited upregulation of total- and phospho-CREB in whole cremasteric tissue was significantly mitigated by treatment with GSK650394 or Tempol.

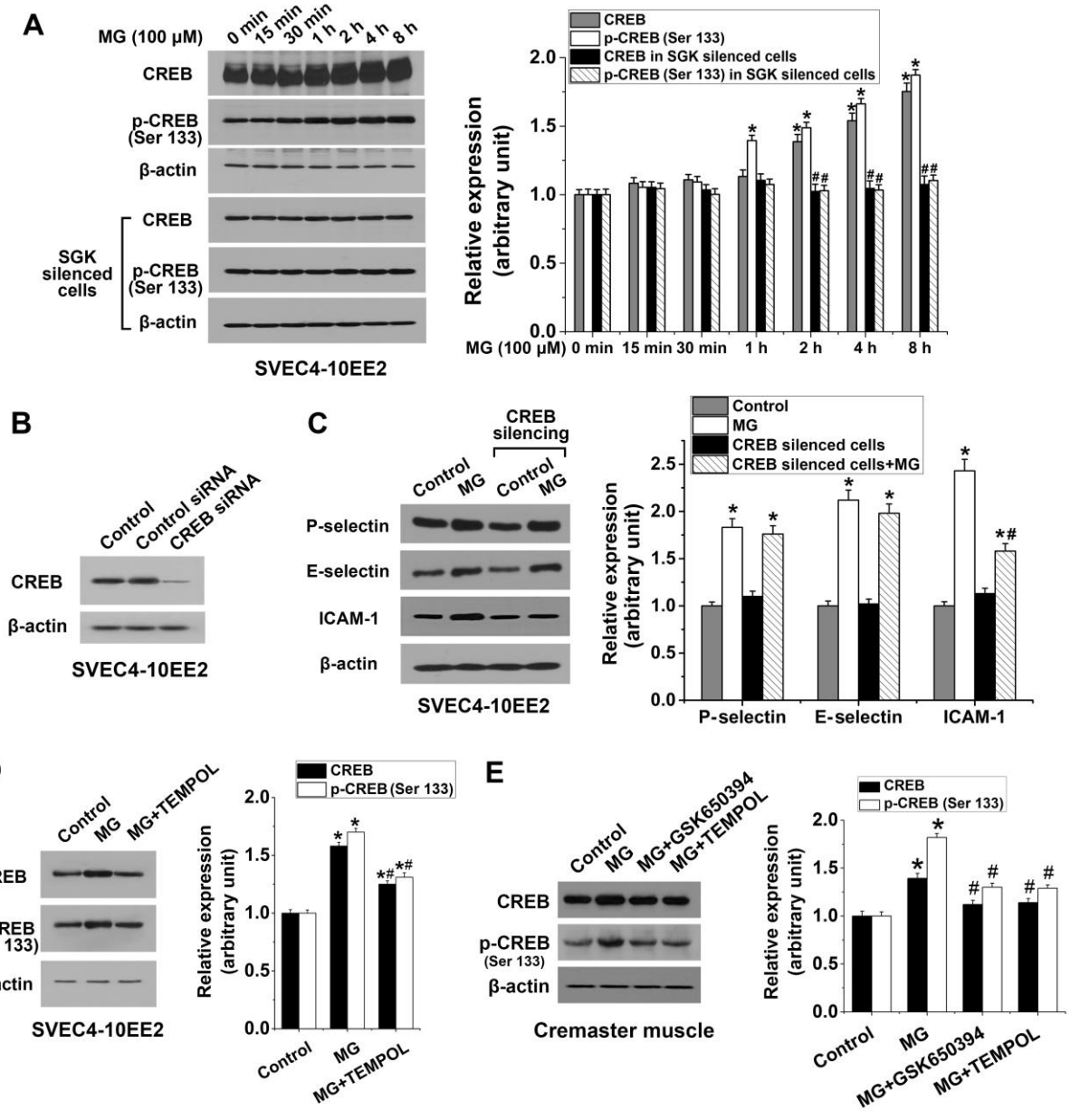

Figure 4-7. Activation of CREB by methylglyoxal. (A) Original Western blot and means ± SEM (n=4) showing total CREB and phosphorylated CREB (Ser-133) determined in MG-treated (100 μM for 0−4 h) EE2 ECs and in MG-treated SGK-silenced EE2 ECs (relative to β-actin). * ($p<0.05$) from 0 min. # ($p<0.05$) from absence of SGK silencing. (B) CREB-targeted siRNA silencing showing decreased CREB protein expression in EE2 ECs. (C) Original Western blot and means ± SEM (n=4) showing P-selectin, E-selectin and ICAM-1 expression (relative to β-actin) in EE2 ECs in the absence (Control) or in the presence of MG (100 μM, 4 h) without or with CREB silencing. * ($p<0.05$) from Control. # ($p<0.05$) from absence of CREB silencing. (D) Original Western blot and means ± SEM (n=4) showing total CREB and phosphorylated CREB (Ser-133) expression determined in EE2 ECs (relative to β-actin) in the absence (Control) or in the presence of MG (100 μM, 4 h) without (MG) or with Tempol (300 μM, 30 min prior to MG). * ($p<0.05$) from Control. # ($p<0.05$) from MG alone. (E) Original Western blot and means ± SEM (n=4) showing total CREB and phosphorylated CREB (Ser-133) expression determined 4 h after an intrascrotal injection of saline (Control), MG (50 mg/kg) or co-treatment of MG with GSK650394 (50 mg/kg) or Tempol (50 mg/kg), both agents administered 30 min prior to MG. * ($p<0.05$) from Control. # ($p<0.05$) from MG alone.

4.5 Discussion

Endothelial adhesion molecules on the vascular lining are requisite elements during leukocyte recruitment at the site of inflammation. The present study unravels signaling mechanisms by which endothelial-expressed GSK3 and SGK1 orchestrate rolling, adhesion and transendothelial migration of leukocytes. By utilizing a previously established mouse model simulating diabetes-associated inflammation [75, 153], we elucidate the hitherto unknown role of endothelial PI3K signaling effectors SGK1 and GSK3 in MG-induced leukocyte-endothelial cell interactions. In this study, we demonstrate the temporal endothelial SGK1 and GSK3 signalling mechanism in MG-induced leukocyte recruitment (depicted in Fig. 4-8). Excessive MG triggers Akt-dependent transient GSK3 activation in endothelial cells, which is responsible for NF-κB activation at early time-points. After 1 h, the GSK3 activity decreases due to the activation of SGK1 and the activated SGK1 maintains the crucial NF-κB activity at later time-points. This temporal activation of GSK3 and SGK1 is pivotal for endothelial adhesion molecules P- and E-selectins and ICAM-1expression

and consequently MG-induced leukocyte recruitment *in vivo*. The activation of SGK1 is also responsible for CREB activation, which regulates the expression of ICAM-1. MG activates GSK3 in neutrophils only after 30 min treatment, an effect, however, not responsible for Mac-1 expression. Both GSK3 and SGK1 in neutrophils are not involved in MG-elicited leukocyte recruitment. The physiological relevance of methylglyoxal (MG) concentrations used in this study is based on previous reports [326, 327]. It has recently been shown that a single administration of 50 mg/kg MG (intrascrotally for 4 h) yielded concentrations of MG at approximately 1.7 μM and 3.9 nmol/mg protein in plasma and tissue respectively [75]. The concentration of MG detected in cremaster tissue is comparable to that detected in other organs [134, 187].

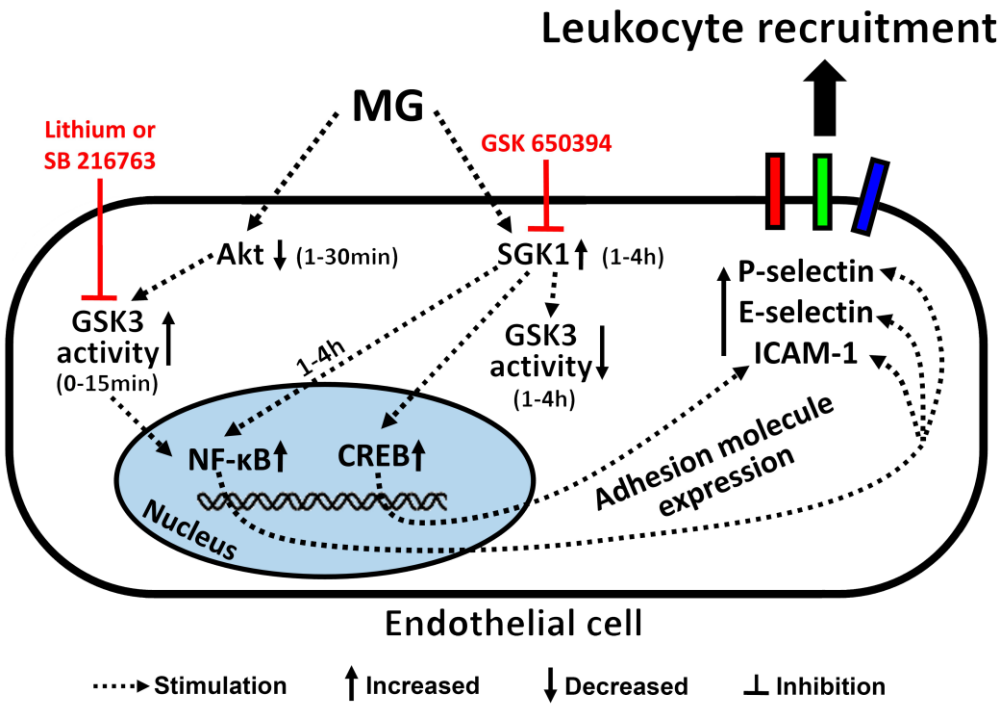

Figure 4-8. Scheme of methylglyoxal-elicited endothelial SGK1/GSK3 signalling. MG first induces Akt-dependent transient GSK3 activation in ECs at early time points (< 30 min). The activation of GSK3 is responsible for NF-κB activation at early time-points. After 1h, MG induces SGK1 activation, which further maintains NF-κB activity and responsible for GSK3 inactivation at later time-points. NF-κB activity is critical for endothelial adhesion molecule expression P-selectin, E-selectin and ICAM-1 expression. The activation of SGK1 is also responsible for CREB activation, which regulates the expression of ICAM-1. The expression of adhesion molecule on ECs finally leads to leukocyte adhesion and transmigration.

Here, we demonstrate that MG-triggered GSK3 activation in endothelial cells, but not in neutrophils, is acute and transient and parallels decreased phosphorylation of the upstream kinase Akt. The inhibitory effect of MG on PI3K signaling and subsequent activation of GSK3 was previously reported in pancreatic beta cells [232]. Similarly, MG was shown to foster platelet aggregation by attenuation of Akt phosphorylation [212]. Consistent with our findings in endothelial cells, short exposure of L6 muscle cells to MG blunted Akt phosphorylation [140]. On the contrary and suggestive of the cell-specific effects of MG, Akt phosphorylation in adipocytes [328] and vascular smooth muscle cells [186] was increased after treatment with MG. Similar to MG treatment, transient activation of GSK3 in endothelial cells was previously observed after treatment with either thrombin or TNFα [329]. Our results also show that following prolonged exposure to MG, inhibitory phosphorylation of endothelial GSK3 was increased. Intriguingly, GSK3 activation in neutrophils, unlike endothelial cells, is enhanced after prolonged exposure to MG.

Our results show that, with transient decrease in inhibitory phosphorylation, GSK3 acquires a proinflammatory activity in the context of MG-induced endothelial activation for leukocyte recruitment which is ameliorated by pharmacological GSK3 inhibition. Paradoxically, we observed that inhibition of SGK1 similarly mitigates leukocyte recruitment *in vivo* given that SGK1 is known to inactivate GSK3. Clearly, endothelial SGK1 is genomically upregulated by exposure to MG and our *in vitro* results show that at later time points (> 1 h), both total and phospho-SGK1 levels are increased in contrast to the acute and transient activation of GSK3. From our *in vitro* results, it is apparent that SGK1 and GSK3 signaling in endothelial cells is temporal with Akt-paralleled GSK3 signaling being decisive at early time points (15 min). At later time points SGK1 silencing virtually abrogated MG-induced phosphorylation of endothelial GSK3 (Ser-21/9). However, biological ramification of this effect on GSK3 is unknown. Furthermore, SGK silencing blunts NF-κB activity at later time points (≥ 1 h) in contrast to GSK3 silencing which curtails NF-κB activation at early time points. It is, therefore, tempting to speculate that at later time points SGK1 directly mediates NF-κB activation independently of its effect on GSK3.

Mechanistically, the role of SGK1 in inflammatory sequelae is largely unknown. Here we unravel that MG treatment potentiates SGK1 transcript levels in endothelial cells. Previously, NADPH

oxidases were shown to be critically involved in the upregulation of SGK1 [241]. MG-induced endothelial SGK1 upregulation is presumably redox-sensitive because MG triggers ROS production which contributes to leukocyte-endothelial cell interactions [152, 153]. Surprisingly, SGK1 was not upregulated in neutrophils exposed to MG in contrast to the effect on GSK3 activation. The role of leukocyte-expressed SGK1, however, is not completely understood. The hematopoietic growth factor granulocyte-macrophage colony-stimulating factor (GM-CSF) was recently shown to augment SGK1 transcript and protein levels in neutrophils and the SGK1 inhibitor GSK650394 reduced GM-CSF-induced neutrophil survival [330]. SGK1 was shown to be effective by regulating Orai1/STIM1 and, thus, influences Ca^{2+}-dependent functions such as cell migration [331]. Along this line, Orai1 was shown to be decisive in neutrophil arrest and migration [332]. From the present study, however, it is unclear whether these mechanisms are operative for SGK1-sensitivity in leukocytes in MG-induced leukocyte-endothelial cell interactions.

Previous observations demonstrated that MG induces NF-κB-dependent upregulation of endothelial adhesion molecules [75]. We observed that targeted gene silencing or pharmacological inhibition of either GSK3 or SGK1 blunted the expression of endothelial adhesion molecules elicited by MG. It is documented that GSK3 inhibition curtails endothelial E-selectin [313], VCAM-1 [329], P-selectin and ICAM-1 expression [333, 334]. Mounting evidence suggests that GSK3 is an essential element for NF-κB activation [223, 329, 335]. Accordingly, our results showed that knockdown of GSK3 gene dramatically reduced both activation of NF-κB and expression of endothelial adhesion molecules, substantiating the *in vivo* effects of GSK3 inhibitors on MG-induced leukocyte recruitment.

Our study is the first to demonstrate the modulatory role of SGK1 in leukocyte recruitment *in vivo* by regulating the expression of endothelial adhesion molecules. SGK1 was previously reported to mediate NF-κB-dependent ICAM-1 expression in mesangial cells [336]. In accordance with our results, knockdown of SGK1 gene was previously shown to attenuate NF-κB activation in renal collecting duct cells [337]. SGK1 phosphorylates and activates NDRG1, a mechanism associated with degradation of NF-κB inhibitory proteins [240]. We demonstrate in this study that upon stimulation with MG, endothelial CREB is phosphorylated in an SGK1-dependent manner. Upon

stimulation with glucocorticoids, the SGK kinases were shown to physically associate with CREB [242]. Recently, CREB was reported to be essential in endothelial ICAM-1 [338, 339] VE-cadherin [340] and VCAM-1 upregulation [338]. Our data show that MG-triggered upregulation of endothelial ICAM-1, but not P- and E-selectins, was at least partially mediated by CREB. Additionally, CREB phosphorylation was documented to be ROS-sensitive [341], a decisive mechanism in MG-elicited leukocyte-endothelial interactions [153]. This mechanism is validated in our present study by the inhibitory effect of the antioxidant Tempol on MG-triggered CREB phosphorylation.

In summary, we provide biological evidence that temporal Akt-dependent GSK3 activity and SGK1 signaling in endothelial cells are pivotal in MG-elicited up-regulation of transcription factors, adhesion molecule expression, and leukocyte interactions with the activated vascular endothelium. Pharmacologically targeting GSK3 or SGK1 alleviates acute inflammation induced by MG, thus, unravelling potential therapeutic targets in inflammation associated with excessive MG levels.

CHAPTER 5

METHYLGLYOXAL MODULATES ENDOTHELIAL NITRIC OXIDE SYNTHASE-ASSOCIATED FUNCTIONS IN EA.HY926 ENDOTHELIAL CELLS

In Chapter 5 and the following Chapter 6, we reveal MG-induced eNOS uncoupling as another mechanism underlying MG-elicited leukocyte recruitment. In this chapter (Chapter 5), we show that MG induces eNOS uncoupling which shifts its function from producing NO to producing superoxide in human endothelial cell line cells. The identification of this novel source of superoxide lays the foundation for investigating the role of eNOS-derived superoxide production in MG-elicited leukocyte recruitment, and the latter will be shown in the next Chapter 6.

This chapter has been published as a research paper by Yang Su, Syed M. Qadri, Lingyun Wu,and Lixin Liu in *Cardiovascular Diabetology 2013 Sep 19; 12:134.* Contents of this chapter have been adapted / reproduced from the published article with permission from the journal *Cardiovascular Diabetology.* In this study, Y.S. conducted all the experiments, acquired and analyzed all the data, and also participated in the design of the study and manuscript writing.

5.1 Abstract

Background

Increased levels of the sugar metabolite methylglyoxal (MG) *in vivo* were shown to participate in the pathophysiology of vascular complications in diabetes. Alterations of endothelial nitric oxide synthase (eNOS) activity by hypophosphorylation of the enzyme and enhanced monomerization are found in the diabetic milieu, and the regulation of this still remains undefined. Using various pharmacological approaches, we elucidate putative mechanisms by which MG modulates eNOS-associated functions of MG-stimulated superoxide ($O_2^{\bullet-}$) production, phosphorylation status and eNOS uncoupling in EA.hy926 human ECs.

Methods

In cultured EA.hy926 ECs, the effects of MG treatment, tetrahydrobiopterin (BH4; 100 µM) and sepiapterin (20 µM) supplementation, NOS inhibition by N^G-nitro-L-arginine methyl ester (L-NAME; 50 µM), and inhibition of peroxynitrite ($ONOO^-$) formation (300 µM Tempol plus 50 µM L-NAME) on eNOS dimer/monomer ratios, Ser-1177 eNOS phosphorylation and 3-nitrotyrosine (3NT) abundance were quantified using immunoblotting. $O_2^{\bullet-}$-dependent fluorescence was determined using a commercially available kit and tissue biopterin levels were measured by fluorometric HPLC analysis.

Results

In EA.hy926 cells, MG treatment significantly enhanced $O_2^{\bullet-}$ generation and 3NT expression and reduced Ser-1177 eNOS phosphorylation, eNOS dimer/monomer ratio and cellular biopterin levels indicative of eNOS uncoupling. These effects were significantly mitigated by administration of BH4, sepiapterin and suppression of $ONOO^-$ formation. L-NAME treatment significantly blunted eNOS-derived $O_2^{\bullet-}$ generation but did not modify eNOS phosphorylation or monomerization.

Conclusion

MG triggers eNOS uncoupling and hypophosphorylation in EA.hy926 ECs associated with $O_2^{\bullet-}$ generation and biopterin depletion. The observed effects of the glycolysis metabolite MG presumably account, at least in part, for endothelial dysfunction in diabetes.

5.2 Introduction

Chronic hyperglycemia fosters endothelial dysfunction that accounts for the pathophysiology of microvascular sequelae in diabetes [342, 343]. The elevated glycolysis metabolite methylglyoxal (MG) has been implicated in vascular complications such as hypertension [344], impaired microcirculation [345] and thrombosis [255] in diabetes. The increased MG affects multi-organ homeostasis by modulating immune cell functions [265], cytokine induction [267], cytosolic Ca^{2+} [213], cellular energy and redox balance [157] and adhesion molecules expression [75] and induces both necrotic [346] and apoptotic cell death [345].

Endothelial nitric oxide synthase (eNOS) is the predominant and constitutively expressed NOS in vascular ECs and catalyzes the reaction for generation of nitric oxide (NO) from L-arginine in the presence of the cofactors tetrahydrobiopterin (BH4) and NADPH [347]. Regulation of eNOS activity is coupled to cytosolic Ca^{2+} [348] whereas the expression is regulated by a wide range of transcriptional and posttranscriptional mechanisms [349]. Alterations of NO balance contribute to the pathophysiology of diabetic complications [350]. Deficiency of either L-arginine or BH4 results in reduced NO but enhanced superoxide ($O_2^{\bullet-}$) production, a functional change of eNOS that is defined as eNOS uncoupling [347]. eNOS uncoupling is associated with increased eNOS monomerization, tyrosine nitration and formation of dihydrobiopterin (BH2) and decreased cellular BH4 [351, 352]. Sepiapterin is a stable precursor of BH4 and serves as a valuable pharmacological agent for the study of eNOS uncoupling due to its high cell permeability as compared to BH4 [353, 354]. $O_2^{\bullet-}$ avidly reacts with NO to form peroxynitrite ($ONOO^-$) which triggers the oxidation of BH4, impairs eNOS activity and induces eNOS uncoupling [347, 351, 355].

Uncoupling of eNOS is the underlying mechanism of endothelial dysfunction associated with cardiovascular conditions such as hypertension, stroke, and heart failure [356, 357]. Recently,

eNOS uncoupling was shown to participate in endothelial dysfunction in diabetic mice [358] and to mediate peripheral neuropathy in diabetic rats [359]. In Zucker diabetic fatty rats, endothelial dysfunction and decreased NO availability were attributed to dissociation of eNOS from HSP90, an effect elicited by increased calpain activity [360]. As a myriad of molecules are dysregulated in diabetes, the specific effects of MG on eNOS uncoupling, however, remain elusive.

Ramifications of elevated MG levels in hyperglycemia include impaired NO production and redox imbalance [115]. Various studies promulgate a possible link between endothelial dysfunction and functional alterations of eNOS after MG treatment. To date, however, discrepant data prevail on MG sensitivity of eNOS functions in different model systems. On the one hand, MG was shown to stimulate transcription of eNOS [361]; while on the other, abundance of eNOS protein was reduced following MG treatment [362, 363]. In contrast, MG was shown to suppress eNOS phosphorylation on serine-1179 without affecting eNOS protein expression [70]. Increased MG levels in preeclamptic vasculature were shown to be coupled with enhanced arginase, LOX-1 and tyrosine nitration [364]. The association between MG-triggered eNOS phosphorylation, eNOS uncoupling, and oxidative stress in vascular endothelial dysfunction, however, remains ill-defined.

The present study explores the mechanisms of MG-induced endothelial dysfunction by examining putative eNOS-associated functions. We elucidate the effects of exogenous BH4 and sepiapterin administration, NOS inhibition and suppression of peroxynitrite ($ONOO^-$) formation on $O_2^{\bullet-}$ generation, eNOS monomerization, cellular biopterin levels, tyrosine nitration, and phosphorylation of eNOS in EA.hy926 ECs *in vitro*.

5.3 Materials and methods

Cell culture and pharmacological treatments

EA.hy926 cells, the hybrid human umbilical vein endothelial cell line cells [365], were obtained from American Type Culture Collection (Rockville, MD, USA) and cultured in Dulbecco's modified Eagle's medium (Cellgro, VA, USA) with 10% fetal bovine serum (Hyclone, UT, USA), 100 U/mL penicillin and 100 μg/mL streptomycin (Amresco, OH, USA) with 5% CO_2 and maximal humidity at 37 ℃. Cells between passage 3 and 6 were used for the experiments. As

indicated in the figure legends, various pharmacological approaches were used to elucidate eNOS-associated functions. To maintain eNOS dimerization, the NOS cofactor 5,6,7,8-tetrahydrobiopterin (BH4, 100 μM; Sigma-Aldrich, Oakville, ON, Canada) or the negative control, a pteridine analogue, 5,6,7,8-tetrahydroneopterin (NH4, 100 μM; Schircks Laboratories, Jona, Switzerland) were freshly-prepared and administered. NH4 has similar antioxidant effects as BH4 but, unlike BH4, is ineffective in restoring uncoupled eNOS [366]. Sepiapterin (20 μM; Cayman, Ann Arbor, MI, USA), a substrate for BH4 synthesis via the pterin salvage pathway, was used to increase cellular BH4 levels [367]. The NOS inhibitor N^G-nitro-L-arginine methyl ester (L-NAME, 50 μM; Sigma-Aldrich), was administered to inhibit uncoupled eNOS-derived $O_2^{\bullet-}$ [258]. For suppression of $ONOO^-$ generation, EA.hy926 cells were treated with a combination of the ROS scavenger 1-oxyl-2,2,6,6-tetramethyl-4-hydroxypiperidine (Tempol, 300 μM; Santa Cruz, Dallas, TX, USA) and NOS inhibitor L-NAME (50 μM) for 24 h prior to the addition of MG [31, 368]. $O_2^{\bullet-}$ reacts with NO at equimolar ratios to generate $ONOO^-$ [31], and from our unpublished observations, pretreatment with a combination of L-NAME and Tempol more potently inhibits $ONOO^-$ formation than pretreatment with either pharmacological agent alone.

Determination of $O_2^{\bullet-}$ production

$O_2^{\bullet-}$ levels were determined using a commercial superoxide detection kit (Enzo, Brockville, ON, Canada) according to the manufacturer's instructions as described previously [369, 370]. The superoxide detection reagent when oxidized produces an orange fluorescent compound which is retained in the cell. Cells were seeded in a 96-well plate and stained with the membrane-permeable and nonfluorescent $O_2^{\bullet-}$ detection probe (5 μM, 30 min, 37 ℃ in the dark). Excessive probe was removed by washing with PBS. The fluorescence in cells was detected using excitation and emission wavelengths of 544 nm and 590 nm respectively. The data are expressed as arbitrary units.

Analysis of biopterin levels by HPLC

Measurement of BH4 and total biopterins was performed by fluorometric HPLC analysis as described previously with slight modifications [258]. After indicated treatments, EA.hy926 cells were lysed in a lysis buffer (pH 7.4; containing 50 mM Tris-HCl, 1 mM DTT and 1 mM EDTA) with 0.1 μM neopterin (Sigma-Aldrich) as an internal recovery standard. The samples were

deproteinated with 10% 1:1 mixture of 1.5 M $HClO_4$ and 2 M H_3PO_4 and centrifuged (12,000 × g for 10 min). The supernatant was split into portions and subjected to acid- and alkali-oxidation respectively. For determination of total biopterins (BH4, BH2 and non-reduced biopterins) by acid-oxidation, 10 µl iodine solution (1% iodine in 2% KI solution) was added into every 90 µl supernatant and for quantification of BH2 and non-reduced biopterins by alkali-oxidation, 10 µl of 1 M NaOH and 10 µl of iodine solution were added to 80 µl supernatant. Following incubation (1 h, room temperature in the dark), the alkali-oxidation samples were acidified with 1 M H_3PO_4, the iodine in both acid- and alkali-oxidation samples was reduced using 5% ascorbic acid (Sigma) and the samples were centrifuged (12,000 ×g for 10 min). The supernatant was collected for HPLC analysis using a Hitachi D-7000 HPLC system (Hitachi, Mississauga, ON, Canada) via Symmetry C18 reverse-phase column with a methanol-water (1.5:98.5, v/v) mobile phase running at 0.5 mL/min. Fluorescence was detected at excitation and emission wavelengths of 348 nm and 444 nm respectively. The level of BH4 was calculated by subtracting BH2 and non-reduced biopterins from total biopterins and expressed as pmol per mg protein. The biopterin levels in NH4-treated cells were calculated without adding 0.1 µM neopterin.

Western blotting

Non-reducing SDS-PAGE was performed to detect eNOS dimers and monomers [258]. Briefly, cultured EA.hy926 cells were harvested and lysed on ice for 30 min by using RIPA buffer (50 mM Tris-HCl, 150 mM NaCl, 1 % NP-40, 0.5% sodium deoxycholate, 0.1 % SDS and protease inhibitors cocktail, pH 8.0). The lysate was centrifuged at 10,000 × g for 10 min, and the supernatant was collected, incubated with 4 × Laemmli buffer without β-mercaptoethanol (200 mM Tris-HCl, 50 % glycerol, 2% SDS, 0.04% bromophenol blue, pH 6.8) at 37℃ for 5 min. Aliquots of cell lysates (50 µg of protein each) were separated on 7% SDS-PAGE. Gels and buffers were equilibrated at 4℃ before electrophoresis, and the buffer tank was placed in an ice bath during electrophoresis to maintain the low temperature. Subsequent to non-reducing SDS-PAGE, the gels were electrotransferred to a nitrocellulose membrane (Bio-Rad, CA, USA), and the blots were probed by primary antibody against eNOS (1:1000; BD Pharmingen, USA) and horseradish peroxidase-conjugated secondary antibody (Santa Cruz) as routine Western blot. In separate gels, total eNOS (1:1000), β-actin (1:1000; Santa Cruz, CA, USA), phospho-eNOS (Ser-1177, 1:1000; BD Pharmingen, CA, USA) and 3-nitrotyrosine (3NT, 1:1000; Enzo) from cell lysates of the same

experiments were detected by routine Western blot under reduced condition. The bands were visualized with enhanced chemiluminescence reagents (GE Healthcare Life Sciences, NJ, USA) and exposed to X-ray film (Kodak scientific imaging film, ON, Canada). Densitometric quantification of the detected bands was performed using Quantity One® Software (Bio-rad). The ratio of eNOS dimer to monomer was normalized to one in the absence of MG.

Statistical analysis

Data are expressed as arithmetic means ± SEM from at least three independent experiments. Statistical analysis was made using one way analysis of variance (ANOVA) with Tukey's post-hoc comparison test. n denotes the number of different batches of cells tested in each treatment group. Values of $p < 0.05$ were considered statistically significant.

5.4 Results

To elucidate the redox imbalance triggered by MG treatment on vascular ECs *in vitro*, we analyzed MG-triggered $O_2^{\bullet-}$ generation using a fluorescence-based assay. Treatment of EA.hy926 ECs with MG (50 – 200 µM) for 2, 4, 6 and 8 h respectively, significantly increased $O_2^{\bullet-}$ production in a concentration- and time-dependent manner (Fig. 5-1A). In another series of experiments, we analyzed the effect of biopterin supplementation (BH4, 100 µM; sepiapterin, 20 µM), pharmacological inhibition of NOS using L-NAME (50 µM) or suppression of $ONOO^-$ formation using combined 24-h pretreatment with Tempol (300 µM) and L-NAME (50 µM) on MG-induced $O_2^{\bullet-}$ production. As shown in Fig. 5-1B, inhibition of NOS, suppression of $ONOO^-$ formation, or supplementation of either BH4 or sepiapterin significantly attenuated MG-induced $O_2^{\bullet-}$ production. Treatment of EA.hy926 cells with the BH4 control NH4 (100 µM), however, did not significantly alter MG-induced $O_2^{\bullet-}$ production (Fig. 5-1B). These results suggest eNOS-derived $O_2^{\bullet-}$ production in MG-treated EA.hy296 ECs.

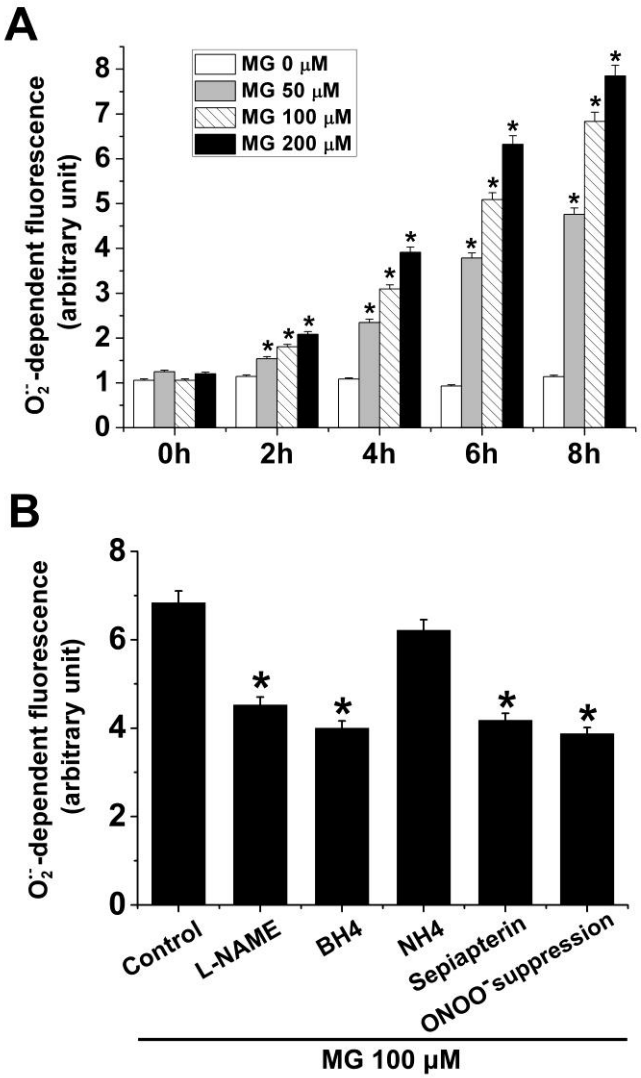

Figure 5-1. Methylglyoxal-stimulated $O_2^{\bullet-}$ production in EA.hy926 ECs. A. $O_2^{\bullet-}$ generation determined in EA.hy296 ECs treated with different concentrations of MG (0, 50, 100 and 200 μM) for 0, 2, 4, 6 and 8 h respectively. Data are arithmetic means ± SEM (n = 6). * indicates significant difference ($p < 0.05$) from the absence of MG (ANOVA). B. $O_2^{\bullet-}$ generation determined in EA.hy296 ECs treated with MG (100 μM) for 8 h in the absence (Control) or in the presence of L-NAME (50 μM), BH4 (100 μM), NH4 (100 μM) or sepiapterin (20 μM) in the last 4 h of MG treatment or 24-h pre-treatment with 300 μM Tempol and 50 μM L-NAME ($ONOO^-$ suppression) prior to the addition of MG. Data are arithmetic means ± SEM (n = 6). * indicates significant difference ($p < 0.05$) from Control (ANOVA).

Next, we explored the effect of MG on eNOS monomerization in EA.hy926 ECs. Treatment of EA.hy926 cells with MG (50 – 200 μM) for 0.5, 2, 4, and 8 h respectively, significantly decreased eNOS dimer/monomer ratio in a concentration- and time-dependent manner (Fig. 5-2A and 5-2B). These results, together with the effect of L-NAME inhibition on MG-induced $O_2^{\bullet-}$ production (Fig. 5-1B), suggest that MG treatment induces eNOS uncoupling in EA.hy926 cells. We further tested the effect of biopterin supplementation, L-NAME addition and suppression of $ONOO^-$ formation on MG-elicited eNOS monomerization. As shown in Fig. 5-2C and 5-2D, treatment of EA.hy926 cells with MG (100 μM) for 8 h significantly reduced eNOS dimer/monomer ratio, an effect that was significantly blunted by the administration of BH4 (100 μM, 4 h), sepiapterin (20 μM, 4 h) or by $ONOO^-$ suppression (300 μM Tempol and 50 μM L-NAME, 24 h). Treatment with L-NAME (50 μM, 4 h) alone or the BH4 control NH4 (100 μM, 4 h) did not modify eNOS dimer/monomer ratio (Fig. 5-2C and 5-2D).

To further elucidate MG-induced eNOS uncoupling, we determined the cellular BH4 levels in EA.hy926 cells following MG treatment. As depicted in Fig. 5-3A, treatment of EA.hy926 cells with MG (50 – 200 μM) for 8 h significantly decreased total cellular biopterin and BH4 levels in a concentration-dependent manner. More importantly, treatment of EA.hy926 cells resulted in a reduction of BH4/total biopterin ratio, an effect reaching statistical significance at 100 μM MG concentration (Fig. 5-3B). We then explored the effect of biopterin supplementation, L-NAME addition and suppression of $ONOO^-$ formation on MG-induced reduction in cellular BH4 levels. As illustrated in Fig. 5-3C, 4-h supplementation of BH4 (100 μM) or sepiapterin (20 μM) in MG-treated EA.hy926 cells significantly increased total cellular biopterin and BH4 levels suggesting that exogenous biopterin repletion dissipated MG-induced reduction in cellular BH4 contents associated with eNOS uncoupling. Suppression of $ONOO^-$, however, did not significantly modify total cellular biopterin levels but significantly increased cellular BH4 levels in MG-treated cells (Fig. 5-3C). Neither the BH4 control NH4 (100 μM) nor L-NAME (50 μM) alone significantly altered cellular BH4 and total biopterin levels (Fig. 5-3C). Similarly, MG-induced reduction of cellular BH4/total biopterin ratio was significantly attenuated by supplementation with BH4 or sepiapterin or by $ONOO^-$ suppression but not by the BH4 control NH4 or by L-NAME alone (Fig. 5-3D).

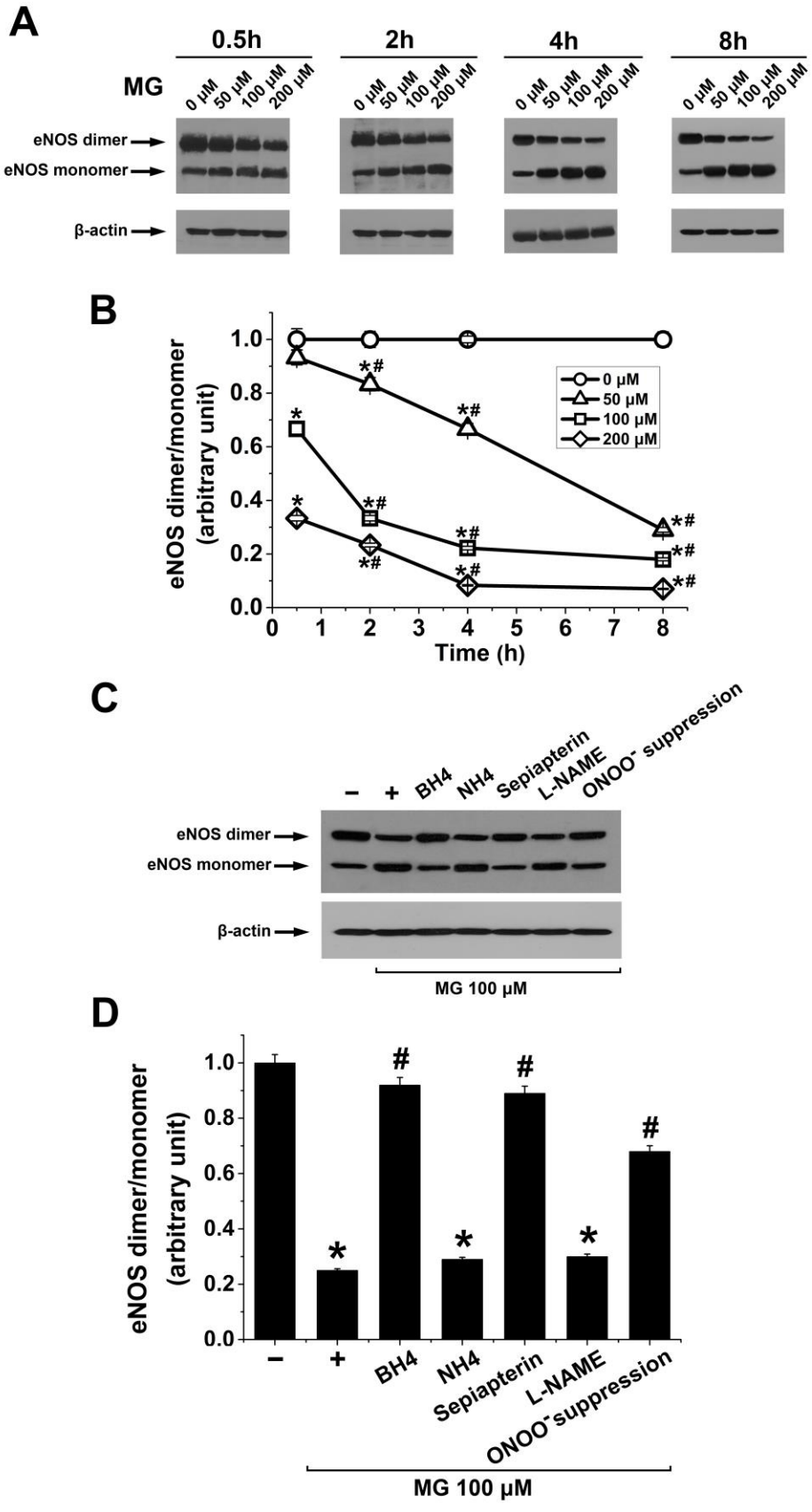
A
0.5h
2h
4h
8h
MG
0 μM
50 μM
100 μM
200 μM
eNOS dimer
eNOS monomer
β-actin
B
eNOS dimer/monomer (arbitrary unit)
Time (h)
0 μM
50 μM
100 μM
200 μM
C
–
+
BH4
NH4
Sepiapterin
L-NAME
ONOO⁻ suppression
eNOS dimer
eNOS monomer
β-actin
MG 100 μM
D
eNOS dimer/monomer (arbitrary unit)
–
+
BH4
NH4
Sepiapterin
L-NAME
ONOO⁻ suppression
MG 100 μM

Figure 5-2. Methylglyoxal-induced eNOS monomerization in EA.hy926 ECs. A and B. Original Western blots (A) and the respective densitometric analysis (B) of the relative abundance of eNOS dimers over eNOS monomers (relative to β-actin) in EA.hy296 ECs treated with different concentrations of MG (0 μM, circles; 50 μM, triangles; 100 μM, squares; and 200 μM, diamonds) for 0.5, 2, 4, and 8 h respectively. Data are arithmetic means ± SEM (A, representative of five experiments; B, n = 5). * indicates significant difference ($p < 0.05$) from the absence of MG (ANOVA). # indicates significant difference ($p < 0.05$) from time 0.5 h (ANOVA).

C and D. Original Western blots (C) and the respective densitometric analysis (D) of the relative abundance of eNOS dimers over eNOS monomers (relative to β-actin) in EA.hy296 ECs incubated in the absence (–) or in the presence of MG (100 μM) for 8 h alone (+) or with 100 μM BH4, 100 μM NH4, 20 μM sepiapterin or 50 μM L-NAME in the last 4 h of MG treatment or with 24-h pre-treatment with 300 μM Tempol and 50 μM L-NAME ($ONOO^-$ suppression). Data are arithmetic means ± SEM (C, representative of four experiments; D, n = 4). * indicates significant difference ($p < 0.05$) from the absence of MG (ANOVA). # indicates significant difference ($p < 0.05$) from MG treatment alone (ANOVA).

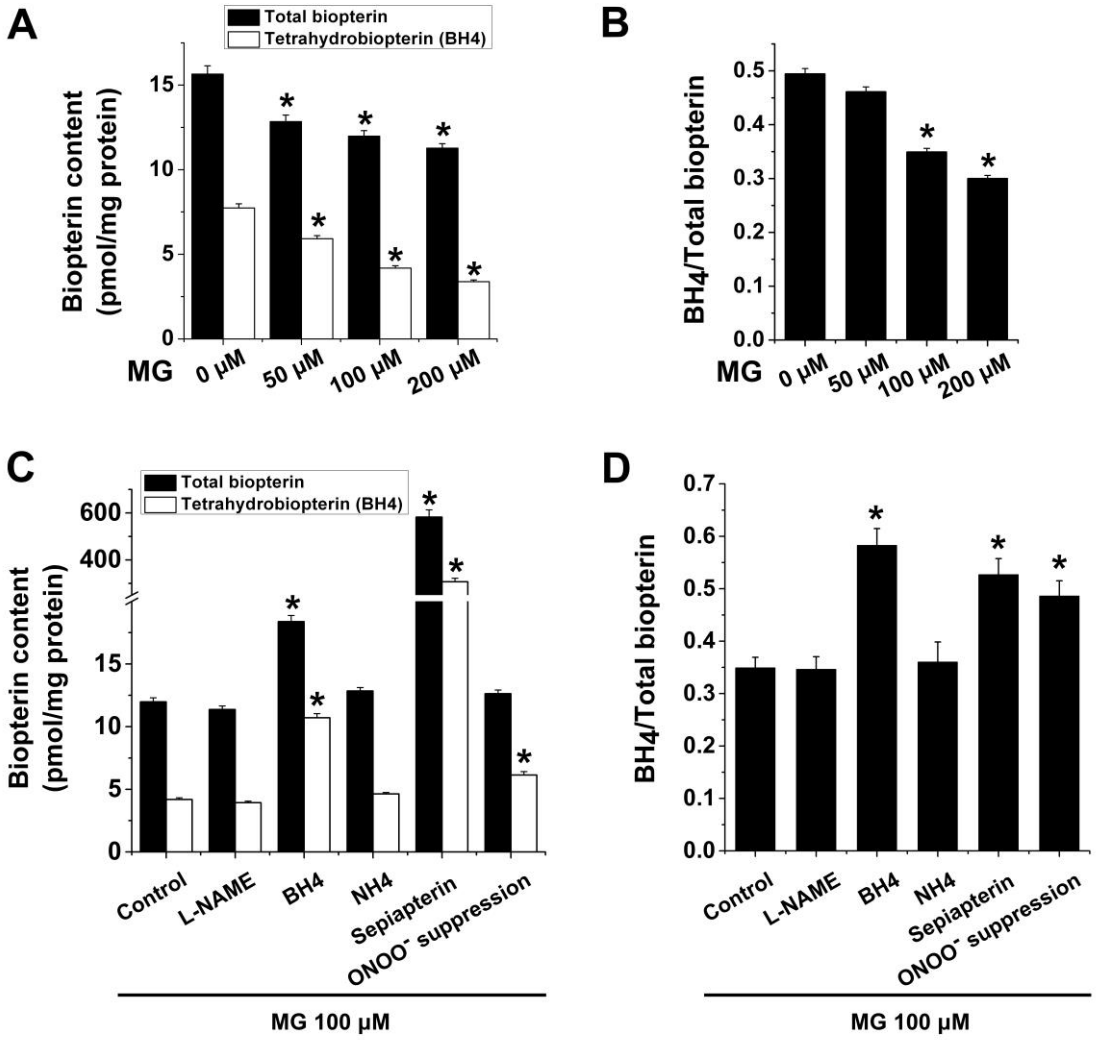

Figure 5-3. Effect of methylglyoxal on cellular biopterin levels in EA.hy926 ECs. A and B. Total cellular biopterin (pmol/mg protein; black bars; A) and BH4 (pmol/mg protein; white bars; A) and the respective BH4/total biopterin ratio (B) determined in EA.hy296 ECs treated with different concentrations of MG (0, 50, 100 and 200 µM) for 8 h. Data are arithmetic means ± SEM (n = 5). * indicates significant difference ($p < 0.05$) from the absence of MG (ANOVA). C and D. Total cellular biopterin (pmol/mg protein; black bars; C) and BH4 (pmol/mg protein; white bars; C) and the respective BH4/total biopterin ratio (D) determined in EA.hy296 ECs treated with MG (100 µM) for 8 h in the absence (Control) or in the presence of L-NAME (50 µM), BH4 (100 µM), NH4 (100 µM) or sepiapterin (20 µM) in the last 4 h of MG treatment or with 24-h pre-treatment with 300 µM Tempol and 50 µM L-NAME ($ONOO^-$ suppression). Data are arithmetic means ± SEM (n = 5). * indicates significant difference ($p < 0.05$) from Control (ANOVA).

Uncoupling of eNOS is associated with enhanced cellular nitration of tyrosine [352]. In a further series of experiments we examined the abundance of 3NT in EA.hy926 cells treated with MG and the effect of biopterins, L-NAME or $ONOO^-$ suppression after MG. As shown in Fig. 5-4, treatment of EA.hy926 cells with 100 μM of MG for 8 h significantly increased the expression of 3NT, an effect that was significantly blunted by BH4 (100 μM, 4 h), sepiapterin (20 μM, 4 h) or $ONOO^-$ suppression (300 μM Tempol and 50 μM L-NAME, 24 h) but not by the BH4 control NH4 (100 μM, 4 h) or L-NAME (50 μM, 4 h) suggesting that biopterin-sensitive eNOS uncoupling was triggered by MG (Fig. 5-4A and 5-4B). The effect of $ONOO^-$ suppression on the reduction of 3NT expression by the combination of Tempol (300 μM) and L-NAME (50 μM) was higher than the administration of Tempol (300 μM) alone (data not shown).

To further unravel the modulation of eNOS functions by MG, we investigated the effect of biopterin supplementation, $ONOO^-$ suppression and NOS inhibition on eNOS phosphorylation (Ser-1177) associated with eNOS uncoupling. To this end, treatment of EA.hy926 cells with 100 μM of MG for 8 h did not modify total eNOS but significantly decreased phosphorylation of eNOS (Ser-1177), an effect that was significantly blunted by BH4 (100 μM), sepiapterin (20 μM) or $ONOO^-$ suppression but not by the BH4 control NH4 (100 μM) or L-NAME (50 μM) suggesting that both eNOS phosphorylation (Ser-1177) and eNOS uncoupling are closely linked to MG-triggered endothelial dysfunction (Fig. 5-5A and 5-5B).

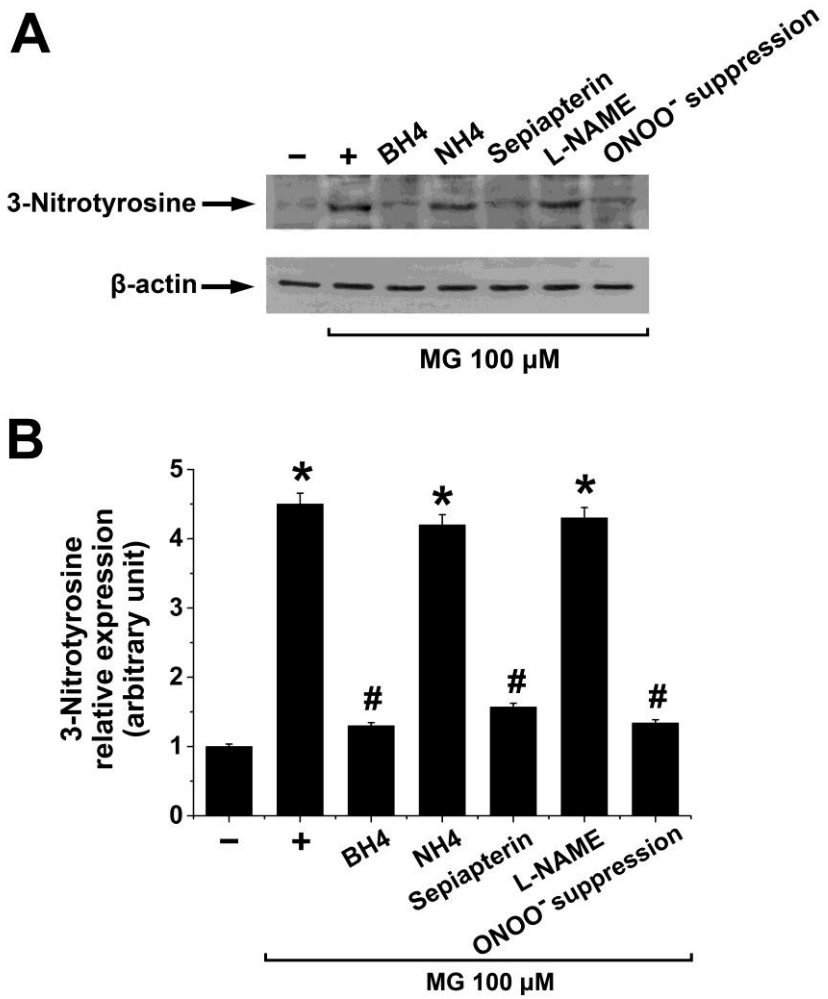

Figure 5-4. Effect of methylglyoxal on tyrosine nitration in EA.hy926 ECs. A and B. Original Western blots (A) and the respective densitometric analysis (B) of the relative abundance of 3-nitrotyrosine (relative to β-actin) in EA.hy296 ECs incubated in the absence (–) or in the presence of MG (100 μM) for 8 h alone (+) or with 100 μM BH4, 100 μM NH4, 20 μM sepiapterin, or 50 μM L-NAME in the last 4 h of MG treatment or with 24-h pre-treatment with 300 μM Tempol and 50 μM L-NAME ($ONOO^-$ suppression). Data are arithmetic means ± SEM (A, representative of three experiments; B, n = 3). * indicates significant difference ($p < 0.05$) from the absence of MG (ANOVA). # indicates significant difference ($p < 0.05$) from MG treatment alone (ANOVA).

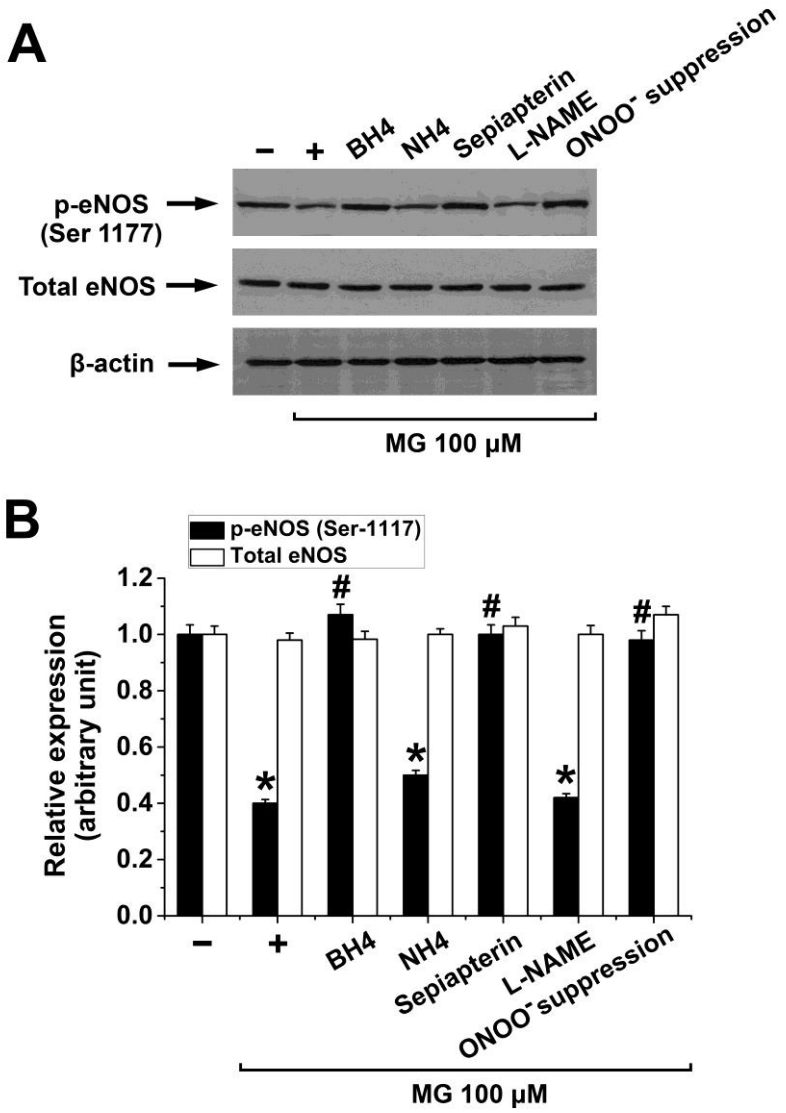

Figure 5-5. Effect of methylglyoxal on eNOS phosphorylation in EA.hy926 ECs. A and B. Original Western blots (A) and the respective densitometric analysis (B) of the relative abundance of total eNOS protein (white bars; relative to β-actin) and Ser-1177 phospho-eNOS (black bars; relative to β-actin) in EA.hy296 ECs incubated in the absence (–) or in the presence of MG (100 μM) for 8 h alone (+) or with 100 μM BH4, 100 μM NH4, 20 μM sepiapterin or 50 μM L-NAME in the last 4 h of MG treatment or with 24 h pre-treatment with 300 μM Tempol and 50 μM L-NAME ($ONOO^-$ suppression). Data are arithmetic means ± SEM (A, representative of three experiments; B, n = 3). * indicates significant difference ($p < 0.05$) from the absence of MG (ANOVA). # indicates significant difference ($p < 0.05$) from MG treatment alone (ANOVA).

5.5 Discussion

In this study we provide conclusive biological evidence that treatment of EA.hy926 ECs with MG triggers eNOS hypophosphorylation and eNOS uncoupling *in vitro*. We show that MG treatment enhances $O_2^{\bullet-}$ generation and 3NT expression and decreases Ser-1177 phosphorylated eNOS, eNOS dimer/monomer ratio and cellular levels of BH4 and BH4/total biopterin ratio in ECs. Moreover, we demonstrate that pharmacological suppression of eNOS uncoupling by L-NAME, exogenous BH4 or sepiapterin administration, and $ONOO^-$ suppression counteracted MG-induced eNOS uncoupling, 3NT upregulation and eNOS hypophosphorylation.

Oxidative stress is a salient feature of the pathophysiology of diabetes. The glycolysis metabolite MG was previously shown to affect redox balance by stimulating ROS production and modulating the expression and functions of cytoprotective molecules such as glutathione [371], superoxide dismutase [174], glyoxalase [372] and H_2S [373]. Increased NADPH oxidase-derived $O_2^{\bullet-}$ reacts with eNOS-derived NO to generate $ONOO^-$ which oxidizes BH4 to BH2. BH4 reduction has been implicated in the pathogenesis of a variety of conditions such as hyperphenylalaninemia [374], diabetes [375], ischemia-reperfusion injury [376], hypertension [377], Alzheimer disease and Parkinson's disease [378], and many of these pathological conditions were shown to be ameliorated by exogenous BH4 [374-377] or sepiapterin [379-381] supplementation. BH4 is critical for the maintenance of eNOS dimers and is functionally related to S-glutathionylation, a powerful regulator of eNOS uncoupling [382]. Our data that MG-triggered $O_2^{\bullet-}$ generation was inhibitable by L-NAME addition, BH4 or sepiapterin supplementation and $ONOO^-$ suppression clearly suggest the presence and contribution of uncoupled eNOS to $O_2^{\bullet-}$ generation in EC functions triggered by MG.

Mounting evidence suggests that phosphorylation of the residue Ser-1177 of eNOS via AKT stimulates NO production [383]. The effects of eNOS phosphorylation on eNOS uncoupling and $O_2^{\bullet-}$ production are not completely understood. Ser-1177 phosphorylation was shown to inhibit the Ca^{2+} sensitivity of eNOS and thus fosters Ca^{2+}-independent $O_2^{\bullet-}$ generation [384]. In this study we tested the effect of BH4 supplementation on the hitherto known reduction of eNOS phosphorylation triggered by MG [70]. Our data show that supplementation of either BH4 or

sepiapterin reversed MG-triggered reduction in Ser-1177 eNOS phosphorylation and enhanced eNOS uncoupling. Similar to BH4, other pharmacological agents such as nifedipine [385], nicorandil [386], and telmisartan [387] were shown to inhibit eNOS uncoupling and enhance eNOS phosphorylation and may, therefore, be beneficial in diabetic endothelial dysfunction. Furthermore, endogenous mediators such as C-reactive protein [388], IGF-1 [389], calcitriol [390], and 20-hydroxyeicosatetraenoic acid [391] were reported to modulate eNOS-associated functions. In this study we demonstrate for the first time the eNOS monomerization induced by the glycolysis metabolite MG and the effects of BH4 and sepiapterin supplementation on MG-modulated eNOS-associated functions in ECs.

Uncoupling of eNOS is characterized by augmented tyrosine nitration which strongly indicates $ONOO^-$-triggered cellular injury in diabetic hyperglycemia [392]. Increased placental protein tyrosine nitration was documented in diabetes patients [393] and, in animal models of diabetes, 3NT was shown to be enhanced in the kidney [394] and in the ventricle and lens [395]. Similarly, 3NT is upregulated in diabetic cardiomyopathy [396]. Our finding that BH4 but not NH4 supplementation abrogated enhanced 3NT expression in MG-treated ECs supports the view that MG-induced depletion of eNOS factor BH4 is critical for MG-triggered eNOS uncoupling and endothelial dysfunction. Similar observations were also made in the diabetic heart subjected to ischemia-reperfusion injury [376], clearly indicating that exogenous BH4 supplementation may ameliorate diabetes-associated multi-organ pathologies.

Conflicting reports on eNOS expression in diabetic endothelial dysfunction suggest the complexity of the signalling mechanisms associated with eNOS during hyperglycemia. Treatment of ECs with high concentrations of glucose was reported to have decreased eNOS protein expression *in vitro* [397]. It was also reported that the abundance of total and phosphorylated eNOS was reduced in internal mammary arteries of diabetes patients [398]. In old Zucker diabetic fatty rats, eNOS protein expression was demonstrated to be decreased [399]. On the contrary, in diabetic and apolipoprotein E-deficient mice, eNOS mRNA levels were augmented [400]. In a contrasting report, however, eNOS expression was shown to be unaltered in type 2 diabetic db/db mice [401]. Along those lines, the discordant effects of MG treatment on eNOS functions reported previously may, thus, not be unexpected [70, 361-363]. It is, however, intriguing to speculate that MG may

be one of the essential metabolites that triggers eNOS hypophosphorylation and uncoupling encountered in diabetes.

5.6 Conclusions

We conclude that the intermediate glycolysis metabolite MG is a powerful modulator of eNOS functions in vascular ECs *in vitro*. Administration of BH4 or its precursor sepiapterin or suppression of $ONOO^-$ formation replenishes cellular BH4 levels, reverse hypophosphorylation of eNOS and ameliorates $O_2^{\bullet-}$ generation, 3NT upregulation and eNOS monomerization that are associated with MG-triggered eNOS uncoupling in ECs. These pharmacological measures may indicate promising therapeutic benefits in MG-sensitive endothelial dysfunction in diabetes.

CHAPTER 6

UNCOUPLING OF eNOS CONTRIBUTES TO REDOX-SENSITIVE LEUKOCYTE RECRUITMENT AND MICROVASCULAR LEAKAGE ELICITED BY METHYLGLYOXAL

For the further exploration of the phenomena shown in Chapter 5, in this chapter, we demonstrate the role of eNOS-derived superoxide in MG-induced leukocyte recruitment. We show that blockade of eNOS-derived superoxide abrogated MG-induced microvascular hyperpermeability, as well as MG-elicited leukocyte adhesion and emigration. Together with Chapter 5, we unravel MG-induced eNOS uncoupling and eNOS-derived superoxide production as another mechanism involved in MG-elicited leukocyte recruitment.

This chapter has been published as a research paper by Yang Su, Syed M. Qadri, Mokarram Hossain, Lingyun Wu and Lixin Liu in *Biochemical Pharmacology 2013 Dec 15;86(12):1762-1774.* Contents of this chapter have been adapted / reproduced from the published article with permission from the journal *Biochemical Pharmacology*. In this study, Y.S. conducted all the experiments, acquired and analyzed all the data, and also participated in the design of the study and manuscript writing.

6.1 Abstract

Elevated levels of the glycolysis metabolite methylglyoxal (MG) have been implicated in impaired leukocyte-endothelial interactions and vascular complications in diabetes, putative mechanisms of which remain elusive. Uncoupling of endothelial nitric oxide synthase (eNOS) was shown to be involved in endothelial dysfunction in diabetes. Whether MG contributes to these effects has not been elucidated. By using intravital microscopy *in vivo*, we demonstrate that MG-triggered reduction in leukocyte rolling velocity and increases in rolling flux, adhesion, emigration and microvascular permeability were significantly abated by scavenging reactive oxygen species (ROS). In murine cremaster muscle, MG treatment reduced tetrahydrobiopterin (BH4)/total biopterin ratio, increased arginase expression and stimulated ROS and superoxide production. The latter was significantly blunted by ROS scavengers Tempol (300 μM) or MnTBAP (300 μM), by BH4 supplementation (100 μM) or by NOS inhibitor N^G-nitro-L-arginine methyl ester (L-NAME; 20 μM). In these tissues and cultured murine and human primary ECs, MG increased eNOS monomerization and decreased BH4/total biopterin ratio, effects that were significantly mitigated by supplementation of BH4 or its precursor sepiapterin but not by L-NAME or tetrahydroneopterin, indicative of MG-triggered eNOS uncoupling. MG treatment further decreased the expression of guanosine triphosphate cyclohydrolase I in murine primary ECs. MG-induced leukocyte recruitment was significantly attenuated by supplementation of BH4 or sepiapterin or suppression of superoxide by L-NAME confirming the role of eNOS uncoupling in MG-elicited leukocyte recruitment. Together, our study uncovers eNOS uncoupling as a pivotal mechanism in MG-induced oxidative stress, microvascular hyperpermeability and leukocyte recruitment *in vivo*.

6.2 Introduction

Inflammatory injury afflicting ECs contributes to the pathophysiology of multiple vascular diseases [402]. In diabetes, chronic hyperglycemia leads to endothelial dysfunction which fosters deranged microcirculation [342, 343]. The underlying mechanisms of impaired endothelial functions and innate immunity in diabetes are, however, not completely understood. Chronic hyperglycemia results in excessive levels of the cytotoxic metabolite methylglyoxal (MG) [115, 403] which serves as a precursor to form advanced glycation end-products [404]. MG has been implicated in the pathogenesis of diabetes [134], neuronal injury [405] and vascular complications

[255, 344, 345]. MG-induced cytotoxicity encompasses both necrotic [346] and apoptotic cell death [345] leading to alterations of muti-organ homeostasis. Moreover, MG is a powerful modulator of mitochondrial functions, thus altering both cellular energy and redox balance [157].

Inflammatory sequelae of pathological MG concentrations comprise functional modulation of various immune cells. MG was shown to stimulate cytokine induction [267], activate macrophages [294, 406], suppress T-cell-mediated immune functions [265] and modulate innate immunity by enhancing neutrophil apoptosis and Mac-1 expression [255]. Recently, MG was shown to stimulate leukocyte-endothelial interactions in an *in vivo* model of acute inflammation [75]. MG treatment up-regulated NF-κB-dependent expression of EC adhesion molecules, mitigated intravascular leukocyte rolling velocity, increased rolling flux and leukocyte adhesion and accelerated leukocyte emigration in mice [75]. In diabetic mice, deranged leukocyte-endothelial interactions were documented [253], but the contribution of the increased metabolite MG alone has not been completely characterized. Mechanisms that mediate pro-inflammatory effects of elevated MG, however, are largely unidentified.

Nitric oxide (NO) homeostasis is an important determinant of physiological cardiovascular functions and its impairment is involved in the pathophysiology of diabetes [350]. Furthermore, NO is a powerful modulator of leukocyte-endothelial interactions [407, 408]. The constitutively expressed endothelial nitric oxide synthase (eNOS) catalyses the reaction for generation of NO and L-citrulline from L-arginine [409] and requires the presence of the essential cofactors tetrahydrobiopterin (BH4) and NADPH [347]. Deficiency of either L-arginine or BH4 reduces the generation of NO by eNOS which triggers superoxide ($O_2^{\bullet-}$) production, a process termed eNOS uncoupling [351]. Ramifications of eNOS uncoupling include increased eNOS monomerization, tyrosine nitration and formation of dihydrobiopterin (BH2) [352, 410]. Guanosine triphosphate cyclohydrolase 1 (GTPCH1) is the rate limiting enzyme that regulates *de novo* BH4 synthesis whereas dihydrofolate reductase (DHFR) reduces BH2, thus, salvaging BH4 from BH2 [411]. eNOS uncoupling-derived $O_2^{\bullet-}$ stimulates platelet aggregation [412] and increased monocyte adhesion to ECs [413], both effects favouring diabetic vasculopathy. Moreover, reactive oxygen species (ROS) are potent regulators of leukocyte-endothelial interactions [414-418]. In fact, redox

imbalance is known to participate in a multitude of pathophysiological processes, the mechanisms of which may in part be secondary to eNOS uncoupling.

MG influences NO and redox balance and contributes to a myriad of hyperglycemia-induced alterations of cellular functions *in vivo* [115], mechanisms of which still remain elusive. eNOS uncoupling was previously shown to be responsible for endothelial dysfunction in diabetic mice [358] and essential in both endothelial dysfunction and peripheral neuropathy in Zucker diabetic fatty rats [359]. It was only recently shown that MG affects eNOS expression or functions. On the one hand, sensitivity of eNOS to MG was increased by the upregulation of eNOS transcription [361], while on the other hand, eNOS protein expression was decreased by MG [362, 363]. Discordantly, MG was reported to modulate eNOS activity without significantly affecting eNOS protein expression but by suppressing phosphorylation of eNOS at serine-1179 [70]. In preeclamptic vasculature, increased MG concentrations were shown to affect the expression of arginase and arginase-dependent lectin-like oxidized low-density lipoprotein receptor 1 (LOX-1) [364], that are associated with enhanced $O_2^{\bullet-}$ production and uncoupling of eNOS [364, 410, 419]. Arginase is further inhibitable by the NOS inhibitor L-NAME [420]. Whether or not MG-sensitive eNOS regulation participates in leukocyte-endothelial interactions is not known.

We hypothesized that MG-elicited leukocyte recruitment and microvascular hyperpermeability are mediated by modulation of eNOS expression or functions, a mechanism common to other MG-induced pathologies [362, 364]. To reveal the presence of eNOS uncoupling and its role in MG-triggered leukocyte recruitment and microvascular hyperpermeability, we quantified BH4 reduction, eNOS monomerization, L-NAME inhibitable $O_2^{\bullet-}$ production and used fluorescence imaging and real-time intravital microscopic analysis to study microvascular permeability changes and leukocyte-endothelial interactions induced by exogenous MG.

6.3 Materials and Methods

Mice

Male C57BL/6 mice (Charles River, Saint-Constant, QC, Canada) between 8 and 12 wk-old and young C57BL/6 mice at 5 − 7 day-old were used in this study. This study was carried out with the

approval of animal protocols from the University Committee on Animal Care and Supply (UCACS; protocol permit # 20070028) at the University of Saskatchewan following the standards of the Canadian Association of Animal Care. All surgery was performed under ketamine/xylazine anesthesia, and all efforts were made to minimize animal suffering.

Intravital microscopy

Mice were anesthetised using an i.p. injection of 10 mg/kg xyalzine (Bayer, Toronto, ON, Canada) and 200 mg/kg ketamine hydrochloride (Rogar, Montreal, QC, Canada). The mouse cremaster muscle preparation was used to study dynamic leukocyte-endothelial interactions in microvasculature as described previously [114, 280]. The cremaster muscle was superfused with 37°C-warmed bicarbonate-buffered saline (pH 7.4; containing in mM 133.9 NaCl, 4.7 KCl, 1.2 $MgSO_4$ and 20 $NaHCO_3$, all reagents purchased from Fisher Scientific, Toronto, ON, Canada). A BX61WI Olympus upright microscope with a LUCPLFLN 20× objective lens was connected to a 3CCD color video camera (DXC-990, Sony) for bright-field intravital microscopy. Throughout the experiment, leukocyte behaviour and hemodynamic changes in the selected cremasteric postcapillary venule (25−40 μm diameter) were visualized, projected on a TV monitor and recorded at real time on a DVD recorder. The number of rolling, adherent, and emigrated leukocytes during offline playback analysis of the recorded video was determined in the cremasteric microvasculature as described previously [75, 114, 280]. MG (25 or 50 mg/kg b.w.; Sigma, Oakville, ON, Canada) dissolved in saline, was administered by an intrascrotal injection for 4 h before the cremaster muscle was exposed for intravital microscopy. Where indicated, the pharmacological agents used to modulate MG-induce leukocyte recruitment were dissolved in the bicarbonate-buffered saline and superfused for 2 h on the exposed cremaster muscle. Manganese (III) tetrakis (4-benzoic acid) porphyrin (MnTBAP, Santa Cruz, Dallas, TX, USA) or 1-oxyl-2,2,6,6-tetramethyl-4-hydroxypiperidine (Tempol, Santa Cruz) was used to suppress ROS production. NOS inhibitor N^G-nitro-L-arginine methyl ester (L-NAME, Sigma), was administered to inhibit uncoupled eNOS-derived $O_2^{\bullet-}$ production [258, 421]. To maintain eNOS dimerization, the NOS cofactor 5,6,7,8-tetrahydroboipterin (BH4; Sigma) or the negative control, a pteridine analogue, 5,6,7,8-tetrahydroneopterin (NH4; Schircks laboratories, Switzerland) was freshly-prepared and administered. NH4 has similar antioxidant effects as BH4 but, unlike BH4, is ineffective in restoring uncoupled eNOS [366]. BH4 availability may be compromised due to

oxidative transformation to 7,8-dihydrobiopterin (BH2) [257, 422]. Thus, BH4- or NH4-containing superfusion buffer was replaced every 30 min by freshly prepared BH4 to maximize BH4 and minimize BH2 availability. Sepiapterin (50 μM; Cayman, Ann Arbor, MI, USA), a substrate for BH4 synthesis via the pterin salvage pathway, was used to increase BH4 levels. Sepiapterin functions as both a precursor as well as a by-product of BH4 synthesis and is also described as a BH4 analog [367].

Measurement of microvascular permeability

MG-triggered microvascular leakage was studied in postcapillary venules of the cremaster muscle as described previously [280, 423, 424]. Briefly, MG (100 μM) was superfused for 1 h over the exposed cremaster muscle and where indicated, BH4 (100 μM) or the ROS scavenger Tempol (300 μM) or MnTBAP (300 μM) was superfused for 30 min prior to and 1 h during MG superfusion. FITC-labelled bovine serum albumin (BSA; Sigma) at 25 mg/kg b.w. was injected to the mice i.v. at the start of the experiment, and FITC-derived fluorescence (excitation at 495 nm, and emission at 525 nm) in the venule was detected using a monochrome deep-cooled CCD digital camera (Retiga SRV, QImaging, Surrey, BC, Canada) mounted on BX61WI Olympus upright microscope. The intensity of FITC-albumin-derived fluorescence within the lumen of the venule and in the adjacent perivascular tissue was recorded and analysed using METAMORPH software (MetaMorph®, Molecular Devices Inc., PA, USA). The index of vascular albumin leakage, permeability index, was determined in the same segment of the venule at different time points as shown previously [423, 424].

Harvest of murine primary endothelial cells

Primary murine ECs were isolated from the lungs or hearts of C57BL/6 mice (aged 5–7 days) according to a previously described protocol [280, 320]. Briefly, ECs were immuno-magnetically isolated utilizing anti-ICAM-2 (CD 102) antibody (clone 3C4; BD Pharmingen, Quebec City, QC, Canada), seeded in 35-mm laminin-coated petri dishes and cultured in microvascular EC culture medium (EBM-2) supplemented with EGM-2 MV bullet kit (Lonza, Mississauga, ON, Canada). After the cells reached confluency, they were passaged on laminin-coated 24-well plates and treated with MG and other pharmacological agents at the indicated concentrations.

Culture of HUVECs

Human umbilical vein ECs (HUVECs) were obtained from American Type Culture Collection (ATCC) and cultured as described previously [70]. Briefly, cells were cultured in Kaighns F12K medium (containing 10% FBS, 0.1 mg/ml heparin and 0.03–0.05 mg/ml EC growth supplement; Sigma), grown to confluency and treated with MG and other pharmacological agents at the indicated concentrations.

Immunoblotting

For the detection of eNOS dimers and monomers, immunoblotting was performed in the non-reduced state as described previously [258]. Briefly, after the indicated treatment, cremaster muscles were excised and snapped frozen in liquid nitrogen. The tissue was homogenized and lysed in lysis buffer (pH 8.0; containing 50 mM Tris-HCl, 150 mM NaCl, 1% NP-40, 0.5% sodium deoxycholate, 0.1% SDS and protease and phosphatase inhibitor cocktails purchased from Fisher Scientific). The same lysis buffer was used to lyse murine primary ECs. Proteins (50 μg) were solubilized in Laemmli sample buffer without β-mercaptoethanol at 37 ℃ for 5 min and resolved by 7% SDS-PAGE with the buffer tank placed on ice during electrophoresis. For immunoblotting, proteins were transferred onto a nitrocellulose membrane and blocked with 5% non-fat milk in TBST at room temperature for 1 h. The blots were then probed by 1:1000 dilution of primary anti-eNOS antibody (clone M221; Abcam), anti-GTPCH1 (Santa Cruz), anti-DHFR (Santa Cruz), anti-LOX-1 (Abcam), anti-arginase II (Santa Cruz) or mouse anti-β-actin antibody (Santa Cruz) and the secondary horseradish peroxidase-conjugated antibody (Santa Cruz). Antibody binding was detected with the ECL detection reagent (GE Healthcare, Baie d'Urfe, QC, Canada). As eNOS monomers and dimers were detected in non-reduced conditions, equal volumes of lysates in reduced conditions were run in separate gels to quantify β-actin expression. Densitometric quantification of the detected bands was performed using Gene Snap Software (Syngene, Frederick, MD, USA).

Determination of ROS generation in whole cremaster muscle

We measured the levels of ROS production in cremaster muscles as previously described [373]. Following the indicated treatments, the cremaster muscle was loaded (30 min, 37 ℃ in the dark) with a membrane-permeable and non-fluorescent 2',7'-dichlorodihydrofluorescein diacetate

(H_2DCFDA; 30 μM, Invitrogen, Burlington, ON, Canada) which oxidizes to fluorescent 2',7'-dichlorofluorescein (DCF) in the presence of ROS. To remove excess probe, the muscle was washed with bicarbonate-buffered saline and fluorescence intensity in the excised muscle was excited at 495 nm and measured at 527 nm emission wavelengths. Data are collected as fluorescence intensity per gram tissue and normalized to the control.

Determination of $O_2^{\bullet-}$ production in whole cremaster muscle

Levels of $O_2^{\bullet-}$ in excised cremaster muscles after various treatments were determined using a commercial superoxide detection kit (Enzo, Brockville, ON, Canada) according to the manufacturer's instructions. After staining with the membrane-permeable and nonfluorescent $O_2^{\bullet-}$ detection probe (10 μM; 30 min, 37 ℃ in the dark) and removal of excess probe by washing with bicarbonate-buffered saline, the muscle was excised and fluorescence detected using excitation and emission wavelengths of 544 nm and 590 nm respectively. Data are collected as fluorescence intensity per gram tissue and normalized to the control.

Confocal microscopy

For estimation of $O_2^{\bullet-}$ generation in MG-treated HUVECs, dihydroethidium (DHE; Cayman) fluorescence staining was used as described previously [425, 426]. After the indicated treatments, HUVECs were incubated with DHE (5 μM) for 30 min. The cells were then washed three times and images were obtained using a laser scanning confocal microscope (ConfoCor2/LSM510, Zeiss, Thornwood, NY, USA) with fluorescence (showing oxidized DHE) detected using excitation and emission wavelengths of 517 nm and 610 nm respectively.

Analysis of biopterin levels by HPLC

Measurement of BH4 and total biopterins was performed by fluorometric HPLC analysis as described previously with slight modifications [258, 259]. After indicated treatments, cremaster muscles were homogenized in 250 μL lysis buffer (pH 7.4; containing 50 mM Tris-HCl, 1 mM DTT and 1 mM EDTA) and 0.1 μM neopterin (Sigma) as an internal recovery standard. The samples were deproteinated with 10% 1:1 mixture of 1.5 M $HClO_4$ and 2 M H_3PO_4 and centrifuged (12,000 × *g* for 10 min). The supernatant was split into portions and subjected to acid-and alkali-oxidation respectively. To determine total biopterins (BH4, BH2 and biopterin) by acid-oxidation,

10 µl iodine solution (1% iodine in 2% KI solution) was added into every 90 µl supernatants and for BH2 and biopterin estimation by alkali-oxidation, 10 µl 1 M NaOH and 10 µl iodine solution were added to 80 µl supernatant. Following incubation (1 h, room temperature in the dark), the alkali-oxidation samples were acidified with 1 M H_3PO_4 and iodine in both acid- and alkali-oxidation samples was reduced using 5% ascorbic acid (Sigma) and the samples were centrifuged (12,000 $\times g$ for 10 min). The supernatant was collected for HPLC analysis using a Hitachi D-7000 HPLC system (Hitachi, Mississauga, ON, Canada) via Symmetry C18 reverse-phase column with a methanol-water (1.5:98.5, v/v) mobile phase running at 0.5 mL/min. Fluorescence was detected at excitation and emission wavelengths of 348 nm and 444 nm respectively. The level of BH4 was calculated by subtracting BH2 and biopterin from total biopterins and expressed as pmol per mg protein. The biopterin levels in NH4 treated cells were calculated without adding neopterins.

Statistical analysis

Data are expressed as arithmetic means ± SEM from at least three independent experiments. Statistical analysis was made using Student *t* test or one way analysis of variance (ANOVA) with Tukey's post-hoc comparison test. *n* denotes the number of different mice and different batches of cremasteric tissues or ECs studied in each group. Values of $p < 0.05$ were considered statistically significant.

6.4 Results

To address the effects of MG treatment on leukocyte-endothelial interactions we used intravital microscopy to analyze real-time dynamics of leukocyte recruitment in post-capillary venules of the cremaster muscle. The captured intravital images of cremasteric microcirculation depicted in Fig. 6-1A show the number of adherent and emigrated cells was increased after treatment with MG (intrascrotal injection of 25 and 50 mg/kg b.w. for 6 h), consistent with previous reports [75]. To elucidate the mechanisms underlying MG-induced leukocyte recruitment, we examined the effects of ROS scavengers on different parameters of dynamic leukocyte recruitment. As shown in Fig. 6-1B, MG (25 and 50 mg/kg b.w. for 6 h) increased rolling flux, an effect that was significantly mitigated by superfusion of MG-stimulated cremaster muscle with either Tempol (300 µM) or MnTBAP (300 µM). Similarly, Tempol or MnTBAP significantly ameliorated the

reduced rolling velocity triggered by MG (25 and 50 mg/kg b.w.; Fig. 6-1C). MG-triggered reduction of rolling velocity fosters leukocyte adhesion to vascular endothelium and subsequent emigration of leukocytes in the extravascular tissue. As a consequence of pharmacological ROS scavenging, either Tempol or MnTBAP significantly attenuated the number of adherent and emigrated cells stimulated by MG-induced ROS generation (Fig. 6-1D and 6-1E). These results indicate that an increase of MG in local tissue triggers ROS-sensitive leukocyte recruitment.

To unravel the redox mechanisms underlying MG-elicited leukocyte recruitment, we measured total ROS and $O_2^{\bullet-}$ generation in MG-treated muscle tissue. We found that treatment of cremaster muscle with MG for 6 h significantly increased both $O_2^{\bullet-}$ and total ROS levels in a dose-dependent manner, an effect reaching statistical significance at 5 mg/kg b.w. dose of MG (Fig. 6-2A). We further investigated the effect of ROS scavengers on $O_2^{\bullet-}$ and total ROS production in MG-treated whole cremaster muscle. As depicted in Fig. 6-2B, in the absence of MG, Tempol (300 μM) or MnTBAP (300 μM) did not modify tissue $O_2^{\bullet-}$ and total ROS levels. However, treatment of the cremaster muscle with MG (25 mg/kg b.w. for 6 h) significantly increased $O_2^{\bullet-}$ and total ROS levels, effects that were significantly blunted by either Tempol or MnTBAP superfusion, suggesting that pharmacological ROS scavenging ameliorates the oxidative stress triggered by MG in the cremaster muscle (Fig. 6-2B). To further explore the mechanism of MG-elicited oxidative stress, we tested the effects of NOS essential cofactor BH4 and its control NH4 [366]. Fig. 6-2C shows that when perfused at the same concentration for 2 h, NH4 did not significantly reduce MG-induced $O_2^{\bullet-}$ production whereas BH4 significantly decreased the $O_2^{\bullet-}$ amount in MG-treated muscle. Because BH4 is an essential cofactor for all NOS and NH4 is not, the different $O_2^{\bullet-}$-dependent fluorescence after BH4 and NH4 treatment suggests the involvement of NOS in the generation of $O_2^{\bullet-}$ in MG-treated tissue. Fig. 6-2D, demonstrates that superfusion of cremaster muscle with L-NAME (20 μM, 2 h) significantly diminished $O_2^{\bullet-}$ production elicited by MG (50 mg/kg b.w.). The reduction of $O_2^{\bullet-}$ in MG-treated muscle by BH4 supplementation and L-NAME treatment indicates that there was an L-NAME-inhibitable $O_2^{\bullet-}$ production by NOS after MG treatment *in vivo*. Together, these results suggest that, after MG treatment, there was possibly uncoupling of NOS in the muscle tissue that was partly responsible for the $O_2^{\bullet-}$ generation and was inhibited by the addition of BH4 or by the NOS inhibitor L-NAME. Additionally, we tested

the effects of BH4 supplementation or L-NAME treatment on MG-induced $O_2^{\bullet-}$ production in HUVECs. As shown in Fig. 6-2E, DHE-dependent fluorescence indicating $O_2^{\bullet-}$ production was higher after treatment with MG and was blunted in the presence of either BH4 or L-NAME suggesting similar sensitivity of HUVECs to MG.

On the basis of these results and to explore whether there is eNOS uncoupling in tissue after MG treatment, we determined whether MG affects tissue levels of BH4 and whether exogenous supplementation of BH4 indeed replenishes tissue BH4 in our *in vivo* model. We found that MG significantly and dose-dependently decreased total biopterin content, BH4 content (Fig. 6-3A) and more importantly, the ratio of BH4/total biopterin (Fig. 6-3B). Moreover, exogenous supplementation of BH4 or its precursor sepiapterin abrogated MG-induced reduction of BH4 levels (Fig. 6-3C) and BH4/total biopterin ratio (Fig. 6-3D) in tissue; whereas NH4, the BH4 control, and L-NAME, the NOS inhibitor, did not significantly alter MG-triggered decreased tissue BH4/total biopterin ratio (Fig. 6-3D). This suggests that exogenous supplementation of BH4 or its precursor sepiapterin efficiently replenishes tissue BH4 levels after MG treatment. To unravel the mechanisms of decreased bioavailability of BH4 we tested the expression of the enzymes GTPCH1 and DHFR in tissue after MG treatment. As depicted in Fig. 6-3E and 6-3F, MG significantly decreased GTPCH1 but not DHFR expression in tissue indicating that MG treatment affects *de novo* synthesis of BH4 but may not affect the reduction of BH2 to BH4.

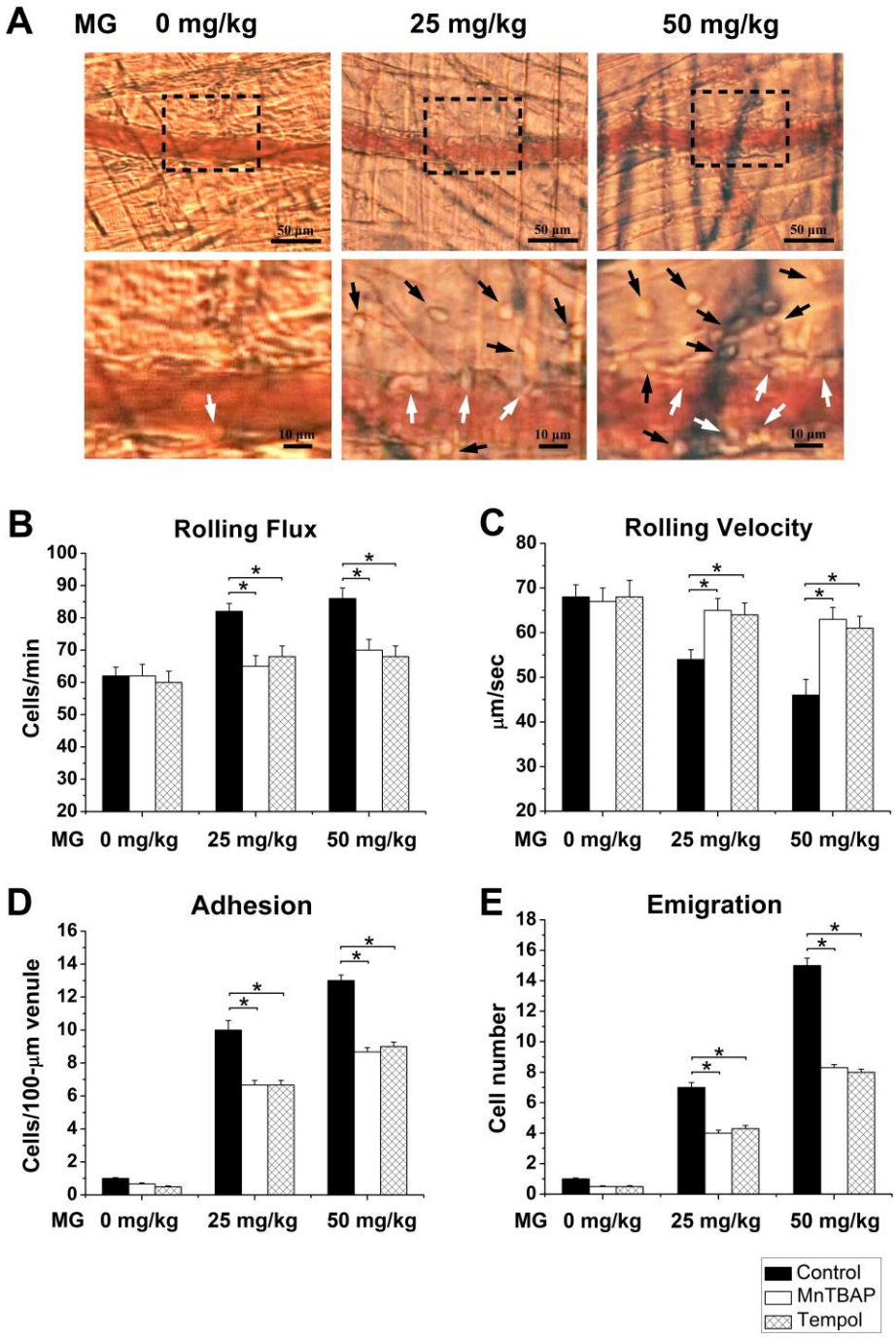

Figure 6-1. Methylglyoxal-elicited redox-sensitive leukocyte recruitment. A. Representative images captured from intravital video microscopy showing a postcapillary venule with adherent leukocytes and the surrounding cremasteric tissue with emigrated leukocytes in the absence (MG 0 mg/kg b.w.; left panel) or in the presence of MG (25 mg/kg b.w., middle panel and 50 mg/kg b.w., right panel, after 6 h intrascrotal MG injection). The images in the lower panels are amplified

areas (with dotted line) from the corresponding images in the upper panels showing the adherent (white arrows) and emigrated (black arrows) leukocytes. B – D. The leukocyte rolling flux (B, cells/min), leukocyte rolling velocity (C, μm/sec), and the number of adherent (D, cells/100-μm venule) and emigrated (E, cells/443×286 μm2 field) leukocytes determined after an intrascrotal injection of saline (0 mg/kg b.w. MG) or MG (25 mg/kg b.w. and 50 mg/kg b.w.) for 6 h with the last 2-h superfusion with bicarbonate buffered-saline (Control; black bars), MnTBAP (300 μM; white bars) or Tempol (300 μM; hatched bars). Data are arithmetic means ± SEM (n = 5). * indicates significant difference ($p < 0.05$) from MG treatment alone (ANOVA).

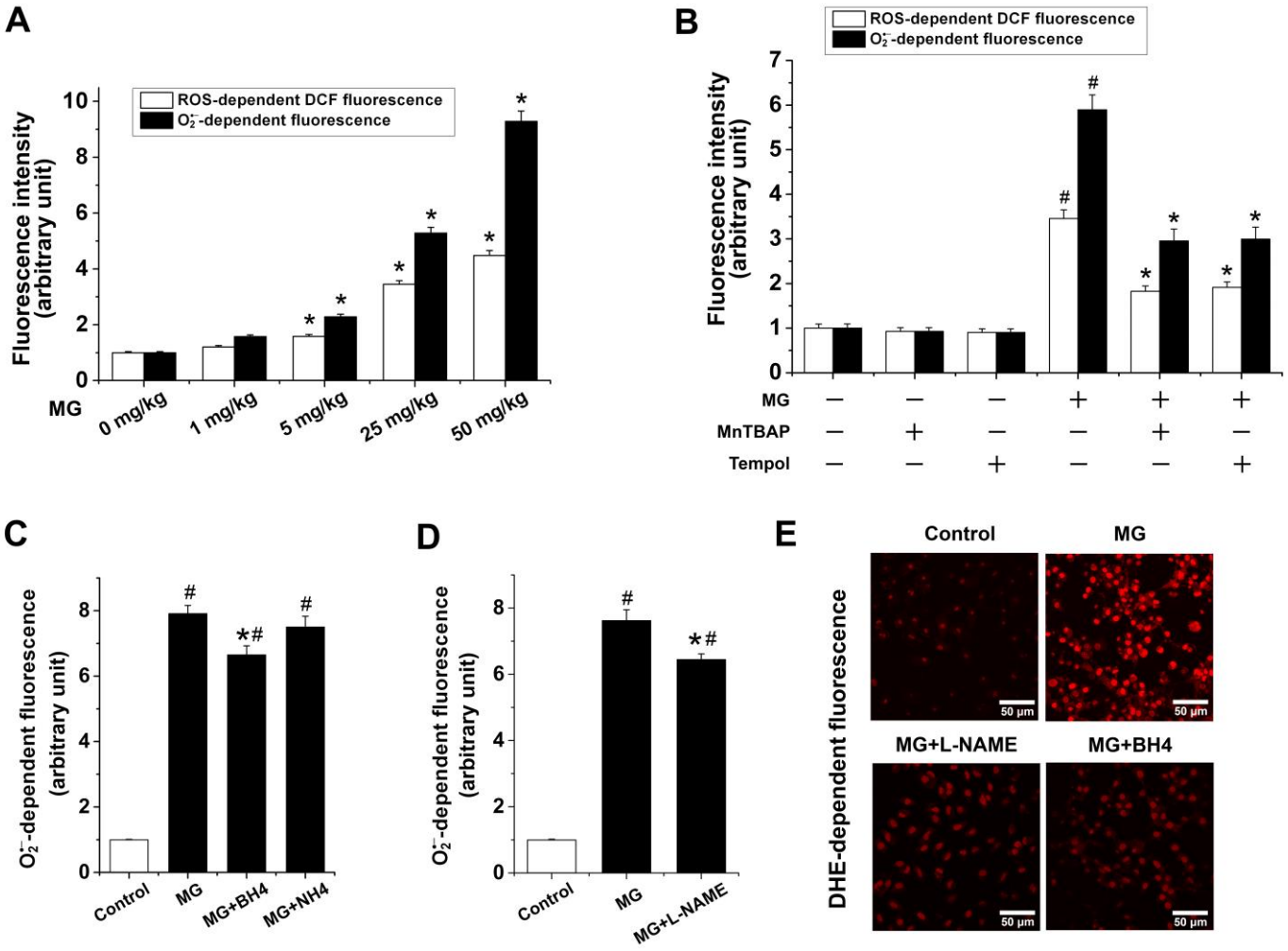

Figure 6-2. Methylglyoxal-triggered oxidative stress. A. The total ROS (white bars) and $O_2^{\bullet-}$ (back bars) generation determined in whole cremaster muscle at 6-h after intrascrotal injection of MG at different doses (0, 1, 5, 25 and 50 mg/kg b.w.) with the last 2-h superfusion with bicarbonate buffered-saline. Data are arithmetic means ± SEM (n = 5). * indicates significant difference ($p < 0.05$) from the absence of MG (0 mg/kg b.w.; ANOVA). B. The total ROS (white bars) and $O_2^{\bullet-}$ (back bars) generation determined in whole cremaster muscle after an intrascrotal injection of saline or MG (25 mg/kg b.w.) for 6 h with the last 2-h superfusion of the cremaster muscle with bicarbonate buffered-saline, MnTBAP (300 μM) or Tempol (300 μM). Data are arithmetic means ± SEM (n = 5). # indicates significant difference ($p < 0.05$) from the absence of MG (ANOVA). * indicates significant difference ($p < 0.05$) from MG treatment alone (ANOVA). C and D. The total $O_2^{\bullet-}$ generation determined in whole cremaster muscle after an intrascrotal injection of saline

(Control; white bar) or MG (50 mg/kg b.w.; black bars) for 6 h with the last 2-h superfusion of the cremaster muscle with bicarbonate buffered-saline (MG), BH4 (100 μM, C), NH4 (100 μM, C) or L-NAME (20 μM, D). Data are arithmetic means ± SEM (n = 5, C and D). * indicates significant difference ($p < 0.05$) from MG treatment alone (ANOVA). # indicates significant difference ($p < 0.05$) from Control (ANOVA). E. Representative laser confocal micrographs (from three independent experiments) of DHE-stained HUVECs incubated in the absence (Control) or in the presence of MG (100 μM) for 6 h with the last 2-h treatment with phosphate-buffered saline (MG), L-NAME (20 μM; MG + L-NAME) or BH4 (100 μM; MG + BH4).

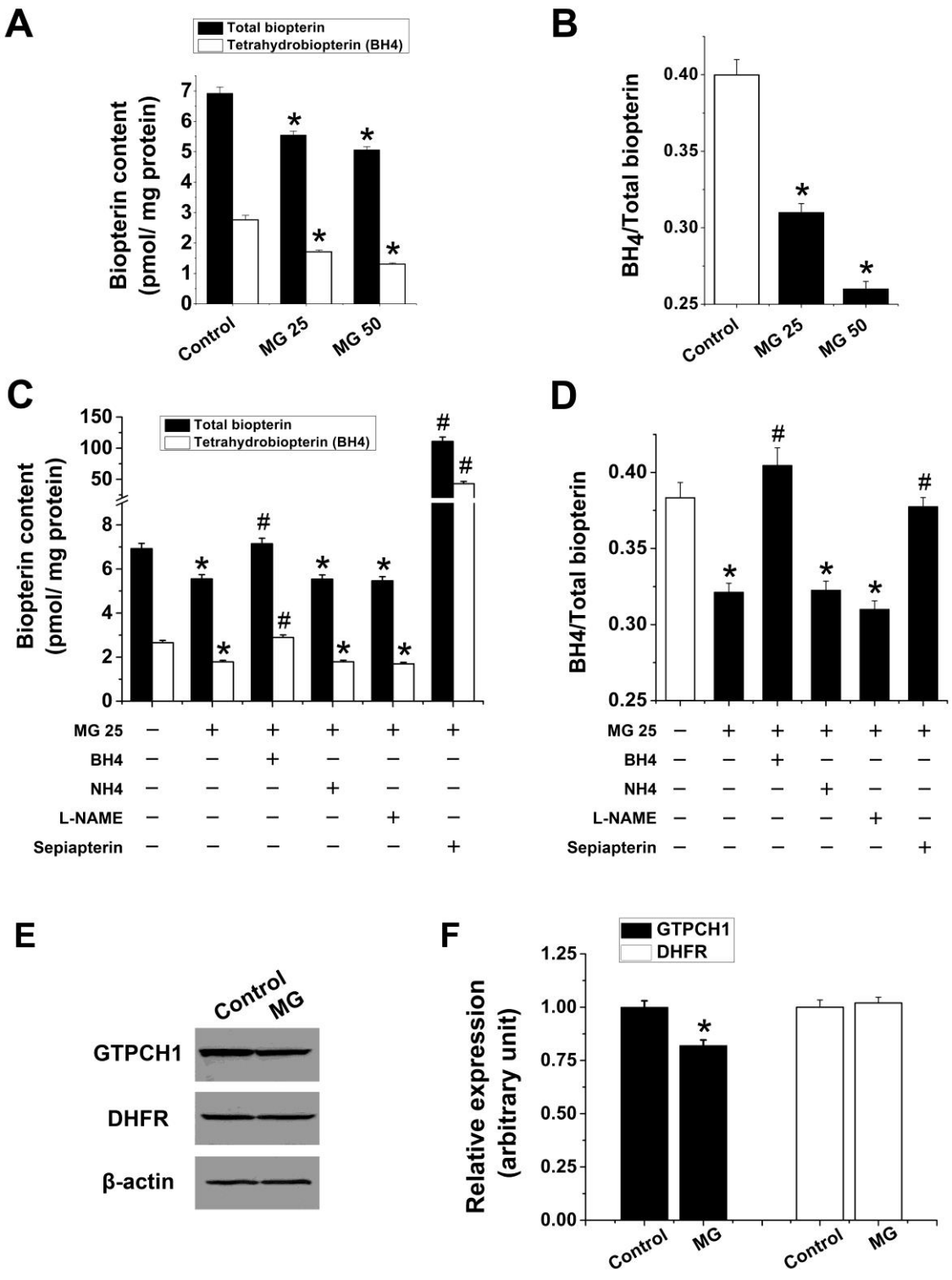

Figure 6-3. Sensitivity of BH4 metabolism to methylglyoxal. A and B. Effect of an intrascrotal injection of MG (0, 25 and 50 mg/kg b.w.) on total cellular biopterin (pmol/mg protein; black bars; A) and BH4 (pmol/mg protein; white bars; A) and the respective BH4/total biopterin ratio (B) in

whole cremaster muscle determined at 6 h after an intrascrotal injection of saline (Control) or MG (25 mg/kg b.w., MG 25 and 50 mg/kg b.w., MG 50) with the last 2-h superfusion with bicarbonate buffered-saline. Data are arithmetic means ± SEM (n = 5). * indicates significant difference ($p < 0.05$) from the Control (ANOVA). C and D. Effect of addition of BH4, NH4, L-NAME or sepiapterin on total cellular biopterin (pmol/mg protein; black bars; C) and BH4 (pmol/mg protein; white bars; C) and the respective BH4/total biopterin ratio (D) in whole cremaster muscle determined at 6 h after an intrascrotal injection of saline or MG (25 mg/kg b.w., MG 25) with the last 2-h superfusion with control saline, BH4 (100 µM), NH4 (100 µM), L-NAME (20 µM) or sepiapterin (50 µM). Data are arithmetic means ± SEM (n = 5). * indicates significant difference ($p < 0.05$) from the saline-control (ANOVA). # indicates significant difference ($p < 0.05$) from MG treatment alone (ANOVA). E and F. Original Western blots (E) and the respective densitometric analysis (F) of the abundance of GTPCH1 (black bars) and DHFR (white bars) relative to β-actin determined in murine primary ECs in the absence (Control) or in the presence of MG (100 µM; MG) for 6 h. Data are arithmetic means ± SEM (E, representative of three experiments; F, n = 3). * indicates significant difference ($p < 0.05$) from the Control (ANOVA).

Elevated MG levels were previously shown to affect arginase and arginase-dependent LOX-1 expression which are associated with $O_2^{\bullet-}$ production [364]. As depicted in Fig. 6-4, expression of arginase was significantly enhanced in whole cremaster muscle after an intrascrotal injection with MG (50 mg/kg b.w. for 6 h) indicating that MG induces the depletion of the substrate L-arginine via increased arginase expression and may thus foster enhanced eNOS uncoupling. MG further increased arginase-dependent LOX-1 expression in whole cremaster muscle (data not shown).

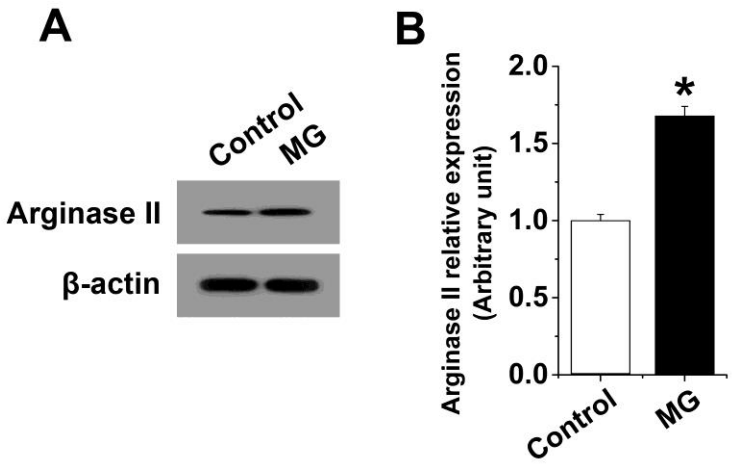

Figure 6-4. Methylglyoxal-sensitive arginase expression in whole cremaster muscle. Original Western blots (A) and the respective densitometric analysis (B) of the relative abundance of arginase II (relative to β-actin) in whole cremaster muscle determined at 6 h after an intrascrotal injection of saline (Control; white bar) or MG (25 mg/kg b.w., MG; black bar) with the last 2-h superfusion with bicarbonate buffered-saline. Data are arithmetic means ± SEM (A, representative of four experiments; B, n = 4). * indicates significant difference ($p < 0.05$) from the Control (Student t test).

Further, we examined the effect of MG on eNOS monomerization in whole cremaster tissue and in isolated primary ECs. As shown in Fig. 6-5A and 6-5B, 6-h treatment of cremaster muscle with MG significantly decreased the abundance of eNOS dimers and elevated eNOS monomers and increased eNOS monomer/dimer ratio in a dose-dependent manner. To further assess the mechanisms regulating eNOS uncoupling by MG, we explored the effects of BH4 supplementation and NOS inhibition on eNOS monomerization. As illustrated in Fig. 6-5C and 6-5D, treatment of cremaster muscle with MG (25 mg/kg b.w.) for 6 h significantly increased eNOS monomer/dimer ratio. Superfusion of BH4 (100 μM, for 2 h) after 4-h MG injection completely reversed the increase in eNOS monomer/dimer ratio induced by MG. However, superfusion of the cremaster muscle with neither the BH4 control NH4 (100 μM) nor the NOS inhibitor L-NAME (20 μM) significantly modified eNOS monomer/dimer ratio, indicating that BH4 addition dissipates the increased monomer/dimer ratio induced by MG and suggesting BH4 being the critical NOS cofactor during eNOS uncoupling (Fig. 6-5C and 6-5D). To confirm the effects of BH4

supplementation on MG-triggered eNOS uncoupling, we further tested the effects of the BH4 precursor sepiapterin. Similar to BH4, superfusion with sepiapterin (50 μM, 2 h) significantly counteracted the increase in eNOS monomer/dimer ratio elicited by MG (Fig. 6-5E and 6-5F).

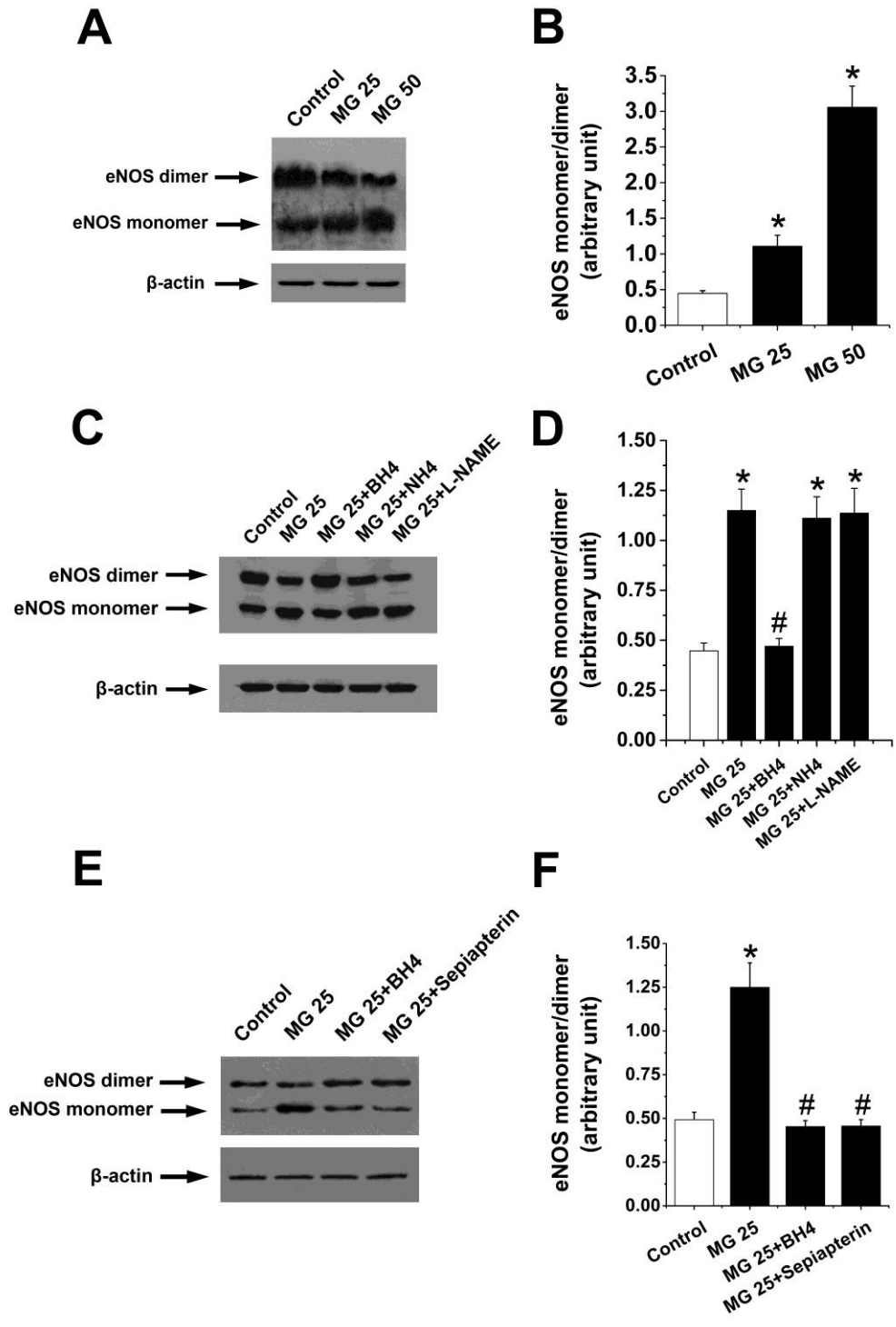

Figure 6-5. Methylglyoxal-sensitive eNOS monomerization in whole cremaster muscle. A and B. Original Western blots (A) and the respective densitometric analysis (B) of the relative abundance of eNOS monomers over eNOS dimers (relative to β-actin) in whole cremaster muscle determined at 6 h after an intrascrotal injection of saline (Control; white bar) or MG (25 mg/kg b.w., MG 25 and 50 mg/kg b.w., MG 50; black bars) with the last 2-h superfusion with bicarbonate buffered-saline. Data are arithmetic means ± SEM (A, representative of four experiments; B, n = 4). * indicates significant difference ($p < 0.05$) from the Control (ANOVA). C – F. Original Western blots (C and E) and the respective densitometric analysis (D and F) of the relative abundance of eNOS monomers over eNOS dimers (relative to β-actin) determined in whole cremaster muscle after an intrascrotal injection of saline (Control; white bar) or MG (25 mg/kg b.w., MG 25; black bars) for 6 h with the last 2-h superfusion with bicarbonate buffered-saline (Control or MG 25), BH4 (100 µM; MG 25 + BH4), NH4 (100 µM; MG 25 + NH4), L-NAME (20 µM; MG 25 + L-NAME) or sepiapterin (50 µM; MG 25 + sepiapterin; in E and F). Data are arithmetic means ± SEM (C and E, representative of four experiments; D and F, n = 4). * indicates significant difference ($p < 0.05$) from Control (ANOVA). # indicates significant difference ($p < 0.05$) from MG treatment alone (ANOVA).

To characterize the specificity of MG-elicited eNOS uncoupling in primary vascular ECs, we cultured and treated HUVECs or murine primary ECs with MG (100 µM) in the presence or absence of BH4 (100 µM) or L-NAME (20 µM). L-NAME did not change MG-induced eNOS monomerization in either type of ECs (Fig. 6-6). Similar to its effects on whole cremaster muscle, BH4 treatment abolished the increase in eNOS monomer/dimer ratio induced by MG (Fig. 6-6) indicating that MG-induced eNOS uncoupling is specific to both murine and human ECs and, thus, ruling out the possibility of indirect effects of BH4 supplementation *in vivo*.

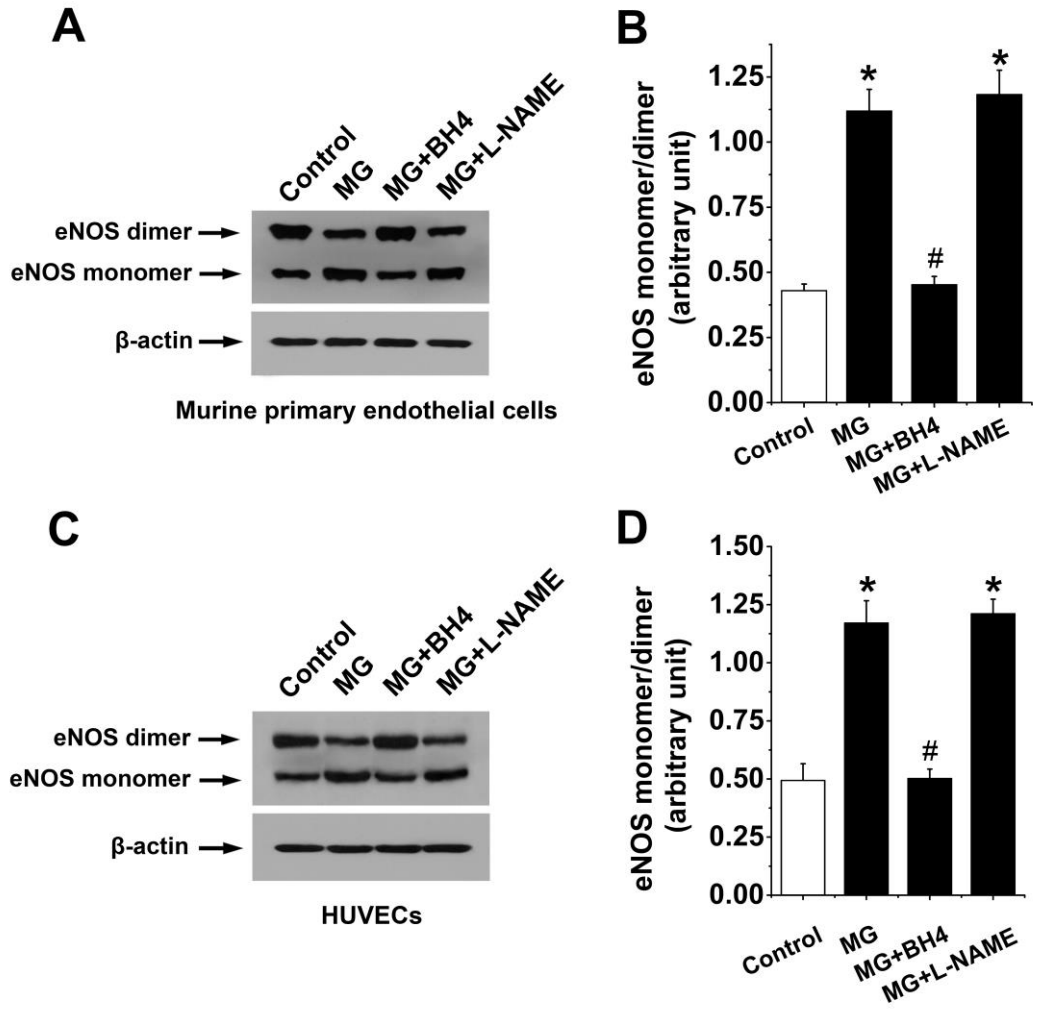

Figure 6-6. Methylglyoxal-sensitive eNOS monomerization in vascular ECs. Original Western blots (A and C) and the respective densitometric analysis (B and D) of the relative abundance of eNOS monomers over eNOS dimers (relative to β-actin) in murine primary ECs (A and B) and in HUVECs (C and D) determined in the absence (Control; white bar) or in the presence of MG (100 μM; black bars) for 6 h with the last 2-h treatment with phosphate-buffered saline (MG), BH4 (100 μM; MG + BH4) or L-NAME (20 μM; MG + L-NAME). Data are arithmetic means ± SEM (A and C, representative of three experiments; B and D, n = 3). * indicates significant difference ($p < 0.05$) from the Control (ANOVA). # indicates significant difference ($p < 0.05$) from MG treatment alone (ANOVA).

To determine whether MG-induced redox imbalance via enhanced eNOS uncoupling is relevant for increased microvascular permeability during leukocyte recruitment, we measured the changes of permeability in cremasteric postcapillary venule after MG treatment. As illustrated in Fig. 6-7A and 7B, superfusion of MG (100 μM, 1 h) on the cremaster muscle time-dependently increased microvascular permeability, an effect that was significantly inhibited by co-superfusion with the ROS scavengers Tempol (300 μM) and MnTBAP (300 μM) 30 min prior to and 1 h following superfusion with MG. To detect the involvement of eNOS uncoupling in permeability changes, we tested whether or not the NOS cofactor BH4 affects MG-induced hyperpermeability. To this end, superfusion of BH4 (100 μM) significantly abated MG-induced increment of microvascular permeability (Fig. 6-7A and 6-7B), an effect clearly highlighting the role of eNOS uncoupling as an essential regulatory mechanism of endothelial barrier impairment sensitive to MG treatment.

Further experiments sought to elucidate the involvement of eNOS uncoupling-derived $O_2^{\bullet-}$ in MG-induced leukocyte recruitment by investigating the effects of L-NAME which modulates $O_2^{\bullet-}$ production as shown previously [258, 421] and in Fig. 6-2D in this study. As a result, superfusion of cremaster muscle with L-NAME (20 μM, for 2 h) following 4 h of MG treatment (50 mg/kg b.w.) tended to decrease enhanced leukocyte rolling flux triggered by MG, an effect, however, not reaching statistical significance (Fig. 6-8A). In the absence of MG, L-NAME alone did not significantly alter rolling flux (Fig. 6-8A). Analysis of rolling velocity revealed that MG-induced reduction in leukocyte rolling velocity was significantly blunted by L-NAME, an effect which reached statistical significance at 5.5–6 h after MG treatment, whereas in the absence of MG, L-NAME alone did not significantly modify rolling velocity (Fig. 6-8B). As is expected and due to its effect in suppressing NO production, L-NAME alone slightly but significantly enhanced both adhesion and emigration, an effect statistically significant at 5 – 6 h for adhesion and at 5.5 h for emigration after normal saline treatment (Fig. 6-8C and 6-8D). Next, we determined the effect of L-NAME treatment on the increased number of adherent and emigrated cells elicited by MG. As illustrated in Fig. 6-8C and 6-8D, L-NAME significantly mitigated MG-induced leukocyte adhesion and emigration, an effect reaching statistical significance at 5 – 6 h after MG injection. Because MG-elicited leukocyte recruitment is dependent on ROS production (Fig. 6-1) and inhibitable by L-NAME (Fig. 6-8), our results suggest that eNOS uncoupling is important in MG-induced leukocyte recruitment.

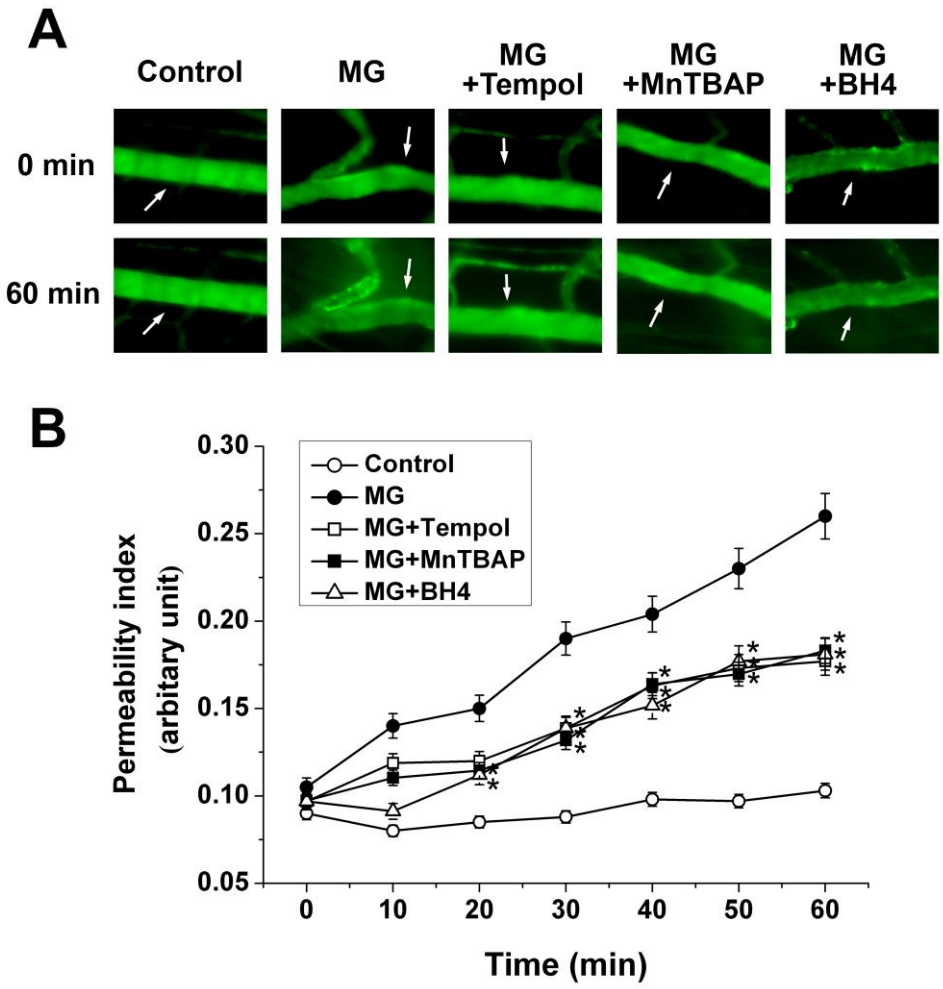

Figure 6-7. Methylglyoxal-induced redox-sensitive and BH4-inhibitable microvascular hyperpermeability. A. Representative fluorescence intravital microscopy images of cremasteric postcapillary venules after i.v. infusion of FITC-labelled BSA (25 mg/kg b.w.) showing leakage of fluorescent BSA before (0 min; upper panels) and 60 min after superfusion (lower panels) with buffered-saline (Control) or MG (100 μM) without (MG) or with Tempol (300 μM; MG + Tempol), MnTBAP (300 μM; MG + MnTBAP) or BH4 (100 μM; MG + BH4). Arrow indicates the venule observed for permeability index measurements. B. The permeability index in the cremasteric postcapillary venules following 1-h superfusion of bicarbonate-buffered saline (Control; white circles) or 100 μM MG in the absence (black cricles) or presence of Tempol (300 μM; white squares), MnTBAP (300 μM; black squares) or BH4 (100 μM; white triangles) 30 min prior to and during 1-h MG superfusion. Data are arithmetic means ± SEM (n = 4). * indicates significant difference ($p < 0.05$) from MG alone (ANOVA).

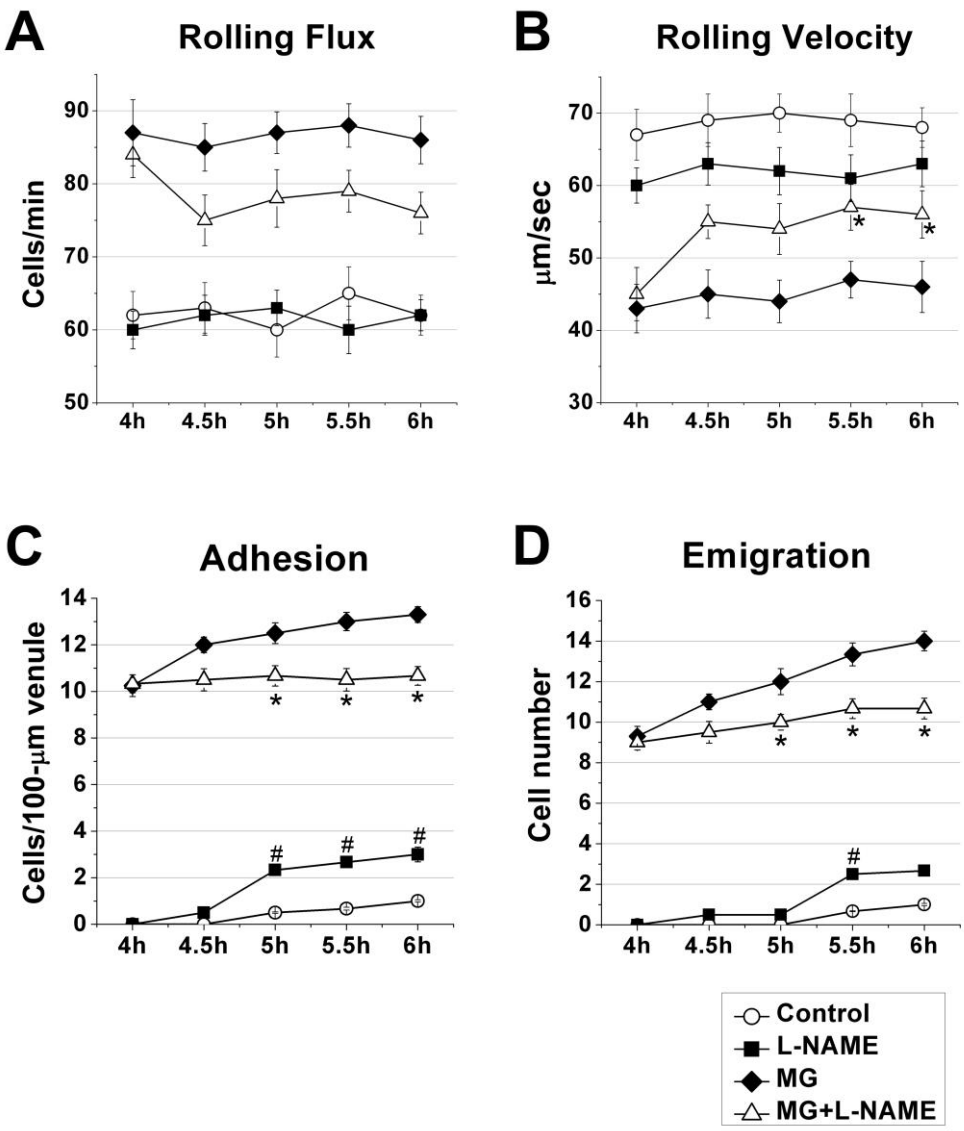

Figure 6-8. Effect of L-NAME on methylglyoxal-induced leukocyte recruitment. The leukocyte rolling flux (A, cells/min), leukocyte rolling velocity (B, µm/sec), the number of adherent (C, cells/100-µm venule) and emigrated (D, cells/443×286 µm2 field) leukocytes determined in cremasteric venules after intrascrotal injection of saline for 6 h with the last 2-h superfusion with control saline (Control; white circles) or L-NAME (20 µM; black squares), or after an intrascrotal injection of MG (50 mg/kg b.w.) for 6 h with the last 2-h superfusion with bicarbonate buffered-saline (MG; black diamonds) or L-NAME (MG + L-NAME; 20 µM; white triangles). Data are arithmetic means ± SEM (n = 5). * indicates significant difference ($p < 0.05$) from MG treatment alone (ANOVA). # indicates significant difference ($p < 0.05$) from control saline (ANOVA).

To confirm the role of eNOS uncoupling on MG-induced leukocyte-endothelial interactions, additional series of experiments were performed to examine the effect of supplementation of NOS cofactor BH4. As a result, superfusion of BH4 (100 μM), but not the analog NH4 (100 μM), significantly blunted MG-stimulated increases in leukocyte rolling flux (Fig. 6-9A). MG-induced reduction in leukocyte rolling velocity was significantly increased in the presence of BH4 but not NH4 (Fig. 6-9B). Moreover, analysis of MG-triggered leukocyte adhesion and emigration revealed that BH4, but not NH4, significantly reduced the number of adherent and emigrated leukocytes elicited by MG, effects statistically significant after 4.5 h (adhesion) and 5 h (emigration) following MG treatment respectively (Fig. 6-9C and 6-9D). To further elucidate the robust effects of BH4 on leukocyte adhesion and emigration, we tested the effects of addition of sepiapterin, a precursor of BH4 synthesis. As shown in Fig. 6-9E and 6-9F, either BH4 (100 μM) or sepiapterin (50 μM) superfusion for 2 h significantly attenuated adhesion and emigration after 4-h MG (25 mg/kg b.w.) administration. Remarkably, the inhibitory potency of both BH4 and sepiapterin on MG-induced leukocyte recruitment is similar, suggesting that BH4 depletion fosters leukocyte recruitment as a result of enhanced eNOS uncoupling following MG treatment.

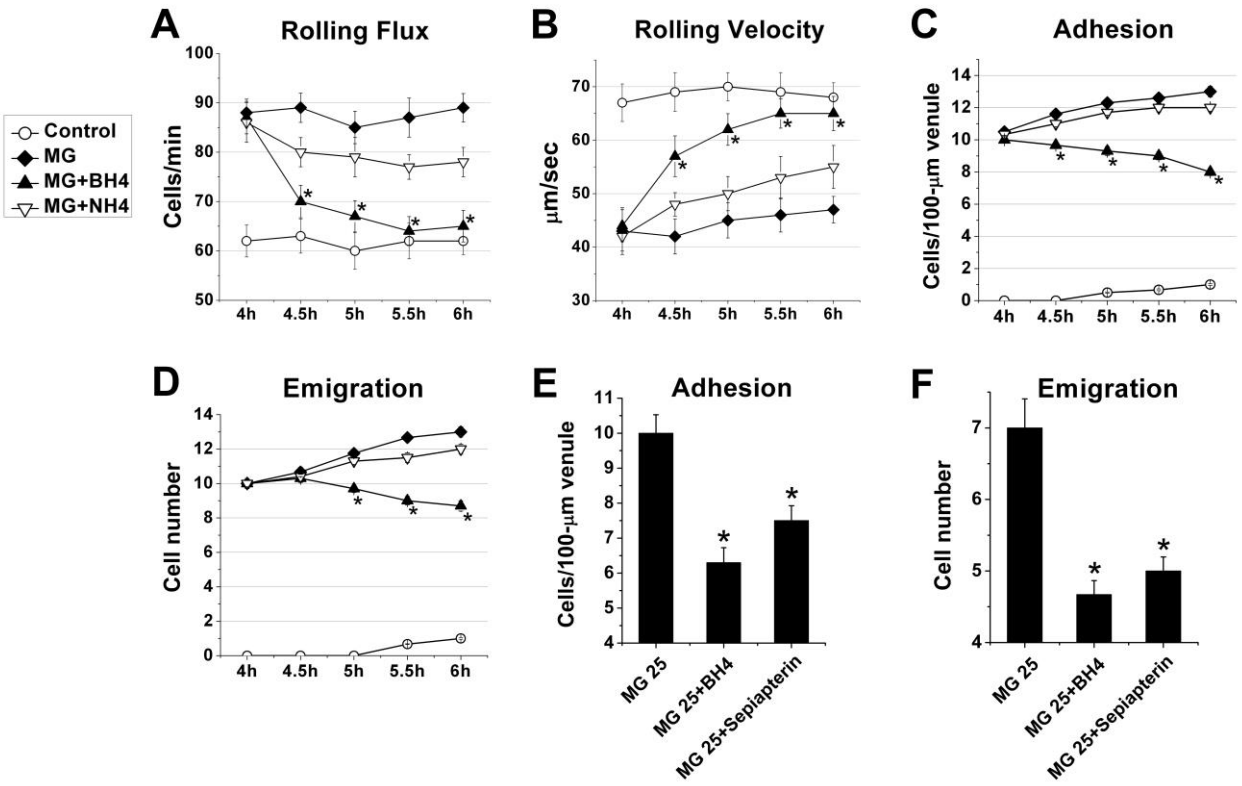

Figure 6-9. Effect of exogenous biopterins on methylglyoxal-induced leukocyte recruitment. A – D. Leukocyte rolling flux (A, cells/min), rolling velocity (B, µm/sec), the number of adherent (C, cells/100-µm venule) and emigrated (D, cells/443×286 µm2 field) leukocytes determined in cremaster venules after an intrascrotal injection of saline for 6 h with the last 2-h superfusion with control saline (Control; white squares), or after an intrascrotal injection of MG (50 mg/kg b.w.) with the last 2-h superfusion with bicarbonate buffered-saline (MG; black diamonds), BH4 (MG + BH4; 100 µM; black triangles) or NH4 (MG + NH4; 100 µM; white triangles). Data are arithmetic means ± SEM (n = 5). * indicates significant difference ($p < 0.05$) from MG treatment alone (ANOVA). E and F. The number of adherent (E, cells/100-µm venule) and emigrated (F, cells/443×286 µm2 field) leukocytes determined in cremasteric venules at 6 h after an intrascrotal injection of MG (25 mg/kg b.w.) with the last 2-h superfusion with bicarbonate buffered-saline (MG 25), BH4 (MG 25 + BH4; 100 µM) or sepiapterin (MG 25 + sepiapterin; 50 µM). Data are arithmetic means ± SEM (n = 4). * indicates significant difference ($p < 0.05$) from MG treatment alone (ANOVA).

6.5 Discussion

The present study reveals that oxidative stress plays a key role in MG-induced leukocyte recruitment, eNOS uncoupling is important for MG-triggered ROS production *in vivo* and the $O_2^{\bullet-}$ produced by uncoupled eNOS contributes to redox-sensitive leukocyte recruitment elicited by MG. MG stimulates dose-dependent monomerization of eNOS, depletion of the NOS cofactor BH4 and generation of ROS and L-NAME-inhibitable $O_2^{\bullet-}$, effects that indicate eNOS uncoupling contributing to the increased leukocyte-endothelial interactions and microvascular hyperpermeability. We provide biological evidence that pharmacologically scavenging ROS, inhibition of NOS, replenishment of the NOS cofactor BH4 or addition of BH4 precursor sepiapterin ameliorates MG-induced leukocyte recruitment (Figure 6-10). Although the concentrations of MG used in this study are higher than those detected in diabetic plasma [427] and tissue [136], they currently serve as an optimal model to elucidate mechanisms involved in pathological changes in animal models of diabetes [187], and in acute MG-induced leukocyte-endothelial interactions *in vivo* [75]. To our knowledge, the role of eNOS uncoupling in MG-induced leukocyte trafficking has never been studied *in vivo*.

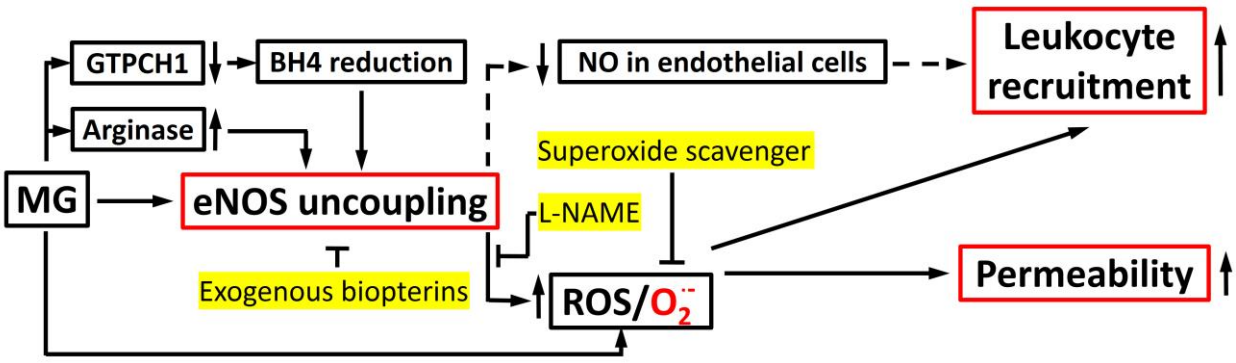

Figure 6-10. Schematic diagram of MG-induced eNOS uncoupling in ECs.

The consequence of the unequivocal link between enhanced ROS generation and MG metabolism is reflected by impaired cellular functions in diabetes. We observed that 16 – 18% of MG-triggered $O_2^{\bullet-}$ production was inhibitable by either BH4 or L-NAME suggesting that previously identified sources such as NADPH oxidase and mitochondrial enzymes are pivotal in MG-elicited $O_2^{\bullet-}$ production in addition to uncoupled eNOS [115]. MG has been shown to impair redox balance

[428] by not only stimulating ROS production but also by modulating the availability and/or functions of cytoprotective molecules such as glutathione [371], superoxide dismutase [174], glyoxalase [372] and H_2S [373]. Whether the increased ROS generation is required for MG-elicited leukocyte-endothelial interactions has not been elucidated. Upregulation of endothelial adhesion molecules such as P-selectin, VCAM-1 and ICAM-1 is associated with ROS generation [429] and the expression of superoxide dismutase [430] and Nox2 [431]. Furthermore, both $O_2^{\bullet-}$ [432] and peroxynitrite ($ONOO^-$) [433] activate endothelial NF-κB signalling. MG was recently shown to induce NF-κB-dependent upregulation of the expression of P- and E-selectins and ICAM-1 on ECs which fosters leukocyte recruitment [75]. MG-induced leukocyte-endothelial interactions could also be elicited by neutrophil-derived ROS [434]. At least in theory, counteracting enhanced ROS production is pivotal to anti-inflammatory therapeutics in diabetes.

An important feature for non-physiological $O_2^{\bullet-}$ induction in endothelium is the uncoupling of eNOS [351]. The activity of eNOS was shown to be substantially affected by MG [70]. Increased NADPH oxidase-derived $O_2^{\bullet-}$ reacts with eNOS-derived NO to generate $ONOO^-$ which oxidizes BH4 [351]. In our study, MG treatment affected *de novo* BH4 synthesis, thereby decreasing its bioavailability. Mounting evidence suggests that the NOS essential cofactor BH4 is critical for the maintenance of eNOS dimers and is functionally related to S-glutathionylation, a powerful regulator of eNOS uncoupling [382]. Exogenous administration of BH4 or overexpression of GTPCH1 gene can increase endothelial BH4 [435] and maintain eNOS dimerization in murine [358] and human [259] diabetic endothelium. Besides increasing NO availability, BH4 treatment blunted Ca^{2+}-independent NOS activation and tissue nitrotyrosine levels essential for inflammation but without appreciable changes in eNOS phosphorylation [436]. Interestingly, BH4 treatment was shown to protect against experimental arthritis [437] and ischemia-reperfusion- and CCl_4-triggered hepatic injury [438-440]. In a cardiac model of ischemia-reperfusion, BH4 was shown to mitigate both leukocyte adhesion and emigration [441]. Supported by the ineffectiveness of NH4 in MG-induced $O_2^{\bullet-}$ generation and leukocyte recruitment, it is tempting to speculate that BH4-elicited inhibitory responses in microvasculature *in vivo* are attributed to maintenance of functional eNOS dimers than BH4 antioxidant effects *per se*.

The robust effects of BH4 reconstitution or administration of its analog sepiapterin on $O_2^{\bullet-}$ and BH4 availability can be translated into its effects on reducing MG-elicited leukocyte recruitment and microvascular hyperpermeability. To corroborate those findings, we used selective NOS inhibitor L-NAME to inhibit $O_2^{\bullet-}$ production by the uncoupled eNOS [442, 443]. L-NAME dissipated MG-induced leukocyte adhesion and emigration. L-NAME alone increased leukocyte recruitment in our model and as was shown elsewhere [407, 408] through the suppression of NO production by NOS. Paradoxically, L-NAME counteracted the effects of MG for $O_2^{\bullet-}$ production and leukocyte recruitment, which underscores its effect on suppressing eNOS for $O_2^{\bullet-}$ production, suggesting eNOS uncoupling following MG increases.

Several studies have shown that compromised endothelial barrier function is an essential phenomenon of the diabetic milieu that contributes to microangiopathy [444, 445]. Hyperglycemia and advanced glycation end-products have been reported to increase microvascular permeability by activation of PKC [446, 447], HIF-1α [448], RhoA/ROCK [449] and AMPK [450] signalling in endothelium. In diabetic rats, retinal VEGF expression and vascular hyperpermeability were shown to be associated with enhanced tyrosine nitration [451]. However, the implication of the increased MG and the mechanism by which it triggers microvascular leakage remains ill-defined. We observed that administration of ROS scavengers or BH4 abated MG-induced microvascular hyperpermeability and by the same token attenuated leukocyte recruitment. In fact, increases in microvascular permeability is associated with both leukocyte-EC interactions [423, 424] and oxidative imbalance [452, 453]. In the blood-retinal barrier, MG was shown to induce hyperpermeability via stimulation of matrix metalloproteinases and subsequent proteolytic degradation of occludin [454]. Clearly, our data highlight that MG-induced $O_2^{\bullet-}$ derived from uncoupled eNOS contributes to, but may not totally account for, the diminished vascular barrier function in diabetes.

In summary, eNOS uncoupling is critical for the regulation of leukocyte-endothelial interactions in MG-triggered inflammation that is associated with diabetes. In the present work, this role was specifically demonstrated *in vivo* for the metabolite MG. Our findings of pharmacological targeting eNOS uncoupling-derived $O_2^{\bullet-}$ may be relevant for the management of inflammation in diabetes.

CHAPTER 7

DISCUSSION AND CONCLUSIONS

7.1 General discussion

Many studies have proposed that elevated MG level in diabetic state could promote endothelial dysfunction that leads to diabetic vascular damage. The studies presented in this thesis suggest leukocyte recruitment can be a contributory factor in this phenomenon. To examine the effect of MG in inducing leukocyte recruitment, the present study used an acute local MG administration to mimic the effect of increased MG on local microvasculature, and showed that there was a clear dose-response relationship between local MG dose and the degree of leukocyte recruitment in the tissue. Based on the intravital microscopy results, we established an acute inflammation model by using 25 mg/kg and 50 mg/kg MG injection to investigate the mechanisms of MG-induced leucocyte recruitment. It is known that plasma MG level in healthy human is about 1 μmol/L or less, but it is increased by 2—6 fold in diabetes patients [112, 131]. Using HPLC, we detected the levels of MG in plasma and cremaster muscle. The results showed that at 50 mg/kg MG local injection, with the significant increase of leukocyte recruitment in cremasteric microvasculature, the plasma MG level was increased only by 1.7 fold. This suggests that the effect of MG may be localised. Under pathological conditions, the vascular complications of diabetes usually occur years after the initial illness. However, the overexpression of adhesion molecules is important in the early stages of diabetic vascular complications [256], which is consistent with what we observed following acute MG treatment (50 mg/kg injection for 4 h). In the present study, the role of each of the three MG-upregulated EC adhesion molecules was characterised by functional blocking studies using specific antibodies. Our data indicate that acute MG treatment increases leukocyte rolling flux by upregulating P-selectin expression, reduces leukocyte rolling velocity by upregulating E-selectin expression, and increases cell adhesion by upregulating ICAM-1 expression. All these contribute to the increased leukocyte-EC interactions that result in leukocyte emigration.

In exploring the mechanisms of MG-induced adhesion molecule expression, we observed that MG-induced expression of endothelial adhesion molecules is NF-κB-dependent. Additionally, gene ablation or pharmacological inhibition of either GSK3 or SGK1 blunted MG-induced NF-κB activity, suggesting the regulatory role of GSK3 and SGK1 in NF-κB activation. The glycogen synthase kinase, GSK3, is a pleiotropic serine/threonine kinase. It is a critical downstream effector of PI3K signalling [307]. GSK3 regulates glucose homeostasis and is inhibited by stimulation of

insulin receptors, thus playing a crucial role in energy metabolism. Remarkably, GSK3 is critical in inflammatory processes by playing either a positive or negative regulatory role [310]. Endothelial GSK3 was reported to regulate E-selectin expression [313] and vascular permeability [314], thus highlighting the importance of GSK3 signalling in ECs. Similarly, SGK1 is activated by PI3K and phosphoinositide-dependent kinase-1 (PDK1). It is regulated by a wide array of stimuli [316] including hyperglycemia [317]. Previous studies have shown SGK1 to be a promising therapeutic target in diabetes [318]. SGK1 was shown to foster the activation of NF-κB [241] and CREB [242], two transcription factors that are important in inflammatory responses. However, the function of SGK1 expressed in ECs is not completely understood. In our study, we showed that NF-κB activity was sequentially regulated by GSK3 and SGK1 in MG-treated ECs. MG induced Akt-regulated transient GSK3 activation in ECs, which was responsible for NF-κB activation at early time-points (< 1 h). After 1 h, the GSK3 activity was decreased due to the up-regulation of SGK1 which sustained the NF-κB activity at later time-points. The activation of SGK1 was also responsible for CREB activity which was partially involved in ICAM-1 expression. In accordance with our results, SGK1 was previously reported to mediate NF-κB-dependent ICAM-1 expression in mesangial cells [336], while the knockdown of SGK1 gene was previously shown to attenuate NF-κB activation in cells isolated from renal collecting ducts [337]. Taken together, our study is the first to demonstrate the modulatory role of GSK3 and SGK1 in leukocyte recruitment *in vivo* by regulating the expression of endothelial adhesion molecules, thus revealing the role of SGK1- and GSK3-dependent signalling in MG-induced inflammation.

Besides its role in activating signalling pathways and upregulating adhesion molecule expression, MG has its damaging effects by promoting ROS generation. In this study, we identified uncoupled eNOS as a new source of superoxide in MG-treated ECs. In hyperglycemia [455], hypertension [456], and aging [457], the eNOS protein expression was increased, yet its function was impaired. It was reported that eNOS uncoupling can be triggered by an oxidative environment, by BH4 depletion, or by decreased BH4/BH2 ratio in cells, leading to the insufficient binding of BH4 to eNOS [257, 458, 459]. Under these circumstances, the electron transport from the C-terminal-bound NADPH to N-terminal heme center is changed, and the oxygen molecule instead of L-arginine is the terminal electron acceptor, leading to the formation of superoxide. For the last a few years, eNOS uncoupling has been related to atherosclerosis, diabetes, hypertension, smoking

and ischemia and reperfusion injury [356]. In ECs and VSMCs, MG decreases eNOS activity and NO production, whereas superoxide and peroxynitrite formation is increased [31, 70]. These findings indicate that eNOS uncoupling might be one of the mechanisms underlying MG-induced vessel damage. However, to our knowledge, the effect of MG on eNOS uncoupling has not been reported previously. In this part of the study, we found that MG-triggered eNOS uncoupling and hypophosphorylation were associated with superoxide generation and biopterin depletion in EA.hy926 ECs and in the endothelium of cremasteric microvasculature. In these tissues and cells, MG increased eNOS monomerization and decreased BH4/total biopterin ratio, effects that were significantly mitigated by supplementation of BH4 or its precursor sepiapterin but not by L-NAME or tetrahydroneopterin, indicative of MG-triggered eNOS uncoupling. We also found that MG-induced leukocyte recruitment was significantly attenuated by supplementation of BH4 or sepiapterin or suppression of superoxide by L-NAME confirming the role of eNOS uncoupling in MG-elicited leukocyte recruitment. Our study further showed that MG treatment decreased the expression of guanosine triphosphate cyclohydrolase 1 and increased the expression of 3-nitrotyrosine (3NT), suggesting that impaired BH4 biosynthesis and increased peroxynitrite formation are responsible for MG-induced eNOS uncoupling. Our results are consistent with previous reports that MG increases peroxynitrite formation [31] and peroxynitrite uncouples eNOS by causing BH4 oxidation in bovine aortic ECs [460]. However, given the multiple effects of MG, other mechanisms may also be involved. Other studies show that PKC activity is elevated under hyperglycemic condition, and eNOS uncoupling seems to be the consequence of PKC activity since PKC inhibitors reverse eNOS uncoupling [442, 461]. It was also shown that MG-induced AGE activates PKC in cultured ECs [462]. Thus, it is reasonable that the activation of PKC may also be involved. However, more evidence is needed to prove the link between AGE formation and PKC activation, and their role in MG-induced eNOS uncoupling.

Taken together, our study reveals two distinct molecular mechanisms of MG-induced leukocyte recruitment which support the role of inflammation in the early stage of diabetic vascular complications. Our findings may unveil the mystery of vascular complications and immune dysfunction in diabetes and may provide a new clue for possible therapeutic strategies.

7.2 Conclusions

The present study explores the mechanism of MG-induced leukocyte recruitment in mouse cremasteric microvasculature. Using biochemical and intravital microscopy techniques, this study shows that administration of MG (25 and 50 mg/kg) dose-dependently induced leukocyte recruitment in cremasteric vasculature, with 84-92% recruited cells being neutrophils. Such MG treatment up-regulated the expression of EC adhesion molecules P-selectin, E-selectin, and ICAM-1 via the activation of NF-κB signalling pathway in ECs, which contributed to the increased leukocyte rolling flux, reduced leukocyte rolling velocity, and increased leukocyte adhesion, respectively. Further study of MG-related signalling pathways revealed that NF-κB activity is sequentially regulated by GSK3 and SGK1 in ECs. Our data suggest that MG induces Akt-regulated transient GSK3 activation in ECs, which was responsible for NF-κB activation at early time-points (< 1 h). After MG activation for 1 h, GSK3 activity was decreased due to the up-regulation of SGK1 which sustained the NF-κB activity at later time-points. Silencing or inhibiting GSK3 or SGK1 attenuated P-selectin, E-selectin and ICAM-1 expression in ECs and abated MG-induced leukocyte recruitment by supressing NF-κB activity. SGK1 also promoted CREB activity which was partially involved in ICAM-1 expression. Silencing CREB blunted ICAM-1 expression with no changes in the expression of P-selectin and E-selectin levels. Additionally, this study reveals MG-triggered eNOS uncoupling as an important source of MG-induced superoxide in ECs. MG increased eNOS monomerization and decreased BH4/total biopterin ratio, effects that were significantly mitigated by supplementation of BH4 or its precursor sepiapterin but not by L-NAME or tetrahydroneopterin. MG-induced leukocyte recruitment was significantly attenuated by supplementation of BH4 or sepiapterin or suppression of superoxide by L-NAME confirming the role of eNOS uncoupling in MG-elicited leukocyte recruitment. MG treatment also decreased the expression of guanosine triphosphate cyclohydrolase I in murine primary ECs, suggesting the impaired BH4 biosynthesis being one of the mechanisms underlying MG-induced eNOS uncoupling.

7.3 Significance of the study

Leukocyte recruitment from the blood stream into the extravascular space is essential for developing an appropriate inflammatory response to injury and infection. However, the interaction

between neutrophils and ECs induced by hyperglycemia brings more damage than cure to the microvasculature. Increased MG levels and increased leukocyte transmigration are both believed to play an important role in the pathogenesis of diabetic vascular complications, but the correlation between these two phenomena has never been studied, neither has the mechanisms underlying MG-induced leukocyte recruitment. In this study, we show, for the first time, that administration of MG to the tissue dose-dependently induced leukocyte recruitment, with 84-92% recruited cells being neutrophils. We also demonstrate two distinct mechanisms that are involved in MG-induced leukocyte recruitment. Firstly, MG sequentially induces the activation of GSK3 and SGK1, which subsequently activates downstream transcriptional factors NF-κB and CREB. NF-κB- and CREB-mediated expression of endothelial adhesion molecules fosters leukocyte adhesion and is also crucial for leukocyte recruitment. Secondly, we show for the first time that MG-induced eNOS uncoupling in ECs, which shifts the functions of eNOS from producing NO to producing superoxide, is at least partially responsible for MG-induced leukocyte recruitment. The change in eNOS function is possibly due to the inhibition of guanosine triphosphate cyclohydrolase I and the reduction of BH4. These novel findings not only uncover the mechanisms of MG-induced leukocyte recruitment, but also suggest the potential therapeutic targets for MG-sensitive endothelial dysfunction in diabetes.

7.4 Limitations of the study

In the study of MG-induced pathological changes, the dose of exogenous MG administered to the animal, the tissue and the cells has been debated. One tends to compare the doses used in the *in vivo* or *in vitro* studies to MG concentrations in the plasma of diabetes patients, and usually the MG doses used in these studies are much higher than the MG concentrations measured in patients. As reviewed in Chapter 1, the progression of diabetes lasts for years, and under hyperglycemic condition, MG is not the only agent that contributes to the damage to the cells and local tissues. Thus, in the study that uses only exogenous MG, it should be reasonable and acceptable to use high MG doses (sometimes even higher than pathological condition) to establish the *in vitro* or *in vivo* model, especially in a short term study [134]. In Sprague-Dawley rats, using MG as the only stimulus, Dhar *et al*. found that it requires 60 mg/kg/day and 28 days of chronic MG infusion by minipump to induce impaired glucose tolerance, apoptosis in pancreatic islets and reduced

pancreatic insulin content in rats [134]. This suggests that large doses of exogenous MG are required to establish a diabetic animal model and reach the similar plasma MG level as in diabetic patients. Besides, in diabetic patients, the data of MG level in the tissue is still missing. Thus it is not known whether the MG level in the local tissue is higher or lower than its level in the plasma. As we mentioned, MG formation is due to glucose or fructose overload and the activation of polyol pathway. Therefore, under pathological condition, cells that are exposed to high glucose or fructose have the potential to produce MG and to have the damaging effects locally. However, exogenous MG is firstly absorbed through the peritoneum into the blood, and then distributed to the whole body. Thus, it is not surprising that it requires large doses of MG to simulate pathological changes in local tissue encountered in diabetic states. The progression of diabetes is a complicated process that involves many active agents with the potential to damage tissues and cells. Without a specific MG inhibitor, it is impossible to study the role of MG alone in the progression of diabetes. Therefore, this leaves the exogenous administration of MG to be the only approach to perform the study, and a higher MG dose is usually required in short term *in vivo* and *in vitro* studies. Diabetes is a complicated disease that requires years to develop, and a large amount of data o MG from the patients is not available. Regardless, the mechanistic studies using animal models and cell models are useful to reveal the molecular mechanisms of MG-induced pathological changes, and to indicate potential therapeutic targets for diabetic patients.

REFFERENCES

1. Longo, D.L., *Harrison's principles of internal medicine*. 18th ed. 2012, New York: McGraw-Hill.
2. *Diabetes in Canada : facts and figures from a public health perspective*. 2011, Ottawa Ont.: Public Health Agency of Canada. 112 p.
3. Public Health Agency of Canada., *Report from the National Diabetes Surveillance System : diabetes in Canada, 2009*. 2009, Ottawa: Public Health Agency of Canada. 26, 28 p.
4. Leroux, C., et al., *Lifestyle and Cardiometabolic Risk in Adults with Type 1 Diabetes: A Review.* Can J Diabetes, 2014. **38**(1): p. 62-69.
5. Public Health Agency of Canada., *Report from the National Diabetes Surveillance System : diabetes in Canada, 2008*. 2009, Ottawa: Public Health Agency of Canada. 25, 25 p.
6. Canada. Health Canada. and Laboratory Centre for Disease Control (Canada). Diabetes Division., *Diabetes in Canada : national statistics and opportunities for improved surveillance, prevention, and control= Le diabète au Canada : statisques nationales et possibilités d'accroître la surveillance, la prévention et la lutte*. 1999, Ottawa: Health Canada. xii, 70, 76, xiii p.
7. Bending, D., P. Zaccone, and A. Cooke, *Inflammation and type one diabetes.* Int Immunol, 2012. **24**(6): p. 339-46.
8. DeSouza, C. and V. Fonseca, *Therapeutic targets to reduce cardiovascular disease in type 2 diabetes.* Nat Rev Drug Discov, 2009. **8**(5): p. 361-7.
9. Israili, Z.H., *Advances in the treatment of type 2 diabetes mellitus.* Am J Ther, 2011. **18**(2): p. 117-52.
10. Barnett, A.H., *New treatments in type 2 diabetes: a focus on the incretin-based therapies.* Clin Endocrinol (Oxf), 2009. **70**(3): p. 343-53.
11. Ramos-Roman, M.A., *Prolactin and lactation as modifiers of diabetes risk in gestational diabetes.* Horm Metab Res, 2011. **43**(9): p. 593-600.

12. Kerimoglu, O.S., et al., *Incidence of diabetes mellitus at postpartum six to twelve months following the diagnosis of gestational diabetes mellitus.* J Turk Ger Gynecol Assoc, 2010. **11**(2): p. 89-94.
13. Cooper, M.E., R.E. Gilbert, and G. Jerums, *Diabetic vascular complications.* Clin Exp Pharmacol Physiol, 1997. **24**(9-10): p. 770-5.
14. Gariano, R.F. and T.W. Gardner, *Retinal angiogenesis in development and disease.* Nature, 2005. **438**(7070): p. 960-6.
15. Cumbie, B.C. and K.L. Hermayer, *Current concepts in targeted therapies for the pathophysiology of diabetic microvascular complications.* Vasc Health Risk Manag, 2007. **3**(6): p. 823-32.
16. Tarr, J.M., et al., *Pathophysiology of Diabetic Retinopathy.* ISRN Ophthalmol, 2013. **2013**: p. 343560.
17. Eleftheriadis, T., et al., *The renal endothelium in diabetic nephropathy.* Ren Fail, 2013. **35**(4): p. 592-9.
18. Pasnoor, M., et al., *Diabetic neuropathy part 1: overview and symmetric phenotypes.* Neurol Clin, 2013. **31**(2): p. 425-45.
19. O'Brien, M.M., P.J. Schofield, and M.R. Edwards, *Polyol-pathway enzymes of human brain. Partial purification and properties of sorbitol dehydrogenase.* Biochem J, 1983. **211**(1): p. 81-90.
20. Shen, B., et al., *Roles of sugar alcohols in osmotic stress adaptation. Replacement of glycerol by mannitol and sorbitol in yeast.* Plant Physiol, 1999. **121**(1): p. 45-52.
21. Karlgren, S., et al., *Conditional osmotic stress in yeast: a system to study transport through aquaglyceroporins and osmostress signaling.* J Biol Chem, 2005. **280**(8): p. 7186-93.
22. Gabbay, K.H., *Hyperglycemia, polyol metabolism, and complications of diabetes mellitus.* Annu Rev Med, 1975. **26**: p. 521-36.
23. Gabbay, K.H., *Aldose reductase inhibition in the treatment of diabetic neuropathy: where are we in 2004?* Curr Diab Rep, 2004. **4**(6): p. 405-8.
24. Phillips, S.A. and P.J. Thornalley, *The formation of methylglyoxal from triose phosphates. Investigation using a specific assay for methylglyoxal.* Eur J Biochem, 1993. **212**(1): p. 101-5.

25. Richard, J.P., *Mechanism for the formation of methylglyoxal from triosephosphates.* Biochem Soc Trans, 1993. **21**(2): p. 549-53.
26. Sharma, Y., et al., *Advanced glycation end products and diabetic retinopathy.* J Ocul Biol Dis Infor, 2012. **5**(3-4): p. 63-69.
27. Shinohara, M., et al., *Overexpression of glyoxalase-I in bovine endothelial cells inhibits intracellular advanced glycation endproduct formation and prevents hyperglycemia-induced increases in macromolecular endocytosis.* J Clin Invest, 1998. **101**(5): p. 1142-7.
28. Bourajjaj, M., et al., *Role of methylglyoxal adducts in the development of vascular complications in diabetes mellitus.* Biochem Soc Trans, 2003. **31**(Pt 6): p. 1400-2.
29. Mostafa, A.A., et al., *Plasma protein advanced glycation end products, carboxymethyl cysteine, and carboxyethyl cysteine, are elevated and related to nephropathy in patients with diabetes.* Mol Cell Biochem, 2007. **302**(1-2): p. 35-42.
30. Shah, S., et al., *Oxidative stress, glucose metabolism, and the prevention of type 2 diabetes: pathophysiological insights.* Antioxid Redox Signal, 2007. **9**(7): p. 911-29.
31. Chang, T., R. Wang, and L. Wu, *Methylglyoxal-induced nitric oxide and peroxynitrite production in vascular smooth muscle cells.* Free Radic Biol Med, 2005. **38**(2): p. 286-93.
32. Bitar, M.S., et al., *Nitric oxide dynamics and endothelial dysfunction in type II model of genetic diabetes.* Eur J Pharmacol, 2005. **511**(1): p. 53-64.
33. Fong, D.S., et al., *Diabetic retinopathy.* Diabetes Care, 2004. **27**(10): p. 2540-53.
34. Keenan, H.A., et al., *Clinical factors associated with resistance to microvascular complications in diabetic patients of extreme disease duration: the 50-year medalist study.* Diabetes Care, 2007. **30**(8): p. 1995-7.
35. Aiello, L.P., et al., *Suppression of retinal neovascularization in vivo by inhibition of vascular endothelial growth factor (VEGF) using soluble VEGF-receptor chimeric proteins.* Proc Natl Acad Sci U S A, 1995. **92**(23): p. 10457-61.
36. Crawford, T.N., et al., *Diabetic retinopathy and angiogenesis.* Curr Diabetes Rev, 2009. **5**(1): p. 8-13.
37. Kadoglou, N.P., et al., *Matrix metalloproteinases and diabetic vascular complications.* Angiology, 2005. **56**(2): p. 173-89.

38. Xu, Y., Z. He, and G.L. King, *Introduction of hyperglycemia and dyslipidemia in the pathogenesis of diabetic vascular complications.* Curr Diab Rep, 2005. **5**(2): p. 91-7.
39. Keidar, S., et al., *Angiotensin II administration to atherosclerotic mice increases macrophage uptake of oxidized ldl: a possible role for interleukin-6.* Arterioscler Thromb Vasc Biol, 2001. **21**(9): p. 1464-9.
40. Kaneto, H., et al., *Role of reactive oxygen species in the progression of type 2 diabetes and atherosclerosis.* Mediators Inflamm, 2010. **2010**: p. 453892.
41. Nishimura, H., *[Diabetes mellitus and atherosclerosis].* Nihon Rinsho, 2011. **69**(1): p. 131-7.
42. Frostegard, J., *Immune Mechanisms in Atherosclerosis, Especially in Diabetes Type 2.* Front Endocrinol (Lausanne), 2013. **4**: p. 162.
43. Vinik, A.I., et al., *Platelet dysfunction in type 2 diabetes.* Diabetes Care, 2001. **24**(8): p. 1476-85.
44. Li, Y., V. Woo, and R. Bose, *Platelet hyperactivity and abnormal Ca(2+) homeostasis in diabetes mellitus.* Am J Physiol Heart Circ Physiol, 2001. **280**(4): p. H1480-9.
45. Boyle, P.J., *Diabetes mellitus and macrovascular disease: mechanisms and mediators.* Am J Med, 2007. **120**(9 Suppl 2): p. S12-7.
46. Beckman, J.A., M.A. Creager, and P. Libby, *Diabetes and atherosclerosis: epidemiology, pathophysiology, and management.* JAMA, 2002. **287**(19): p. 2570-81.
47. Pickup, J.C., *Inflammation and activated innate immunity in the pathogenesis of type 2 diabetes.* Diabetes Care, 2004. **27**(3): p. 813-23.
48. Das, A. and S. Mukhopadhyay, *The evil axis of obesity, inflammation and type-2 diabetes.* Endocr Metab Immune Disord Drug Targets, 2011. **11**(1): p. 23-31.
49. Deans, K.A. and N. Sattar, *"Anti-inflammatory" drugs and their effects on type 2 diabetes.* Diabetes Technol Ther, 2006. **8**(1): p. 18-27.
50. Al-Shukaili, A., et al., *Analysis of inflammatory mediators in type 2 diabetes patients.* Int J Endocrinol, 2013. **2013**: p. 976810.
51. Xia, F., et al., *Luteolin Protects HUVECs from TNF-alpha-induced Oxidative Stress and Inflammation via its Effects on the Nox4/ROS-NF-kappaB and MAPK Pathways.* J Atheroscler Thromb, 2014.

52. Seybold, J., et al., *Tumor necrosis factor-alpha-dependent expression of phosphodiesterase 2: role in endothelial hyperpermeability.* Blood, 2005. **105**(9): p. 3569-76.
53. Nieto-Vazquez, I., et al., *Dual role of interleukin-6 in regulating insulin sensitivity in murine skeletal muscle.* Diabetes, 2008. **57**(12): p. 3211-21.
54. Plomgaard, P., et al., *Tumor necrosis factor-alpha induces skeletal muscle insulin resistance in healthy human subjects via inhibition of Akt substrate 160 phosphorylation.* Diabetes, 2005. **54**(10): p. 2939-45.
55. Draznin, B., *Molecular mechanisms of insulin resistance: serine phosphorylation of insulin receptor substrate-1 and increased expression of p85alpha: the two sides of a coin.* Diabetes, 2006. **55**(8): p. 2392-7.
56. Sykiotis, G.P. and A.G. Papavassiliou, *Serine phosphorylation of insulin receptor substrate-1: a novel target for the reversal of insulin resistance.* Mol Endocrinol, 2001. **15**(11): p. 1864-9.
57. Franke, T.F., *PI3K/Akt: getting it right matters.* Oncogene, 2008. **27**(50): p. 6473-88.
58. Long, S.D. and P.H. Pekala, *Regulation of GLUT4 mRNA stability by tumor necrosis factor-alpha: alterations in both protein binding to the 3' untranslated region and initiation of translation.* Biochem Biophys Res Commun, 1996. **220**(3): p. 949-53.
59. Meguro, S., M. Ishibashi, and I. Takei, *[The significance of high sensitive C reactive protein as a risk factor for cardiovascular diseases]*. Rinsho Byori, 2012. **60**(4): p. 356-61.
60. Jin, C., et al., *Association of serum glycated albumin, C-reactive protein and ICAM-1 levels with diffuse coronary artery disease in patients with type 2 diabetes mellitus.* Clin Chim Acta, 2009. **408**(1-2): p. 45-9.
61. Nguyen, M.T., et al., *A subpopulation of macrophages infiltrates hypertrophic adipose tissue and is activated by free fatty acids via Toll-like receptors 2 and 4 and JNK-dependent pathways.* J Biol Chem, 2007. **282**(48): p. 35279-92.
62. Lee, J.Y., et al., *Saturated fatty acids, but not unsaturated fatty acids, induce the expression of cyclooxygenase-2 mediated through Toll-like receptor 4.* J Biol Chem, 2001. **276**(20): p. 16683-9.

63. Gao, Z., et al., *Inhibition of insulin sensitivity by free fatty acids requires activation of multiple serine kinases in 3T3-L1 adipocytes.* Mol Endocrinol, 2004. **18**(8): p. 2024-34.
64. Hirosumi, J., et al., *A central role for JNK in obesity and insulin resistance.* Nature, 2002. **420**(6913): p. 333-6.
65. Wellen, K.E. and G.S. Hotamisligil, *Inflammation, stress, and diabetes.* J Clin Invest, 2005. **115**(5): p. 1111-9.
66. Schalkwijk, C.G. and C.D. Stehouwer, *Vascular complications in diabetes mellitus: the role of endothelial dysfunction.* Clin Sci (Lond), 2005. **109**(2): p. 143-59.
67. Colwell, G.A., *Inflammation and diabetic vascular complications.* Diabetes Care, 1999. **22**(12): p. 1927-8.
68. Yamagishi, S., *Advanced glycation end products and receptor-oxidative stress system in diabetic vascular complications.* Ther Apher Dial, 2009. **13**(6): p. 534-9.
69. Inoguchi, T. and H. Nawata, *NAD(P)H oxidase activation: a potential target mechanism for diabetic vascular complications, progressive beta-cell dysfunction and metabolic syndrome.* Curr Drug Targets, 2005. **6**(4): p. 495-501.
70. Dhar, A., et al., *Methylglyoxal scavengers attenuate endothelial dysfunction induced by methylglyoxal and high concentrations of glucose.* Br J Pharmacol, 2010. **161**(8): p. 1843-56.
71. Dimmeler, S. and A.M. Zeiher, *Nitric oxide-an endothelial cell survival factor.* Cell Death Differ, 1999. **6**(10): p. 964-8.
72. Basta, G., A.M. Schmidt, and R. De Caterina, *Advanced glycation end products and vascular inflammation: implications for accelerated atherosclerosis in diabetes.* Cardiovasc Res, 2004. **63**(4): p. 582-92.
73. Basta, G., et al., *Advanced glycation end products activate endothelium through signal-transduction receptor RAGE: a mechanism for amplification of inflammatory responses.* Circulation, 2002. **105**(7): p. 816-22.
74. DiDonato, J.A., et al., *A cytokine-responsive IkappaB kinase that activates the transcription factor NF-kappaB.* Nature, 1997. **388**(6642): p. 548-54.
75. Su, Y., et al., *The role of endothelial cell adhesion molecules P-selectin, E-selectin and intercellular adhesion molecule-1 in leucocyte recruitment induced by exogenous methylglyoxal.* Immunology, 2012. **137**(1): p. 65-79.

76. Bobryshev, Y.V., *Monocyte recruitment and foam cell formation in atherosclerosis.* Micron, 2006. **37**(3): p. 208-22.
77. Patel, S.S., et al., *Inhibition of alpha4 integrin and ICAM-1 markedly attenuate macrophage homing to atherosclerotic plaques in ApoE-deficient mice.* Circulation, 1998. **97**(1): p. 75-81.
78. Cai, H. and D.G. Harrison, *Endothelial dysfunction in cardiovascular diseases: the role of oxidant stress.* Circ Res, 2000. **87**(10): p. 840-4.
79. Sprague, A.H. and R.A. Khalil, *Inflammatory cytokines in vascular dysfunction and vascular disease.* Biochem Pharmacol, 2009. **78**(6): p. 539-52.
80. Hattori, Y., et al., *High-glucose-induced nuclear factor kappaB activation in vascular smooth muscle cells.* Cardiovasc Res, 2000. **46**(1): p. 188-97.
81. Schmidt, A.M., et al., *Activation of receptor for advanced glycation end products: a mechanism for chronic vascular dysfunction in diabetic vasculopathy and atherosclerosis.* Circ Res, 1999. **84**(5): p. 489-97.
82. Duguid, J.B. and G.S. Anderson, *The pathogenesis of hyaline arteriolosclerosis.* J Pathol Bacteriol, 1952. **64**(3): p. 519-22.
83. Gamble, C.N., *The pathogenesis of hyaline arteriolosclerosis.* Am J Pathol, 1986. **122**(3): p. 410-20.
84. Hansson, G.K., *Inflammation, atherosclerosis, and coronary artery disease.* N Engl J Med, 2005. **352**(16): p. 1685-95.
85. Smith, J.P., *Hyaline arteriolosclerosis in the kidney.* J Pathol Bacteriol, 1955. **69**(1-2): p. 147-68.
86. Bastard, J.P., et al., *Recent advances in the relationship between obesity, inflammation, and insulin resistance.* Eur Cytokine Netw, 2006. **17**(1): p. 4-12.
87. Goral, J. and E.J. Kovacs, *In vivo ethanol exposure down-regulates TLR2-, TLR4-, and TLR9-mediated macrophage inflammatory response by limiting p38 and ERK1/2 activation.* J Immunol, 2005. **174**(1): p. 456-63.
88. Milanski, M., et al., *Saturated fatty acids produce an inflammatory response predominantly through the activation of TLR4 signaling in hypothalamus: implications for the pathogenesis of obesity.* J Neurosci, 2009. **29**(2): p. 359-70.

89. Boisvert, W.A., et al., *A leukocyte homologue of the IL-8 receptor CXCR-2 mediates the accumulation of macrophages in atherosclerotic lesions of LDL receptor-deficient mice.* J Clin Invest, 1998. **101**(2): p. 353-63.
90. Kim, C.S., et al., *Circulating levels of MCP-1 and IL-8 are elevated in human obese subjects and associated with obesity-related parameters.* Int J Obes (Lond), 2006. **30**(9): p. 1347-55.
91. Gerszten, R.E., et al., *MCP-1 and IL-8 trigger firm adhesion of monocytes to vascular endothelium under flow conditions.* Nature, 1999. **398**(6729): p. 718-23.
92. Ogawa, M., *Differentiation and proliferation of hematopoietic stem cells.* Blood, 1993. **81**(11): p. 2844-53.
93. Haslett, C., *Resolution of acute inflammation and the role of apoptosis in the tissue fate of granulocytes.* Clin Sci (Lond), 1992. **83**(6): p. 639-48.
94. Sallusto, F. and M. Baggiolini, *Chemokines and leukocyte traffic.* Nat Immunol, 2008. **9**(9): p. 949-52.
95. Petri, B., M. Phillipson, and P. Kubes, *The physiology of leukocyte recruitment: an in vivo perspective.* J Immunol, 2008. **180**(10): p. 6439-46.
96. Kolaczkowska, E. and P. Kubes, *Neutrophil recruitment and function in health and inflammation.* Nat Rev Immunol, 2013. **13**(3): p. 159-75.
97. Kubes, P. and P.A. Ward, *Leukocyte recruitment and the acute inflammatory response.* Brain Pathol, 2000. **10**(1): p. 127-35.
98. Kubes, P., *Polymorphonuclear leukocyte--endothelium interactions: a role for pro-inflammatory and anti-inflammatory molecules.* Can J Physiol Pharmacol, 1993. **71**(1): p. 88-97.
99. Liu, L. and P. Kubes, *Molecular mechanisms of leukocyte recruitment: organ-specific mechanisms of action.* Thromb Haemost, 2003. **89**(2): p. 213-20.
100. Kubes, P. and S.M. Kerfoot, *Leukocyte recruitment in the microcirculation: the rolling paradigm revisited.* News Physiol Sci, 2001. **16**: p. 76-80.
101. Kelly, M., J.M. Hwang, and P. Kubes, *Modulating leukocyte recruitment in inflammation.* J Allergy Clin Immunol, 2007. **120**(1): p. 3-10.
102. McDonald, B. and P. Kubes, *Cellular and molecular choreography of neutrophil recruitment to sites of sterile inflammation.* J Mol Med (Berl), 2011. **89**(11): p. 1079-88.

103. Rao, R.M., et al., *Endothelial-dependent mechanisms of leukocyte recruitment to the vascular wall.* Circ Res, 2007. **101**(3): p. 234-47.
104. Ley, K., *Molecular mechanisms of leukocyte recruitment in the inflammatory process.* Cardiovasc Res, 1996. **32**(4): p. 733-42.
105. Shaw, S.K., et al., *Real-time imaging of vascular endothelial-cadherin during leukocyte transmigration across endothelium.* J Immunol, 2001. **167**(4): p. 2323-30.
106. Muller, W.A., *Leukocyte-endothelial-cell interactions in leukocyte transmigration and the inflammatory response.* Trends Immunol, 2003. **24**(6): p. 327-34.
107. Snyderman, R. and E.J. Goetzl, *Molecular and cellular mechanisms of leukocyte chemotaxis.* Science, 1981. **213**(4510): p. 830-7.
108. Heit, B., et al., *An intracellular signaling hierarchy determines direction of migration in opposing chemotactic gradients.* J Cell Biol, 2002. **159**(1): p. 91-102.
109. Galkina, E. and K. Ley, *Leukocyte recruitment and vascular injury in diabetic nephropathy.* J Am Soc Nephrol, 2006. **17**(2): p. 368-77.
110. Binder, C.J., et al., *Innate and acquired immunity in atherogenesis.* Nat Med, 2002. **8**(11): p. 1218-26.
111. Taniyama, Y. and K.K. Griendling, *Reactive oxygen species in the vasculature: molecular and cellular mechanisms.* Hypertension, 2003. **42**(6): p. 1075-81.
112. Wang, H., et al., *Proinflammatory and proapoptotic effects of methylglyoxal on neutrophils from patients with type 2 diabetes mellitus.* Clin Biochem, 2007. **40**(16-17): p. 1232-9.
113. Hanses, F., et al., *Reduced neutrophil apoptosis in diabetic mice during staphylococcal infection leads to prolonged Tnfalpha production and reduced neutrophil clearance.* PLoS One, 2011. **6**(8): p. e23633.
114. Xu, N., X. Lei, and L. Liu, *Tracking neutrophil intraluminal crawling, transendothelial migration and chemotaxis in tissue by intravital video microscopy.* J Vis Exp, 2011(55).
115. Desai, K.M., et al., *Oxidative stress and aging: is methylglyoxal the hidden enemy?* Can J Physiol Pharmacol, 2010. **88**(3): p. 273-84.
116. Kalapos, M.P., *Methylglyoxal in living organisms: chemistry, biochemistry, toxicology and biological implications.* Toxicol Lett, 1999. **110**(3): p. 145-75.

117. Hopper, D.J. and R.A. Cooper, *The purification and properties of Escherichia coli methylglyoxal synthase.* Biochem J, 1972. **128**(2): p. 321-9.
118. Hopper, D.J. and R.A. Cooper, *The regulation of Escherichia coli methylglyoxal synthase; a new control site in glycolysis?* FEBS Lett, 1971. **13**(4): p. 213-216.
119. Ray, S. and M. Ray, *Isolation of methylglyoxal synthase from goat liver.* J Biol Chem, 1981. **256**(12): p. 6230-3.
120. Brownlee, M., *Biochemistry and molecular cell biology of diabetic complications.* Nature, 2001. **414**(6865): p. 813-20.
121. Koop, D.R. and J.P. Casazza, *Identification of ethanol-inducible P-450 isozyme 3a as the acetone and acetol monooxygenase of rabbit microsomes.* J Biol Chem, 1985. **260**(25): p. 13607-12.
122. Deng, Y. and P.H. Yu, *Simultaneous determination of formaldehyde and methylglyoxal in urine: involvement of semicarbazide-sensitive amine oxidase-mediated deamination in diabetic complications.* J Chromatogr Sci, 1999. **37**(9): p. 317-22.
123. Yu, P.H., et al., *Physiological and pathological implications of semicarbazide-sensitive amine oxidase.* Biochim Biophys Acta, 2003. **1647**(1-2): p. 193-9.
124. Desai, K. and L. Wu, *Methylglyoxal and advanced glycation endproducts: new therapeutic horizons?* Recent Pat Cardiovasc Drug Discov, 2007. **2**(2): p. 89-99.
125. Chang, T. and L. Wu, *Methylglyoxal, oxidative stress, and hypertension.* Can J Physiol Pharmacol, 2006. **84**(12): p. 1229-38.
126. Wu, L. and B.H. Juurlink, *Increased methylglyoxal and oxidative stress in hypertensive rat vascular smooth muscle cells.* Hypertension, 2002. **39**(3): p. 809-14.
127. Bonnefont-Rousselot, D., *Glucose and reactive oxygen species.* Curr Opin Clin Nutr Metab Care, 2002. **5**(5): p. 561-8.
128. Goldin, A., et al., *Advanced glycation end products: sparking the development of diabetic vascular injury.* Circulation, 2006. **114**(6): p. 597-605.
129. Adams, C.J., et al., *Isolation by HPLC and characterisation of the bioactive fraction of New Zealand manuka (Leptospermum scoparium) honey.* Carbohydr Res, 2008. **343**(4): p. 651-9.
130. Nagao, M., et al., *Mutagens in coffee and other beverages.* Environ Health Perspect, 1986. **67**: p. 89-91.

131. McLellan, A.C., et al., *Glyoxalase system in clinical diabetes mellitus and correlation with diabetic complications.* Clin Sci (Lond), 1994. **87**(1): p. 21-9.
132. Lapolla, A., et al., *Glyoxal and methylglyoxal levels in diabetic patients: quantitative determination by a new GC/MS method.* Clin Chem Lab Med, 2003. **41**(9): p. 1166-73.
133. Beisswenger, P.J., et al., *Metformin reduces systemic methylglyoxal levels in type 2 diabetes.* Diabetes, 1999. **48**(1): p. 198-202.
134. Dhar, A., et al., *Chronic methylglyoxal infusion by minipump causes pancreatic beta-cell dysfunction and induces type 2 diabetes in Sprague-Dawley rats.* Diabetes, 2011. **60**(3): p. 899-908.
135. Dhar, I., et al., *Increased methylglyoxal formation with upregulation of renin angiotensin system in fructose fed Sprague Dawley rats.* PLoS One, 2013. **8**(9): p. e74212.
136. Randell, E.W., S. Vasdev, and V. Gill, *Measurement of methylglyoxal in rat tissues by electrospray ionization mass spectrometry and liquid chromatography.* J Pharmacol Toxicol Methods, 2005. **51**(2): p. 153-7.
137. Sowers, J.R., M. Epstein, and E.D. Frohlich, *Diabetes, hypertension, and cardiovascular disease: an update.* Hypertension, 2001. **37**(4): p. 1053-9.
138. Taniguchi, C.M., B. Emanuelli, and C.R. Kahn, *Critical nodes in signalling pathways: insights into insulin action.* Nat Rev Mol Cell Biol, 2006. **7**(2): p. 85-96.
139. Guo, Q., et al., *Methylglyoxal contributes to the development of insulin resistance and salt sensitivity in Sprague-Dawley rats.* J Hypertens, 2009. **27**(8): p. 1664-71.
140. Riboulet-Chavey, A., et al., *Methylglyoxal impairs the insulin signaling pathways independently of the formation of intracellular reactive oxygen species.* Diabetes, 2006. **55**(5): p. 1289-99.
141. Jia, X. and L. Wu, *Accumulation of endogenous methylglyoxal impaired insulin signaling in adipose tissue of fructose-fed rats.* Mol Cell Biochem, 2007. **306**(1-2): p. 133-9.
142. Jia, X., et al., *Structural and functional changes in human insulin induced by methylglyoxal.* FASEB J, 2006. **20**(9): p. 1555-7.
143. Maritim, A.C., R.A. Sanders, and J.B. Watkins, 3rd, *Diabetes, oxidative stress, and antioxidants: a review.* J Biochem Mol Toxicol, 2003. **17**(1): p. 24-38.
144. Chung, S.S., et al., *Contribution of polyol pathway to diabetes-induced oxidative stress.* J Am Soc Nephrol, 2003. **14**(8 Suppl 3): p. S233-6.

145. Gerrits, P.M. and E. Tsalikian, *Diabetes and fructose metabolism.* Am J Clin Nutr, 1993. **58**(5 Suppl): p. 796S-799S.
146. Basciano, H., L. Federico, and K. Adeli, *Fructose, insulin resistance, and metabolic dyslipidemia.* Nutr Metab (Lond), 2005. **2**(1): p. 5.
147. Delbosc, S., et al., *Involvement of oxidative stress and NADPH oxidase activation in the development of cardiovascular complications in a model of insulin resistance, the fructose-fed rat.* Atherosclerosis, 2005. **179**(1): p. 43-9.
148. Hwang, I.S., et al., *Fructose-induced insulin resistance and hypertension in rats.* Hypertension, 1987. **10**(5): p. 512-6.
149. Wu, L., *The pro-oxidant role of methylglyoxal in mesenteric artery smooth muscle cells.* Can J Physiol Pharmacol, 2005. **83**(1): p. 63-8.
150. Du, J., et al., *Superoxide-mediated early oxidation and activation of ASK1 are important for initiating methylglyoxal-induced apoptosis process.* Free Radic Biol Med, 2001. **31**(4): p. 469-78.
151. Kalapos, M.P., A. Littauer, and H. de Groot, *Has reactive oxygen a role in methylglyoxal toxicity? A study on cultured rat hepatocytes.* Arch Toxicol, 1993. **67**(5): p. 369-72.
152. Su, Y., et al., *Methylglyoxal modulates endothelial nitric oxide synthase-associated functions in EA.hy926 endothelial cells.* Cardiovasc Diabetol, 2013. **12**: p. 134.
153. Su, Y., et al., *Uncoupling of eNOS contributes to redox-sensitive leukocyte recruitment and microvascular leakage elicited by methylglyoxal.* Biochem Pharmacol, 2013. **86**(12): p. 1762-74.
154. Turrens, J.F., *Mitochondrial formation of reactive oxygen species.* J Physiol, 2003. **552**(Pt 2): p. 335-44.
155. Yu, T., et al., *Mitochondrial fission mediates high glucose-induced cell death through elevated production of reactive oxygen species.* Cardiovasc Res, 2008. **79**(2): p. 341-51.
156. Russell, J.W., et al., *High glucose-induced oxidative stress and mitochondrial dysfunction in neurons.* FASEB J, 2002. **16**(13): p. 1738-48.
157. Wang, H., J. Liu, and L. Wu, *Methylglyoxal-induced mitochondrial dysfunction in vascular smooth muscle cells.* Biochem Pharmacol, 2009. **77**(11): p. 1709-16.
158. Rosca, M.G., et al., *Alterations in renal mitochondrial respiration in response to the reactive oxoaldehyde methylglyoxal.* Am J Physiol Renal Physiol, 2002. **283**(1): p. F52-9.

159. Suh, K.S., et al., *Methylglyoxal induces oxidative stress and mitochondrial dysfunction in osteoblastic MC3T3-E1 cells.* Free Radic Res, 2014. **48**(2): p. 206-17.
160. de Arriba, S.G., et al., *Methylglyoxal impairs glucose metabolism and leads to energy depletion in neuronal cells--protection by carbonyl scavengers.* Neurobiol Aging, 2007. **28**(7): p. 1044-50.
161. Ho, C., et al., *Methylglyoxal-induced fibronectin gene expression through Ras-mediated NADPH oxidase activation in renal mesangial cells.* Nephrology (Carlton), 2007. **12**(4): p. 348-56.
162. Wautier, M.P., et al., *Activation of NADPH oxidase by AGE links oxidant stress to altered gene expression via RAGE.* Am J Physiol Endocrinol Metab, 2001. **280**(5): p. E685-94.
163. Pacher, P. and C. Szabo, *Role of peroxynitrite in the pathogenesis of cardiovascular complications of diabetes.* Curr Opin Pharmacol, 2006. **6**(2): p. 136-41.
164. Julius, U., et al., *Nitrosylated proteins in monocytes as a new marker of oxidative-nitrosative stress in diabetic subjects with macroangiopathy.* Exp Clin Endocrinol Diabetes, 2009. **117**(2): p. 72-7.
165. el-Remessy, A.B., et al., *Oxidative stress inactivates VEGF survival signaling in retinal endothelial cells via PI 3-kinase tyrosine nitration.* J Cell Sci, 2005. **118**(Pt 1): p. 243-52.
166. Shibuki, H., et al., *Lipid peroxidation and peroxynitrite in retinal ischemia-reperfusion injury.* Invest Ophthalmol Vis Sci, 2000. **41**(11): p. 3607-14.
167. Dickhout, J.G., et al., *Peroxynitrite causes endoplasmic reticulum stress and apoptosis in human vascular endothelium: implications in atherogenesis.* Arterioscler Thromb Vasc Biol, 2005. **25**(12): p. 2623-9.
168. Vareniuk, I., et al., *Nitrosative stress and peripheral diabetic neuropathy in leptin-deficient (ob/ob) mice.* Exp Neurol, 2007. **205**(2): p. 425-36.
169. Drel, V.R., et al., *A peroxynitrite decomposition catalyst counteracts sensory neuropathy in streptozotocin-diabetic mice.* Eur J Pharmacol, 2007. **569**(1-2): p. 48-58.
170. Obrosova, I.G., et al., *Role for nitrosative stress in diabetic neuropathy: evidence from studies with a peroxynitrite decomposition catalyst.* FASEB J, 2005. **19**(3): p. 401-3.

171. Forstermann, U. and H. Kleinert, *Nitric oxide synthase: expression and expressional control of the three isoforms.* Naunyn Schmiedebergs Arch Pharmacol, 1995. **352**(4): p. 351-64.
172. Dhar, A., et al., *Methylglyoxal production in vascular smooth muscle cells from different metabolic precursors.* Metabolism, 2008. **57**(9): p. 1211-20.
173. Park, Y.S., et al., *Identification of the binding site of methylglyoxal on glutathione peroxidase: methylglyoxal inhibits glutathione peroxidase activity via binding to glutathione binding sites Arg 184 and 185.* Free Radic Res, 2003. **37**(2): p. 205-11.
174. Kang, J.H., *Modification and inactivation of human Cu,Zn-superoxide dismutase by methylglyoxal.* Mol Cells, 2003. **15**(2): p. 194-9.
175. Droge, W., *Free radicals in the physiological control of cell function.* Physiol Rev, 2002. **82**(1): p. 47-95.
176. Chelikani, P., I. Fita, and P.C. Loewen, *Diversity of structures and properties among catalases.* Cell Mol Life Sci, 2004. **61**(2): p. 192-208.
177. Rahimi, R., et al., *A review on the role of antioxidants in the management of diabetes and its complications.* Biomed Pharmacother, 2005. **59**(7): p. 365-73.
178. Choudhary, D., D. Chandra, and R.K. Kale, *Influence of methylglyoxal on antioxidant enzymes and oxidative damage.* Toxicol Lett, 1997. **93**(2-3): p. 141-52.
179. Frye, E.B., et al., *Role of the Maillard reaction in aging of tissue proteins. Advanced glycation end product-dependent increase in imidazolium cross-links in human lens proteins.* J Biol Chem, 1998. **273**(30): p. 18714-9.
180. Schalkwijk, C.G., et al., *Amadori albumin in type 1 diabetic patients: correlation with markers of endothelial function, association with diabetic nephropathy, and localization in retinal capillaries.* Diabetes, 1999. **48**(12): p. 2446-53.
181. Tan, K.C., et al., *Advanced glycation end products and endothelial dysfunction in type 2 diabetes.* Diabetes Care, 2002. **25**(6): p. 1055-9.
182. Ogawa, S., et al., *Methylglyoxal is a predictor in type 2 diabetic patients of intima-media thickening and elevation of blood pressure.* Hypertension, 2010. **56**(3): p. 471-6.
183. Oldfield, M.D., et al., *Advanced glycation end products cause epithelial-myofibroblast transdifferentiation via the receptor for advanced glycation end products (RAGE).* J Clin Invest, 2001. **108**(12): p. 1853-63.

184. Stitt, A.W., et al., *Advanced glycation end products (AGEs) co-localize with AGE receptors in the retinal vasculature of diabetic and of AGE-infused rats.* Am J Pathol, 1997. **150**(2): p. 523-31.
185. Westwood, M.E. and P.J. Thornalley, *Molecular characteristics of methylglyoxal-modified bovine and human serum albumins. Comparison with glucose-derived advanced glycation endproduct-modified serum albumins.* J Protein Chem, 1995. **14**(5): p. 359-72.
186. Chang, T., et al., *Modification of Akt1 by methylglyoxal promotes the proliferation of vascular smooth muscle cells.* FASEB J, 2011. **25**(5): p. 1746-57.
187. Dhar, A., K.M. Desai, and L. Wu, *Alagebrium attenuates acute methylglyoxal-induced glucose intolerance in Sprague-Dawley rats.* Br J Pharmacol, 2010. **159**(1): p. 166-75.
188. Tanaka, Y., et al., *Effect of metformin on advanced glycation endproduct formation and peripheral nerve function in streptozotocin-induced diabetic rats.* Eur J Pharmacol, 1999. **376**(1-2): p. 17-22.
189. Johnson, G.L. and R. Lapadat, *Mitogen-activated protein kinase pathways mediated by ERK, JNK, and p38 protein kinases.* Science, 2002. **298**(5600): p. 1911-2.
190. Purves, T., et al., *A role for mitogen-activated protein kinases in the etiology of diabetic neuropathy.* FASEB J, 2001. **15**(13): p. 2508-14.
191. Liu, Z. and W. Cao, *p38 mitogen-activated protein kinase: a critical node linking insulin resistance and cardiovascular diseases in type 2 diabetes mellitus.* Endocr Metab Immune Disord Drug Targets, 2009. **9**(1): p. 38-46.
192. Yang, R. and J.M. Trevillyan, *c-Jun N-terminal kinase pathways in diabetes.* Int J Biochem Cell Biol, 2008. **40**(12): p. 2702-6.
193. Du, J., et al., *Involvement of MEKK1/ERK/P21Waf1/Cip1 signal transduction pathway in inhibition of IGF-I-mediated cell growth response by methylglyoxal.* J Cell Biochem, 2003. **88**(6): p. 1235-46.
194. Ren, J., et al., *High glucose induces cardiac insulin-like growth factor I resistance in ventricular myocytes: role of Akt and ERK activation.* Cardiovasc Res, 2003. **57**(3): p. 738-48.
195. Blanc, A., N.R. Pandey, and A.K. Srivastava, *Synchronous activation of ERK 1/2, p38mapk and PKB/Akt signaling by H2O2 in vascular smooth muscle cells: potential involvement in vascular disease (review).* Int J Mol Med, 2003. **11**(2): p. 229-34.

196. Du, J., et al., *Methylglyoxal induces apoptosis in Jurkat leukemia T cells by activating c-Jun N-terminal kinase.* J Cell Biochem, 2000. **77**(2): p. 333-44.
197. Yamawaki, H., et al., *Methylglyoxal mediates vascular inflammation via JNK and p38 in human endothelial cells.* Am J Physiol Cell Physiol, 2008. **295**(6): p. C1510-7.
198. Saatian, B., et al., *Transcriptional regulation of lysophosphatidic acid-induced interleukin-8 expression and secretion by p38 MAPK and JNK in human bronchial epithelial cells.* Biochem J, 2006. **393**(Pt 3): p. 657-68.
199. Thiefes, A., et al., *Simultaneous blockade of NFkappaB, JNK, and p38 MAPK by a kinase-inactive mutant of the protein kinase TAK1 sensitizes cells to apoptosis and affects a distinct spectrum of tumor necrosis factor [corrected] target genes.* J Biol Chem, 2005. **280**(30): p. 27728-41.
200. Ovrevik, J., et al., *p38 and Src-ERK1/2 pathways regulate crystalline silica-induced chemokine release in pulmonary epithelial cells.* Toxicol Sci, 2004. **81**(2): p. 480-90.
201. Zhong, J., et al., *GCK is essential to systemic inflammation and pattern recognition receptor signaling to JNK and p38.* Proc Natl Acad Sci U S A, 2009. **106**(11): p. 4372-7.
202. Steinberg, S.F., *Structural basis of protein kinase C isoform function.* Physiol Rev, 2008. **88**(4): p. 1341-78.
203. Dempsey, E.C., et al., *Protein kinase C isozymes and the regulation of diverse cell responses.* Am J Physiol Lung Cell Mol Physiol, 2000. **279**(3): p. L429-38.
204. Rossi, F., et al., *De novo synthesis of diacylglycerol from glucose. A new pathway of signal transduction in human neutrophils stimulated during phagocytosis of beta-glucan particles.* J Biol Chem, 1991. **266**(13): p. 8034-8.
205. Srivastava, A.K., *High glucose-induced activation of protein kinase signaling pathways in vascular smooth muscle cells: a potential role in the pathogenesis of vascular dysfunction in diabetes (review).* Int J Mol Med, 2002. **9**(1): p. 85-9.
206. Quagliaro, L., et al., *Intermittent high glucose enhances apoptosis related to oxidative stress in human umbilical vein endothelial cells: the role of protein kinase C and NAD(P)H-oxidase activation.* Diabetes, 2003. **52**(11): p. 2795-804.
207. Morigi, M., et al., *Leukocyte-endothelial interaction is augmented by high glucose concentrations and hyperglycemia in a NF-kB-dependent fashion.* J Clin Invest, 1998. **101**(9): p. 1905-15.

208. Kinsella, J.L., et al., *Protein kinase C regulates endothelial cell tube formation on basement membrane matrix, Matrigel.* Exp Cell Res, 1992. **199**(1): p. 56-62.
209. Michell, B.J., et al., *Coordinated control of endothelial nitric-oxide synthase phosphorylation by protein kinase C and the cAMP-dependent protein kinase.* J Biol Chem, 2001. **276**(21): p. 17625-8.
210. Geraldes, P. and G.L. King, *Activation of protein kinase C isoforms and its impact on diabetic complications.* Circ Res, 2010. **106**(8): p. 1319-31.
211. Thallas-Bonke, V., et al., *Attenuation of extracellular matrix accumulation in diabetic nephropathy by the advanced glycation end product cross-link breaker ALT-711 via a protein kinase C-alpha-dependent pathway.* Diabetes, 2004. **53**(11): p. 2921-30.
212. Hadas, K., et al., *Methylglyoxal induces platelet hyperaggregation and reduces thrombus stability by activating PKC and inhibiting PI3K/Akt pathway.* PLoS One, 2013. **8**(9): p. e74401.
213. Jan, C.R., et al., *Effect of methylglyoxal on intracellular calcium levels and viability in renal tubular cells.* Cell Signal, 2005. **17**(7): p. 847-55.
214. Rasheed, Z. and T.M. Haqqi, *Endoplasmic reticulum stress induces the expression of COX-2 through activation of eIF2alpha, p38-MAPK and NF-kappaB in advanced glycation end products stimulated human chondrocytes.* Biochim Biophys Acta, 2012. **1823**(12): p. 2179-89.
215. Shi, L., et al., *Advanced glycation end products induce human corneal epithelial cells apoptosis through generation of reactive oxygen species and activation of JNK and p38 MAPK pathways.* PLoS One, 2013. **8**(6): p. e66781.
216. Liu, X., et al., *Effect of pioglitazone on insulin resistance in fructose-drinking rats correlates with AGEs/RAGE inhibition and block of NADPH oxidase and NF kappa B activation.* Eur J Pharmacol, 2010. **629**(1-3): p. 153-8.
217. Haslbeck, K.M., et al., *The AGE/RAGE/NF-(kappa)B pathway may contribute to the pathogenesis of polyneuropathy in impaired glucose tolerance (IGT).* Exp Clin Endocrinol Diabetes, 2005. **113**(5): p. 288-91.
218. Feng, L., et al., *Chronic vascular inflammation in patients with type 2 diabetes: endothelial biopsy and RT-PCR analysis.* Diabetes Care, 2005. **28**(2): p. 379-84.

219. Wautier, J.L., et al., *Receptor-mediated endothelial cell dysfunction in diabetic vasculopathy. Soluble receptor for advanced glycation end products blocks hyperpermeability in diabetic rats.* J Clin Invest, 1996. **97**(1): p. 238-43.
220. Schmidt, A.M., et al., *Advanced glycation endproducts interacting with their endothelial receptor induce expression of vascular cell adhesion molecule-1 (VCAM-1) in cultured human endothelial cells and in mice. A potential mechanism for the accelerated vasculopathy of diabetes.* J Clin Invest, 1995. **96**(3): p. 1395-403.
221. Okamoto, T., et al., *Angiogenesis induced by advanced glycation end products and its prevention by cerivastatin.* FASEB J, 2002. **16**(14): p. 1928-30.
222. Jope, R.S., C.J. Yuskaitis, and E. Beurel, *Glycogen synthase kinase-3 (GSK3): inflammation, diseases, and therapeutics.* Neurochem Res, 2007. **32**(4-5): p. 577-95.
223. Hoeflich, K.P., et al., *Requirement for glycogen synthase kinase-3beta in cell survival and NF-kappaB activation.* Nature, 2000. **406**(6791): p. 86-90.
224. Nikoulina, S.E., et al., *Potential role of glycogen synthase kinase-3 in skeletal muscle insulin resistance of type 2 diabetes.* Diabetes, 2000. **49**(2): p. 263-71.
225. Ring, D.B., et al., *Selective glycogen synthase kinase 3 inhibitors potentiate insulin activation of glucose transport and utilization in vitro and in vivo.* Diabetes, 2003. **52**(3): p. 588-95.
226. Smith, S.A., et al., *Rosiglitazone, but not glyburide, reduces circulating proinsulin and the proinsulin:insulin ratio in type 2 diabetes.* J Clin Endocrinol Metab, 2004. **89**(12): p. 6048-53.
227. Yue, T.L., et al., *Rosiglitazone treatment in Zucker diabetic Fatty rats is associated with ameliorated cardiac insulin resistance and protection from ischemia/reperfusion-induced myocardial injury.* Diabetes, 2005. **54**(2): p. 554-62.
228. Henriksen, E.J., et al., *Modulation of muscle insulin resistance by selective inhibition of GSK-3 in Zucker diabetic fatty rats.* Am J Physiol Endocrinol Metab, 2003. **284**(5): p. E892-900.
229. Cline, G.W., et al., *Effects of a novel glycogen synthase kinase-3 inhibitor on insulin-stimulated glucose metabolism in Zucker diabetic fatty (fa/fa) rats.* Diabetes, 2002. **51**(10): p. 2903-10.

230. Plotkin, B., et al., *Insulin mimetic action of synthetic phosphorylated peptide inhibitors of glycogen synthase kinase-3.* J Pharmacol Exp Ther, 2003. **305**(3): p. 974-80.
231. Pearce, N.J., et al., *Development of glucose intolerance in male transgenic mice overexpressing human glycogen synthase kinase-3beta on a muscle-specific promoter.* Metabolism, 2004. **53**(10): p. 1322-30.
232. Fiory, F., et al., *Methylglyoxal impairs insulin signalling and insulin action on glucose-induced insulin secretion in the pancreatic beta cell line INS-1E.* Diabetologia, 2011. **54**(11): p. 2941-52.
233. Li, X.H., et al., *Methylglyoxal induces tau hyperphosphorylation via promoting AGEs formation.* Neuromolecular Med, 2012. **14**(4): p. 338-48.
234. Lang, F., A. Gorlach, and V. Vallon, *Targeting SGK1 in diabetes.* Expert Opin Ther Targets, 2009. **13**(11): p. 1303-11.
235. Lang, F., et al., *(Patho)physiological significance of the serum- and glucocorticoid-inducible kinase isoforms.* Physiol Rev, 2006. **86**(4): p. 1151-78.
236. Wu, C., et al., *Induction of pathogenic TH17 cells by inducible salt-sensing kinase SGK1.* Nature, 2013. **496**(7446): p. 513-7.
237. Yang, M., et al., *Serum-glucocorticoid regulated kinase 1 regulates alternatively activated macrophage polarization contributing to angiotensin II-induced inflammation and cardiac fibrosis.* Arterioscler Thromb Vasc Biol, 2012. **32**(7): p. 1675-86.
238. Kobayashi, S.D., et al., *Spontaneous neutrophil apoptosis and regulation of cell survival by granulocyte macrophage-colony stimulating factor.* J Leukoc Biol, 2005. **78**(6): p. 1408-18.
239. Catela, C., et al., *Serum and glucocorticoid-inducible kinase 1 (SGK1) is necessary for vascular remodeling during angiogenesis.* Dev Dyn, 2010. **239**(8): p. 2149-60.
240. Zarrinpashneh, E., et al., *Ablation of SGK1 impairs endothelial cell migration and tube formation leading to decreased neo-angiogenesis following myocardial infarction.* PLoS One, 2013. **8**(11): p. e80268.
241. BelAiba, R.S., et al., *The serum- and glucocorticoid-inducible kinase Sgk-1 is involved in pulmonary vascular remodeling: role in redox-sensitive regulation of tissue factor by thrombin.* Circ Res, 2006. **98**(6): p. 828-36.

242. David, S. and R.G. Kalb, *Serum/glucocorticoid-inducible kinase can phosphorylate the cyclic AMP response element binding protein, CREB.* FEBS Lett, 2005. **579**(6): p. 1534-8.
243. Gilmore, T.D., *Introduction to NF-kappaB: players, pathways, perspectives.* Oncogene, 2006. **25**(51): p. 6680-4.
244. Baldwin, A.S., Jr., *The NF-kappa B and I kappa B proteins: new discoveries and insights.* Annu Rev Immunol, 1996. **14**: p. 649-83.
245. Karin, M. and F.R. Greten, *NF-kappaB: linking inflammation and immunity to cancer development and progression.* Nat Rev Immunol, 2005. **5**(10): p. 749-59.
246. Barnes, P.J. and M. Karin, *Nuclear factor-kappaB: a pivotal transcription factor in chronic inflammatory diseases.* N Engl J Med, 1997. **336**(15): p. 1066-71.
247. Hoare, G.S., et al., *Role of oxidant stress in cytokine-induced activation of NF-kappaB in human aortic smooth muscle cells.* Am J Physiol, 1999. **277**(5 Pt 2): p. H1975-84.
248. Kim, J., et al., *Methylglyoxal induces apoptosis mediated by reactive oxygen species in bovine retinal pericytes.* J Korean Med Sci, 2004. **19**(1): p. 95-100.
249. Dhar, I., et al., *Methylglyoxal, a reactive glucose metabolite, increases renin angiotensin aldosterone and blood pressure in male Sprague-Dawley rats.* Am J Hypertens, 2014. **27**(3): p. 308-16.
250. Tak, P.P. and G.S. Firestein, *NF-kappaB: a key role in inflammatory diseases.* J Clin Invest, 2001. **107**(1): p. 7-11.
251. Lu, J., et al., *Increased plasma methylglyoxal level, inflammation, and vascular endothelial dysfunction in diabetic nephropathy.* Clin Biochem, 2011. **44**(4): p. 307-11.
252. Dhar, A., et al., *Methylglyoxal scavengers attenuate endothelial dysfunction induced by methylglyoxal and high concentrations of glucose.* Br J Pharmacol, 2010.
253. Pettersson, U.S., et al., *Increased recruitment but impaired function of leukocytes during inflammation in mouse models of type 1 and type 2 diabetes.* PLoS One, 2011. **6**(7): p. e22480.
254. Berlanga, J., et al., *Methylglyoxal administration induces diabetes-like microvascular changes and perturbs the healing process of cutaneous wounds.* Clin Sci (Lond), 2005. **109**(1): p. 83-95.

255. Gawlowski, T., et al., *AGEs and methylglyoxal induce apoptosis and expression of Mac-1 on neutrophils resulting in platelet-neutrophil aggregation.* Thromb Res, 2007. **121**(1): p. 117-26.
256. Zhang, M., et al., *Effects of eicosapentaenoic acid on the early stage of type 2 diabetic nephropathy in KKA(y)/Ta mice: involvement of anti-inflammation and antioxidative stress.* Metabolism, 2006. **55**(12): p. 1590-8.
257. Crabtree, M.J., et al., *Quantitative regulation of intracellular endothelial nitric-oxide synthase (eNOS) coupling by both tetrahydrobiopterin-eNOS stoichiometry and biopterin redox status: insights from cells with tet-regulated GTP cyclohydrolase I expression.* J Biol Chem, 2009. **284**(2): p. 1136-44.
258. Yang, Y.M., et al., *eNOS uncoupling and endothelial dysfunction in aged vessels.* Am J Physiol Heart Circ Physiol, 2009. **297**(5): p. H1829-36.
259. Cai, S., J. Khoo, and K.M. Channon, *Augmented BH4 by gene transfer restores nitric oxide synthase function in hyperglycemic human endothelial cells.* Cardiovasc Res, 2005. **65**(4): p. 823-31.
260. Aleksandrovskii, Y.A., *Antithrombin III, C1 inhibitor, methylglyoxal, and polymorphonuclear leukocytes in the development of vascular complications in diabetes mellitus.* Thromb Res, 1992. **67**(2): p. 179-89.
261. Nilsson, J., et al., *Inflammation and immunity in diabetic vascular complications.* Curr Opin Lipidol, 2008. **19**(5): p. 519-24.
262. Zhang, W., et al., *Inflammation and diabetic retinal microvascular complications.* J Cardiovasc Dis Res, 2011. **2**(2): p. 96-103.
263. Desai, K.M., et al., *Oxidative stress and aging: Is methylglyoxal the hidden enemy?* Canadian Journal of Physiology and Pharmacology, 2010. **88**(3): p. 273-284.
264. Liu, J., et al., *Upregulation of aldolase B and overproduction of methylglyoxal in vascular tissues from rats with metabolic syndrome.* Cardiovasc Res, 2011. **92**(3): p. 494-503.
265. Price, C.L., et al., *Methylglyoxal modulates immune responses: relevance to diabetes.* J Cell Mol Med, 2010. **14**(6B): p. 1806-15.

266. Webster, L., et al., *Induction of TNF alpha and IL-1 beta mRNA in monocytes by methylglyoxal- and advanced glycated endproduct-modified human serum albumin.* Biochem Soc Trans, 1997. **25**(2): p. 250S.
267. Kuntz, S., C. Kunz, and S. Rudloff, *Carbonyl compounds methylglyoxal and glyoxal affect interleukin-8 secretion in intestinal cells by superoxide anion generation and activation of MAPK p38.* Mol Nutr Food Res, 2010. **54**(10): p. 1458-67.
268. Akhand, A.A., et al., *Glyoxal and methylglyoxal trigger distinct signals for map family kinases and caspase activation in human endothelial cells.* Free Radic Biol Med, 2001. **31**(1): p. 20-30.
269. Biswas, S., et al., *Selective inhibition of mitochondrial respiration and glycolysis in human leukaemic leucocytes by methylglyoxal.* Biochem J, 1997. **323 (Pt 2)**: p. 343-8.
270. Adams, J.L., et al., *p38 MAP kinase: molecular target for the inhibition of pro-inflammatory cytokines.* Prog Med Chem, 2001. **38**: p. 1-60.
271. Zhang, D., et al., *Porphorymonas gingivalis induces intracellular adhesion molecule-1 expression in endothelial cells through the nuclear factor-kappaB pathway, but not through the p38 MAPK pathway.* J Periodontal Res, 2011. **46**(1): p. 31-8.
272. Butcher, E.C., *Leukocyte-endothelial cell recognition: three (or more) steps to specificity and diversity.* Cell, 1991. **67**(6): p. 1033-6.
273. Sun, L., et al., *Inflammatory reaction versus endogenous peroxisome proliferator-activated receptors expression, re-exploring secondary organ complications of spontaneously hypertensive rats.* Chin Med J (Engl), 2008. **121**(22): p. 2305-11.
274. Illoh, K., et al., *Mucosal tolerance to E-selectin and response to systemic inflammation.* J Cereb Blood Flow Metab, 2006. **26**(12): p. 1538-50.
275. Bruno, C.M., et al., *Plasma ICAM-1 and VCAM-1 levels in type 2 diabetic patients with and without microalbuminuria.* Minerva Med, 2008. **99**(1): p. 1-5.
276. Jublanc, C., et al., *Serum levels of adhesion molecules ICAM-1 and VCAM-1 and tissue inhibitor of metalloproteinases, TIMP-1, are elevated in patients with autoimmune thyroid disorders: Relevance to vascular inflammation.* Nutr Metab Cardiovasc Dis, 2010.

277. Papayianni, A., et al., *Circulating levels of ICAM-1, VCAM-1, and MCP-1 are increased in haemodialysis patients: association with inflammation, dyslipidaemia, and vascular events.* Nephrol Dial Transplant, 2002. **17**(3): p. 435-41.
278. Kressel, G., et al., *Systemic and vascular markers of inflammation in relation to metabolic syndrome and insulin resistance in adults with elevated atherosclerosis risk.* Atherosclerosis, 2009. **202**(1): p. 263-71.
279. Dhar, A., et al., *Methylglyoxal, protein binding and biological samples: are we getting the true measure?* J Chromatogr B Analyt Technol Biomed Life Sci, 2009. **877**(11-12): p. 1093-100.
280. Liu, L., et al., *LSP1 is an endothelial gatekeeper of leukocyte transendothelial migration.* J Exp Med, 2005. **201**(3): p. 409-18.
281. O'Driscoll, J. and J.P. Ryan, *A modified haematoxylin and eosin stain for histologicl sections of lymph nodes.* J Clin Pathol, 1978. **31**(7): p. 700.
282. Lapolla, A., et al., *Evaluation of advanced glycation end products and carbonyl compounds in patients with different conditions of oxidative stress.* Mol Nutr Food Res, 2005. **49**(7): p. 685-90.
283. Chaplen, F.W., W.E. Fahl, and D.C. Cameron, *Evidence of high levels of methylglyoxal in cultured Chinese hamster ovary cells.* Proc Natl Acad Sci U S A, 1998. **95**(10): p. 5533-8.
284. Balciunas, M., et al., *Markers of endothelial dysfunction after cardiac surgery: soluble forms of vascular-1 and intercellular-1 adhesion molecules.* Medicina (Kaunas), 2009. **45**(6): p. 434-9.
285. Schram, M.T. and C.D. Stehouwer, *Endothelial dysfunction, cellular adhesion molecules and the metabolic syndrome.* Horm Metab Res, 2005. **37 Suppl 1**: p. 49-55.
286. Song, Y., et al., *Circulating levels of endothelial adhesion molecules and risk of diabetes in an ethnically diverse cohort of women.* Diabetes, 2007. **56**(7): p. 1898-904.
287. Dogruel, N., et al., *Serum soluble endothelial-cell specific adhesion molecules in children with insulin-dependent diabetes mellitus.* J Pediatr Endocrinol Metab, 2001. **14**(3): p. 287-93.
288. Skyrme-Jones, R.A. and I.T. Meredith, *Soluble adhesion molecules, endothelial function and vitamin E in type 1 diabetes.* Coron Artery Dis, 2001. **12**(1): p. 69-75.

289. Fornoni, A., et al., *Role of inflammation in diabetic nephropathy.* Curr Diabetes Rev, 2008. **4**(1): p. 10-7.
290. Wong, C.K., et al., *Aberrant expression of soluble co-stimulatory molecules and adhesion molecules in type 2 diabetic patients with nephropathy.* J Clin Immunol, 2008. **28**(1): p. 36-43.
291. Bavbek, N., et al., *Elevated concentrations of soluble adhesion molecules and large platelets in diabetic patients: are they markers of vascular disease and diabetic nephropathy?* Clin Appl Thromb Hemost, 2007. **13**(4): p. 391-7.
292. Soedamah-Muthu, S.S., et al., *Soluble vascular cell adhesion molecule-1 and soluble E-selectin are associated with micro- and macrovascular complications in Type 1 diabetic patients.* J Diabetes Complications, 2006. **20**(3): p. 188-95.
293. Akhand, A.A., et al., *Glyoxal and methylglyoxal induce lyoxal and methyglyoxal induce aggregation and inactivation of ERK in human endothelial cells.* Free Radic Biol Med, 2001. **31**(10): p. 1228-35.
294. Pal, A., et al., *Methylglyoxal induced activation of murine peritoneal macrophages and surface markers of T lymphocytes in sarcoma-180 bearing mice: involvement of MAP kinase, NF-kappa beta signal transduction pathway.* Mol Immunol, 2009. **46**(10): p. 2039-44.
295. Fukunaga, M., et al., *Methylglyoxal induces apoptosis through activation of p38 MAPK in rat Schwann cells.* Biochem Biophys Res Commun, 2004. **320**(3): p. 689-95.
296. Fortes, Z.B., et al., *Direct vital microscopic study of defective leukocyte-endothelial interaction in diabetes mellitus.* Diabetes, 1991. **40**(10): p. 1267-73.
297. Ghosh, M., et al., *In vivo assessment of toxicity and pharmacokinetics of methylglyoxal. Augmentation of the curative effect of methylglyoxal on cancer-bearing mice by ascorbic acid and creatine.* Toxicol Appl Pharmacol, 2006. **212**(1): p. 45-58.
298. Watanabe, K., et al., *Methylglyoxal (MG) and cerebro-renal interaction: does long-term orally administered MG cause cognitive impairment in normal Sprague-Dawley rats?* Toxins (Basel), 2014. **6**(1): p. 254-69.
299. Apple, M.A. and D.M. Greenberg, *Arrest of cancer in mice by therapy with normal metabolites. II. Indefinite survirors among mice treated with mixtures of 2-oxopropanal*

(NSC-79019) and 2,3-dihydroxypropanal (NSC67934). Cancer Chemother Rep, 1968. **52**(7): p. 687-96.

300. Egyud, L.G. and A. Szent-Gyorgyi, *Cancerostatic action of methylglyoxal.* Science, 1968. **160**(3832): p. 1140.
301. Talukdar, D., et al., *A brief critical overview of the biological effects of methylglyoxal and further evaluation of a methylglyoxal-based anticancer formulation in treating cancer patients.* Drug Metabol Drug Interact, 2008. **23**(1-2): p. 175-210.
302. Paramasivan, S., et al., *Methylglyoxal-augmented manuka honey as a topical anti-Staphylococcus aureus biofilm agent: safety and efficacy in an in vivo model.* Int Forum Allergy Rhinol, 2014. **4**(3): p. 187-95.
303. Distler, M.G., et al., *Glyoxalase 1 increases anxiety by reducing GABAA receptor agonist methylglyoxal.* J Clin Invest, 2012. **122**(6): p. 2306-15.
304. Smolock, A.R., et al., *Protein kinase C upregulates intercellular adhesion molecule-1 and leukocyte-endothelium interactions in hyperglycemia via activation of endothelial expressed calpain.* Arterioscler Thromb Vasc Biol, 2011. **31**(2): p. 289-96.
305. Cain, R.J., B. Vanhaesebroeck, and A.J. Ridley, *Different PI 3-kinase inhibitors have distinct effects on endothelial permeability and leukocyte transmigration.* Int J Biochem Cell Biol, 2012. **44**(11): p. 1929-36.
306. Liu, L., et al., *Leukocyte PI3Kgamma and PI3Kdelta have temporally distinct roles for leukocyte recruitment in vivo.* Blood, 2007. **110**(4): p. 1191-8.
307. Cross, D.A., et al., *Inhibition of glycogen synthase kinase-3 by insulin mediated by protein kinase B.* Nature, 1995. **378**(6559): p. 785-9.
308. Wyatt, A.W., et al., *DOCA-induced phosphorylation of glycogen synthase kinase 3beta.* Cell Physiol Biochem, 2006. **17**(3-4): p. 137-44.
309. Dong, M., et al., *Chronic Akt activation attenuated lipopolysaccharide-induced cardiac dysfunction via Akt/GSK3beta-dependent inhibition of apoptosis and ER stress.* Biochim Biophys Acta, 2013. **1832**(6): p. 848-63.
310. Cortes-Vieyra, R., et al., *Role of glycogen synthase kinase-3 beta in the inflammatory response caused by bacterial pathogens.* J Inflamm (Lond), 2012. **9**(1): p. 23.

311. Tang, W., et al., *A PLCbeta/PI3Kgamma-GSK3 signaling pathway regulates cofilin phosphatase slingshot2 and neutrophil polarization and chemotaxis.* Dev Cell, 2011. **21**(6): p. 1038-50.
312. Bhavsar, S.K., et al., *AKT/SGK-sensitive phosphorylation of GSK3 in the regulation of L-selectin and perforin expression as well as activation induced cell death of T-lymphocytes.* Biochem Biophys Res Commun, 2012. **425**(1): p. 6-12.
313. Gong, R., A. Rifai, and L.D. Dworkin, *Hepatocyte growth factor suppresses acute renal inflammation by inhibition of endothelial E-selectin.* Kidney Int, 2006. **69**(7): p. 1166-74.
314. Yang, J., et al., *Antipermeability function of PEDF involves blockade of the MAP kinase/GSK/beta-catenin signaling pathway and uPAR expression.* Invest Ophthalmol Vis Sci, 2010. **51**(6): p. 3273-80.
315. Avrahami, L., et al., *GSK-3 inhibition: achieving moderate efficacy with high selectivity.* Biochim Biophys Acta, 2013. **1834**(7): p. 1410-4.
316. Lang, F. and E. Shumilina, *Regulation of ion channels by the serum- and glucocorticoid-inducible kinase SGK1.* FASEB J, 2013. **27**(1): p. 3-12.
317. Lang, F., et al., *Deranged transcriptional regulation of cell-volume-sensitive kinase hSGK in diabetic nephropathy.* Proc Natl Acad Sci U S A, 2000. **97**(14): p. 8157-62.
318. Ullrich, S., et al., *Serum- and glucocorticoid-inducible kinase 1 (SGK1) mediates glucocorticoid-induced inhibition of insulin secretion.* Diabetes, 2005. **54**(4): p. 1090-9.
319. Sherk, A.B., et al., *Development of a small-molecule serum- and glucocorticoid-regulated kinase-1 antagonist and its evaluation as a prostate cancer therapeutic.* Cancer Res, 2008. **68**(18): p. 7475-83.
320. Hossain, M., et al., *ICAM-1-mediated leukocyte adhesion is critical for the activation of endothelial LSP1.* Am J Physiol Cell Physiol, 2013. **304**(9): p. C895-904.
321. Scoditti, E., et al., *PPARgamma agonists inhibit angiogenesis by suppressing PKCalpha-and CREB-mediated COX-2 expression in the human endothelium.* Cardiovasc Res, 2010. **86**(2): p. 302-10.
322. Xu, N., M. Hossain, and L. Liu, *Pharmacological inhibition of p38 mitogen-activated protein kinases affects KC/CXCL1-induced intraluminal crawling, transendothelial migration, and chemotaxis of neutrophils in vivo.* Mediators Inflamm, 2013. **2013**: p. 290565.

323. Overbeek, S.A., et al., *Chemo-attractant N-acetyl proline-glycine-proline induces CD11b/CD18-dependent neutrophil adhesion.* Biochim Biophys Acta, 2013. **1830**(1): p. 2188-93.
324. Ackermann, T.F., et al., *EMD638683, a novel SGK inhibitor with antihypertensive potency.* Cell Physiol Biochem, 2011. **28**(1): p. 137-46.
325. Mansley, M.K. and S.M. Wilson, *Effects of nominally selective inhibitors of the kinases PI3K, SGK1 and PKB on the insulin-dependent control of epithelial Na+ absorption.* Br J Pharmacol, 2010. **161**(3): p. 571-88.
326. Nagaraj, R.H., et al., *Effect of pyridoxamine on chemical modification of proteins by carbonyls in diabetic rats: characterization of a major product from the reaction of pyridoxamine and methylglyoxal.* Arch Biochem Biophys, 2002. **402**(1): p. 110-9.
327. Thornalley, P.J., et al., *The human red blood cell glyoxalase system in diabetes mellitus.* Diabetes Res Clin Pract, 1989. **7**(2): p. 115-20.
328. Jia, X., et al., *Methylglyoxal mediates adipocyte proliferation by increasing phosphorylation of Akt1.* PLoS One, 2012. **7**(5): p. e36610.
329. Eto, M., et al., *Glycogen synthase kinase-3 mediates endothelial cell activation by tumor necrosis factor-alpha.* Circulation, 2005. **112**(9): p. 1316-22.
330. Burgon, J., et al., *Serum and glucocorticoid-regulated kinase 1 regulates neutrophil clearance during inflammation resolution.* J Immunol, 2014. **192**(4): p. 1796-805.
331. Eylenstein, A., et al., *Stimulation of Ca2+-channel Orai1/STIM1 by serum- and glucocorticoid-inducible kinase 1 (SGK1).* FASEB J, 2011. **25**(6): p. 2012-21.
332. Schaff, U.Y., et al., *Orai1 regulates intracellular calcium, arrest, and shape polarization during neutrophil recruitment in shear flow.* Blood, 2010. **115**(3): p. 657-66.
333. Collino, M., et al., *Insulin reduces cerebral ischemia/reperfusion injury in the hippocampus of diabetic rats: a role for glycogen synthase kinase-3beta.* Diabetes, 2009. **58**(1): p. 235-42.
334. Cuzzocrea, S., et al., *Inhibition of glycogen synthase kinase-3beta attenuates the development of carrageenan-induced lung injury in mice.* Br J Pharmacol, 2006. **149**(6): p. 687-702.
335. Demarchi, F., et al., *Glycogen synthase kinase-3 beta regulates NF-kappa B1/p105 stability.* J Biol Chem, 2003. **278**(41): p. 39583-90.

336. Terada, Y., et al., *Aldosterone-stimulated SGK1 activity mediates profibrotic signaling in the mesangium.* J Am Soc Nephrol, 2008. **19**(2): p. 298-309.
337. Leroy, V., et al., *Aldosterone activates NF-kappaB in the collecting duct.* J Am Soc Nephrol, 2009. **20**(1): p. 131-44.
338. Corsini, M., et al., *Cyclic adenosine monophosphate-response element-binding protein mediates the proangiogenic or proinflammatory activity of gremlin.* Arterioscler Thromb Vasc Biol, 2014. **34**(1): p. 136-45.
339. Hadad, N., et al., *Endothelial ICAM-1 protein induction is regulated by cytosolic phospholipase A2alpha via both NF-kappaB and CREB transcription factors.* J Immunol, 2011. **186**(3): p. 1816-27.
340. Devi, T.S., et al., *GSK-3beta/CREB axis mediates IGF-1-induced ECM/adhesion molecule expression, cell cycle progression and monolayer permeability in retinal capillary endothelial cells: Implications for diabetic retinopathy.* Biochim Biophys Acta, 2011. **1812**(9): p. 1080-8.
341. Shimizu, H., et al., *CREB, NF-kappaB, and NADPH oxidase coordinately upregulate indoxyl sulfate-induced angiotensinogen expression in proximal tubular cells.* Am J Physiol Cell Physiol, 2013. **304**(7): p. C685-92.
342. Hartge, M.M., T. Unger, and U. Kintscher, *The endothelium and vascular inflammation in diabetes.* Diab Vasc Dis Res, 2007. **4**(2): p. 84-8.
343. Kitasato, L., et al., *Postprandial hyperglycemia and endothelial function in type 2 diabetes: focus on mitiglinide.* Cardiovasc Diabetol, 2012. **11**: p. 79.
344. Chen, X., et al., *Carbonyl stress induces hypertension and cardio-renal vascular injury in Dahl salt-sensitive rats.* Hypertens Res, 2013. **36**(4): p. 361-7.
345. Nicolay, J.P., et al., *Stimulation of suicidal erythrocyte death by methylglyoxal.* Cell Physiol Biochem, 2006. **18**(4-5): p. 223-32.
346. Chan, W.H. and H.J. Wu, *Methylglyoxal and high glucose co-treatment induces apoptosis or necrosis in human umbilical vein endothelial cells.* J Cell Biochem, 2008. **103**(4): p. 1144-57.
347. Tejero, J. and D. Stuehr, *Tetrahydrobiopterin in nitric oxide synthase.* IUBMB Life, 2013. **65**(4): p. 358-65.

348. Buckley, B.J., Z. Mirza, and A.R. Whorton, *Regulation of Ca(2+)-dependent nitric oxide synthase in bovine aortic endothelial cells.* Am J Physiol, 1995. **269**(3 Pt 1): p. C757-65.
349. Fleming, I. and R. Busse, *Molecular mechanisms involved in the regulation of the endothelial nitric oxide synthase.* Am J Physiol Regul Integr Comp Physiol, 2003. **284**(1): p. R1-12.
350. Wheatcroft, S.B., et al., *Pathophysiological implications of insulin resistance on vascular endothelial function.* Diabet Med, 2003. **20**(4): p. 255-68.
351. Montezano, A.C. and R.M. Touyz, *Reactive oxygen species and endothelial function--role of nitric oxide synthase uncoupling and Nox family nicotinamide adenine dinucleotide phosphate oxidases.* Basic Clin Pharmacol Toxicol, 2012. **110**(1): p. 87-94.
352. Ravi, K., et al., *S-nitrosylation of endothelial nitric oxide synthase is associated with monomerization and decreased enzyme activity.* Proc Natl Acad Sci U S A, 2004. **101**(8): p. 2619-24.
353. Sawabe, K., et al., *Cellular uptake of sepiapterin and push-pull accumulation of tetrahydrobiopterin.* Mol Genet Metab, 2008. **94**(4): p. 410-6.
354. Shimazu, T., et al., *Sepiapterin enhances angiogenesis and functional recovery in mice after myocardial infarction.* Am J Physiol Heart Circ Physiol, 2011. **301**(5): p. H2061-72.
355. Lorin, J., et al., *Arginine and nitric oxide synthase: regulatory mechanisms and cardiovascular aspects.* Mol Nutr Food Res, 2014. **58**(1): p. 101-16.
356. Kietadisorn, R., R.P. Juni, and A.L. Moens, *Tackling endothelial dysfunction by modulating NOS uncoupling: new insights into its pathogenesis and therapeutic possibilities.* Am J Physiol Endocrinol Metab, 2012. **302**(5): p. E481-95.
357. Srivastava, K., P.M. Bath, and U. Bayraktutan, *Current therapeutic strategies to mitigate the eNOS dysfunction in ischaemic stroke.* Cell Mol Neurobiol, 2012. **32**(3): p. 319-36.
358. Cai, S., et al., *Endothelial nitric oxide synthase dysfunction in diabetic mice: importance of tetrahydrobiopterin in eNOS dimerisation.* Diabetologia, 2005. **48**(9): p. 1933-40.
359. Shevalye, H., et al., *Metanx alleviates multiple manifestations of peripheral neuropathy and increases intraepidermal nerve fiber density in Zucker diabetic fatty rats.* Diabetes, 2012. **61**(8): p. 2126-33.
360. Stalker, T.J., Y. Gong, and R. Scalia, *The calcium-dependent protease calpain causes endothelial dysfunction in type 2 diabetes.* Diabetes, 2005. **54**(4): p. 1132-40.

361. Lin, X., et al., *Effect of glucose degradation products, glucose-containing dialysate and icodextrin on AQP1 and eNOS expression in cultured endothelial cells.* J Nephrol, 2009. **22**(1): p. 117-22.
362. Wang, X., et al., *Attenuation of hypertension development by scavenging methylglyoxal in fructose-treated rats.* J Hypertens, 2008. **26**(4): p. 765-72.
363. Mukohda, M., et al., *Long-term methylglyoxal treatment causes endothelial dysfunction of rat isolated mesenteric artery.* J Vet Med Sci, 2013. **75**(2): p. 151-7.
364. Sankaralingam, S., et al., *Evidence for increased methylglyoxal in the vasculature of women with preeclampsia: role in upregulation of LOX-1 and arginase.* Hypertension, 2009. **54**(4): p. 897-904.
365. Targosz-Korecka, M., et al., *Stiffness memory of EA.hy926 endothelial cells in response to chronic hyperglycemia.* Cardiovasc Diabetol, 2013. **12**: p. 96.
366. Heitzer, T., et al., *Tetrahydrobiopterin improves endothelium-dependent vasodilation in chronic smokers : evidence for a dysfunctional nitric oxide synthase.* Circ Res, 2000. **86**(2): p. E36-41.
367. Woo, H.J., et al., *Production of sepiapterin in Escherichia coli by coexpression of cyanobacterial GTP cyclohydrolase I and human 6-pyruvoyltetrahydropterin synthase.* Appl Environ Microbiol, 2002. **68**(6): p. 3138-40.
368. Wang, H., et al., *Fructose-induced peroxynitrite production is mediated by methylglyoxal in vascular smooth muscle cells.* Life Sci, 2006. **79**(26): p. 2448-54.
369. Batandier, C., et al., *Determination of mitochondrial reactive oxygen species: methodological aspects.* J Cell Mol Med, 2002. **6**(2): p. 175-87.
370. Tarpey, M.M. and I. Fridovich, *Methods of detection of vascular reactive species: nitric oxide, superoxide, hydrogen peroxide, and peroxynitrite.* Circ Res, 2001. **89**(3): p. 224-36.
371. Price, C.L. and S.C. Knight, *Methylglyoxal: possible link between hyperglycaemia and immune suppression?* Trends Endocrinol Metab, 2009. **20**(7): p. 312-7.
372. Di Loreto, S., et al., *Methylglyoxal causes strong weakening of detoxifying capacity and apoptotic cell death in rat hippocampal neurons.* Int J Biochem Cell Biol, 2008. **40**(2): p. 245-57.

373. Chang, T., et al., *Interaction of methylglyoxal and hydrogen sulfide in rat vascular smooth muscle cells.* Antioxid Redox Signal, 2010. **12**(9): p. 1093-100.
374. Kim, H.K., S.H. Ha, and J. Han, *Potential therapeutic applications of tetrahydrobiopterin: from inherited hyperphenylalaninemia to mitochondrial diseases.* Ann N Y Acad Sci, 2010. **1201**: p. 177-82.
375. Abudukadier, A., et al., *Tetrahydrobiopterin has a glucose-lowering effect by suppressing hepatic gluconeogenesis in an endothelial nitric oxide synthase-dependent manner in diabetic mice.* Diabetes, 2013. **62**(9): p. 3033-43.
376. Okazaki, T., et al., *Reversal of inducible nitric oxide synthase uncoupling unmasks tolerance to ischemia/reperfusion injury in the diabetic rat heart.* J Mol Cell Cardiol, 2011. **50**(3): p. 534-44.
377. Khoo, J.P., et al., *Pivotal role for endothelial tetrahydrobiopterin in pulmonary hypertension.* Circulation, 2005. **111**(16): p. 2126-33.
378. Foxton, R.H., J.M. Land, and S.J. Heales, *Tetrahydrobiopterin availability in Parkinson's and Alzheimer's disease; potential pathogenic mechanisms.* Neurochem Res, 2007. **32**(4-5): p. 751-6.
379. Cheng, H., et al., *Improvement of endothelial nitric oxide synthase activity retards the progression of diabetic nephropathy in db/db mice.* Kidney Int, 2012. **82**(11): p. 1176-83.
380. Thida, M., et al., *Effects of sepiapterin supplementation and NOS inhibition on glucocorticoid-induced hypertension.* Am J Hypertens, 2010. **23**(5): p. 569-74.
381. Tiefenbacher, C.P., et al., *Sepiapterin reduces postischemic injury in the rat heart.* Pflugers Arch, 2003. **447**(1): p. 1-7.
382. Crabtree, M.J., et al., *Integrated redox sensor and effector functions for tetrahydrobiopterin- and glutathionylation-dependent endothelial nitric-oxide synthase uncoupling.* J Biol Chem, 2013. **288**(1): p. 561-9.
383. McCabe, T.J., et al., *Enhanced electron flux and reduced calmodulin dissociation may explain "calcium-independent" eNOS activation by phosphorylation.* J Biol Chem, 2000. **275**(9): p. 6123-8.
384. Chen, C.A., et al., *Phosphorylation of endothelial nitric-oxide synthase regulates superoxide generation from the enzyme.* J Biol Chem, 2008. **283**(40): p. 27038-47.

385. Yamamoto, E., et al., *Nifedipine prevents vascular endothelial dysfunction in a mouse model of obesity and type 2 diabetes, by improving eNOS dysfunction and dephosphorylation.* Biochem Biophys Res Commun, 2010. **403**(3-4): p. 258-63.
386. Serizawa, K., et al., *Nicorandil prevents endothelial dysfunction due to antioxidative effects via normalisation of NADPH oxidase and nitric oxide synthase in streptozotocin diabetic rats.* Cardiovasc Diabetol, 2011. **10**: p. 105.
387. Wenzel, P., et al., *AT1-receptor blockade by telmisartan upregulates GTP-cyclohydrolase I and protects eNOS in diabetic rats.* Free Radic Biol Med, 2008. **45**(5): p. 619-26.
388. Singh, U., et al., *C-reactive protein decreases endothelial nitric oxide synthase activity via uncoupling.* J Mol Cell Cardiol, 2007. **43**(6): p. 780-91.
389. Ren, J., et al., *IGF-I alleviates diabetes-induced RhoA activation, eNOS uncoupling, and myocardial dysfunction.* Am J Physiol Regul Integr Comp Physiol, 2008. **294**(3): p. R793-802.
390. Hirata, M., et al., *22-Oxacalcitriol prevents progression of endothelial dysfunction through antioxidative effects in rats with type 2 diabetes and early-stage nephropathy.* Nephrol Dial Transplant, 2013. **28**(5): p. 1166-74.
391. Cheng, J., et al., *20-hydroxyeicosatetraenoic acid causes endothelial dysfunction via eNOS uncoupling.* Am J Physiol Heart Circ Physiol, 2008. **294**(2): p. H1018-26.
392. Ceriello, A., et al., *Vitamin C further improves the protective effect of GLP-1 on the ischemia-reperfusion-like effect induced by hyperglycemia post-hypoglycemia in type 1 diabetes.* Cardiovasc Diabetol, 2013. **12**(1): p. 97.
393. Johnston, P.C., et al., *Placental protein tyrosine nitration and MAPK in type 1 diabetic pre-eclampsia: Impact of antioxidant vitamin supplementation.* J Diabetes Complications, 2013. **27**(4): p. 322-7.
394. Osorio, H., et al., *Sodium-glucose cotransporter inhibition prevents oxidative stress in the kidney of diabetic rats.* Oxid Med Cell Longev, 2012. **2012**: p. 542042.
395. Sakul, A., et al., *Age- and diabetes-induced regulation of oxidative protein modification in rat brain and peripheral tissues: consequences of treatment with antioxidant pyridoindole.* Exp Gerontol, 2013. **48**(5): p. 476-84.

396. Huynh, K., et al., *Targeting the upregulation of reactive oxygen species subsequent to hyperglycemia prevents type 1 diabetic cardiomyopathy in mice.* Free Radic Biol Med, 2013. **60**: p. 307-17.
397. Ding, Y., et al., *Effects of simulated hyperglycemia, insulin, and glucagon on endothelial nitric oxide synthase expression.* Am J Physiol Endocrinol Metab, 2000. **279**(1): p. E11-7.
398. Okon, E.B., et al., *Compromised arterial function in human type 2 diabetic patients.* Diabetes, 2005. **54**(8): p. 2415-23.
399. Lu, X., et al., *Rosiglitazone reverses endothelial dysfunction but not remodeling of femoral artery in Zucker diabetic fatty rats.* Cardiovasc Diabetol, 2010. **9**: p. 19.
400. Ding, H., et al., *Endothelial dysfunction in the streptozotocin-induced diabetic apoE-deficient mouse.* Br J Pharmacol, 2005. **146**(8): p. 1110-8.
401. Pannirselvam, M., et al., *Pharmacological characteristics of endothelium-derived hyperpolarizing factor-mediated relaxation of small mesenteric arteries from db/db mice.* Eur J Pharmacol, 2006. **551**(1-3): p. 98-107.
402. Libby, P., *Inflammation in atherosclerosis.* Arterioscler Thromb Vasc Biol, 2012. **32**(9): p. 2045-51.
403. Phillips, S.A., D. Mirrlees, and P.J. Thornalley, *Modification of the glyoxalase system in streptozotocin-induced diabetic rats. Effect of the aldose reductase inhibitor Statil.* Biochem Pharmacol, 1993. **46**(5): p. 805-11.
404. Yamawaki, H. and Y. Hara, *Glyoxal causes inflammatory injury in human vascular endothelial cells.* Biochem Biophys Res Commun, 2008. **369**(4): p. 1155-9.
405. Di Loreto, S., et al., *Methylglyoxal induces oxidative stress-dependent cell injury and up-regulation of interleukin-1beta and nerve growth factor in cultured hippocampal neuronal cells.* Brain Res, 2004. **1006**(2): p. 157-67.
406. Rachman, H., et al., *Critical role of methylglyoxal and AGE in mycobacteria-induced macrophage apoptosis and activation.* PLoS One, 2006. **1**: p. e29.
407. Hossain, M., S.M. Qadri, and L. Liu, *Inhibition of nitric oxide synthesis enhances leukocyte rolling and adhesion in human microvasculature.* J Inflamm (Lond), 2012. **9**(1): p. 28.

408. Hickey, M.J., D.N. Granger, and P. Kubes, *Inducible nitric oxide synthase (iNOS) and regulation of leucocyte/endothelial cell interactions: studies in iNOS-deficient mice.* Acta Physiol Scand, 2001. **173**(1): p. 119-26.
409. Andrew, P.J. and B. Mayer, *Enzymatic function of nitric oxide synthases.* Cardiovasc Res, 1999. **43**(3): p. 521-31.
410. Xia, Y., et al., *Nitric oxide synthase generates superoxide and nitric oxide in arginine-depleted cells leading to peroxynitrite-mediated cellular injury.* Proc Natl Acad Sci U S A, 1996. **93**(13): p. 6770-4.
411. Zhou, Z.W., et al., *Mechanism of reversal of high glucose-induced endothelial nitric oxide synthase uncoupling by tanshinone IIA in human endothelial cell line EA.hy926.* Eur J Pharmacol, 2012. **697**(1-3): p. 97-105.
412. Quinn, K.L., et al., *Human neutrophil peptides mediate endothelial-monocyte interaction, foam cell formation, and platelet activation.* Arterioscler Thromb Vasc Biol, 2011. **31**(9): p. 2070-9.
413. Bayat, H., et al., *Activation of thromboxane receptor modulates interleukin-1beta-induced monocyte adhesion--a novel role of Nox1.* Free Radic Biol Med, 2012. **52**(9): p. 1760-6.
414. Grommes, J., et al., *Simvastatin reduces endotoxin-induced acute lung injury by decreasing neutrophil recruitment and radical formation.* PLoS One, 2012. **7**(6): p. e38917.
415. Bonder, C.S., et al., *Chimeric SOD2/3 inhibits at the endothelial-neutrophil interface to limit vascular dysfunction in ischemia-reperfusion.* Am J Physiol Gastrointest Liver Physiol, 2004. **287**(3): p. G676-84.
416. Minegishi, K., et al., *Reactive oxygen species mediate leukocyte-endothelium interactions in prostaglandin F2alpha -induced luteolysis in rats.* Am J Physiol Endocrinol Metab, 2002. **283**(6): p. E1308-15.
417. Lo, S.K., et al., *Hydrogen peroxide-induced increase in endothelial adhesiveness is dependent on ICAM-1 activation.* Am J Physiol, 1993. **264**(4 Pt 1): p. L406-12.
418. Wood, J.G., et al., *Systemic hypoxia promotes leukocyte-endothelial adherence via reactive oxidant generation.* J Appl Physiol (1985), 1999. **87**(5): p. 1734-40.

419. Cominacini, L., et al., *The binding of oxidized low density lipoprotein (ox-LDL) to ox-LDL receptor-1 reduces the intracellular concentration of nitric oxide in endothelial cells through an increased production of superoxide.* J Biol Chem, 2001. **276**(17): p. 13750-5.
420. Robertson, C.A., et al., *Effect of nitric oxide synthase substrate analog inhibitors on rat liver arginase.* Biochem Biophys Res Commun, 1993. **197**(2): p. 523-8.
421. Heimfarth, L., et al., *Methylglyoxal-induced cytotoxicity in neonatal rat brain: a role for oxidative stress and MAP kinases.* Metab Brain Dis, 2013. **28**(3): p. 429-38.
422. Hasegawa, H., et al., *Delivery of exogenous tetrahydrobiopterin (BH4) to cells of target organs: role of salvage pathway and uptake of its precursor in effective elevation of tissue BH4.* Mol Genet Metab, 2005. **86 Suppl 1**: p. S2-10.
423. Lei, X., et al., *Different microvascular permeability responses elicited by the CXC chemokines MIP-2 and KC during leukocyte recruitment: role of LSP1.* Biochem Biophys Res Commun, 2012. **423**(3): p. 484-9.
424. Petri, B., et al., *Endothelial LSP1 is involved in endothelial dome formation, minimizing vascular permeability changes during neutrophil transmigration in vivo.* Blood, 2011. **117**(3): p. 942-52.
425. Rajapakse, A.G., et al., *Hyperactive S6K1 mediates oxidative stress and endothelial dysfunction in aging: inhibition by resveratrol.* PLoS One, 2011. **6**(4): p. e19237.
426. Rosado, E., et al., *Interaction between NO and COX pathways modulating hepatic endothelial cells from control and cirrhotic rats.* J Cell Mol Med, 2012. **16**(10): p. 2461-70.
427. Han, Y., et al., *Plasma methylglyoxal and glyoxal are elevated and related to early membrane alteration in young, complication-free patients with Type 1 diabetes.* Mol Cell Biochem, 2007. **305**(1-2): p. 123-31.
428. Liu, J., et al., *Aldolase B knockdown prevents high glucose-induced methylglyoxal overproduction and cellular dysfunction in endothelial cells.* PLoS One, 2012. **7**(7): p. e41495.
429. Takano, M., et al., *Rapid upregulation of endothelial P-selectin expression via reactive oxygen species generation.* Am J Physiol Heart Circ Physiol, 2002. **283**(5): p. H2054-61.
430. Lin, S.J., et al., *Superoxide dismutase inhibits the expression of vascular cell adhesion molecule-1 and intracellular cell adhesion molecule-1 induced by tumor necrosis factor-*

alpha in human endothelial cells through the JNK/p38 pathways. Arterioscler Thromb Vasc Biol, 2005. **25**(2): p. 334-40.

431. Chen, C.Y., et al., *Inhibitory effect of delphinidin on monocyte-endothelial cell adhesion induced by oxidized low-density lipoprotein via ROS/p38MAPK/NF-kappaB pathway.* Cell Biochem Biophys, 2011. **61**(2): p. 337-48.
432. Xie, H., P.E. Ray, and B.L. Short, *NF-kappaB activation plays a role in superoxide-mediated cerebral endothelial dysfunction after hypoxia/reoxygenation.* Stroke, 2005. **36**(5): p. 1047-52.
433. Cooke, C.L. and S.T. Davidge, *Peroxynitrite increases iNOS through NF-kappaB and decreases prostacyclin synthase in endothelial cells.* Am J Physiol Cell Physiol, 2002. **282**(2): p. C395-402.
434. Ward, R.A. and K.R. McLeish, *Methylglyoxal: a stimulus to neutrophil oxygen radical production in chronic renal failure?* Nephrol Dial Transplant, 2004. **19**(7): p. 1702-7.
435. Sawabe, K., K.O. Wakasugi, and H. Hasegawa, *Tetrahydrobiopterin uptake in supplemental administration: elevation of tissue tetrahydrobiopterin in mice following uptake of the exogenously oxidized product 7,8-dihydrobiopterin and subsequent reduction by an anti-folate-sensitive process.* J Pharmacol Sci, 2004. **96**(2): p. 124-33.
436. Yan, J., G. Tie, and L.M. Messina, *Tetrahydrobiopterin, L-arginine and vitamin C act synergistically to decrease oxidant stress and increase nitric oxide that increases blood flow recovery after hindlimb ischemia in the rat.* Mol Med, 2012. **18**: p. 1221-30.
437. Haruna, Y., et al., *Endothelial dysfunction in rat adjuvant-induced arthritis: vascular superoxide production by NAD(P)H oxidase and uncoupled endothelial nitric oxide synthase.* Arthritis Rheum, 2006. **54**(6): p. 1847-55.
438. Dai, Y., et al., *Tetrahydrobiopterin ameliorates hepatic ischemia-reperfusion Injury by coupling with eNOS in mice.* J Surg Res, 2012. **176**(2): p. e65-71.
439. Elrod, J.W., et al., *eNOS gene therapy exacerbates hepatic ischemia-reperfusion injury in diabetes: a role for eNOS uncoupling.* Circ Res, 2006. **99**(1): p. 78-85.
440. Matei, V., et al., *The eNOS cofactor tetrahydrobiopterin improves endothelial dysfunction in livers of rats with CCl4 cirrhosis.* Hepatology, 2006. **44**(1): p. 44-52.

441. Chen, Q., et al., *The role of tetrahydrobiopterin and dihydrobiopterin in ischemia/reperfusion injury when given at reperfusion.* Adv Pharmacol Sci, 2010. **2010**: p. 963914.
442. Li, H., et al., *Reversal of endothelial nitric oxide synthase uncoupling and up-regulation of endothelial nitric oxide synthase expression lowers blood pressure in hypertensive rats.* J Am Coll Cardiol, 2006. **47**(12): p. 2536-44.
443. Landmesser, U., et al., *Oxidation of tetrahydrobiopterin leads to uncoupling of endothelial cell nitric oxide synthase in hypertension.* J Clin Invest, 2003. **111**(8): p. 1201-9.
444. Yuan, S.Y., et al., *Microvascular permeability in diabetes and insulin resistance.* Microcirculation, 2007. **14**(4-5): p. 363-73.
445. Perrin, R.M., S.J. Harper, and D.O. Bates, *A role for the endothelial glycocalyx in regulating microvascular permeability in diabetes mellitus.* Cell Biochem Biophys, 2007. **49**(2): p. 65-72.
446. Dang, L., J.P. Seale, and X. Qu, *High glucose-induced human umbilical vein endothelial cell hyperpermeability is dependent on protein kinase C activation and independent of the Ca2+-nitric oxide signalling pathway.* Clin Exp Pharmacol Physiol, 2005. **32**(9): p. 771-6.
447. Murakami, T., et al., *Protein kinase cbeta phosphorylates occludin regulating tight junction trafficking in vascular endothelial growth factor-induced permeability in vivo.* Diabetes, 2012. **61**(6): p. 1573-83.
448. Yan, J., Z. Zhang, and H. Shi, *HIF-1 is involved in high glucose-induced paracellular permeability of brain endothelial cells.* Cell Mol Life Sci, 2012. **69**(1): p. 115-28.
449. Wang, J., et al., *RhoA/ROCK-dependent moesin phosphorylation regulates AGE-induced endothelial cellular response.* Cardiovasc Diabetol, 2012. **11**: p. 7.
450. Liu, C., J. Wu, and M.H. Zou, *Activation of AMP-activated protein kinase alleviates high-glucose-induced dysfunction of brain microvascular endothelial cell tight-junction dynamics.* Free Radic Biol Med, 2012. **53**(6): p. 1213-21.
451. El-Remessy, A.B., et al., *Experimental diabetes causes breakdown of the blood-retina barrier by a mechanism involving tyrosine nitration and increases in expression of*

vascular endothelial growth factor and urokinase plasminogen activator receptor. Am J Pathol, 2003. **162**(6): p. 1995-2004.

452. Jin, B.Y., et al., *MARCKS protein mediates hydrogen peroxide regulation of endothelial permeability.* Proc Natl Acad Sci U S A, 2012. **109**(37): p. 14864-9.

453. Basuroy, S., C.W. Leffler, and H. Parfenova, *CORM-A1 prevents blood-brain barrier dysfunction caused by ionotropic glutamate receptor-mediated endothelial oxidative stress and apoptosis.* Am J Physiol Cell Physiol, 2013. **304**(11): p. C1105-15.

454. Kim, J., et al., *Methylglyoxal induces hyperpermeability of the blood-retinal barrier via the loss of tight junction proteins and the activation of matrix metalloproteinases.* Graefes Arch Clin Exp Ophthalmol, 2012. **250**(5): p. 691-7.

455. Cosentino, F., et al., *High glucose increases nitric oxide synthase expression and superoxide anion generation in human aortic endothelial cells.* Circulation, 1997. **96**(1): p. 25-8.

456. Bouloumie, A., et al., *Endothelial dysfunction coincides with an enhanced nitric oxide synthase expression and superoxide anion production.* Hypertension, 1997. **30**(4): p. 934-41.

457. Cernadas, M.R., et al., *Expression of constitutive and inducible nitric oxide synthases in the vascular wall of young and aging rats.* Circ Res, 1998. **83**(3): p. 279-86.

458. Schulz, E., et al., *Nitric oxide, tetrahydrobiopterin, oxidative stress, and endothelial dysfunction in hypertension.* Antioxid Redox Signal, 2008. **10**(6): p. 1115-26.

459. Alderton, W.K., C.E. Cooper, and R.G. Knowles, *Nitric oxide synthases: structure, function and inhibition.* Biochem J, 2001. **357**(Pt 3): p. 593-615.

460. Kuzkaya, N., et al., *Interactions of peroxynitrite, tetrahydrobiopterin, ascorbic acid, and thiols: implications for uncoupling endothelial nitric-oxide synthase.* J Biol Chem, 2003. **278**(25): p. 22546-54.

461. Hink, U., et al., *Mechanisms underlying endothelial dysfunction in diabetes mellitus.* Circ Res, 2001. **88**(2): p. E14-22.

462. Mamputu, J.C. and G. Renier, *Advanced glycation end products increase, through a protein kinase C-dependent pathway, vascular endothelial growth factor expression in retinal endothelial cells. Inhibitory effect of gliclazide.* J Diabetes Complications, 2002. **16**(4): p. 284-93.